NOTE TO USERS

This reproduction is the best copy available.

UNIVERSITÉ DE SHERBROOKE

Faculté de génie
Département de génie civil

Nouveau système cimentaire : cas de la Fritte de verre (New Cementitious System: the case of Glass Frit)

Thèse de doctorat ès sciences appliquées

Spécialité : génie civil

Les membres du jury :

Arezki Tagnit-Hamou	Directeur de recherche
Patrice Rivard	Rapporteur
Benoit Fournier	Examinateur
Laila Raki	Examinateur

Galal Fares

Sherbrooke (Québec), Canada **Juillet 2008**

Your file Votre référence
ISBN: 978-0-494-52830-3
Our file Notre référence
ISBN: 978-0-494-52830-3

Abstract

Canada ranks as the world's third largest aluminium producer, and more than 80% of its aluminum industry is concentrated in Quebec. However, the spent pot-liner waste produced by the aluminium smelters accumulates with time into a considerable amount threatening the Canadian environment, especially that of Quebec. A new-engineered material, known as glass frit (GF) has been developed through the chemical treatment of such waste. GF shows potential hydraulic and pozzolanic properties. GF has been studied as a binder itself and as a supplementary cementitious material (SCM).

The activation of industrial by-products into clinkerless binders is a novel trend that has attracted the attention of many researchers. The activation of GF into binder to produce paste, mortar and concrete was the first aim of this study. Potential activation of GF using different types and combinations of inorganic activators and temperatures of activation was successfully achieved and high strength concretes were obtained. Moreover, mortars with high compressive strength were obtained with well-formulated activators at ambient temperature.

On the other hand, the utilization of industrial by-products as a partial replacement for cement in concrete is a widespread practice. As GF contains a high concentration of sodium in its structure, there is a concern as to the effect of sodium content on the development of alkali-silica reaction (ASR) expansion of concrete. Therefore, this study also aimed to investigate the effect of GF sodium content in the enhancement of ASR expansion and to find new synergistic mixtures that can effectively mitigate ASR expansion in the long term. We observed that ASR expansion decreases with the replacement level of GF. Different synergistic diagrams containing known SCM (silica fume, fly ash, and slag) were achieved from which different effective mixtures can effectively alleviate ASR expansion.

In conclusion, the use of GF in the manufacture of concrete has great benefits. Economically, it could save millions of Canadian dollars needed for the treatment and landfilling of spent pot-liner waste. Ecologically, it could reduce GHG emissions associated with the production of cement clinkers. In this study, most of the well-known by-products are used according to the sustainability theory.

Résumé

Le Canada se situe au troisième rang mondial des pays producteurs d'aluminium, et plus de 80% de l'industrie canadienne de l'aluminium est concentrée au Québec. Cependant, les brasques usées provenant des fonderies d'aluminium s'accumulent à un rythme considérable, menaçant ainsi l'environnement du Canada et spécialement celui du Québec. Un nouveau matériau conçu à partir d'un traitement chimique de ces brasques usées a été produit. Ce nouveau matériau, appelé Fritte de Verre (FV), montre d'excellentes propriétés hydrauliques dans les matériaux cimentaires. La FV a été utilisée comme liant hydraulique et comme matériau cimentaire supplémentaire (MCS). La production de béton sans « clinker » de ciment, réduit ainsi les émissions de gaz à effet de serre (GES) liées à la production de « clinker » de ciment.

L'activation des sous-produits industriels en liants hydrauliques sans clinker est une nouvelle tendance qui a attiré l'attention de beaucoup de chercheurs. L'activation de FV en liants hydrauliques sans clinker pour produire des pâtes, des mortiers et des bétons était l'objectif général de cette étude. L'activation potentielle de FV en utilisant différents types et combinaisons d'activateurs inorganiques et différentes températures d'activation ont été réalisées avec succès. Cette réalisation a permis d'obtenir différents bétons à hautes résistances. De plus, en formulant bien les activateurs, des mortiers à hautes résistances ont été obtenus à la température ambiante.

Comme la FV contient une grande concentration de sodium, nous prévoyons donc qu'elle aura un effet sur le développement de la réaction alcalis-silice (RAS) causant une expansion du béton. Le but de cette partie de l'étude était donc d'étudier l'effet de la teneur en sodium de la FV sur le développement de RAS et sur l'expansion du béton. Par la suite, le deuxième objectif était de formuler de nouveaux mélanges synergétiques pouvant mitiger efficacement les RAS à long terme. Nous avons observé que l'expansion associable à la RAS diminue selon le taux de remplacement de ciment par la FV. Différents diagrammes synergétiques contenant un apport de MCS connus (fumées de silice, cendres volantes et laitier) ont été dessinés desquels différents mélanges synergétiques peuvent mitiger efficacement les RAS.

En conclusion, l'utilisation de la FV dans le béton est très bénéfique. Du point de vue économique, elle peut réduire les coûts liés au traitement et à l'enfouissement des brasques usées. Du point de vue écologique, elle peut réduire les émissions de GES associées à la production de « clinker de ciment ». Dans cette étude, la plupart des sous-produits industriels sont utilisés selon la théorie du développement durable.

Mots clés : Ajouts cimentaires, caractérisation, activation, nouveau liant, réaction alcali-silice

Acknowledgement

The work involved with this dissertation has been extensive and trying, but first and foremost, it has been exciting, instructive, and enjoyable. Without help, support, and encouragement from several persons, I would never have been able to finish this work.

First of all, I would like to thank my supervisor, Arezki Tagnit-Hamou, for the inspiring and encouraging way he has guided me to a deeper understanding of topic and his valuable comments through my work on this dissertation. During my years as a Ph.D. student, I have known Prof. Tagnit-Hamou as a sympathetic and principle-centered person. His great enthusiasm and integral view of research, as well as his mission for providing "high-quality work", has made a deep impression on me. I am deeply indebted to him for having shown me this way of conducting research. He does not realize how much I have learned from him and how grateful I owe to him. I am very glad to have come to know Prof. Arezki Tagnit-Hamou.

I would also like to extend special thanks to Dr. Said Laldji for his fruitful collaboration and help during my experimental work.

I would like to thank Nova Pb who provided me with GF that they created with their own CAlSiFrit process in which aluminium waste product was transformed into a remarkable engineered commercial product, CAlSiFrit™, or as I call it in this work GF. Thanks also to all my colleagues at the Department of Civil Engineering for providing a good working atmosphere, especially those who are responsible for the Civil Engineering lab.

Last but not least, there are hardly words enough to thank my late parents for all they have done for me. I also want to mention my family, Seham, Mohamed, Youssef, and Yara who sometimes had to suffer from a "mentally" absent partner and father; many thanks to them for always supporting me over the past several years.

Table of Contents

List of Tables

Page

List of Figures

Page

CHAPTER 1
INTRODUCTION

1.1 General

The cement industry is a vital part of the national economies of most cement producing countries across the world. The production of Portland cement not only consumes limestone, clay, coal, and electric power, but also releases waste gases, such as CO_2, which can contribute to the greenhouse effect. Hence, the development of the cement industry is closely bound to a sustainable development strategy. It is important to extract the benefits of using industrial by-products as additives to cement. The goal of sustainable development for cement and concrete is very important, and it can be reached through serious effort toward the complete utilization of cementitious and pozzolanic by-products from thermal power plants and metallurgical industries (silicon, ferrosilicon, iron, and aluminium industries).

The Canadian primary aluminium industry has a total production capacity of 2.3 million tonnes per year. The production is concentrated in Quebec (more than 2 million metric tonnes annually), while British Columbia produces the remainder of the national production. Quebec ranks as the world's third largest producer behind the United States and Russia. The aluminium industry makes a permanent and growing contribution to Quebec and Canada's economic wealth. The aluminium industry was first established in Quebec at the turn of the century. Canada has no bauxite mines, the basic raw material needed to produce aluminium. However, both Quebec and British Columbia have competitive hydroelectric power costs, a qualified labour force, and modern public infrastructures that are in the vicinity of the large North American markets. The first aluminium smelter was established at the turn of the century in Quebec, more precisely in Shawinigan.

Aluminium smelter plants produce, among other wastes, spent pot-liner (SPL) waste material during the electrolytic production of aluminium. SPL contains a small amount of cyanide, as well as considerable amounts of sodium and fluoride. SPL is basically made up of two layers: a conductive carbon layer and a non-conductive insulation layer.

Most aluminium manufacturers split these layers into the first cut (the carbon layer) and the second cut (refractory layer). The EPA (Environmental Protection Agency) has classified the first cut (but not the second cut) as a hazardous waste, assigning the waste code number K088. For every tonne of aluminium produced, approximately 25 to 35 kg of spent pot-liner (SPL) is generated. Annual worldwide generation of this waste is estimated at 637,500 tonnes per year (tpy) of SPL, of which 40 to 45% by weight is a hazardous waste that requires treatment (which could cost the United States an estimated $33 million dollars and Canada an estimated $20 million dollars for treatment and landfill disposal). No land fill without treatment has been allowed in North America since 1997. Over 100,000 tpy of SPL are generated in the United States, while Canada generates approximately and 60,000 tpy of SPL [PARADIS, 1998; MINTO, 2003]. SPL contain 0.1 to 1.0% cyanides and high sodium compounds.

Nova Frit International proposes a state-of-the-art technology, known as the CAlSiFrit process, which transforms SPL into a viable commercial product with a stable composition that guarantees unique properties. The CAlSiFrit process is not a treatment process to detoxify the SP leaving residues to be eliminated in one way or another; it is a recycling process making complete use of the fed material to elaborate new value-added commercial products showing completely different mechanical, physical, and chemical properties than those of the original material. This process is characterized by zero effluent and absolutely no residuals accompanied by very low atmospheric emissions. The SPL are transformed into a remarkable engineered commercial product, CAlSiFrit™, which is also referred to by its technical name, glass frit (GF).

The CAlSiFrit process is environmentally sound as it produces no residue, neither solid nor liquid. This pyrometallurgical process is highly viable and sustainable as it succeeds in bringing solutions to two worldwide industries, namely the aluminium smelting industry and the concrete industry. The process also results in a credit relative to greenhouse gas emissions (GHG) and the Kyoto Agreement.

After the transformation of SPL into a valuable non-hazardous engineered product, intensive research to explore and find different ways of recycling GF as a cement additive and as a

clinker-free binder was conducted. GF has a high alkali content of approximately 10% Na_2O_{eq}, which is a matter of concern with respect to alkali-aggregate reaction (AAR) expansion.

1.2 Objective and originality

The aim of the present study is to evaluate GF as a new binder and as a cementitious material. A trial to convert GF into a new binder (clinker-free) using a chemo-thermal activation process was undertaken. Different combinations of GF-slag and GF-fly ash were activated to investigate the beneficial effect of their presence. It is important to note that no such study has previously been done on GF as a clinker-free binder (hydraulic binder). Moreover, studying the effect of alkali content of GF on the alkali-silica reaction (ASR) in mortar and concrete, especially when an alkali-active constituent exists, is of great importance. Several tests related to alkali-silica reaction were carried out to assess and optimize GF for use in the concrete industry.

The objectives of the present study are as follows:

i - Evaluation of the pozzolanicity and chemical reactivity of GF;

ii- Study of the hydraulic reactivity of GF and the possible ways it can be chemically activated;

iii- Development of alkali-activated GF (AAGF) binder that has reasonable workability while achieving one-day strength surpassing that of equivalent OPC binder at elevated temperature;

vi- Investigation of different activators and combinations of activators and selection of the most efficient ones;

v- Optimization of the GF-to-sand ratio by conducting different mixtures using the best activators;

vi- Assessment of some concrete mixtures made with AAGF binder.

vii- Determination of the effect of alkali content of GF used as a mineral admixture by determining the effect of GF content on ASR;

viii- Investigation of the synergistic interaction between GF and other mineral admixtures as well as drawing the synergistic diagrams needed to determine the efficient ternary combinations of GF-based mineral admixtures;

ix- Study of the effect of quaternary combinations of GF and other mineral admixtures on alleviating ASR;

x- Study of the pore solution chemistry, pore system, and microstructure of different combinations of GF and other mineral admixtures on assessing ASR expansion.

This study is divided into two main phases: in the first phase, GF was evaluated as a clinkerless binder for fabricating paste, mortar, and concrete. Therefore, different activators were tested to select the most efficient activators and combinations of activators. Moreover, the best activation temperature was selected. In the second phase, GF was assessed as a new cementitious material for its efficiency in mitigating ASR expansion in mortar and concrete using different standards and techniques.

1.3 Methodology

The above objectives were achieved through the two main phases mentioned previously. The first phase included the development of GF activators, the activation of GF into a novel clinkerless binder using the chemo-thermal activation method, and some applications involving the determination of the best GF-to-sand ratio in different GF mortar mixtures. Afterwards, different concrete mixtures using the best activators and the best conditions of activation were fabricated. At the same time, intensive microstructure development was monitored in all GF pastes fabricated during this part of the study.

The first phase of the experimental program included the following studies:

i- Study of the interaction of GF with different activators at different curing temperatures;

ii- Study of the interaction of GF with different activators and different mineral admixtures at different curing temperatures;

iii- Study of the interaction of GF with different combinations of activators including different single, binary, and ternary activator mixtures.

The second phase included intensive studies on mortar bars and concrete prisms made up of Portland cement-GF binder with and without other mineral admixtures to study ASR expansion. As well, it included examination of the pore solution chemistry of these binder-based mixtures. All tests were performed in accordance with CSA A23.2-14A (equivalent to ASTM C1293), CSA A23.2-25A (equivalent to ASTM C1260), and ASTM C227 specification with and without certain modifications as well as different aggregates with different reactivities.

This second phase of the experimental program included the following studies and parameters:

i- Comparison between Portland cement-GF mortar bar mixtures and different binary mortar bar mixtures including slag, fly ash, and silica fume in presence of alkali-silica reactive aggregate (Spratt aggregate) in severe alkaline condition (1N NaOH at 80°C);

ii- Comparison between different OPC-GF binary, ternary and quaternary mortar bar mixtures with different types of aggregates and curing conditions;

iii- Comparison between different OPC-GF binary, ternary and quaternary concrete prism mixtures with Spratt (reactive aggregate) in presence and absence of admixed alkali, and at curing conditions of 100 % R.H., at 38°C;

iv- Comparison between different OPC-GF binary, ternary and quaternary cement pastes by following-up the change in pH, concentration of available ions (Na^+, K^+, Ca^{2+}, etc.), pore-size distribution inside these pastes and their microstructure analysis with time;

v- Comparison of the effect of different parameters such as curing conditions and type of both aggregate and mineral admixture.

1.4 Structure of the thesis

The structure of the thesis is summarized in Figure 1.1.

Chapter 2 introduces a brief literature review of most of the research related to the current study. The materials used in fabricating paste, mortar, and concrete including cementitious binders, as well as different activators, fine and coarse aggregates and chemical admixtures

are described in Chapter 3. The most important tests needed for the characterization of cementitious binders used throughout this study are presented indepth in Chapter 4.

Chapter 5 details the development of alkali activators suitable for activation of GF. The effect of different activators and combinations of activators needed for producing reasonable compressive strengths in pastes, mortar, and concrete, in addition to microstructure exploration during fabrication, are investigated. Optimum GF-to-sand ratio, using different mixtures of AAGF mortars and activators, is determined. Different concrete mixtures with different activator, w/b ratios, and combinations of activators were tested for compressive strength with time for up to more than two years.

Chapter 6 discusses the concern related to alkali content of GF and its effect on alkali-silica reaction. Different testing methods related to alkali-silica reaction in mortar and concrete were conducted. The effect of GF content on the alkali-silica reaction in mortar and concrete was investigated. The synergistic interaction of GF and different mineral admixtures was assessed and the synergistic diagrams were drawn. Different ternary and quaternary systems in mortar and concrete were evaluated. Alkali-silica reaction was tested in concrete for more than two years. A direct correlation between accelerated mortar bar test (AMBT) and concrete prism test (CPT) was drawn. Pore solution chemistry, pore size distribution, and microstructural changes for different cementitious systems, including GF, were investigated.

Chapter 7 presents a brief conclusion drawn from the test results found throughout the thesis and discusses further tests and recommendations to be conducted in the future.

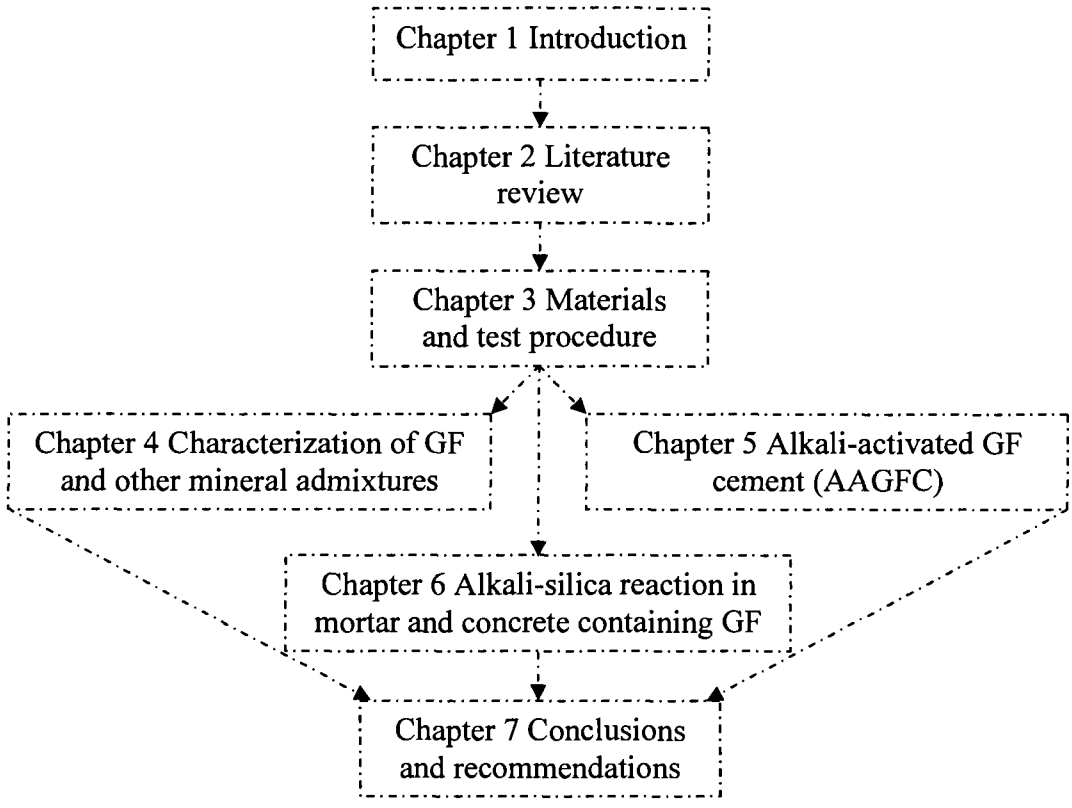

Figure 1. 1 Structure of the thesis

Throughout this study, the latent properties of GF, as well as the synergistic interaction of GF with other mineral admixtures, were explored through:

i- Investigation of the use of GF as a new binder using the chemo-thermal activation method in presence and absence of other active additives and different activators;

ii- Evaluation of the resulting new binder and optimization of the best mixtures during compressive strength testing at different curing ages;

iii- Evaluation of the chemical and physical properties and durability characteristics of mortar and concrete mixtures containing GF in different aggressive media to ensure successful use of GF as a new cementitious material;

iv- Study of the effect of alkali content of GF on expansion due to alkali-silica reaction (ASR) through different tests conducted under different curing conditions. As well, the synergistic interaction of GF with different active additives (fly ash, slag, and silica fume) on the mitigation of ASR expansion was evaluated.

v-

CHAPTER 2
LITERATURE REVIEW

2.1 General

Deposits of mineral waste by-products are growing year after year all over the world. Most of this waste could be reused as valuable raw materials, since they usually contain many useful ingredients. Based on the physico-chemical nature of mineral waste, studies have been undertaken to evaluate the potential of converting them into building materials. In many cases, the hydraulic activity of normally passive materials could be increased, so that an activated mineral waste would behave like a binder for concrete. The significance of the wastes stems from their high silicate and/or aluminium silicate components content, preferably in glassy form as in the case of fly ash or blast-furnace slag. For this type of waste an alkaline activator can be used.

2.2 Glass frit background

Glass frit is the industrial by-product of thermally treated SPL waste resulting from a mixture of the conductive carbon and refractory layers used to line the pots, in the electrolytic process used in aluminium production from the raw material known as alumina. SPL is actually made up of two layers, a conductive carbon layer and a non-conductive insulation layer. Most aluminium manufacturers split these layers into the first cut (the carbon layer) and the second cut (the refractory layer). The EPA (Environmental Protection Agency) has classified the first cut (but not the second cut) as a hazardous waste, assigning waste code number K088, as shown in Figure 2.1 [CONSTANS, 1998]

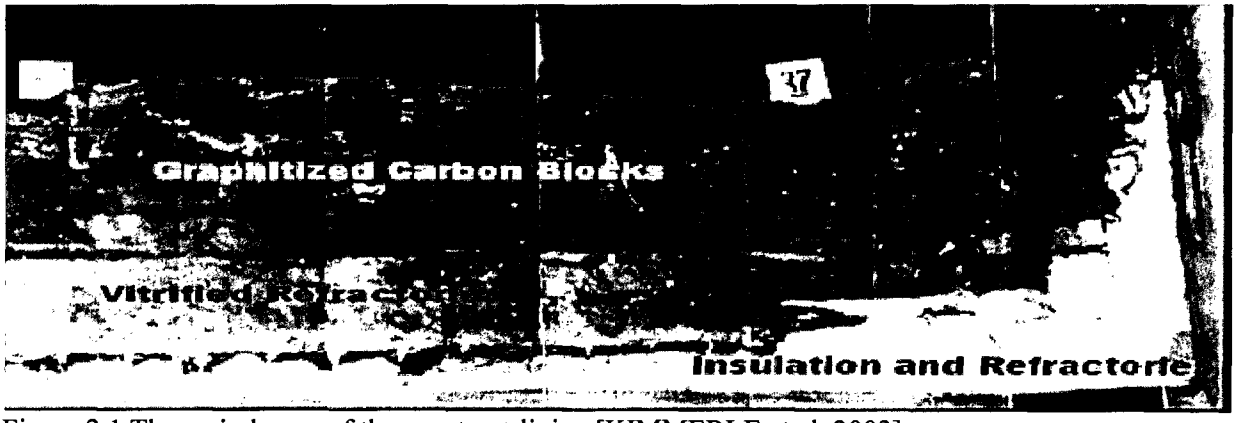

Figure 2.1 The main layers of the spent pot-lining [KIMMERLE et al, 2003]

This layer, which is contaminated by cyanides and fluorides (used in aluminium manufacture as fluxing materials), is thermally treated to rid it of these dangerous elements by the addition of silicate and carbonate compounds at high temperature and with the aid of high tech filters, followed by sudden quenching. The resulting material, known as glass frit, has a high alkali content of approximately 10% (Na_2Oeq). Glass frit is composed largely of SiO_2, Al_2O_3, CaO, Fe_2O_3, and MgO which are also the major components of slag and other pozzolanic materials, in addition to high percentages of Na_2O and F, as shown in Figure 2.2 and Table 2.1. Due to its high alkali content, glass frit requires deep investigation to explore its latent properties and assess the effect of its alkalis on alkali-reactive aggregates in mortar and concrete.

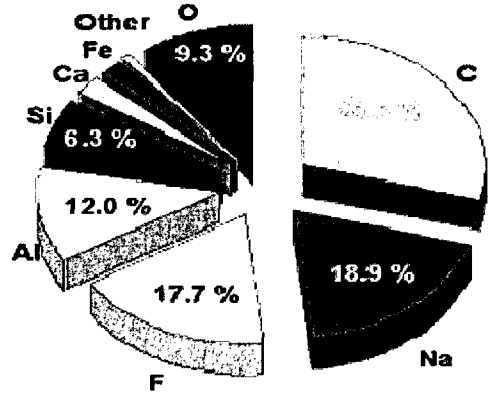

Figure 2.2 Average composition of spent pot-lining [KIMMERLE et al., 2003]

TABLE 2.1 CHEMICAL COMPOSITION OF SPL [CONSTANS, 1998] AND GLASS FRIT [NOVA PB]

Oxide Weight %	Typical First Cut K088	Typical Second Cut (non hazardous) K088	Glass frit
SiO_2	1.5-8	14-45	33.8
Al_2O_3	8-20	21-50	25.1
Fe_2O_3	0.3-1.0	2-15	3.4
CaO	1.5-2.25	1.5-4.2	14.6
MgO	0.05-0.25	0.3-0.6	0.76
Na_2O_{eq}	10-15	15-24	10.12
CaF_2	-	-	12.1
F	9-12	9-15	-
C	54-66	1.3-4.5	0.40

2.3 Definition of a pozzolan

The American Society for Testing and Materials (ASTM C 125, 2000) defines a pozzolan as "a siliceous or siliceous and aluminous material which in itself possesses little or no cementitious value but which will, in finely divided form and in the presence of moisture, chemically react with calcium hydroxide at ordinary temperature to form compounds possessing cementitious properties".

2.4 Investigation of the pozzolanicity and hydraulic reactivity of the active additives

SHI [2001] indicated that lime-natural pozzolan mortars have been used for many years. He mentioned that the examination of a concrete slab discovered in southern Galilee proves that the invention of lime and lime-pozzolan concrete dates back to the Neolithic period (7000 BC) rather than Greek and Roman times [MALINOWSKI AND GARFINKEL, 1991]. Many up-to-date Roman monuments, stand as a concrete fact to the durability of lime-pozzolan mortars [LEA, 1974]. Lime-Surkhi mixtures (Surkhi is pulverized fire clay or brick-earth) have commonly been used since Greek and Roman times and are still widely used in India [SHI, 2001].

It was not until the 7^{th} century that England started to use lime-Dutch trass mixtures. Such mixtures were also used extensively in Holland for construction of harbours and sea defences [SHI, 2001]. In Iceland, mortars made of lime and volcanic ash were used in the construction of many of the early stone buildings. These mortars were found to be very strong, rock-like, and durable, having survived for periods of 90 to 400 years [SHI, 2001].

In North America, a natural pozzolan was first used for the Los Angeles aqueduct in 1912. In this structure, 50% of the Portland cement was replaced by deeply altered Rhyolite tuff [SHI, 2001]. About $700,000 was saved due to the use of this pozzolan [PRICE, 1975].

Pozzolans are widely used as cement replacement in Portland cement concrete. The use of pozzolans is advantageous resulting in lower cost, reduction in heat evolution, decreased permeability, alkali-aggregate expansion control, increased chemical resistance, reduced

concrete drying shrinkage, improvement of the properties of fresh concrete and better durability [SHI, 2001].

2.5 General use of pozzolans

In modern cement and concrete technology, addition of active mineral additives (fly ash, silica fume, slag, natural pozzolan, etc.) is of great technical significance. It is well known that the clinker minerals C_3S and C_2S that make up about 75% of Portland cement will form high basic calcium hydrosilicates (C/S> 1.5) with a lime/silica ratio of 1.6-1.9 and a large amount of calcium hydroxide. In comparison with low basic calcium hydrosilicates (C/S < 1.5), they have much lower strength. In particular, the free lime has a rather low strength and poor stability, which leads to lower strength and durability of cement and concrete. With the addition of a proper amount of active mineral additives, the active SiO_2 will gradually have a secondary reaction with $Ca(OH)_2$ and high basic calcium hydrosilicate in cement paste, as the so-called pozzolanic reaction, forming low basic calcium hydrosilicates. Thus, as a result, there will be an increase not only in quality of hydrates, but in the quantity as well, and the strength of cement paste and other properties can be improved greatly [PU, 1999].

This part of the literature review focuses on the use of pozzolans as ecological binders and as active additives (mineral admixtures) for both improving durability and alleviating the harmful effect of the alkali-silica reaction (ASR) in concrete.

Supplementary cementitious materials (SCMs), also known as mineral admixtures, contribute to the properties of hardened concrete through hydraulic or pozzolanic activity. Typical examples are natural pozzolans (volcanic tuff, pumicites, metakaolin, rice husk ash, etc.), artificial pozzolan (such as fly ash-class F and class C, silica fume) and ground granulated blast-furnace slag, which can be used individually with Portland or blended cement or in different combinations. These materials react chemically with calcium hydroxide released from the hydration of Portland cement to form cement compounds. These materials are often added to concrete to make concrete mixtures more economical, reduce permeability, increase strength, or influence other concrete properties. Fly ash, the most commonly used pozzolan in concrete, is a very fine residue that is extracted from the combustion of pulverized coal and is

carried from the combustion chamber of the furnace by exhaust gases [BERRY AND MALHOTRA, 1980]. Fly ash is commercially available as a by-product of thermal power generating stations.

Blast-furnace slag, or iron blast-furnace slag, is a non-metallic product consisting essentially of silicates, calcium aluminosilicates, and other compounds that are developed in a molten condition simultaneously with the iron in the blast-furnace [JOHN EGGERS, 2002]. Silica fume, also known as condensed silica fume and microsilica, is a finely divided residue resulting from the production of elemental silicon or ferro-silicon alloys that is carried from the furnace by the exhaust gases [KHEDR AND ABOU-ZEID, 1994]. Silica fume with or without fly ash or slag, is often used to make high-strength concrete.

2.6 Evaluation of pozzolanic reactivity

Many methods have been used to evaluate pozzolanic reactivity, where Vicat [LEA, 1938] proposed the first method, a lime absorption test for the evaluation of pozzolans reactivity. DAY (1992) and SHI (1992) have reviewed different evaluation test methods. All these methods are summarized in Table 2.2 [SHI, 2001]. The effect of curing temperature on strength development of lime-natural pozzolan pastes is shown in Figure 2.3 [SHI AND DAY, 1993].

TABLE 2.2 SUMMARY OF TEST METHODS FOR THE EVALUATION OF POZZOLANIC REACTIVITY OF POZZOLANS [SHI, 2001]

Method		Evaluation criteria
Lime absorption		- Amount of absorbed lime in a pozzolan/ Saturated $Ca(OH)_2$ solution at different ages
Setting time		setting time of 1:4 lime pozzolan pastes by Vicat test
Solubility	In saturated Ca(OH)2 Solution	- Decrease of Ca^{2+} in solution due to addition of a pozzolan
	In alkali	Dissolved SiO_2 or $SiO_2 + R_2O_3$ of pozzolan in alkaline solution
	In acid	- Dissolved $SiO_2 + R_2O_3$ of pozzolan in acid
	In alkali then in acid	- Dissolved $SiO_2 + R_2O_3$ of pozzolan after treatment in acid then in alkali solution
Mechanical Strength		
Pozzolan +Portland cement		- Tensile strength difference of mortars cured at 18°C and 50°C. Strength ratio of Portland pozzolan cement to pure Portland cement mortars
	Pozzolan + lime	- Strength of lime-pozzolan mixtures cured under controlled conditions at specified age

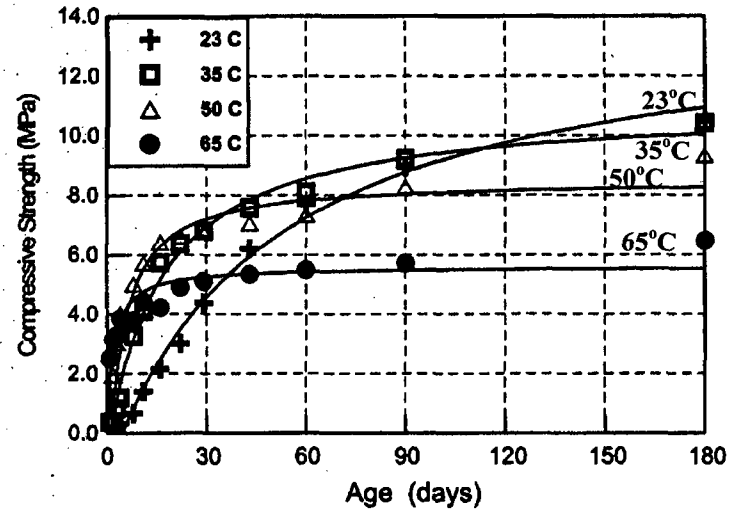

Figure 2.3 Effect of curing temperatures on strength development of lime-natural pozzolan pastes [SHI, DAY, 1993]

The relationship between the compressive strength of lime-natural pozzolan pastes and the Blaine fineness of the natural pozzolan is also shown in Figure 2.4 [DAY, SHI, 1994].

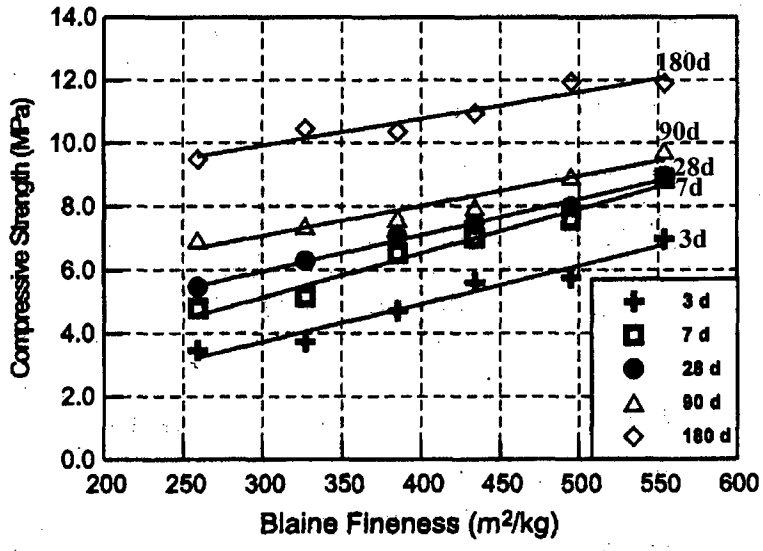

Figure 2.4 Relationship between the compressive strength of lime-natural pozzolan pastes and the Blaine fineness of the natural pozzolan [DAY, SHI, 1994]

Various chemical formulas have been proposed for predicting the hydraulic activity of granulated blast-furnace slag, as shown in Table 2.3 [MANTEL, 1994].

MANTEL (1994) reported that he could not find a correlation between compressive strength and any of the commonly used hydraulic indices. None of those formulas provided generally valid information as to the effect of the chemical composition of slag on strength development.

TABLE 2.3 FORMULAS PROPOSED FOR ASSESSMENT OF HYDRAULICITY OF GRANULATED BLAST-FURNACE SLAGS [MANTEL, 1994].

	Formula	Requirement for good performance	Preference
1	CaO/SiO_2	1.3-1.4	1
2	(CaO + MgO)/SiO2	>1.4	1
3	$(CaO + MgO)/(SiO_2 + Al_2O_3)$	1.0 – 1.3	1
4	$(CaO + 0.56Al_2O_3 + 1.4MgO)/SiO_2$	>= 1.65	2
5	$(CaO + Al_2O_3 + MgO)/SiO_2$	>= 1	3

MALQUORI (1960) suggested that an evaluation of pozzolanic materials for purposes of their addition to Portland cement must be based on two factors: (1) the mechanical strength of mortars and concretes made with a Portland-pozzolan mixture, and (2) the reduction of free calcium hydroxide in the hardened pozzolanic cement. The pozzolans consume the $Ca(OH)_2$ to generate further cementitious hydrate materials (Gehlenite and Tobermorite), thereby increasing the strength and quality of the concrete concerned.

JAMBOR (1963) studied the relation between phase composition, overall porosity, and strength of hardened lime-pozzolan pastes by means of X-ray analysis, differential and gravimetric thermal analysis, electron microscopy, and chemical analysis. The main hydration products of 22 pastes made from lime and various pozzolanic materials and hardened in water for 400 days were found to be calcium hydro-silicates of the tobermorite group and Stratling's compound, C_2ASHn. A formula was developed giving the compressive strength of the pastes in terms of the volume of the hydration products produced.

The quality of natural or artificial pozzolanic cements should be evaluated using strength tests. Many standards now use the compressive or tensile strength of mortars [SHI, 2001]. The mortars are prepared with a specified ratio of pozzolan to Portland cement or pozzolan to lime, and cured under closely controlled conditions. LEA (1974) has confirmed that the strength differences of Portland pozzolan cements, under two different curing temperatures, increases as the pozzolan content goes up. DAY (1988) has obtained similar results.

SIBBICK AND NIXON (2000) have investigated the effect of metakaolin as a cement replacement material in ASR reactive concrete and suggested that a cement replacement rate of 7.5% metakaolin is adequate. They also reported on the reactivity of different pozzolans determined using the Chapelle test, measuring the reduction in the $Ca(OH)_2$ in milligram per gram of the pozzolanic material as shown in Table 2.4.

TABLE 2.4 REACTIVITY OF POZZOLANS USING THE CHAPELLE TEST [SIBBICK AND NIXON, 2000]

Pozzolan type	Pozzolan reactivity measured as mg of $Ca(OH)_2$ consumed per g of pozzolan
Ground granulated blast-furnace slag	40
Microsilica	427
Pulverized fuel ash	875
Metakaolin	1050

McCARTER and EZIRIM (1998) have used electrical methods to follow the early hydration characteristics of pozzolanic materials activated with powdered calcium hydroxide at room temperature (20°C). The electrical response was measured in terms of conductance and capacitance. Four materials were studied: ground granulated blast-furnace slag, microsilica, metakaolin and pulverized fuel ash. Their work has shown that monitoring the temporal change in electrical parameters can be exploited as a potentially useful test for identifying the hydration stages and studying the rate of reaction over these stages.

BALL and CARROL (1999) have studied autoclaved pulverized fuel ash/calcium hydroxide pastes (C/S ratio approximately 0.8) at 184°C for periods of up to 12 hours. The pastes were analyzed for loss of calcium hydroxide and ash, release of silicon, aluminium and alkalis, and by X-ray diffraction. Calcium hydroxide was consumed within 6 hours, which coincides with the most rapid periods of ash reaction. A semicrystalline C-S-H phase appears initially, which converts to crystalline tobermorite at later stages. Hydrogarnet formed readily and was stable under the conditions investigated. Differences in the behaviour of the ash samples were evident that seemed to be related to particle-size distribution rather than to the amount of glassy phase present or to other measures of reactivity.

PAPAYIANNI (1987) has investigated the pozzolanicity and hydraulic reactivity of high-lime fly ashes (lignite fly ashes) which often have self-cementing as well as pozzolanic properties, due to their high lime content. Neat lignite fly ash mortars develop strengths 60 to 70% those of similar OPC mixtures at 28 days. Ground lignite fly ashes can therefore be used on their own as a binding agent in suitable product or constructions, while other fly ashes (i.e.

low-calcium fly ash) react only as pozzolanic materials in concrete. The hydraulic reactivity of ground lignite fly ashes is associated with the presence of free lime and active silica within the ash. Strength development is due to the interaction of these constituents and the formation of C-S-H gel.

Finally, MEHTA (1989) has classified pozzolans according to their degree of reactivity as shown in Table 2.5.

TABLE 2.5 MEHTA'S POZZOLANS CLASSIFICATION [MEHTA, 1989]

Class	Description	Example
I	Cementitious	Granulated blast-furnace slag
II	Cementitious: Pozzolanic	High-calcium fly ash
III	High active pozzolans	Silica fume, rice husk ash
IV	Normal pozzolans	Low-calcium fly ash
V	Weak pozzolans	Slow cooled blast-furnace slag, Field-burnt rice husk ash

2.7 Activation of pozzolans into clinker-free binders

The aim of this part of the study is to evaluate the potential to convert glass frit into a cementitious material. If successful, demonstration could be achieved due to the dual nature of the glass frit both as a mineral admixture and as a clinker-free binder (such as slag and fly ash). In many cases, the hydraulic activity of normally passive materials could be increased, so that an activated mineral waste would behave like a binder. Many methods have been used to activate the potential reactivity of pozzolanic material. These methods can be divided into three groups: chemical methods, thermal methods, and mechanical methods, some of which are not very efficient while others are not practical. Therefore, the literature review will focus on the methods used to activate slag and fly ash, including the types of activators, mix proportions, alkalinity, and curing temperature.

In addition to their use as mineral admixtures for the above-mentioned reasons, pozzolans are also used in the manufacture of clinkerless cements. Ground granulated blast-furnace slag and fly ash have latent hydraulic properties giving rise to their extensive use as partial replacement

for Portland cement, where they are activated by alkali and lime generated by Portland cement hydration. They can also be activated directly with alkali salts to give a clinker-free binder. Slag is often used in concrete as a supplementary cementitious material and partial replacement of Portland cement. The major advantages of making concrete with slag replacement are the superior durability and lower hydration heat as compared with 100% Portland cement binder. It should be noted that, in the case of slag replacement, carbonation resistance and freeze-thaw resistance decreases with increasing slag content. In addition, the low early strength of these concretes is a limitation in many applications. The problem of low early strength can be overcome by using alkali-activated slag (AAS) concretes that can potentially yield high-early strength.

Evidently, the use of slag and fly ash offers benefits with respect to the cost of concrete manufacturing, because these raw materials are produced as by-products or waste materials and can replace purpose-made Portland clinker. The same applies for the effects of cement and concrete products on the environment as lower primary energy and fewer raw materials are required in producing concrete, while durability of structures is generally improved. In both slag and fly ash, the amorphous glass is the active part. The glass in slag consists of mono-silicates like those in Portland clinker, Q^0 type, while fly ash glass consists of cross-linked silica-tetrahedra, Q^4 type [BIJEN, 1996]. When activated, slag dissolves, while in fly ash, Si-O-Si links have to be broken. Fly ash does not dissolve but decomposes. The activation of slag needs low pH of less than 12, while the activation of fly ash needs higher pH value of more than 13 [BIJEN, 1996].

In the last few years, the notion of ecological binder, which defines a binder obtained with little impact on the environment, has become used more and more frequently. Activated blast-furnace slag binder is part of this category of binders. Alkali-activated blast-furnace slag binders were first achieved by [PURDON, 1940], but their investigation and testing have continued to develop, leading in the last few decades to industrially produced cement with strengths of over 100 MPa. Blast-furnace slag used to make blended cements can be activated with suitable chemicals and be used as principal binding component in mortar and concrete

that contain no ordinary Portland cement (OPC). This binder component is referred to as alkali-activated blast-furnace slag cement (AABFC).

Unlike OPC, AABFC requires little energy to produce, since it is a by-product of the iron industry. Consequently, its use represents a considerable economic and environmental benefit through energy conservation and by-product utilization. AABFC technology has been used successfully in practice in the cement and concrete industry in Eastern Europe and China for many years. However, research interest has only been roused in Canada in more recent times [DOUGLAS AND BRANSTETR, 1990, DOUGLAS et al., 1991; SHI 1992, SHI AND DAY 1995; GIFFORD, GILLOT 1994, 1996a, 1996b]. Plastic ABFSC mortars and concretes are of sticky consistency, and they stiffen rapidly when compared with OPC mixtures. These mixtures require the use of caustic chemicals, such as sodium silicate, while mixing. These characteristics probably account partly for their slow recognition. Certainly, the development of both effective and less caustic activators and admixtures to enhance workability would encourage acceptance.

Blast-furnace slag and OPC may not be very different in chemical composition, but blast-furnace slag is mainly glassy and even the small crystalline fraction normally contains no tricalcium aluminate (C_3A) or unstable calcium sulphoaluminate phases in its hydration products. Consequently, AABFS concretes are less prone to associated durability problems. Hydrated AABFSC contains alkaline aluminosilicate and low-basic calcium silicate hydrates (C-S-H) which are better crystallized than the hydration products of OPC.

GLUKHOVSKY et al. (1980) give the solubility of C-S-H as 0.035-0.05 g/L with that of the alkaline aluminosilicates still lower and make a comparison with the high-basic calcium aluminate and silicate hydrates of OPC and free lime at 0.5-1.3 g/L. It follows that hydrated AABFSC is less reactive and chemically more stable than hydrated OPC. Furthermore, the pore structure of hardened AABFSC is finer than that of OPC paste. However, micro-cracks are commonly observed. Hydrated AABFSC has been shown to exhibit higher coefficients of capillary suction than hydrated OPC [COLLINS AND SANJAYAN, 2001]. This suggests that hardened AABFSC paste can be expected to exhibit greater permeability. Notwithstanding, air-entrained AABFSC concrete has been shown to perform as well as OPC concrete under

severe freezing-and-thawing test conditions [DOUGLAS et al., 1992; GILLOTT 1995]. Furthermore, ABFSC concrete has been shown to exhibit lower expansion due to alkali-silica reaction while being more prone to excessive expansion and cracking due to alkali-carbonate reaction [GIFFORD AND GILLOTT, 1996b].

Alkali-activated slag cement concretes are compounded by ground slag (granulated blast-furnace slag, phosphorus slag, etc.), and alkali components (water glass, KOH, NaOH, Na_2CO_3, and even alkali-containing industrial waste material, aggregates, and water in particular proportions [TALLING, BRANDSTETS, 1989].

2.7.1 Types of Alkali activators

Alkali activators were classified into different types according to GLUKHOWSKY et al. (1980), as follows:

i) Alkali metal hydroxide, ROH;

ii) Non-silicate salts of weak acids, R_2CO_3, R_2SO_3, R_2S, R_2PO_4, RF, etc;

iii) Silicate salts, $R_2O.SiO_2$ (Ms = SiO_2/R_2O = 0.5 to 2.5);

iv) Aluminates, $R_2O.nAl_2O_3$;

v) Aluminosilicates, $R_2O.Al_2O_3.nSiO_2$ (Si/R_2O = 2 to 6);

vi) Non-silicate strong acid salts R_2SO_4; where R represents an alkali metal ion.

WANG (1991) has reported that the highest strength of alkali-activated slag concrete attainable at present using water-reducing and set-retarding admixture is about 150 MPa. Alkali-activated slag concretes have many other advantages over ordinary concrete, such as low production cost, low consumption of energy, good durability and high resistance to chemical attacks. However, the following problems remain to be solved [WANG, 1991]:

a) The practical infeasibility of utilizing alkaline waste and many other types of slag instead of industrial alkalis and granulated blast-furnace slag.

b) The difficulty of retarding alkali-aggregate reaction.

c) Effective control of setting time.

d) Mitigation of the brittleness of alkali-activated slag concrete having relatively high strength.

e) Minimizing of quality fluctuation.

2.7.2 Alkali activation of slag

A. Hydration of alkali-activated slag (AAS) cement

HUANHAI et al. (1993) have reported a kinetic study of alkali-activate slag (AAS) made with blast-furnace slag and water glass (sodium silicate). They found that the calorimetric curves of AAS and OPC are similar, but the mechanism of each is different. It is proposed that the hydration process of AAS could also be classified into five stages: initial, induction, acceleration, deceleration, and decay. Meanwhile, the hypotheses developed for OPC may also be used to explain the hydration process of AAS. The calorimetric curve of AAS consists of two thermal peaks: the first peak represents the reaction of silicate ions from water glass with Ca ions from slag, producing C-S-H; the second peak is related to the reaction of silicate and aluminate ions with metal ions (Ca, Na, Mg, etc.) from the degraded slag, forming secondary C-S-H and other hydrates. Third, the main factor of hydration of AAS is the pH value of the solution, while the silicate concentration only affects early hydration.

Various studies of cementitious material suggested that the pH of the solution plays an important role in the hydration process and in determining the nature of C-S-H. It was reported that C-S-H does not form in a solution with a pH below 9.5 [GREENBERG, CHANG, 1965]. The effect of pH on the structure and composition of C-S-H, however, is still controversial.

SHI and LI (1989); and SHI and DAY (1996b) have found that due to the variation of activator, the hydration of alkali-slag cements can be described by three models: type I- one initial peak of hydration occurs during the first few minutes and no more peaks appear thereafter; type II- one initial peak appears before the induction period and one accelerated hydration peak appears after the induction period; type III- two peaks (one initial and additional initial) appear before the induction period and one accelerated hydration peak appears after the induction period

SONG and JENNINGS (1999) have determined the chemical composition and pH of the pore solution extracted from six different ground granulated blast-furnace slag pastes. The pH of the mixing solution is expected to have a significant effect on the nature of C-S-H by affecting the chemistry of the pore solution. They have found that the composition of Si, Ca, Al and Mg are function at the pH of the aqueous phase, with high pH associated with the higher concentrations of Si and Al and the lower concentration of Ca and Mg. When slag was mixed with an aqueous phase with higher pH than 11.5. The reaction is activated or accelerated. The main hydration product was identified as C-S-H, and hydrotalcite ($Mg_6Al_2CO_3(OH)_{16}.4H_2O$), at later stages of hydration, was observed in the pastes with an aqueous phase of high pH. At pH lower than 11.5 the equilibrium solubility of silica is low and slag simply does not dissolve. Hydrotalcite seems to be a phase that should form when a high degree of hydration is reached in slag pastes. SHI and LI (1989); and SHI and DAY (1996a) have found that all caustic alkalis and alkali compounds that are less soluble than $Ca(OH)_2$ can act as activators of slags.

As a result of the reaction between the aluminosilicate phases, which are present in blast-furnace slag and an alkaline activator, hydrated products are formed of the thomsonite-($NaCa_2Al_5Si_5O_{20}.6H_2O$), hydronepheline- ($Na[AlSi_2O_6].1.1H_2O$) and natrolite-type ($Na_2Al_2Si_3O_{10}.2H_2O$), as well as hydrated silicates from the tobermorite group such as C-S-H (I). Furthermore, calcite, hydrogarnet (C_3AH_6), and hydrated magnesium silicates could also be formed according to VAN AARDT and VISSER (1977) who have pointed out that hydrogarnet can be produced due to hydroxide attack on clay minerals. Thus, these compounds could also be encountered in alkali-activated hydrated systems including silicates and aluminosilicates. The efficiency of an activator is very strongly related to the physico-chemical nature of the material to be activated. The hydraulic activity of slag and fly ash depends on the quantity and quality of the amorphous phase present in the material [SLOTA, 1987].

LI et al. (2002) have summarized the relationship between structure, composition, and activity of glass cementitious materials with low-calcium additions including slag and fly ash. The difference between slag and fly ash is that aluminate hydrates of the slag sample

obviously increase at the same hydration time. This is due to the fact that the alumina oxygen ions of slag more easily dissolve and react. Under high alkalinity, the glass structure of fly ash was easily broken. Because of the lower calcium content of the fly ash, only a little C-S-H gel forms. Therefore, pore structure results showed that there are many pores in the fly ash paste. Only in higher alkalinity condition is the glass structure of fly ash easily broken, and its activation and hydration properties are improved.

B. Activation with sodium silicate and sodium hydroxide

The use of sodium silicate as an activator that would yield equivalent one-day strength to ordinary Portland cement at normal curing temperature, while having reasonable workability, was the aim of many researchers. Activation with sodium silicate (water glass) has been widely reported to give rise to rapid hardening and high compressive strengths [DOUGLAS et al., 1991; QING-HUA et al., 1992; SHI, 1992; WANG AND SCRIVENER, 1995].

DOUGLAS et al. (1991) have presented results of a preliminary investigation dealing with the compressive strength development of alkali-activated ground granulated blast-furnace slag concretes; these concretes incorporated sodium silicate as an activator, but did not contain any Portland cement. The five concrete mixtures were proportioned using sodium silicate and small amounts of hydrated lime. The water-to-binder ratio of mixtures ranged from 0.34 to 0.5. The air-entrained concrete produced satisfactory workability. The 1-day and 28-day compressive strengths of the concretes ranged from 20.4 to 38.9 MPa and from 45.5 to 59.6 MPa respectively. They concluded that combined-alkali-activated slag could be used as high compressive strength cementitious materials. As well, the use of fly ash can increase the strength and decreases the shrinkage.

QING-HUA et al. (1992) have reported that small amount of immediate reaction takes place when pure slag is mixed with water. Therefore, pure slag paste is capable of self-activation only to a small extent and the principle hydrate formed is C-S-H. The soluble sodium silicate (water glass) used had a composition of 10.8% Na_2O, 29.7% SiO_2 and 59.5% H_2O. The silica modulus (Ms = SiO_2/Na_2O)) was 2.85 and it was regulated to be 1.5 by adding NaOH solution. They used two amounts of water glass, 11 and 5.6%. The compressive strength of the

activated slag pastes has reached 68 MPa at 28 days for water glass content of 11% and lower compressive strengths with lower water glass content (5.6%). Hydrated lime (CH) influences the hydration rate at early age. With addition of CH, a silica rich gel is initially formed. The amount of water glass added is directly proportional to the compressive strength. In the alkali-lime-activated slag pastes, the hydrates are C-S-H and possibly zeolite.

BROUGH and ATKINSON (2002) have used sodium silicate activator with higher modulus (silicate-to-alkali ratio) that is less corrosive and thus safer, and which also partly alleviated set time difficulties. The slag samples used in this study were predominantly glassy, with very little crystalline material. High strengths were developed rapidly on activation with 1.5 M $Na_2O(SiO_2)_2$ solution (M_s = 2). After the initial exotherm due to the wetting of the slag, two peaks were observed in the calorimetry of this system, the first corresponds to gelation and set of the sodium silicate, and the second to bulk hydration of the slag responsible for strength development.

KRIZAN and ZIVANOVIC (2002) have activated slag with water glass ($Na_2O.nSiO_2$) and sodium metasilicate ($Na_2O.SiO_2.5H_2O$). The *n* modulus of liquid water glass was 3.01 with 9.62% Na_2O and 29.0% SiO_2. Sodium hydroxide was added to change the *n* modulus; water glass with *n* moduli of 0.6, 0.9, 1.2, and 1.5 was used in the experiments. It was found that the mass of Na_2O, rather than the total mass of activators, correlated best with the physical properties of alkali-slag cements; accordingly, all activators were added as percentage by mass of Na_2O. Quartz sand (0-0.2mm) was used as aggregate in mortar specimens, with a water-to-binder ratio of 0.43 and a weight ratio between binder and aggregate of 1:3. The cumulative heat of hydration increases by increasing the *n* modulus as well as the dosage of water glass, but is still lower than that of Portland cement. The compressive strength of normal-cured water glass slag cements is higher than Portland cement mortars. Drying shrinkage of alkali–slag cements is considerably higher than that of Portland cement. Consequently, industrial use of alkali–slag cement needs better understanding of the hardening mechanism and requires further research based on presented observations and results.

JOLICOEUR et al. (1992) have studied the effect of using of 2% Na_2O to activate slag paste, where they obtained low one-day strength, while when 4% Na_2O was used, the early strength increased with increasing Ms from 0 to 0.5 and remained relatively constant with increasing Ms up to 2.0 with accompanying loss of workability.

DOUGLAS et al. (1990) have studied the activation of slag by sodium silicate solution with Ms of 1.21, in combination with 2% lime and 1% Na_2SO_4, which produced comparable strength to Portland cement mortar.

XINCHENG et al. (1992) have reported one-day strength as high as 68.1 MPa for slag activated by sodium silicate solution with Ms of 0.77.

QING-HUA and SARKAR (1994) have reported high one-day strength of slag pastes that contained a combination of liquid sodium silicate (5% Na_2O dosage) with Ms of 1.5 in combination with 1.7% to 5.0% lime. The workability was found to decrease with increasing dosage of activator and the optimum lime dosage was found to be 2%. Use of lime successfully retarded the setting time.

WANG et al. (1994) have achieved high one-day strength up to 37.9 MPa with the use of liquid sodium silicates. The best alkali dosages were within the range 3.0 to 5.5% Na_2O by weight of slag and optimum range of Ms was 0.9 to 1.3 for neutral slag and 1.0 to 1.5 for basic slag; however, time of the initial set was less than 20 minutes. This was considered too short for most normal civil engineering applications.

BAKHAREV et al. (1999) have studied the alkali activation of Australian slag using sodium silicate, sodium hydroxide, sodium carbonate, sodium phosphate, and a combination of these. The compressive strength obtained for sodium silicate-activated slag cements was in the range of 20 to 40 MPa, and depends on the modulus of the solution and concentration of alkalis, as shown in Figures 2.5 and 2.6. At a high modulus, early strength decreased and the setting time was significantly shortened; heat treatment (at 60°C) also had a significant accelerating effect on strength development of slag pastes. OPC/slag mixtures activated by alkalis showed lower

strength than the slag alone activated by an alkali solution. A mixture of sodium silicate solution of Ms of 0.75 and 4% Na was recommended for use in AAS concrete based on study of workability and compressive strength. It was noted that the replacement of 30% of slag by fly ash has reduced compressive strength.

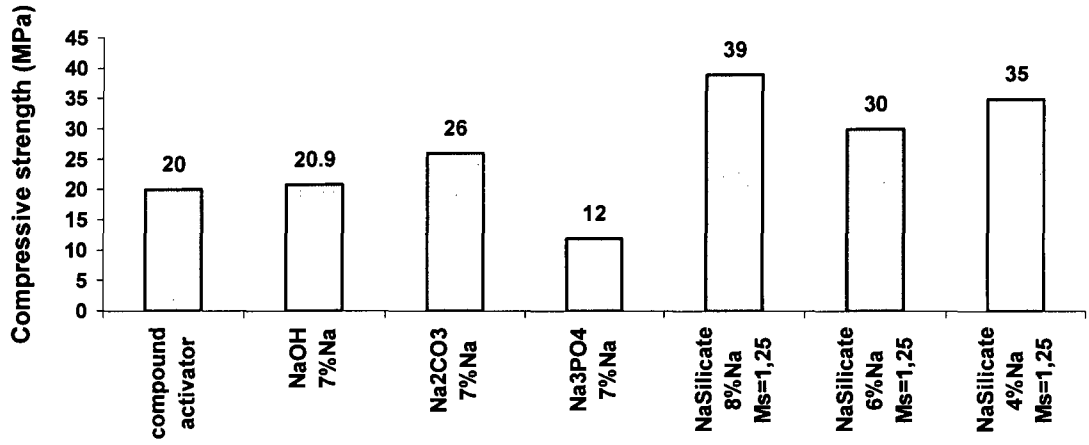

Figure 2.5 The 28-day compressive strength of alkali-activated slag pastes [BAKHAREV et al., 1999]

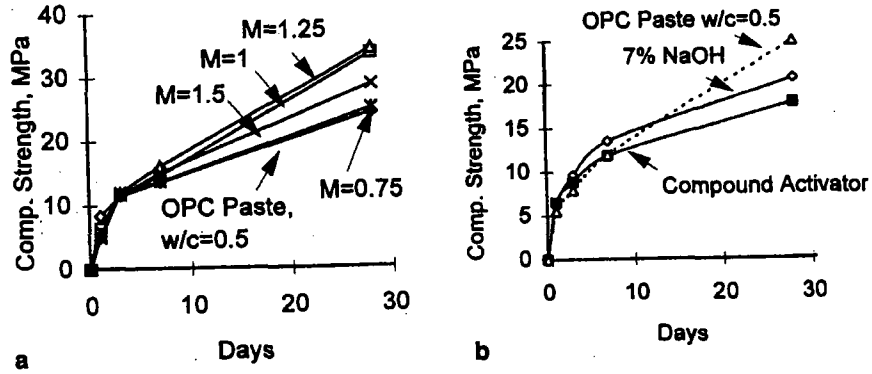

Figure 2.6 Compressive strength of pastes activated with (a) Na silicate with 4% of Na in the mixture and (b) sodium hydroxide and compound activator [BAKHAREV et al., 1999]

COLLINS and SANJAYAN (2001) have used powdered sodium silicate with Ms of 1.0 and Na dosage of 4% (% by weight of slag) plus 1% lime, which yielded equivalent one-day strength to OPC and demonstrated better workability than OPC at water-to-cementitious ratio of 0.5. One-day strength and workability decrease with increasing Ms. They have also reported that the addition of lignosulphonate water-reducing retarder brought the workability up to the OPC control and the increasing addition of naphthalene sulphonate-based superplasticizer moderately improved workability, however, the paste is not workable as OPC

with W/B of 0.5. A mixture of lignosulphonate water-reducing retarder plus naphthalene sulphonate-based superplasticizer showed a significant improvement in workability, although still not as good as OPC with W/B of 0.5.

SUGAMA (2007) has evaluated the usefulness of sodium-silicate-activated slag (SSAS) cement for completing geothermal wells containing highly concentrated H_2SO_4 and some CO_2. Using a 20wt% sodium silicate solution (SiO_2/Na_2O mol ratio of 3.22) as the alkali activator, the following observation were made for the SSAS cements autoclaved at two temperatures:

• At 200°C, an outstanding compressive strength of more than 80 MPa, and a minimum water permeability of less than $3{\cdot}0 \times 10^{-5}$ Darcy were displayed. The combination of C-S-H and tobermorite phases was responsible for strengthening and densifying the autoclaved cement.

• At 300°C, an excessive growth of well-formed tobermorite and xonotlite crystals generated an undesirable porous microstructure, causing the retrogression of strength and enhancing water permeability. Although all the phases formed in the autoclaved cements were vulnerable to reactions with H_2SO_4, so depositing bassanite scales as corrosion product over the cement's surfaces, the C-S-H phase played an important role in retarding the rate of acid erosion. Thus, after the uptake of Ca by the H_2SO_4, Ca-destitute C-S-H preferentially reacted with the Mg from the slag to form the lizardite phase that not only retarded the rate of acid erosion, but also retained the integrity of the cementitious structure. Therefore, SSAS cement has good potential as acid-resistant geothermal well cement at temperatures up to 200°C.

It is important to mention that the setting time of this cement at room temperature depended primarily on the SiO_2/Na_2O molar ratio in the sodium silicate activator; actually, using 3.22 and 2.50 ratios contributed to long setting time of more than 100min. In contrast, the slurry made with the ratio of 2.5, it set rapidly in less than 25 min. However, when the ratio of 2.5 was used and 50wt% of slag was replaced by fly ash, the setting time was changed from 617 to 1767 min.

BAKHAREV (2005) has reported in his study that the influence of elevated temperature curing on phase composition, microstructure, and strength development in geopolymeric materials prepared using Class F fly ash, sodium silicate and sodium hydroxide solutions as activators. Fly ash was mixed with sodium hydroxide and sodium silicate solutions, providing up to 10% Na in the mixtures. Water-to-binder ratio of 0.3 and curing temperatures of 75 and 90°C for 24 hours were applied. It was concluded that long obtained at room temperature is beneficial for strength development of geopolymeric materials. For materials utilizing fly ash activated by sodium silicate, 6-hour heat curing is more beneficial for strength development than 24-hour heat treatment. Fly ash mixtures activated by sodium hydroxide had more stable strength properties than the same mixtures activated by sodium silicate. The composition of aluminosilicate gel depended on treatment history.

WANG (2000) has investigated the hydration process and development of the microstructure of alkali-activated slag (4NNaOH and liquid/binder ratio of 0.25), and concluded that dissolution-precipitation is the dominant mechanism for early reactions. The hydration products formed in AAS have been determined. Poorly crystalline C-S-H(I) gel of low Ca/Si ratio, hydrotalcite ($Mg_6Al_2CO_3(OH)_{16}.4H_2O$), AFm phases, and CH are the major hydration products for all the AAS pastes. Hydrotalcite-type phase with Mg/Al ratio of about 2 is identified on a submicrometer scale; such that it cannot be observed by the scanning electron microscope (SEM). CH may be formed at early ages if the Ca/Si ratio of slag is relatively high. Afm-type phases are formed at the expense of CH. This work was also confirmed by similar work done by [LOTHENBACH AND GRUSKOVNJAK, 2007].

PAN et al. (2002) have studied and developed a new kind of alkali-slag-red mud cementitious material (ASRC), with both high early and ultimate strength and excellent resistance against chemical attacks, by the application of composite solid activator into slag-red mud mixture system. The alkali activator is composed by solid water glass with a modulus of 1.2 and sodium aluminate clinker. The hydrated specimens were cured either at ambient temperature or in steam at 80°C (steam curing). The hydration products of ASRC cement are mostly C-S-H gel with a very low Ca/Si ratio of 0.8-1.2.

BAKHAREV et al. (2002) have investigated the durability of alkali-activated slag (AAS) concrete in sulphate environment. AAS concrete was prepared using sodium silicate glass (Ms of 2) and sodium hydroxide solution (60% w/v) as activators. Liquid sodium silicate and sodium hydroxide were blended providing the modulus in solution (Ms) equal to 0.75, and 5.4% Na_2O in mixture with slag. The AAS concrete had a nominal strength of 40 MPa at 28 days (w/b ratio of 0.5). Two tests were used to determine resistance of AAS concrete to sulphate attack. These tests involved immersion in 5% magnesium sulphate and 5% sodium sulphate solution. The main parameters studied were evolution of compressive strength, products of degradation, and microstructural changes. In the case of sodium sulphate solution, the compressive strength of AAS concrete decreased by up to 17%, while in the case of magnesium sulphate solution, the compressive strength decrease was more substantial, up to 37%.

SHI and LI (1989) have studied the properties of alkali-phosphorus slag cement and how they were influenced by the modulus of water glass, soluble phosphates, water to binder ratio and the fineness of the slag. When water glass was used as an activator of alkali granulated phosphorus slag cement, the anions of water glass react with Ca^{2+} dissolving from the surface of phosphorus slag grains and primary calcium silicate hydrate formed at the primary stage of hydration. If the dosage of Na_2O is the same, the setting time of the cement shortens with the increase in the modulus of water glass. If the modulus is the same, the setting shortens with the increase in the dosage of Na_2O. The modulus of water glass has a large effect on the early compressive strength of cement and almost no effect after 90 days. Soluble phosphates have hardly any effect on the setting time of alkali granulated phosphorus cement.

COLLINS (1999) has concluded from his studies on the chemical activation of Australian slag that powdered sodium silicate (Na=4%, Ms=1) and 1% lime is the most suitable activator of Australian slag, based on one-day strength and workability. At W/B of 0.5, alkali-activated slag pastes (AASP), based on powdered sodium silicate activator have better dispersion than ordinary Portland cement pastes and showed minimal slump loss. However, liquid-based alkali-activated slag pastes, based on liquid NaOH and sodium silicate activators, showed considerable slump loss over two hours. A small difference in workability was mentioned

when gypsum was added to slag. The use of a small dosage of hydrated lime in AASP based on powdered sodium silicate improved the workability and one-day strength, as shown in the following Figures 2.7-2.10.

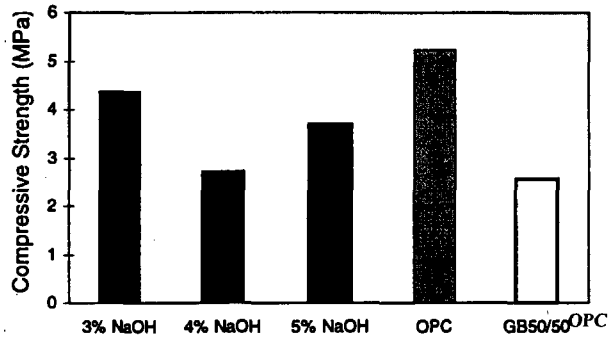

Figure 2.7 One-day compressive strength for NaOH compared with control pastes [COLLINS, 1999]

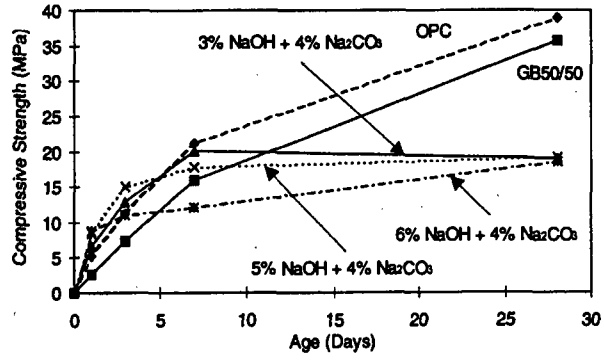

Figure 2.8 Compressive strength versus time for NaOH + Na_2CO_3 AASP with w/b = 0.5 [COLLINS, 1999]

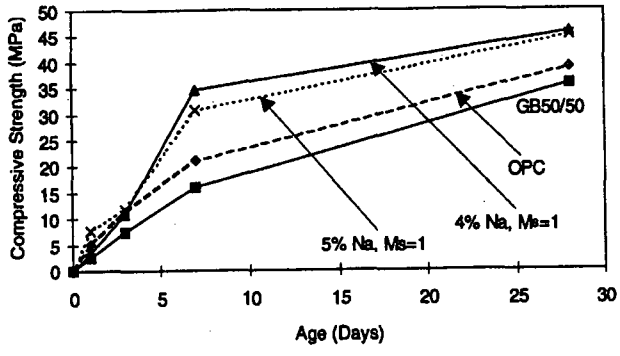

Figure 2.9 Compressive strength versus time for sodium silicate AASP with w/b = 0.5 [COLLINS, 1999]

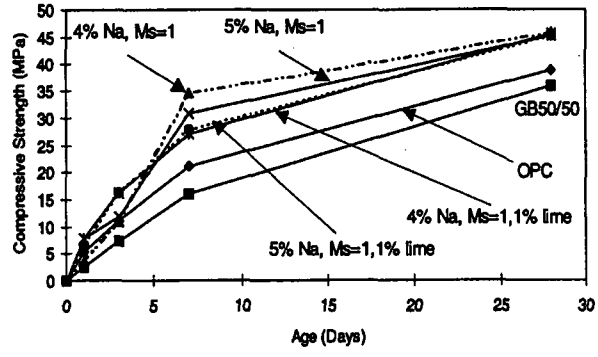

Figure 2.10 Compressive strength versus time for sodium silicate AASP with w/b = 0.5; effects of hydrated lime additions [COLLINS, 1999]

In summary, the review of literature and results from experimentation show that alkaline activators have selectivity; that is, different activators have variable activation effects on slags from different origins. Analysis of hydration chemistry indicates that selectivity results from the variation of hydration products and microstructure from different combinations of slag and activator. Selectivity of activators suggests that strength of a blast-furnace slag with NaOH solution (ASTM C 1073) is better used as an internal quality control index rather than a quality evaluation index. To improve the sensitivity of the quality control test, the alkali may be selected based on activator-optimization testing rather than specifying an alkali [SHI AND DAY, 1996a].

2.7.3 Alkali-activation of fly ash

Fly ash is widely produced industrial waste in many places in the world. While fly ash is used to form blended cements; only about 20% is currently used for this purpose [MEHTA, 1989]. Most fly ashes from combustion of coal are made up of aluminosilicate and silicate glass plus small amounts of crystalline materials, including mullite, quartz, hematite, and magnetite. The glasses in these ashes are pozzolanic and consume calcium hydroxide upon hydration [MEHTA, 1989]. The research on alkali activation of fly ash is relatively new. The intrinsic reactivity of a fly ash depends upon various factors, primarily its chemical and mineralogical composition and fineness [DIAMOND, 1986].

SHI and DAY (1995) have performed experiments to determine the effect of various chemical activators on strength of lime fly-ash pastes manufactured with two types of fly ash — a low and a high calcium subbituminous ash. Blends of 80% fly ash and 20% hydrated lime were used. Pastes were continuously moist-cured at 50°C. The result indicated that the addition of small amounts of Na_2SO_4 and $CaCl_2$ can increase the pozzolanic reactivity of both types of fly ash; this resulted in a significant improvement in strength. Na_2SO_4 has its predominant influence at early ages; its effect at later ages varies with the nature of the fly ash used. In general, early-age strength increases with the amount of Na_2SO_4 dosage. The extent of strength improvement at later ages depends upon the dosage and type of fly ash used. The addition of calcium chloride has a variable influence on strength at early and intermediate ages. However, strengths at 90 days and 180 days are significantly improved.

FRAAY et al. (1989) have examined the dissolution of class F-fly ash particles in a NaOH solution with a lime buffer at 7 days using transmission electron microscopy (TEM). At 28 days, there is evidence of surface precipitation of CH and needle-like structure on fly ash grains. Only glass particles appear to react while mullite, quartz, and iron containing particles act only as nucleation sites. They have also shown that the reaction of fly ash in cement-bsed pastes is at first controlled by the rate of CH precipitation on the surface of the fly ash and that this rate is decreased by the precipitation of C-S-H from clinker phases on the surface of the ash. The precipitation of CH is controlled by the pH of the system and increases as the extent

of the hydration reaction increases, which causes release of OH- ions into the pore water forming C-S-H. The reaction rate between fly ash and CH is a function of the of fly ash dissolution rate.

MA et al. (1995) have shown the formation of hydrate products around fly ash grains in the system 90% fly ash: 10% CH after 24 hours at 100°C. There was no formation of product at 25 °C for the same period. The authors have suggested that this difference in the hydration rate is due to the increased dissociation of glass structure at high temperature.

WILLIAMS et al. (2002) have investigated different systems of alkali-activated fly ash–portlandite (CH) paste mixtures, which were analyzed using thermogravimetric analysis (TGA) and synchrotron X-ray diffraction (XRD) to determine the effect of varying the fly ash/CH ratio on the rate of reaction. In these studies, several different weight ratios of constituents and temperatures ranging from 25 to 60°C were investigated. NaOH solution was added. The water/solids ratio was kept constant at 0.8. This concentration of NaOH was chosen to give an initial pH above 13.2 because it has been suggested that the rate of reaction of ash is very slow below this value, as indicated by the authors. They have found out that the formation of a C-S-H type reaction product with a Ca/Si ratio is somewhat lower than that of hydrated neat Portland cement. Similar work was done on fly ash and CH by other researchers [LUXAN et al., 1989; MA AND BROWN, 1997; BIERNACKI et al., 2001]

FERNÁNDEZ-JIMENEZ et al. (2005) have shown a descriptive mechanism for the activation of class F fly ash and classified the activation process into different steps i.e., dissolution and polymerization. In the first step of the reaction (nucleation), the vitreous aluminosilicate component of the fly ash dissolves in the alkaline solution, favouring the formation of a certain amount of aluminosilicate gel. During nucleation, gel composition is significantly affected by thermodynamic and kinetic parameters. In the second step of the reaction, gel polymerizes into zeolitic structure. In this study, fly ash was mixed with an 8 M solution of NaOH, (solution/ash = 0.35). The resulting paste was poured into small plastic moulds and oven-cured at 85°C for 5 h, 24 h and 60 days. As well, FERNÁNDEZ-JIMENEZ and PALOMO [2005] have studied the effect of activator on the composition and

microstructure of alkali-activated fly ash binder. They used three types of inorganic activators such as NaOH, Na_2CO_3, and water glass solutions. Furthermore, this work was supported by another research on quantitative determination of phases in the alkali activation of fly ashes [FERNÁNDEZ-JIMENEZ et al., 2006].

PALOMO et al. (2007) have studied blended cements containing 30% Portland cement clinker and 70% fly ash. The powdery material was mixed with deionized water for "normal" hydration, and with two different alkaline solutions for "normal" alkaline activation. The mechanical strength developed by this type of cement differed significantly depending on the hydrating solution used. XRD, FTIR and ^{29}Si MAS-NMR characterization studies were conducted to obtain information on the complex structural nature of the hardened matrices, which in all cases consisted of a mixture of amorphous gels (C-S-H + N-A-S-H gel). PALOMO, CRIADO, and FERNÁNDEZ-JIMENEZ have covered the area of fly ash activation in an intensive way and they form excellent research group [CRIADO et al., 2007; CRIADO et al., 2005].

2.7.4 Alkali-activation of fly ash/slag combination

The preparation of ecological cementing material with slag and fly ash has drawn worldwide attention and much progress has been made in recent years, as previously shown in this part of the study. However, there is no much work done on combined use of the both; existing bibliography about the joint activation of fly ashes and slags is limited. From the knowledge of both materials, it is known that the disadvantages of one activation process can be balanced by the other.

SHI AND DAY (1999) have studied the effect of two types of fly ash and the addition of lime on the strength development and hydration of sodium hydroxide- and sodium silicate (6% Na_2O by mass)-activated slag/fly ash blends, which consisted of 50% fly ash and 50% slag by mass. Performance was compared to that of 100% slag cements. When NaOH was used as an activator, the slag replacement with ASTM Type F fly ash did not show significant effect on either strength development or hydration; Type C fly ash did not affect strength development, but chemically affected the hydration and strength development when Na_2SiO_3 was used as an

activator. The addition of a small amount of hydrated lime significantly increased early-age strength, but slightly decreased later-age strength of the activated slag/fly ash blends. Measurement of the heat evolution during hydration indicated that the addition of the hydrated lime had a slight effect on hydration during the pre-induction period, but accelerated hydration thereafter.

PUERTAS et al. (2000) have studied the activation of fly ash/slag pastes with NaOH solutions. The parameters of the process studied are: activator concentration (NaOH 2 and 10 M), curing temperature (25°C and 65°C), and fly ash/slag ratios (100/0, 70/30, 50/50, 30/70, and 0/100). The equations of the models describing the mechanical behaviour of these pastes have been established as a function of the factors and levels considered. The ratio of fly ash/slag and the activator concentration always result to be significant factors. The influence of curing temperature in the development of pastes strength is lower than the contribution due to other factors. At 28 days of reaction, the mixture 50% fly ash/50% slag activated with 10 M NaOH and cured at 25°C, developed compressive mechanical strengths of about 50 MPa. The nature of the reaction products in these pastes has been studied by insoluble residue in HCl acid, XRD, FTIR and MAS NMR. It has been verified that slag reacts almost completely. It has also been determined that the fly ash is partially dissolved and participates in the reactive process, even in pastes activated at ambient temperature. The main reaction product in these pastes is a hydrated calcium silicate, like CSH gel, with high amounts of tetracoordinated Al in its structure, as well as Na ions in the interlayer spaces. No hydrated alkaline alumino-silicates with three-dimensional structure characteristics of the alkaline activation of fly ashes were formed.

LI and LIU (2007) have used slag as an additive for fly ash-based geopolymers in their study. It was found that the incorporation of slag could significantly increase the compressive strength of the geopolymer. The compressive strength of geopolymer with 4.0% slag reached 50 and 70 MPa when cured for 14 days at 30 and 70°C, respectively. XRD and Fourier transform infrared (FTIR) results showed that the addition of slag could generate more amorphous products and accelerate the reaction rate of raw materials. From X-ray photoelectron spectroscopy (XPS) results, the decrease of binding energy and a broadening of

peaks were observed for Si 2p, Al 2p, and O 1s elements due to the Ca^{2+} provided by slag. The decrease in binding energy was more favorable to zeolite formation. The results of MIP suggested that 4% slag addition significantly influenced pore structure of geopolymer. A refinement of pore size was exhibited after 4% slag addition, especially for specimens being cured at 70°C. For these reasons, the compressive strength of geopolymer made with 4% slag addition was greatly improved.

ZHAO et al. (2007) have presented the results of the preparation of an ecological cementing material from granulated blast-furnace slag (GBFS) and Class C fly ash (CCFA). The desulphurization gypsum, calcined at 600-800°C for 0.5-1.5 h, works as the main ingredient of the activator in the cementing material. The optimized formulation of the cementing material was obtained with the aid of factorial design method: slag, 70%; CCFA, 18%; activator, 12%. The "partial super-fine grinding process" was adopted to improve the performance, in such a way that 85% of the mixture is ground to Blaine fineness of 3500 cm^2/g, 15% further ground to around 5000 cm^2/g. The compressive strength of 28 days of the cement mortar is up to 49 MPa and flexural strength 8.4 MPa. The hydration products, investigated by SEM and X-ray diffraction, are mainly ettringite and C-S-H gel. The fineness has significant influence on the strength of cementing material, but the particle size distribution is more important. Partial super-fine grinding process provides an efficient method to improve the particle size distribution and thus the mechanical strength of the cementing material. The mass ratio of CCFA/GBFS has remarkable influence on the mechanical strength of the cementing material. Proper amount of CCFA can reduce cost without negative contribution to flexural strength.

Finally, and according to ROY (1999) and SHI et al. (2006), the bibliographic history of alkali-activated and alkaline cement are summarized as shown in Table 2.6.

TABLE 2. 6 THE BIBLIOGRAPHIC HISTORY OF ALKALI-ACTIVATED BINDERS

Author(s)	Year	Significance
Kuhl	1930	Investigated setting behavior of slag in presence of caustic ash
Chassevent	1937	Measured reactivity of slags using caustic potash and soda solution
Feret	1939	Slag used for cement
Purdon	1940	Investigated clinker-free cements consisting of slag and alkali
Glukhovsky	1957	Created soil cement that composed of hydrous and anhydrous aluminosilicates and alkalis
Glukhovsky	1959	Theoritical basis and development of alkaline cements
Glukhovsky	1965	First called "alkaline cement" because natural substances used as components
Davidovits	1979	"Geopolymer term"-emphasizes greater polymerization
Malinowski	1979	Ancient aqueducts characterized
Davidovits	1982	Mixed alkalis with a burnt mixture of kaolinite, limestone and dolomite and used several trade marks as Geopolymer, Pyrament
Forss	1983	F-cement (slag-alkali-superplasticizer)
Langton and Roy	1984	Ancient building materials characterized
Davidovits and Sawyer	1985	Patent of ''Pyrament'' cement
Krivenko	1986	D.Sc. thesis, R2O–RO–R2O3-SiO2–H2O
Malolepsy and Petri	1986	Activation of synthetic melilite slags
Malek. et al.	1986	Slag cement-low level radioactive wastes forms
Davidovits	1987	Ancient and modern concretes compared
Deja and Malolepsy	1989	Resistance to chlorides shown
Kaushal et al.	1989	Adiabatic cured nuclear wastes forms from alkaline mixtures
Roy and Langton	1989	Ancient concretes analogs
Majundar et al.	1989	C12A7 – slag activation
Talling and Brandstetr	1989	Alkali-activated slag
Wu et al	1990	Activation of slag cement
Roy et al.	1991	Rapid setting alkali
Roy and Silsbee	1992	Alkali-activated cements: an overview
Palomo and Glasser	1992	CBC with metakaolin
Roy and Malek	1993	Slag cement
Glukhovsky	1994	Ancient, modern, and future concretes
Krivenko	1994	Alkaline cements
Wang and Scrivener	1995	Slag and alkali-activated microstructure

2.8 Conclusions

- Clinkerless alkali-activated slag cements characterized by their high strength, dense structure, low energy cost, and simple production technology compared with Portland cement.
- Alkali activation of slag needs low concentration of alkali activator (pH lower than 12)
- Slags exhibit selectivity towards the anion or anion groups of activators that have the same content of Na.
- Sodium silicate provides the best activation with compressive strength of pastes and mortars exceeding that of OPC pastes of the same w/b ratio.
- A mixture of powdered sodium silicate and a small dosage of lime improve the workability and one-day strength of alkali-activated slag pastes.
- The hydration products of alkali-activated slag cement are mostly C-S-H gel with a very low Ca/Si ratio.
- Heat treatment had a significant accelerating effect on strength development of slag pastes.
- The reaction of fly ash and lime is very weak at room temperature, while the reaction of slag and lime is much more rapid than that of fly ash; therefore, at room temperature, slag can react with more lime and alkali can speed up this reaction.
- The alkali-slag cement, as a low-cost product providing the possibility of using by-products and wastes in alkali-activated slag mixtures, can be seen as a solution to today's ecological problems.
- Alkali activation of class F fly ash needs more concentrated alkali activator (pH higher than 13) and higher temperature of activation due to its crystalline structure.
- Bibliography existing about the joint activation of fly ashes and slags is limited.
- The incorporation of slag with fly ash during alkali activation could significantly increase the compressive strength of the geopolymer.
- The mass ratio of fly ash/slag has remarkable influence on the mechanical strength of the activated cementing material.

2.9 Use of pozzolans as supplementary cementitious materials (SCMs)

2.9.1 Pozzolanic and cementitious reactions of some active additives in blended cement pastes

MARSH and DAY (1988) have reported results of thermogravimetric tests on hardened cement pastes containing fly ash. Ashes derived from subbituminous and lignite coals were used at replacement levels of 30% and 50% by weight. Thermal analysis was performed on samples which were water cured for various ages from 3 days to one year. An analytical technique was used to split the non-evaporable water content of cement pastes into two components: water held by calcium hydroxide, and water held in other reaction products. The technique is used to identify and monitor the progress of the different types of fly ash. There are distinct differences in the manner in which various ash/cement pastes hydrate. The subbituminous ash relies more upon the "pozzolanic reaction" between calcium silicate and calcium hydroxide to provide the strength-giving hydration product. Conversely, the lignite ash produces a substantial amount of hydrate by direct reaction between compounds of the ash and water. At early and intermediate ages, the hydrate produced from the reaction of fly ash may combine substantially more water per unit weight than the hydrates normally produced through the reaction of cement.

MARSH et al. (1986) have investigated hardened cement paste specimens, with and without partial replacement of the cement by fly ash for various ages up to one year at temperatures between 20 and 80°C. The pozzolanic reaction of fly ash in cement, as measured by reduction in calcium hydroxide content and contribution to compressive strength, is accelerated by an increase in curing temperature. The acceleration of pozzolanic reaction is greater than the acceleration of Portland cement hydration for a given curing temperature. The maximum strength of cement paste which contains 30% by weight of cement replaced by fly ash is greater than that of plain cement paste for all curing temperatures. Consumption of calcium hydroxide with no corresponding gain in strength, or with a reduction in strengths, was observed for ash-pastes cured at 50°C and above. Changes in mercury porosity, on the other hand, correlate well with changes in strength during the early strength-gain periods and also during the later strength-decreasing period. Measurement of calcium hydroxide (CH) content

is of special interest in Portland cement/fly ash system as it provides an indication of the progress of the pozzolanic reaction.

OHSAWA et al. (1985) have reported a selective dissolution method which, in principle, only dissolves pozzolan-cement hydration products, hydrated cement products, and cement components while leaving the remaining unreacted pozzolan undissolved. Where this test was used for the quantitative determination of fly ash in hydrated fly ash-$CaSO_4.2H_2O$-$Ca(OH)_2$ system, various kinds of selective dissolution were evaluated using pastes made from a single representative fly ash. Selective dissolution using picric acid, (trinitrophenol)-methanol solution was found to be adequate. Selective dissolution using picric acid-methanol-water was also used. Reproducibility of the determination by both methods was found to be satisfactory.

LI et al. (1985) have used the same method as OHSAWA for the qualitative determination of unhydrated fly ash and silica fume, respectively. Their experimental results have shown that a selective dissolution method using a picric acid (trinitrophenol)-methanol-water solution is suitable to remove reacted cementitious products, and leave a residue of unhydrated pozzolans, such as fly ash and silica fume when mixed with cement. This enables their quantitative determination at various ages of hydration. Silica fume was found to have a much earlier stage reactivity than low-calcium fly ash, although only 78% of silica fume in a 10% silica fume:90% cement mixture reacted in 90 days at 38°C.

JAMES and RAO (1986) have studied the chemical interaction of rice husk ash (about 96 % SiO_2) with lime and water. The setting process for lime-excess and lime-deficient mixtures was investigated. The product of the reaction has been shown to be a calcium silicate hydrate, C-S-H (I) by a combination of thermal analysis, XRD, and electron microscopy. Formation of C-S-H (I) accounts for the strength of lime-rice husk ash cement.

MOUKWA (1990) has reported that cobalt furnace slag yields medium strength cements by addition of lime or Portland cement clinker in a small amount. Hydration can be accelerated by addition of sodium sulphate. Cements of sufficient quality for general use were obtained

with this material. The compressive and the tensile strength measured with cobalt slag concrete may justify its use as replacement for Portland cement.

WENG et al. (1997) have studied the pozzolanic reaction between Portland cement, silica fume, and fly ash mixtures, where results indicated that silica fume additions reduce calcium hydroxide content in the paste as early as 12 hours. The reduction was in linear proportion with the silica fume dosage. Most of the silica fume reacted before 3 days, and a small portion remained for later slow reaction. The higher is the w/b ratio, the greater the silica fume reaction at early ages. Fly ash was found to depress calcium hydroxide formation at 12 hours. The pozzolanic reaction can begin at 3 days, but significant reaction did not occur until after 7 days. The reactivity of silica fume was delayed by the presence of fly ash and its influence began at 1 day rather than 12 hours. A significant increase in hydrate water content was found between 3 and 7 days. At earlier ages, the hydrate water content was lower.

LI et al. (2002) have concluded that the reaction of fly ash and lime is very weak at room temperature. The additions of sulphate and alkali improve the activation of the fly ash-lime system. The effect of alkali is more outstanding than that of sulphate. The reaction of slag and lime is much more rapid than that of fly ash. Therefore, at room temperature, slag can react with more lime while alkali can speed up this reaction. From the analysis of the balance system of hydrates, slag is an ideal substance in producing cementitious materials with low calcium, requiring only some $Ca(OH)_2$ and a little activator to its composition. XRD, SEM, TGA, and DSC-TG results show this conclusion. The difference between slag and fly ash is that aluminate hydrates of slag sample obviously increase at the same hydration time. It is because the alumina oxygen ions of slag more easily dissolve and react. Under high alkalinity, the glass structure of fly ash was easily broken and its activation and hydration properties were improved.

2.9.2 Use of pozzolans as durability-improving materials

Durable concrete will retain its original form, quality, and serviceability when exposed to a given environment [ACI Committee 201, 1992]. In many environmental conditions, concrete is subjected only to mild attack. In others, attack can be so severe that the concrete structure

requires repairs, and often replacement, before the end of the design service life has been reached. Forms of attack may include any of the following:

a) Abrasion;
b) Alkali-silica reaction;
c) Alkali-carbonate reaction;
d) Carbonation;
e) Freezing and thawing and de-icer scaling;
f) Reinforcing-steel corrosion; and
g) Sulphate attack

Resistance to various forms of these attacks can be improved by reducing concrete permeability, thus reducing the intrusion of water or aggressive chemicals and their capillary transmission within the cement-paste matrix. Using pozzolans, ground granulated blast-furnace slag, fly ash, and silica fume can reduce permeability while also imparting other desirable properties to the concrete [KECK, 2001].

Research concerning the use of mineral admixtures to enhance the properties of concrete has been ongoing for several decades. Recently, the use of mineral admixtures has dramatically increased, due to an increase in environmental awareness. Higher early strength can be found in some modern cements due to more $Ca(OH)_2$ formation, but this may adversely affect the durability and cost of concrete [CHAN AND WU 2000]. Since many mineral admixtures are by-products of other necessary reactions, these waste by-products can be used to reduce the amount of cement required, thus, in some cases, reducing the cost and the CO_2 signature of the concrete.

Pozzolans are not binders as such, but in the presence of water they can react with lime liberated by Portland cement hydration to become hydraulic cementitious systems. Cementitious materials, however, need only a small amount of chemical "activator", such as Portland cement, to become hydraulic cements. These limits generally range from as low as 2% for silica fume, to some 60% in case of granulated blast-furnace slag, which is one of the most widely used supplementary cementitious materials. The estimated worldwide availability

of these mineral cement additives, in millions of tonnes per year, is as follows: fly ash 370, granulated blast-furnace slag 35, silica fume 2, and rice husk ash 20. By comparison, Portland cement production is almost 1.5 billion tonnes per year [MALHOTRA, 2000].

Blast-furnace slag, with high glassy phase content, possesses potential cementitious ability and forms C-S-H gel after reacting with calcium hydroxide [PRICE, 1975]. It can therefore, be used as a partial substitute for cement. Similarly, fly ash is a pozzolanic material and also often serves as cement replacement. Fly ash is suitable for massive concrete structures because its addition as a partial substitute for cement will reduce thermal hydration and bleeding, thereby, improving the overall durability of the concrete [KECK, 2001].

Silica fume or microsilica, when incorporated into concrete, increases its early strength [RAO, 2001]. The hydration process is actually quite complicated, requiring the production and dissolution of various compounds at different stages. During these stages, several reactions occur. The combination of these reactions determines the progression of strength development. One belief is that strength can be derived from three mechanisms. First, as silica fume is added, pore size is refined and the resulting matrix is denser. Silica fume causes large pores to become smaller, while the production of certain compounds increases the density of the matrix, thus increasing the strength of the resulting bonds. Secondly, silica fume reduces $Ca(OH)_2$(CH) content. Finally, silica fume concrete undergoes a cement paste-aggregate refinement process. This process describes the enhancement of the transition zones between the cement paste and the aggregate [RAO 2001; TOUTANJI AND BAYASI 1999; MOHD ZAIN AND RADIN, 2000].

The addition of silica fume increases the early strength of concrete. C-S-H is considered the main carrier of strength in hardened cement. It is formed through the transformation of weak $Ca(OH)_2$ to strong C-S-H gel through the pozzolanic reaction [RAO, 2001; TOUTANJI, BAYASI, 1999; MOHD ZAIN, RADIN, 2000]. Although many believe that the above reaction produces C-S-H gel, it does not mean that strength can be directly obtained through measurement of this parameter. In fact, concrete strength and durability can at best be determined indirectly by knowing C-S-H, CH, H content, and porosity [PAPADAKIS, 1999].

HWANG and SHEN (1988) have reported the effect of varying blast-furnace slag content, fly ash content, and water/solid ratio on the behaviour of cement paste and concluded that increasing the slag content resulted in longer setting times. Furthermore, increasing the water/solid ratio also exhibited a similar tendency. The effect of fly ash on the setting behaviour of cement paste paralleled that of slag.

FU et al. (2002) have studied the influence of clinker, activator, and fly ash contents on the properties of blended cement with high fly-ash content. Experimental data from XRD and pore size distribution indicated that the main hydration product of the fly ash blended cement was C-S-H gel, ettringite, and a small amount of $Ca(OH)_2$. The amount of chemically combined water increased with the duration of curing age, while $Ca(OH)_2$ content was reduced after 7 days. The strength of the mortars made with the blended cements decreased with increased fly ash content in the blended cement, especially at early ages. This phenomenon was overcome by introducing compound activators (CA) (Na_2CO_3 and molasses) to the blended cement, with strengths significantly improved at 28 and 90 days when 1.15% CA was added to the blended cement; the activators destroyed the glass pearl surface structure of fly ash to dissolve the silicate and aluminate ions and accelerate the hydration of fly ash grain.

LAFAVE et al. (2002) have reported that ground granulated blast-furnace slag improved the long-term corrosion resistance of concrete by filling and reducing the concrete pore structure, thereby decreasing permeability. As slag content increased, concrete chloride permeability typically decreased and permeability of slag concrete was less affected by increase in w/b ratio than ordinary Portland concrete. Carbonation can progress faster in slag concrete and slag content had to be limited to about 35% cement replacement if early strength development similar to control concrete was desired.

Strength development in ternary blended cements based on Portland cement, ground granulated blast-furnace slag, and fly ash was studied in several countries in the 50s and 60s. Literature concerning fly ash made no mention of an optimum quantity for use in concrete

mixtures; however, recommendations have been made suggesting the use of 40% or less. Furthermore, if early strength is not an important factor, fly ash as high as 60% can be used [NAIK AND RAMME, 1989].

HUSSAIN and RASHEEDUZZAFAR (1994) have indicated that the use of fly ash could increase the resistance of concrete to chloride-induced corrosion of steel reinforcement, because fly ash concrete was less permeable to chloride ingress than concrete without fly ash. It was also able to bind some of the chlorides, thereby reducing the amount of free chloride available to initiate steel corrosion, but without reducing concrete pH below 12.5. Fly ash dosage of less than 15% by mass of cement was not effective in preventing reinforcing steel corrosion, and concrete with a fly ash dosage greater than 20% addition by mass of cement could be susceptible to carbonation at cracks [BERKE et al., 1991].

Slag has low strength at early ages when used in large quantities in concrete. This is due to the slow initial hydration of slag. Unlike fly ash, slag's reactivity is dependent more on temperature [MIURA AND IWAKI, 2000; SIVASUNDARAM AND MALHOTRA, 1992]. Like fly ash, two processes govern slag's reaction rate during the initial period of hydration. The first, nucleation and the growth rate of hydration phases, is the ability to provide sites for the bonding of $Ca(OH)_2$ compounds. These compounds are then transformed into C-S-H gel. The second is the phase boundary interactions or the interactions that occur between the old compounds and the newly formed compounds. It has also been found that the initial rate of hydration is dependent on the initial lime content. This can be observed in the sharp decreases in free lime contents that occur in slag mixtures during the first day [MOSTAFA, et al., 2001].

When a proper ratio between fly ash and slag is used, the strength of the combination exceeds that of slag cement [SHI AND DAY, 1999].

RODRIGUEZ-CAMACHO et al. (2002) have reported results of different Portland-pozzolan cements containing different natural pozzolans, and they were compared with ASTM Types I, II, and V cements. The susceptibility to sulphate attack was studied by measuring the expansion in mortar bars at different ages for 78 weeks. The pozzolanic

cements containing Type I and V Portland clinker and pozzolans with high pozzolanic activity have a better sulphate resistance than Type V cement, even after 52 weeks. The pozzolans containing alumina between 11.6% and 14.7% and high pozzolanic activity have the best sulphate resistance in cement than those containing at least 16% alumina. Pozzolanic cement with Type I clinker is more effective in increasing sulphate resistance.

MEMON et al. (2002) have investigated the effect of mineral and chemical admixtures, namely fly ash, ground granulated blast-furnace slag, silica fume, and superplasticizers, on the porosity, pore size distribution, and compressive strength development of high-strength concrete in seawater curing conditions exposed to tidal zones. In this study, two levels of cement replacement (30% and 70%, by weight) were used. The total cementitious content used was 420 kg/m^3. A water/binder ratio of 0.4 was used to produce concrete having target compressive strength ranging between 54 and 63 MPa at 28 days of age. At the age of 364 days, the compressive strength of the specimens produced ranged between 59 and 74 MPa. The pore-size distribution of both high-strength concrete was significantly finer and the mean volume radii at the age of 6 months were reduced about three-fold compared to OPC concrete. Results of this study indicate that both concrete mixtures (30% and 70%) exhibited better performance than the OPC concrete in seawater exposed to tidal zone. Hence, it is believed that both high-strength concretes produced would withstand severe seawater exposure without serious deterioration.

In Canada, laboratory studies on ternary blended cement mortars at constant w/b ratio were done at CANMET using ASTM class F and ASTM class C fly ashes [BERRY, 1980; FOURNIER et al., 2001]. The availability of ground granulated blast-furnace slag in Canada, as well as the availability of fly ash from existing and future power plant installations justify further investigation of ternary binder systems for the optimization of compressive strength. Replacing large amounts of cement with mineral admixtures such as slag, fly ash, and silica fume can reduce the high cost. As a result, extensive research has been carried out, or is in the process of being performed on these admixtures in order to determine their usefulness.

2.9.3 Use of pozzolans for mitigating the alkali-silica reaction (ASR)

In 1940, STANTON showed that damage in concrete could sometimes result from reaction between the hydration ions in the pore water of concrete and certain forms of silica which are occasionally present in the aggregate. Destruction of concrete structures caused by alkali-aggregate reaction (AAR) has been found in many regions of the world.

Pozzolans such as silica fume, pulverized fly ash, and pulverized blast-furnace slag are known to reduce alkali silica reactivity (ASR) in concrete. Examination of the types and properties of reactive aggregates suggests that the aggregates that are either glassy, poorly crystallized, or those that have an imperfect or damaged silicate lattice are effective. Pozzolans likewise contain very fine particles of glassy silica. The pozzolanic activity is essentially the reaction of the cement's calcium hydroxide with the glassy silica. The reaction is relatively rapid because the silica particles are very fine and present a very large surface area per unit mass. Silica fume, fly ash, and ground granulated blast-furnace slag (slag) are widely used as concrete additives and cement replacements, both for economic reasons and to improve quality of concrete and guard against ASR. One property they share in common is that they are essentially very fine-grained silicate or silicate-aluminate glasses. Because of its fine particles, large surface area, and high silica content, silica fume is a very reactive pozzolan when used in concrete. It has the highest SiO_2 content of the three at > 90%; the average silica content of fly ash and slag is 38% (bituminous) to 48% (sub-bituminous) and 36%, respectively [MEHTA, 1983].

A. Alkali-Aggregate Reaction (AAR)

This reaction can be defined as the chemical reaction in concrete between alkali hydroxides (hydroxyl ions associated with sodium and potassium [high alkaline pore solution]) from Portland cement and other constituents, such as admixtures and pozzolans, and certain constituents of some aggregates. Under certain conditions, this reaction can result in deleterious expansion of the mortar or concrete resulting in cracking, and is divided into two main types:

Alkali-carbonate reaction is a chemical reaction in concrete between alkali hydroxides and certain carbonate rocks, particularly certain calcitic dolomite and dolomitic limestone aggregates [GRATTAN-BELLEW AND MITCHELL, 2002]. The reaction and products of the reaction may cause abnormal expansion and cracking of concrete in service.

Alkali-silica reaction is a chemical reaction in either mortar or concrete between alkali hydroxides and certain siliceous rocks or minerals, such as opaline chert, strained quartz, and certain volcanic glasses, present as constituents of some aggregates. The product of the reaction, a silica gel, can cause expansion and cracking of the concrete or mortar.

Factors that affect the rate and severity of AAR are [FOURNIER AND BÉRUBÉ, 2000]:
i) Potential reactivity of the aggregate;
ii) Alkali content of the cement;
iii) Amount of water present in the concrete;
vi) Humidity of the environment;
v) Aggregate particle size;
vi) External applied stress (or confinement)

The alkali-silica reaction (ASR) has been identified as one of the major causes of deterioration of concrete structures, and can be explained by the surface phenomena of materials and crystalline structure of quartz (SiO_2). The structure of crystalline quartz is built by repetition of a basic unit – silicon tetrahedron – in an oriented three-dimensional framework. A silicon ion, Si^{4+}, is in the centre of the tetrahedron, surrounded by four oxygen ions at the corners. The silicon tetrahedrons are joined with each other through their vertices by oxygen atoms, and each of these is linked to two silicon atoms to attain electrical neutrality. However, on the surface of quartz, a complete tetrahedron does not evolve, and unsatisfied charges develop [LI et al., 1999]. In the presence of NaOH and KOH solution, unsatisfied charges on the silica surface are neutralized by the ions OH- and Na+, or K+. After the hydroxyl groups on the surface of the silica have been neutralized, if an excess of NaOH or KOH still exists, then the internal -Si-O-Si- can be disrupted. LI et al. (1999) pointed out that, in alkaline solutions, silica is much more easily dissolved, the hydroxyl ions being the catalyst. The

dissolved silicate ions, together with the readily ionized Na^+ or K^+ ions, form a colloidal suspension (alkali-silica gel). ASR can be simply described as [LI et al., 1999]:

$$SiO_2 + Na^+, K^+ + OH^- \rightarrow \text{amorphous alkali silicate ('gel')} \qquad (2.1)$$

Some authors [DAVIES AND OBERHOLSTER, 1988; CHATTERJI et al., 1988] have pointed out that ASR is not merely a reaction between the alkalis present in the porous solution and the reactive aggregate, but sufficient Ca^{2+} ions are also required (which are supplied by the portlandite ($Ca(OH)_2$) in the OPC pastes. The general outlines of this process [FERNANDEZ-JIMENEZ et al., 2002] are:

$$Ca(OH)_2 + SiO_2 + NaOH + H_2O \rightarrow n_1Na_2O.n_2CaO.n_3SiO_2.n_4H_2O \qquad (2.2)$$

The resulting gel has an expansive nature depending on CaO content [DAVIES AND OBERHOLSTER, 1988; CHATTERJI et al., 1988].The gel product from ASR will expand through osmotic action in the presence of pore water or moisture and become deleterious to concrete structures. This expansive pressure can sometimes reach 6-7 MPa [DIAMOND, 1989], which is enough to crack concrete structures. A deleterious expansion is commonly regarded as an expansion greater than 0.05%, since at this level small cracks are often visible on the surface of a concrete [HOBBS, 1986].

In general, it is known that adding mineral additives to concrete is an effective measure for preventing ASR. Many investigations have been carried out on the effect of silica fume, fly ash, and blast-furnace slag used as mineral additives for suppressing ASR in some countries. In 1940, STANTON was the first to explain the possibility of reducing expansion due to ASR by using pozzolanic cement containing finely ground 'Monterrey Shale' or by replacement of 25% high-alkali cement with pozzolana. Now several hundreds of papers dealing with this subject have been published and most of them discuss the effectiveness of blast-furnace slag, fly ash, and silica fume. The effectiveness of mineral admixtures in preventing alkali-aggregate reactions depends upon adequate dosage and its alkali content, these two parameters determining the increase or depletion of the alkalinity of pore fluids. Because the hydration

kinetics of these materials, and consequently their pozzolanic activity, are slow, accelerated methods can provide useful information by simulating their possible behaviour after long periods.

The effectiveness of slag in preventing expansion due to alkali-aggregate reaction (AAR) was first reported by COX et al. (1950) and since then a number of papers have been published in many countries. Various theories have been presented regarding the mechanism of slag's action in reducing alkali-aggregate reaction (AAR) expansion [BAKKER, 1981; DIAMOND, 1983; CHATTERJI, 1984; HOBBS, 1982]. A number of investigators have carried out tests on OPC/fly ash [NIXON AND GAZE, 1981; HOBBS, 1982; GAZE AND NIXON, 1983] and OPC/slag mortars [HOBBS, 1982; HOGAN, 1983] containing natural aggregate, but few tests have been carried out on concrete up to 1983 [NIXON, GAZE, 1983]. However, extensive work has been done and published related to the use of slag and fly ash in mitigating ASR expansion [LANE AND OZYILDIRIM, 1999; KERENIDIS, 2007]. Aggregate reactivity, alkali content of the concrete, chemical composition of the SCM, and exposure conditions affect the necessary level of SCM replacement for adequate protection.

Silica fume has been used in concrete for some decades now. Initially, it was used as a cement replacement material, but in recent years silica fume has been used more and more as solid additive (microfiller) in concrete. Increased strength and improved durability are the main benefits. Incorporation of superplasticizer and silica fume offers flowable concrete with low W/C ratio. In other words, silica fume affects concrete quality in many ways, and when properly proportioned, it will greatly improve the quality of both fresh and hardened concrete [GUDMUNDSSON et al., 2000].

In 1979, ASGEIRSSON and GUDMUNDSSON first documented the use of silica fume to control ASR in concrete. A review of the extensive amount of research on this topic has revealed that the efficiency of silica fume in suppressing ASR expansion is primarily dependent upon the alkali contribution of Portland cement [THOMAS, BLESZYNSKI, 2000]. Based on this review, THOMAS and BLESZYNSKI (2000) have proposed the following relationship:

$$SF = K^* Al \qquad (2.3)$$

Where SF = silica fume as percentage of cementitious material, Al = Alkali content of concrete (kg/m^3 of Na_2Oeq) contributed by the Portland cement, K = 2.5.
Canadian standard practice CSA A23-27A (2004) proposes to adopt this approach using different values of K (from 2 to 3) depending on the level of prevention required. A minimum replacement level of 7 % is imposed when silica fume is sole supplementary cementing material.

Canadian standard practice CSA A23-27A (2004) covers the use of ternary blends to counteract alkali-silica reaction. It states that when two or more SCMs are used in combination to control ASR, the minimum replacement levels for the individual SCMs may be partially reduced provided that the sum of the parts of each SCM is greater than, or equal to, one. For example, for a ternary blend with silica fume and slag, if the silica fume replacement level is reduced to a third of the recommended level, the slag replacement level must be at least two thirds of the minimum specified level.

It is a common misunderstanding that most of the silica fume used in concrete is a very fine powder. It has been shown,; however, that some of the silica fume can remain in relatively large lumps in hardened concrete [PETTERSON, 1992; SHAYAN et al., 1993, JUENGER, OSTERTAG, 2004]. These lumps are typically from 50 to 100 μm in diameter, but much larger lumps have been observed [MARUSIN, SHOTWELL, 1995]. If the bulk density of the densified silica fume is too high, it may be difficult to disperse in the concrete. Poorly dispersed silica fume larger than 50 μm could act as alkali-silica reactive aggregate, and obviously large amounts of lumps will reduce the beneficial filling role of silica fume in the cement paste matrix. The effectiveness of silica fume, measured as ASTM C 1260 expansion, was not affected by the presence of lumps up to few hundred micrometers in diameter [GUDMUNDSSON et al., 2000]. However, there are documented cases [JUENGER, OSTERTAG, 2004; MARUSIN et al., 1995] where relatively large lumps acted themselves as reactive aggregates. Therefore, if the lumps are smaller than the threshold value in terms of

size, they are pozzolanic in nature but, if the lumps are larger than the threshold they become alkali-silica reactive [GUDMUNDSSON et al., 2000].

BLACKWELL, et al. (1992) have studied concrete mixtures with a range of alkali contents and various levels of fly ash cast using two sources of greywacke aggregate. After 15 months, deleterious expansion was observed in OPC concrete (without fly ash) with alkali content in excess of 5.18 kg/m^3 Na_2O_{eq}. It is clear, from the results of this study, that in concrete specimens containing above 5 kg/m^3 Na_2O_{eq}, replacement of 25% or more of OPC with fly ash was effective in eliminating damaging reactivity at 15 months. This is the case even when the alkalis derived from the Portland cement and added salts (i.e. disregarding any alkali contribution from the fly ash) are sufficient to promote considerable expansion in concrete without fly ash.

WANG and GILLOT (1992) have studied the effectiveness of combining air-entrainment with partial silica fume replacement of cement as a means of controlling expansion caused by alkali-silica reaction (ASR). The expansion of mortar bars due to ASR was reduced by the partial replacement of cement with silica fume and was also reduced by incorporation of air-entraining agent (AEA). The combination of AEA and silica fume was far more effective in reducing expansion due to alkali-silica reaction than either AEA or silica fume used separately. The alkali-expansivity of mortar bars containing 2% opal as alkali-reactive aggregate was assessed using ASTM C 227 method, as shown in Figure 2.11.

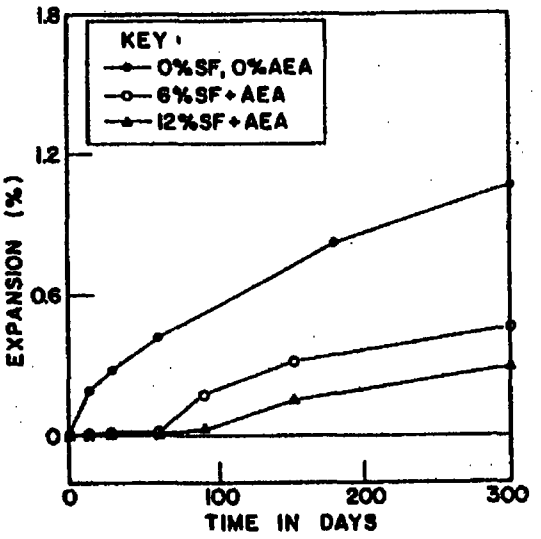

Figure 2.11 Effect of combined AEA and SF on ASR expansion of mortar bars ASTM C227 [WANG, GILLOT, 1992]

THOMAS (1996) has presented the findings from field studies of fly ash concrete structures containing reactive (alkali-silica) aggregates. The Nant-y-Moch Dam in Wales and Lower Noch Dam in Ontario were both constructed using fly ash (20% to 30% by mass of cementitious material) and greywacke-type aggregate. The study was extended to include other dams in the vicinity built with similar reactive aggregate, but without the benefit of fly ash. The fly ash structures are in excellent condition after over 25 years of service in contrast to the dams without fly ash, which exhibited various degrees of deterioration attributed to ASR. Damaging ASR was identified in the plain concrete structures at alkali contents significantly below the commonly adopted 3 kg/m^3 Na_2Oe limit. Both fly ash structures had soluble alkali contents in excess of this value. Microstructural and pore solution analysis showed that much of the alkali in the fly ash concrete was "bound" in the C-S-H and not available to the pore solution for ASR.

FENG AND TINGYU (1998) have studied the mechanism by which natural zeolite powder (NZP) prevented alkali-silica reaction, where a decrease in alkaline-ion concentration in the pore solution of concrete through ion exchange, adsorption, and pozzolanic reaction of the NZP prevented the formation of alkali-silicate gel and improved the interface. Also, in adding NZP to saturated $Ca(OH)_2$ solution stirred with NaOH, concentrations of Na^+, Ca^{2+} and OH^- ions are all reduced. The fineness of NZP influenced its effect while the pH showed greater

decrease when NZP was finer. The alkalinity of the pore solution in NZP mortar bar decreased with an increase in NZP content. The ability of the NZP to reduce mortar bar expansion has a connection with its capacity to reduce OH^- concentration in the pore solution.

FENG et al. (1998) have studied the effect and mechanism of natural zeolite on preventing expansion due to alkali-aggregate reaction. The results confirmed that expansion can be minimized by increasing the fineness of natural zeolite powder or by a previous heat treatment for the zeolite additive. When 30% natural zeolite powder (alkali content varied from 3.3% to 4.3% Na_2O_e) was used to replace the same cement content, AAR did not take place in concrete. The inhibiting effect of natural zeolite powder on AAR was also related to its fineness.

LI et al. (1999) have carried out tests to investigate the effects of calcium nitrite, fly ash, microsilica, and their combination on the alkali-silica reaction in accordance with ASTM C 227 (mortar bar test). The chemically combined water, X-ray diffraction, and compressive strength of each batch of specimens were also measured to explore the mechanism of these effects. The results show that both the mineral admixture and the calcium nitrite solution have positive effects in preventing ASR expansion (20-50% reduction in expansion). It has been found that the addition of a calcium nitrite solution in this experiment has additional effects, which are favourable for strength development.

LANE (2000) has reported that since 1992, The Virginia Department of Transport (VDOT) has required the use of pozzolans or slag in most concrete for the purpose of avoiding deleterious ASR with aggregates that contain microcrystalline or strained quartz. Laboratory studies of these materials in rapid and longer-term tests indicate that they are effective in preventing expansion when used in the proper amount. The rapid tests (Pyrex and AMBT), provide conservative indications of the amount of low-lime fly ash or slag needed to suppress the expansion of a highly reactive Virginia aggregate and thus can be used to quickly evaluate materials. The results indicate that the minimum amounts of low-lime fly ash or slag needed to prevent excessive expansion of Virginia aggregates are 15% and 35% by mass, respectively, with Portland cements having alkali contents up to 1.05% Na_2O_{eq}. Concretes

containing low-lime fly ash or slag have been used in Virginia in these amounts since 1984 and appear to be providing good service.

DUCHESNE and BÉRUBÉ (1992, 2000) have studied the long-term effectiveness of six supplementary cementitious material (SCM) tested in the presence of two highly reactive alkali-silica aggregates from Canada; one siliceous limestone (Spratt Quarry) and one rhyolitic tuff (Beauceville Quarry). Three fly ashes (FA-A, FA-B, FA-C, alkalis varying from 2.34 and 3.07 to 8.55% Na_2O_{eq}, respectively), two silica fumes (alkalis vary from 0.77 to 3.64% Na_2O_{eq}), and one granulated blast-furnace slag (GGBFS, alkali content of 0.64% Na_2O_{eq}) were selected based on their elemental composition in order to represent a wide range of compositions. Concrete prism specimens were made with various contents of SCM and tested according to the CSA A23.2-14A specification for concrete prism test. The performance of SCM in suppressing expansion due to alkali-silica reaction was compared with that obtained by low-alkali cement (LA, 0.74% Na_2Oeq). The SCMs were tested with the high-alkali cement (HA, 1.05% Na_2Oeq). The cement alkali content was increased to 1.25% Na_2Oeq of the mass of cement by adding NaOH to the mixing water. After 9 years of experiment, the control mixtures made with low-alkali cement show expansions of nearly 0.04%. The use of 40% FA-A and FA-B (Na_2Oeq equal to 2.34, 3.07%, respectively), as well as the use of 50% slag decreases expansions lower than those obtained with low-alkali cement. They obtained excellent correlation between the drop of alkali ions in pore solution and expansion reduction in concrete. Increasing the alkali ion content produced deleterious expansion even if a great amount of good SCM were used. The total alkali content of the concrete prism and the amount of SCM used are the key factors governing expansion behavior of concrete containing SCM. The expansion curves are shown in Figures 2.12 and 2.13. Results show that expansion curves flatten out after around two years of curing for all mixtures tested. This phenomenon was due to alkali ions leaching from the concrete prism stored over water in sealed plastic containers with wicks. This behavior is supported by very low alkali ions concentrations measured on concrete samples at the end of the experiment. A two-year limit is then suggested when using the CAN/CSA-A23.2-14A method to evaluate the expansion potential of mixtures containing SCM.

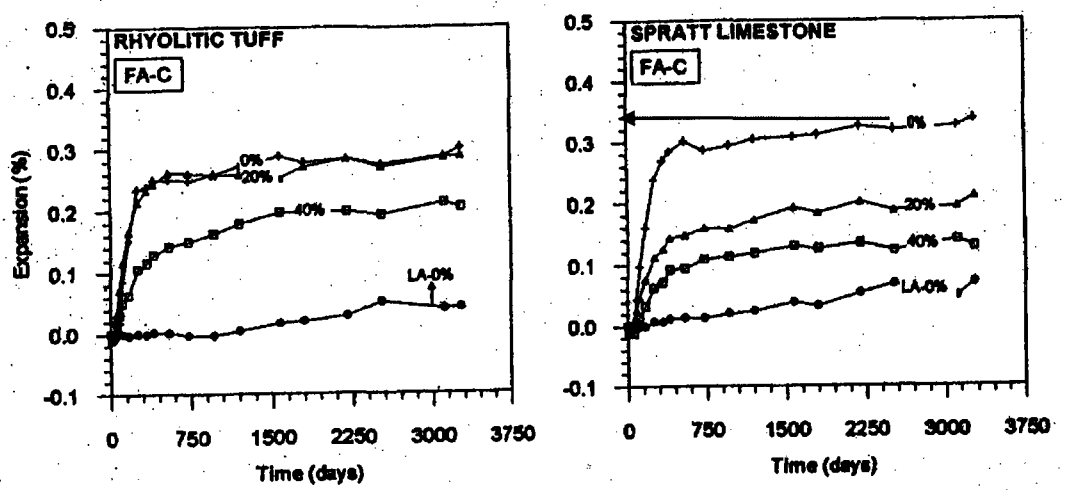

Figure 2.12 Expansion of concrete prisms (CSA A23.2-14A) made with two reactive aggregates and various amounts of fly ash at 100% RH and 38°C [DUCHESNE, BÉRUBÉ, 1992, 2000]

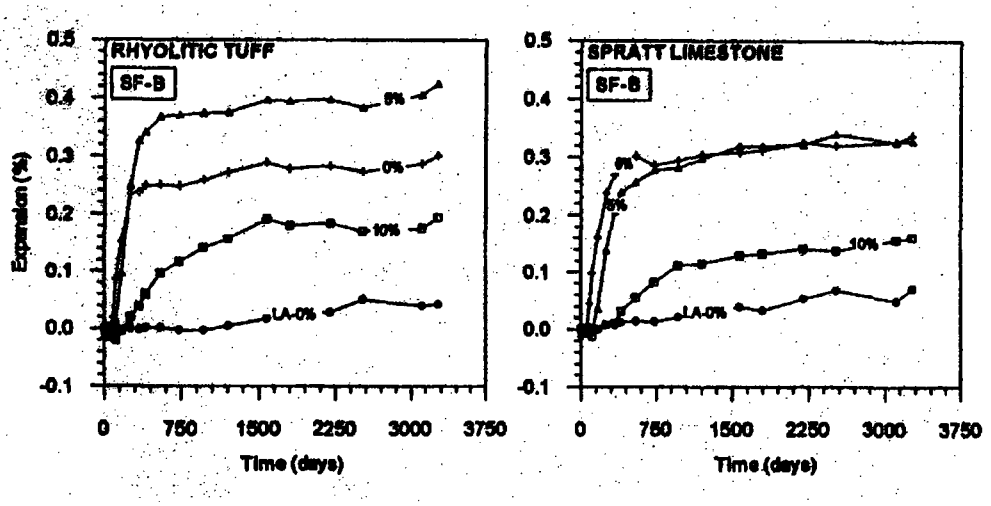

Figure 2.13 Expansion of concrete prisms (CSA A23.2-14A) made with two reactive aggregates and various amounts of silica fume at 100% RH and 38°C [DUCHESNE, BÉRUBÉ, 1992, 2000]

DUCHESNE and BÉRUBÉ (1992) have studied an accelerated autoclave mortar bar method to evaluate the same SCMs using the same reactive aggregates in their studies on the expansion of mortar bars after 5 hours of autoclaving under low temperature-pressure conditions (130°C-0.17 MPa or 25 psi) and after 14 days in 1N NaOH at 80°C. The results of concrete tests after 6, 12, and 18 months and the autoclave mortar-bar results were in good agreement with those from CSA concrete prism and ASTM accelerated mortar bar test using a limit of 0.1% expansion in the autoclave test and ASTM C 1260. It is worth noting that the expansion values for the control specimens with Spratt aggregate were 0.301% after 18

months, 0.324% after 5 hours, and 0.323% after 14 days according to CSA concrete prism, autoclave, and ASTM accelerated methods, respectively.

HUDEC and GHAMARI (2000) have shown that waste glass (approximately 18% Na_2O_{eq} content) has pozzolanic properties, since it also consists of amorphous silica. Experiments were carried out to determine the type, proportion, and size of crushed and powdered waste glass that would be most effective in reducing ASR. The glass was used both as replacement of a given size of reactive Spratt aggregate fraction (4%) and as an additive (8%). The rapid 80°C 1N NaOH mortar bar method was used for comparative testing. The results showed that the glass fractions coarser than sieve No. 200 (75 μm) acted as a highly-reactive aggregate and increased the ASR expansion of mortar. Smaller size fractions decreased ASR expansivity, and the decrease was a function of the total glass surface area. Colored (lower quality) bottle glass was slightly more effective than white bottle glass. The ASR reduction by powdered glass was equivalent to that produced by the same amount of silica fume.

KOJIMA et al. (2000) have carried out mortar bar tests in order to evaluate the reactivity of glass powder (contains about 13% Na_2Oeq) produced from waste bottles in the alkali-silica reaction. Five levels of glass powder replacement ratio (0 to 40%) and two levels of water to cementitious material ratio (30% and 50%) were chosen. Glass powder was incorporated as the replacement for fine aggregate or cement. River sand was used as the natural fine aggregate. Large expansive strain was not observed under the accelerated condition (1.2% Na_2Oeq content) and its value was smaller than 0.1% at the age of 6 months, even if a larger amount of glass powder (30 to 40% replacement ratio) was used. It is suggested that glass powder is sound for the alkali-silica reaction, when used as replacement material for fine aggregate or cement, this work was also confirmed by [SHAYAN AND XU, 2004; SHI et al., 2005]. The alkali in glass powder does not accelerate the alkali-silica reaction, though it contains a larger amount of alkali (13 % Na_2Oeq). The glass powder produced from waste bottles has the potential to be used as an ingredient of concrete. Also, the use of waste glass as an aggregate and its effect on mechanical properties and ASR has been studied by several other researchers, including SCHMIDT and SAIA (1963), JOHNSTON (1974), and FIGG (1981), whose results suggested that the use of glass aggregate generally produces highly

unsatisfactory concrete due to ASR and poor strength development. FIGG (1981) has also noted that the ASR involving glass aggregate is qualitatively different from ASR involving more porous natural aggregates, exhibiting a pessimum with respect to particle size. POLLEY et al. (1998) have indicated in their study that glass aggregate is a satisfactory substitute for natural fine aggregate, at replacement levels of up to 20% of total aggregate, the glass gradation must be between 75μm and 1.5mm. A comparable strength to control concrete was obtained at comparable water-to-cementitious ratio when fly ash in a proportion of 0 to 35% of the total cementitious material was obtained.

YAMAMOTO and KANAZU (2000) have studied the relation between pozzolanic activity and preventive effect on ASR of fly ash, and proposed an accelerated chemical test to estimate the effectiveness of fly ash in preventing ASR expansion in concrete. The chemical test estimated the consumption ratios of Ca^{2+} in normal Portland cement and fly ash blended suspensions. The consumption ratio of Ca^{2+} was named API (assessed pozzolanic-activity index):

$$API = (([Ca(c)] - [Ca(f+c)]) / [Ca(c)]) * 100\ \% \qquad (2.4)$$

The characters Ca, c, and f stand for Ca^{2+} ion concentration, cement and fly ash, respectively, where the time taken to obtain the results is about one day (reacting condition: 80°C - 18 hours). There was a linear correlation between API and the preventive effect on ASR derived from mortar bar tests; the higher the API, the higher the preventive effect. The results suggested that the proposed chemical testing method might be a useful and convenient method to estimate the effect of fly ash in preventing ASR. The proposed chemical method resulted in evaluating not only the effect of fly ash in preventing ASR, but also the pozzolanic activity. The pozzolanic activity index (AI) of each fly ash sample was determined as a ratio of compressive strength of the mortar with fly ash to the control mortar without fly ash at 28 days of age.

One of the most popular recommendations is replacing 50% or more of the ordinary Portland cement (OPC) by ground granulated blast-furnace slag. However, there have been a number of results from laboratory tests indicating that this process may not always be effective.

LUMLEY (1992) has reported in some laboratory tests that a slag of moderate alkali content, used to replace 30% of a high-alkali Portland cement only marginally alleviated ASR expansion in mortar bars containing natural opaline aggregates. In another test, a second slag of lower alkali content than the cement used actually increased expansion. In 1982, HOBBS reported experiments using mortar bars made with high alkali cement and opal as reactive aggregate. He found that "if the cement has an alkali content of 1.1% and the cement content is 550 kg/m3, damage due to ASR may be avoided if 50% of the cement is replaced by slag." He concluded that slag acts as an "alkali diluter" and that it may be assumed to contain no available alkali, however, HOBBS (1986) has quoted other examples of slag alleviating ASR to a lesser extent than expected.

Slag has variable alkali content, and it seems that under certain circumstances, some proportion of these alkalis might become released within concrete, especially if the concrete alkali content derived from other sources is comparatively low. However, the extent to which any such released alkalis will promote ASR expansion remains uncertain. There is conflicting evidence concerning the contribution of alkalis from fly ash to the reaction, and it has been suggested that one-sixth of the total (acid-soluble) alkalis in fly ash should be considered when calculating the total available alkalis in concrete [HOBBS, 1986]. In contrast, other researchers have shown that fly ash concrete can tolerate higher alkali contents than concrete without fly ash, even when the alkalis from fly ash are disregarded [NIXON et al., 1984; THOMAS et al., 1991; OBERHOLSTER AND WESTRA, 1981; DUNCAN et al., 1973].

The replacement level of a single SCM needed to prevent deleterious ASR expansion and cracking may create other problems or concerns. For example, there is a perception that the incorporation of 50% slag or greater than 20% fly ash needed to ensure adequate protection against ASR expansion may lead to poor resistance to deicer-salt scaling [THOMAS, 1996; MEHTA, 1989]. Likewise, incorporating silica fume at levels greater than 10% by mass of

cement may lead to dispersion and workability concerns. However, it is possible to alleviate these and other concerns by using ternary blends with reduced amounts of fly ash or slag in combination with silica fume. There has been increased interest in the use of ternary blends of cementitious materials in recent years, partly due to the development of high-performance concrete. Such blends contain Portland cement together with two other supplementary cementitious materials (e.g. silica fume with either fly ash or slag). These ternary blends are known for producing concrete with excellent fresh and mechanical properties.

THOMAS and BLESZYNSKI (2000) have studied ternary blend combinations of silica fume, blast-furnace slag, and Portland cement. The performance of these blends in terms of controlling deleterious expansion due to ASR shows that there is a synergistic effect when appropriate combinations of silica fume and slag are used. Mixtures with relatively low levels of silica fume (4 to 6%) combined with moderate levels of slag (20 to 35%) are very effective in controlling expansion in concrete containing high-alkali cement and highly reactive aggregate. The use of an appropriately proportioned ternary blend causes a marked reduction in expansion equal to, or greater than the superposition of the individual influences of a single SCM. A preliminary study was conducted using the accelerated mortar bar test (CSA A23.2-25A) to evaluate appropriate mix combinations of silica fume and blast-furnace slag. Expansion levels less than 0.1% at 14 days were used to evaluate effective mix combinations. The straight line drawn between the single SCM points represents the "theoretical" effective ternary blend combinations. It is interesting to note that ternary mixtures that have sufficiently controlled ASR expansion extend beyond this theoretical threshold. This implies a synergistic effect exits between the SCMs resulting in reductions in expansion greater than the sum of the individual SCMs acting alone, as shown in Figure 2.14.

SHEHATA and THOMAS (2002) have investigated the effect of cementitious system containing Portland cement, silica fume, and fly ash on expansion due to alkali-silica reaction. Concrete prisms were prepared and tested in accordance with CSA A23.2-14A standard. Paste samples were cast using the same or similar cementitious material and proportions as were used in the concrete prism test. It was found that practical levels of silica fume with low-, moderate- or high-calcium fly ash were effective in maintaining expansion below 0.04 % after

2 years. Pore solution chemistry showed that while pastes containing silica fume yield pore solutions of increasing alkalinity at ages beyond 28 days, the shortfall of the increased pore solution alkalinity with age obtained for cementitious systems containing silica fume was overcome by using fly ash together with silica fume. In other words, ternary blends resulted in pore solution of low alkalinity throughout the testing period (3 years).

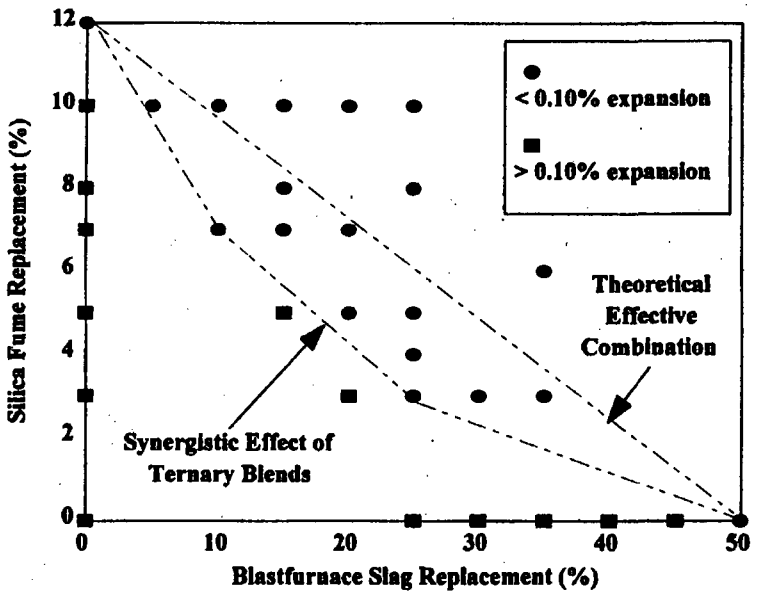

Figure 2.14 Performance of mortar ternary blend combinations with Spratt aggregate (BLESZYNSKI, THOMAS, 2000)

TEMIZ and KARAKECI (2002) have used high-calcium fly ash (HCFA) and silica fume (SF) as mineral admixtures. The effect of these admixtures on the microstructure of cement paste was investigated using X-ray diffraction (XRD) and scanning electron microscopy (SEM). The reaction of HCFA and SF with portlandite, which occurs in Portland cement (PC), forms a new calcium-silicate-hydrate (C-S-H) gel. Thus, the amount of $Ca(OH)_2$, which is harmful for concrete decreased.

FOURNIER et al. (2000) have summarized new proposed standards for the determination of the potential alkali reactivity of aggregates, and selection of appropriate measure for preventing deleterious expansion due to AAR. The proposed approach for selecting preventive measures against ASR involves a risk evaluation process based on the following factors: (1) the degree of reactivity of the particular reactive aggregate, (2) the size of the concrete

element and the environmental conditions to which it will be subjected, and (3) the expected service life of the structure. Proposed preventive measures are then determined according to the following approaches: (1) limit the alkali content in the concrete to a selected level, and/or (2) use of an effective supplementary cementing material (SCM) or an effective combination of supplementary cementing materials (SCMs) in sufficient amount.

ICHIKAWA and MIURA (2007) have proposed that OH^- and R^+ ions in the pore solution de-polymerize silica-rich aggregate to convert to fluid hydrated alkali silicate. The surface region of the aggregate is homogeneously covered with the alkali silicate. Consumption of OH^- ions by the reaction assists the dissolution of calcium into the solution. The Ca^{2+} ions easily penetrate into the soft alkali silicate to re-polymerize the silicate. The aggregate is now tightly packed with a rigid reaction rim that allows the penetration not of alkali silicate but R^+, Ca^{2+} and OH^- ions. The Ca^{2+} ions penetrate much slower than the R^+ ions. The OH^- and R^+ ions penetrate through the reaction rim to convert the fresh silicate into bulky alkali silicate. The resultant expansive pressure is stored in the aggregate. The accumulated pressure cracks the aggregate and the surrounding cement paste when the pressure exceeds the tolerance of the aggregate surrounded by the reaction rim and the cement paste. In this study, Portland cement and ASR-reactive andesite containing significant amount of glassy silicate were used. The content of alkali was enriched to 2.5 times while keeping the Na_2O/K_2O ratio constant. The concrete block wrapped with a cloth was kept at 40°C under 100% relative humidity for 4 months. The concrete block was then kept in a closed plastic bag at room temperature.

2.9.4 Alkali release from fly ash and slag

In the context of the alkali-silica reaction in mortar and concrete, the question of how much alkali is released from latent hydraulic binders and are actually available for the reaction has been the subject of a great deal of work and controversy over the last decade. Although the reaction itself is the result of the attack on reactive silica by hydroxyl ions, the concentration or amount of these that become available is generally influenced, though not always, by the concentration or amount of alkali available [BARLOW AND JACKSON, 1987]. Some authorities accept that the water-soluble alkali content of the hydraulic binder provides a

quantitative measure of the alkalis available in concrete. The ASTM C311 method for "available alkali" acknowledges that in the case of concrete, we are not dealing with water, but a high pH solution with the possibility that this solution may attack the glass in which the alkalis in fly ash and granulated blast-furnace slag are mainly bound. The ASTM method uses calcium hydroxide to provide an alkaline environment, but, as has been established by BUTTLER et al. (1981), the amount of alkali released is dependent upon the relative proportions of the constituents in the paste.

Both fly ash and slag can have alkali content markedly higher than Portland cement. GLASSER and MARR (1984) and COX et al. (1950) have shown that alkalis can be released by fly ash and slag into the pore solution and that the alkalis released can be in greater quantity than those from a Portland cement. DIAMOND (1981), however, has concluded from tests using two Danish fly ashes that one fly ash, which had a total alkali content of 2.4% by mass, acted as an inert diluter whilst the other, which had a total alkali content of 3.3 % by mass, extracted a small proportion of alkalis from the pore solution.

CANHAM and NIXON (1987) have reported that fly ashes, when blended with Portland cement of moderate alkali content, were generally capable of reducing the concentration of hydroxyl ions in the pore solution phase to a greater extent than would be expected if they were assumed to behave as cement of zero alkalinity. The reduction in alkalinity of the pore solution caused by fly ash proceeded over a relatively long time, which suggested that it is probably associated with the incorporation of alkalis into C-S-H gel formed by the slow pozzolanic reaction. On the other hand, ground granulated slags, when blended with Portland cement tend to reduce the hydroxyl ion concentration of the pore solution phase, through generally to a lesser extent than would be expected if they were assumed to behave as cement of zero alkalinity. The effectiveness of slags in lowering the hydroxyl ions concentration of cement pore liquid is not primarily controlled by the alkali content of the slag, and it appears that other factors influencing the nature and composition of the C-S-H gel formed may be important.

DUCHESNE and BÉRUBÉ (1994) have studied the pore solution chemistry of cement pastes made with two condensed silica fumes, three pulverized fly ashes(with different alkali contents vary from 2.34 to 8.55%) and one ground granulated blast furnace slag. The extracted solutions were tested at 7, 28, 84, 182, 364 and 545 days of curing (38°C and 100% R.H.). Results were compared to expansions obtained for a 2 year time period in the CAN/CSA A23.2-14A Concrete Prism Method for concrete specimens made with two very alkali-silica reactive aggregates and tested at the same conditions and water/cement/SCM. A long-term threshold in alkali hydroxide concentration was observed around 0.65N, below which no significant expansion occurred in corresponding concretes. The lower the SCM alkali content and the concrete alkali content as well, and the higher the SCM content, the easier this limit is satisfied. They observed that a large proportion of alkalis released by the fly ash sample, with high alkali content (8.55%), remains in solution and is available for ASR (88% at 28 days and 62% at 1.5 year with 20% fly ash; 52% at 28 days and 36% at 1.5 year for 40% fly ash). Moreover, they have concluded that a threshold in alkali concentration was observed around 0.65N NaOH+KOH over a long time period, which corresponds in this study to a 30% drop with respect to the controls; below this value, no significant expansion occurred in corresponding concretes made with very reactive aggregates.

2.9.5 Influence of fluorides on the degree of cement hydration

SAUMAN (1989) has studied the influence of fluorides and silicofluorides on the degree of cement hydration. The following compounds were selected: CaF_2, NaF, $CaSiF_6$, Na_2SiF_6, and K_2SiF_6. A basic mixture was employed which consisted of clinker and natural gypsum in the weight ratio 93 parts:7 parts. The addition of fluoride or silicofluoride was always converted to 7% of natural gypsum; the hydration period (22°C, 100% relative humidity) corresponded to 24 hours. After this period the samples were freed by a chemical process from the mechanically bound water. The degree of hydration was determined on the basis of the liberated portlandite $Ca(OH)_2$, which was determined thermogravimetrically and converted together with the secondarily formed $CaCO_3$ into CaO. The results can be seen from the illustration shown in Figure 2.15 from which one can conclude that no retardation of the hydration process can be proved either in the case of CaF_2 or NaF, but pronounced retardation effect is exhibited due to the presence of Na_2SiF_6.

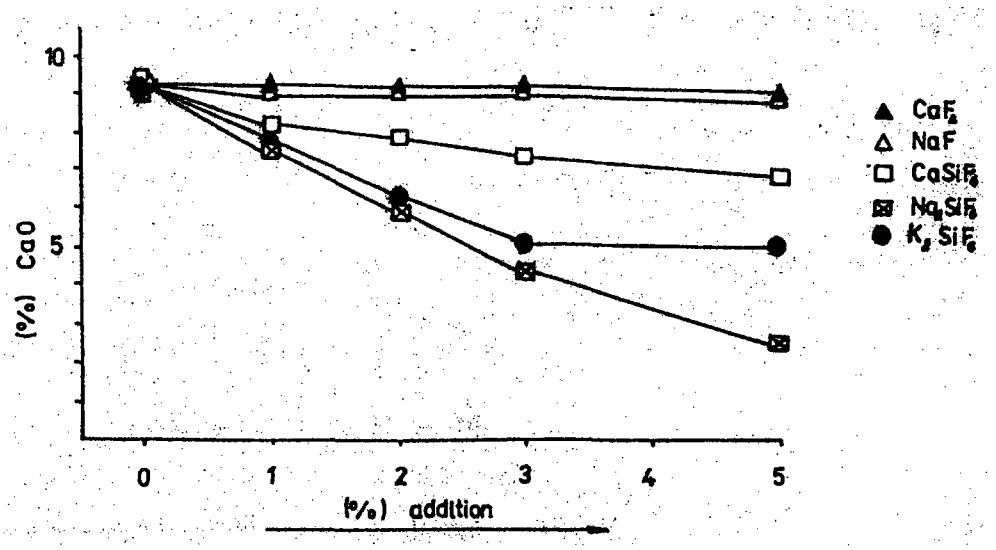

Figure 2.15 Quantity of liberated lime versus addition of fluorides or silicofluorides [SAUMAN, 1989]

SHANBA and ZHONGHUI (1989) have studied the effect of fluoride on hydration of C_3S by burning a stoichiometric mixture of C_3S with CaF_2, specified at 1500°C for 3 hours, and repeating the burning twice. All samples were ground to about 3000 cm^2/g (Blaine) and studied by chemical analysis, XRD, conduct calorimeter, SEM, and compressive strength tests. The results showed that the hydration degree, the chemical bound water, the rate of heat evolution, and the compressive strength were decreased with increasing F content in C_3S samples at 1 day, but increased at 3 days. As the content of F in C_3S increased, the time at which Ca^{2+} and OH^- ion concentrations in liquid phase reach maximum was delayed. The higher the F in C_3S, the more time delayed by the concentrations of Ca^{2+} and OH- were more the same for all samples at 3 days. The addition of CaF_2 as an admixture during hydration has little effect on compressive strength and the Ca^{2+} and OH^- concentration in liquid phase.

2.10 Conclusions

- The reactivity of pozzolans could be significantly increased by several methods, such as elevated temperature curing and the addition of proper chemical activators to their pastes.
- There is obvious correlation between the pozzolanic activities of mineral admixtures and preventive effects on alkali-silica expansion.
- Microstructural and pore solution analysis showed that much of the alkali in the fly ash and slag concrete was bound in the C-S-H and not available to the pore solution for alkali-silica reaction.

- C-S-H reaction product of glassy phase of mineral admixtures with CH, with lower Ca/Si ratio, has the ability to entrap alkalis.
- CaF_2 has no harmful effect on the hydration of cement phases.
- Many studies support the high effectiveness of fly ash and slag in suppressing alkali-aggregate reaction, where their concrete can tolerate higher alkali content than concrete that does not incorporate then -
- The partial replacement of Portland cement with single SCM such as fly ash, slag, or silica fume affects the reduction in ultimate expansion, but may lead to durability concerns.
- The use of appropriately proportioned ternary mixtures causes a marked reduction in expansion equal to, or greater than, the superposition of the individual influences of a single SCM and decrease durability concerns.
- When blended cements are used, the influence of alkali contained in the admixtures (fly ash, slag, etc.) on expansion is very small.
- Particle-size distribution mainly influences both fly ash and slag reactivity at early ages, while the chemical composition and amorphous phase content play a prevailing role at later ages.
- Poorly dispersed silica fume (densified silica fume) larger than 50μm could act as alkali-silica reactive aggregate.
- Accelerated test CSA C23.2-25A (1N NaOH at 80°C) is suitable to detect alkali reactive aggregate and can be used to evaluate the effectiveness of mineral admixtures against alkali-silica reaction.

CHAPTER 3

MATERIALS AND TEST PROCEDURES

3.1 Introduction

The materials used in the current study are frequently referred to, and therefore this chapter concentrates on the properties of these materials in order to avoid repetition in subsequent chapters. It should be noted that this chapter is divided into two parts. Part I deals with glass frit used as clinkerless binder, while part II examines glass frit as a supplementary cementitious material and its effect on alkali-silica reaction (ASR).

3.2 Cementitious binders

Combinations of cement with various combinations of GF and cementitious materials to form different cementitious systems were used to study potential synergetic effects. The term water-to-binder ratio is used rather than the conventional water-to-cement ratio, to take into account all of the binders mentioned hereafter. The physical and chemical properties of the cementitious binders, which were obtained from the NOVA Pb and St. Lawrence Cement company, are summarized in Table 4.1.

3.3 Ordinary Portland cement (OPC)

Ordinary Portland GU cement, sourced from St. Lawrence Cement company and meeting the requirements of CSA A3001 specification, was used as the main binder to which other cementitious materials were added as partial cement replacements. An adequate quantity of OPC from the same silo was stored during work on this part of the study in their original bags as one batch and with sealed airtight plastic covers in a storage room where the temperature remained between 20 and 22°C. The physical and chemical properties of OPC used in this investigation, which were tested by the supplier, are shown in Table 4.1.

3.4 Glass frit (GF)

Glass frit was supplied by the company NOVA Pb Inc. of Sainte-Catherine, Quebec, Canada. An adequate quantity of glass frit was obtained to ensure all mixtures done in this part of the study were from the same batch. The glass frit was stored in large sealed and airtight barrels from one single source, where the temperature remained between 20 and 22°C. The physical

and chemical properties of glass frit were tested by NOVA Pb and Université de Sherbrooke laboratories, respectively, and are summarized in Table 4.1.

3.5 Ground granulated iron blast-furnace slag (slag)

The ground granulated iron blast-furnace slag (slag) used in this study was provided by the St. Lawrence Cement company. It complies with Canadian specification CAN/CSA A3000 (Canadian Specification for Supplementary Cementing Materials). An adequate quantity of slag was stored to ensure all mixtures containing slag as binder originated from a single source and were of uniform composition. Slag was stored in sealed airtight barrels in a large storage room where the temperature remained between 20 and 22°C. The physical and chemical properties of the slag used in this study were tested by Université de Sherbrooke laboratories and are shown in Table 4.1.

3.6 Fly ash (Fa)

The pulverized fly ash (Fa) used in this study, classified as Class F, was supplied by the Lafarge Canada Company. It complies with CAN/CSA A3000 and ASTM C-618 specifications. An adequate quantity of Pfa was stored to ensure all mixtures containing Pfa as binder originated from a single source and were of uniform composition. Pfa was stored in sealed airtight barrels in a large storage room where the temperature remained between 20 and 22°C. The physical and chemical properties of Pfa used in this work were tested by Université de Sherbrooke laboratories and are shown in Table 4.1.

3.7 Condensed silica fume (CSF)

The condensed silica fume (CSF) used was supplied by SKW Canada Inc., Bécancour, Quebec. It complies with CAN/CSA A3000 specification. An adequate quantity of CSF was stored to ensure all mixtures that contained CSF as binder originated from a single source and were of uniform composition. CSF was stored in sealed airtight barrels in a large storage room where the temperature remained between 20 and 22°C. The physical and chemical properties of CSF used in this study were tested by Université de Sherbrooke laboratories and are summarized in Table 4.1.

3.8 Coarse and fine aggregates

3.8.1 Fine aggregates

Five types of fine aggregates were used in this work.

i) The Ottawa sand used as standard sand was supplied in bags. Ottawa sand is unique, its rounded grains of clear colorless quartz, diamond-like in hardness, are pure silica (silicon dioxide) uncontaminated by clay, loam, iron compounds, or other foreign substances. Ottawa sand was obtained from the St. Peter sandstone quarry. It meets the requirements of Canadian specification CSA A23.1(ASTM C33), as shown in Figure 3.1.

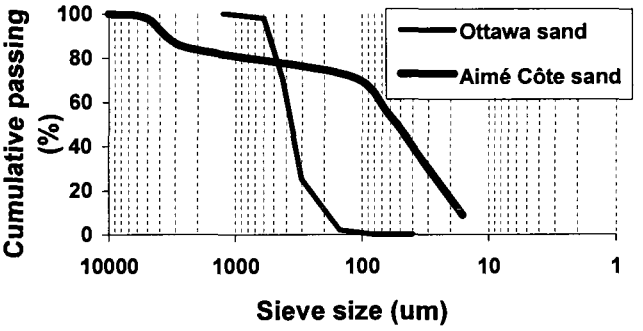

Figure 3.1 Grade distribution of fine aggregates

ii) Aimé Côté sand, which consists of river sand, was used as regular sand and was supplied in barrels. It complies with Canadian specification CSA A23.1(ASTM C33), as shown in Figure 3.1.

iii) LG sand is provided by Bau-Val Inc. The company, located in Saint-Hippolyte in the Lower Laurentians area, operates a quarry with very rich deposits of granite aggregates that it offers to various specialized markets in the Laurentians and elsewhere, including the construction market.

iv) Spratt (limestone) and Mirabel (dolostone) coarse aggregates were crushed to pass through different sieves according to ASTM C227, as shown in Table 3.1. The size fractions thus obtained were recombined to be used in accelerated mortar bar testing.

TABLE 3.1 GRADE PROPORTION OF TESTED AGGREGATES

Sieve size (mixture of 4 bars)			
Passing	Retained	Mass (%)	Mass (g)
5 mm	2.50 mm	10	135
2.5 mm	1.25 mm	25	337.5
1.25 mm	630 μm	25	337.5
630 μm	315 μm	25	337.5
315 μm	160 μm	15	202.5

3.8.2 Coarse aggregate

Spratt aggregate is commonly used as standard aggregate in AAR investigation. Spratt aggregate was crushed and sieved into three-grain sizes according to CSA A23.2-14A, i.e. 20-14mm, 14-10mm, and 10-5mm sieves.

Aimé Côté coarse aggregate used in three-grain sizes - 10, 14 and 20 mm - was supplied by the Aimé Côté Company. It meets the requirements of CSA A23.1 (ASTM C33) specification and its particle size distribution is shown in Figure 3.2.

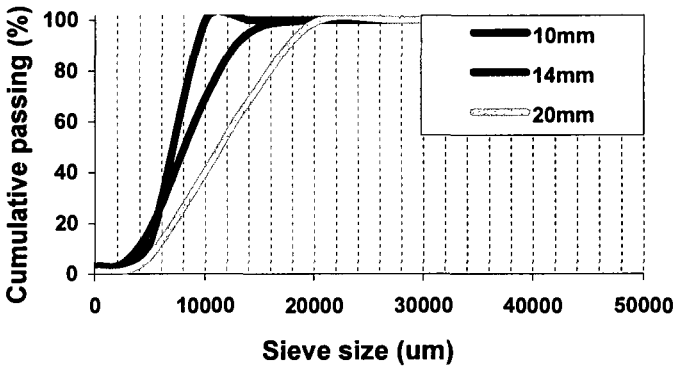

Figure 3.2 Aimé Côté aggregate particle size distribution

The physical properties of both fine and coarse Aimé Côté and Ottawa aggregates are given in Table 3.2. These properties were used in the mix design for the concrete prism test.

TABLE 3.2 PHYSICAL PROPERTIES OF FINE AND COARSE AGGREGATES

Properties	Coarse aggregate	Coarse aggregate	Fine aggregate	Fine aggregate
Name	Aimé Côté	Aimé Côté	Aimé Côté	Ottawa sand
Type	Crushed (calcareous)	Crushed (calcareous)	River sand	excavated
Maximum diameter	10mm	14mm	≤5mm	<0.6mm
Modulus of fineness	6.4	-	2.5	-
Density	2.64	2.63	2.73	2.65
Absorption coefficient	0.57	0.44	1.27	-

The above-mentioned materials were used in the two main phases of this thesis. The other materials specific to each phase are mentioned in each part separately, as follows:

3.9 Alkali-activated GF cement

3.9.1 Alkali-activators

The activators used in this study were as follows:

i) Technical grade sodium hydroxide, which was in pellet form, with a purity of 97.0%. This activator is referred to as NaOH;

ii) Technical grade sodium carbonate;

iii) Technical grade potassium carbonate;

iv) Technical grade hydrated lime;

v) Technical grade sodium metasilicate;

vi) Technical grade sodium sulfate.

3.10 Alkali-silica reaction

The aggregates used in this part of the study were evaluated according to the requirements of CSA A23.2-25A, A23.2-14A, and ASTM C 227 Canadian specifications, as shown later.

3.10.1 Mortar bar tests

The fine aggregates used in this part of the study were Ottawa sand, Aimé Côté sand, LG sand, and ground Mirabel and Spratt coarse aggregates. The coarse aggregates used were previously crushed, then passed through a series of sieves, as shown in Table 3.1.

3.10.2 Concrete prism test

The fine aggregates used in this part were Ottawa and Aimé Côté sands, while Spratt aggregate was the only coarse aggregate used. Spratt aggregate was sieved into three grades and proportioned into three equal parts according to CSA A23.2-14A, i.e. 20-14mm, 14-10mm, and 10-5mm sieves.

3.10.3 NaOH pellets

Technical grade sodium hydroxide, provided in pellet form with a purity of 97 %, was used to increase the alkalinity of the surrounding or internal environment presents in mortar bar or concrete prism tests.

3.10.4 Chemical admixtures

The only superplasticizer (SP) used is a polynaphthalene-sulfonate-based material (PNS). It was mainly used as a dispersing agent for those mixtures containing condensed silica fume and as a dispersing agent and water-reducer for the other mixtures. The specific density of SP is 1.21 and the solid content is 42%.

3.11 Experimental program

3.11.1 Introduction

The main objective of this research program is to assess the effective utilization of GF in concrete and "green" concrete manufacturing. This main objective is divided into two sub-objectives. The first sub-objective is to improve the pozzolanic and hydraulic properties of GF as an ecological binder for manufacturing of clinkerless paste, mortar, and concrete. The second sub-objective is to use GF as an alternative supplementary cementitious material as OPC cement replacement, and assess the effect of the alkali content of GF on ASR expansion in mortar and concrete. During the experimental program, different Canadian and American specifications, as well as modified specifications, were used, as shown in Figure 3.3.

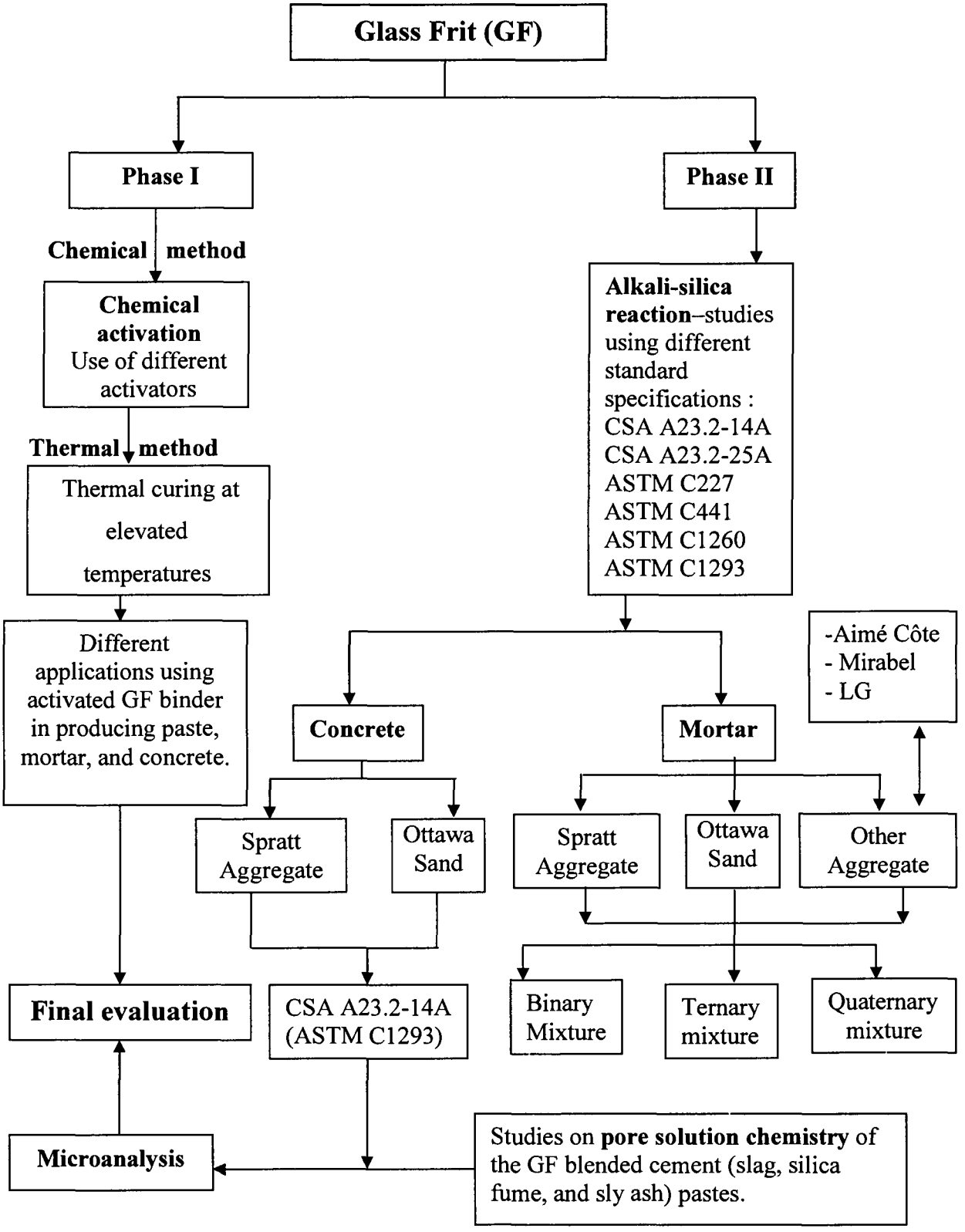

Figure 3.3 Schematic diagram of the main steps in the experimental program.

The experimental program is divided into two main phases as described hereafter and illustrated in Figure 3.3.

A. Use of GF as an activated cementitious binder by using combinations of two methods:

i)- The chemical method;

ii)- The thermal method (heat curing).

The aim of this part of the study was to obtain a GF clinker-free binder by using different activators and combinations of activators, under different conditions, that enhance the latent pozzolanic and hydraulic properties of GF. Tests were conducted on series of different pastes, mortars, and concretes. The improvement of binding properties of GF by partial replacement with a small amount of given mineral admixtures (partial replacement), such as silica fume, fly ash, and slag, was carried out. This part of the study showed the potential of using various methods to improve the binding properties of GF.

B. Use of GF as an alternative supplementary cementitious material (active additive)

This part of the study was conducted to show the actual effect of the alkali content in GF on ASR expansion in mortar and concrete, both in the short and long term.

3.12 Alkali-activated glass frit binder (AAGFB)

In this part of the study, the pozzolanic and hydraulic activities of GF incorporating different activators and tested at different temperatures of activation were evaluated. To begin this evaluation, a few trial mixtures were done.

3.12.1 Trial mixtures

Trial mixtures to determine the actual binding ability of GF as a clinkerless binder were first carried out. Preliminary results showed that GF is highly reactive with most alkaline salts at elevated temperatures. Some of these mixtures contained fly ash and slag to estimate the effect of their presence with GF before proceeding with the detailed experimental program, as shown in Table 3.3.

TABLE 3.3 ACTIVATED TRIAL MIXTURES OF GF ALONE OR IN COMBINATIONS WITH SLAG OR FLY ASH

Sample No.	Glass frit (%)	Slag (%)	Fly ash (%)	Lime (%)	w/b ratio	Ottawa sand	b/sand ratio	Na_2O (%)(to mixing water)	Activation temperature (°C) and time	Notes
1	33.3	40	-	26.7	0.29	-	-	-	80°C-18hrs	Set
2	38.0	-	31	31.0	0.29	-	-	-		Set
3	80	-	-	20.0	0.23	-	-	-		Set
4	80	20	-	-	0.29	-	-	3		50MPa
5	80	20	-	-	0.32	+	1	3.3		28MPa
6	100	-	-	-	0.14	-	-	3		35MPa
7	100	-	-	-	0.19	+	0.44	3		23MPa
8	100	-	-	-	0.19	+	1	3		18MPa

+ stands for mortar (added sand), 50mm test cubes were used to test compressive strength

Table 3.3, and Figures 3.4 and 3.5 have shown that GF could be activated alone or in combination with slag or fly ash. Both NaOH and lime could be used as effective and primary activators. The initial activation of GF alone using NaOH gave a compressive strength of 35 MPa (sample 6), while the activation of GF replaced by 20% slag using the same activator increased the compressive strength to about 50 MPa (an increase of about 43%) in less than 24 (sample 4) hours. Based on the results of these preliminary tests intensive work on the activation of GF into a clinkerless binder and its utilization in manufacturing pastes, mortars, and concretes has been carried out.

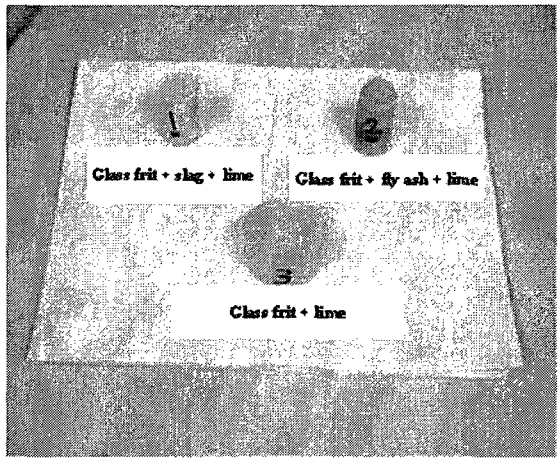

Figure 3.4 Different lime-activated glass frit mixtures alone or in combination with slag or fly ash

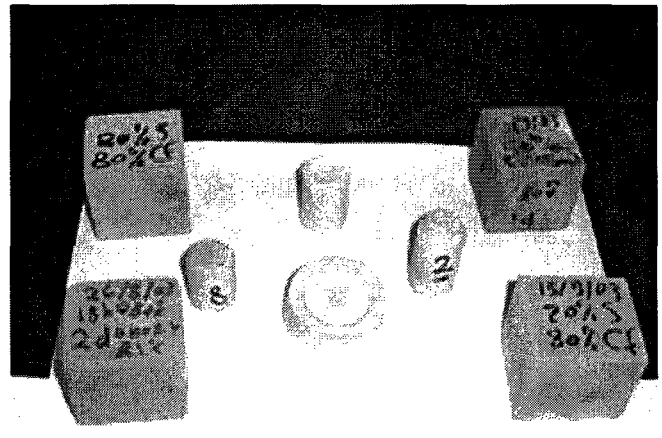

Figure 3.5 Different alkali-activated glass frit mixtures alone or in combination with slag giving a 1-day compressive strength of up to 50 MPa

3.12.2 Detailed laboratory program

The experimental laboratory program is divided into three main parts. In the first part, different glass frit pastes incorporating different activators and subjected to different temperatures of activation were tested. Slag and fly ash were used as co-binders (in small ratios) to improve mechanical properties. The presence of slag and fly ash with GF was tested at low temperature of activation, as the main aim of their presence with GF was to decrease the need for high temperature of activation. In the second phase, which is strongly related to the first phase, different mortars were fabricated based on the best mixtures of the first phase, and mechanical strengths were determined to obtain the best sand-to-GF ratio. In the third part, a series of concrete mixtures were made and their mechanical properties, represented by compressive strengths, were determined.

A. Inorganic activator

The activators used in this part were as follows:

1- NaOH, and Ca $(OH)_2$ and various combinations of the two;

2- Na $_2CO_3$, K $_2CO_3$, CaCO3 and various combinations of the three;

3- Na_2 SO_4;

4- $Na_2SiO_3.9H_2O$.

Binary and ternary combinations of these salts were used through the activation process. All the other inorganic and organic basic salts are also recommended. The characteristics of the mixtures tested in each part are summarized in the next section for paste, mortar, and concrete. A variety of concentrations and temperatures were chosen. A temperature of 21°C and 100% R.H. were chosen as curing conditions to monitor compressive strength development after the completion of the activation process.

3.12.3 Test procedures

A. Steam-curing reactor

The reactor is mainly composed of a small humidity chamber measuring 50 X 50 X 70 cm and a temperature-control unit, as shown in Figure 3.6 and 3.7. All of the activated mixtures tested in this part of the study were cured in this reactor.

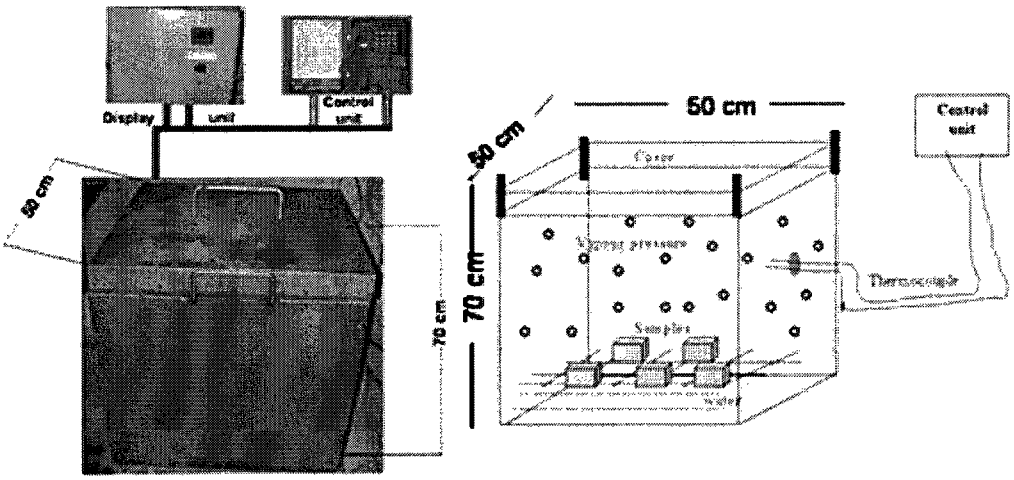

Figure 3.6 Actual and schematic diagrams of the reactor used

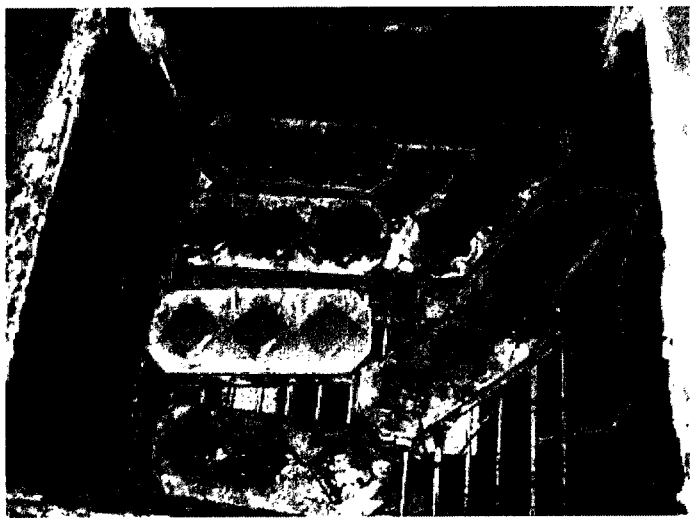

Figure 3.7 Top view of the reactor used

3.12.4 Mixing method

The mixing of paste was carried out in a 5-litre stainless steel mixing bowl. The total amount of binder used for any given batch ranged from 1.25 to 2.5 kg. Mixing was conducted using a two-speed switch mixer. Pastes were prepared by mixing the pre-weighed NaOH pellets and water in the mixing bowl, and then adding the pre-weighed GF powder to this solution and mixing for 2 minutes at slow speed. The mixing was then stopped for 2 minutes and finally mixed for another 2 minutes at high speed. The resulting paste was then cast into moulds with 2-inch cubes made of brass, which is a thermally conductive material. The moulds were placed 5 cm above water by means of a steel rack with four vertical support legs as shown in

the reactor diagram in Figures 3.6 and 3.7. The temperature is automatically controlled and the unit is attached to an LCD screen as well as an electronic recorder to register the temperature reading over time.

This system is ideal for carrying out the activation process of such materials and it is highly recommended. Both the temperature and the pressure can be controlled and maintained at constant level, in addition to the relative humidity, which can be maintained at 100% during the activation process. This activation process can be schematically represented, as in Figure 3.8, to show the overall activation process used after thermal curing. The samples were removed from the reactor after selected time periods and covered with an isolator to let them cool down slowly. They were then demoulded and cured in the humidity chamber (20 ± 2°C and 100% R.H.) until they reached testing age. Many other activators and SCMs could be used in this system. After the activation energy surpasses the threshold activation energy, GF and any other SCM combinations with GF can be easily transferred into a new binder.

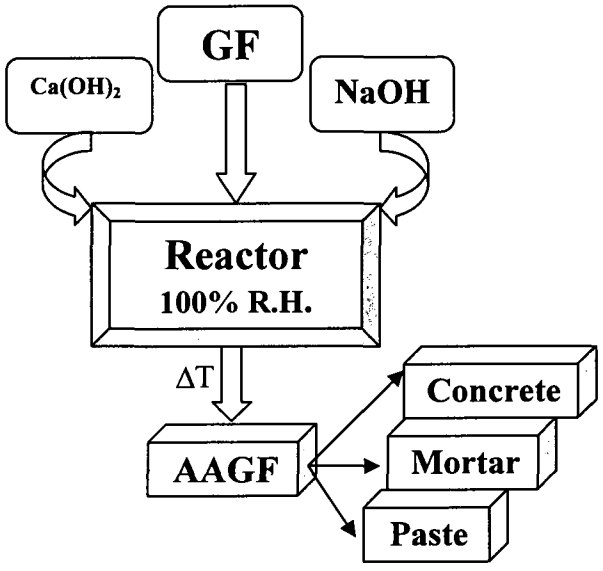

Figure 3.8 Schematic diagrams of the activation process

3.12.5 Mix characteristics of GF clinkerless cement pastes made with NaOH activator

As the most effective activator, NaOH was chosen as the first activator to begin with in preparing the first series of clinkerless GF pastes. Three temperatures of activation of 50, 60 and 80°C were chosen.

A. Paste mix design

In the first mix at 50°C, a constant GF content was used with w/GF ratio changing according to the apparent workability, which in turn changes according to NaOH concentration, as seen in Table 3.4. It can be seen that as NaOH increases, so does the w/GF ratio just as the hygroscopic effect of NaOH increases water demand. The same observation was noted with the other mixtures at 60 and 80°C, as shown in Tables 3.4 and 3.5. The molar concentrations of NaOH have been calculated with respect to the mixing water. It is more practical to express NaOH concentration in molar value than in percentage value, as the molar value is more representative of the pore solution in the paste. The mixture proportions of these series are given in Tables 3.4 and 3.5.

TABLE 3.4 MIXTURE CHARACTERISTICS OF SAMPLES TESTED AT 50 AND 60°C

Mixtures	50°C		60°C	
	W/GF	Na_2O (molar)	W/GF	Na_2O (molar)
C0.5	0.312	0.26	0.315	0.26
C1	0.310	0.52	0.315	0.51
C1.5	0.307	0.79	0.319	0.76
C2	0.308	1.05	0.318	1.01
C2.5	0.308	1.31	0.320	1.26
C3	0.316	1.53	0.319	1.52
C3.5	0.315	1.79	0.319	1.77
C4	0.318	2.03	0.319	2.02
C4.5	0.322	2.25	0.319	2.27
C5	0.324	2.49	0.319	2.53

TABLE 3.5 MIXTURE CHARACTERISTICS OF SAMPLES TESTED AT 80°C

Mixtures	W/GF	Na_2O (molar)	Remarks
C1	0.290	0.556	
C1-sp	0.290	0.556	0.74% (solid SP)
C2	0.306	1.054	
C3	0.302	1.603	
C3-sp	0.250	1.603	1.29 (solid SP)
C4	0.306	2.110	
C5	0.308	2.618	

3.12.6 Other single activators used

In this part of the activation process, a temperature of 60°C was used with the other activators in their different forms. The activators used varied from single to binary and ternary activators, as shown in the following part:

A. $Ca(OH)_2$ activator (CH)

As previously mentioned, this activator was tested during the determination of the pozzolanic properties of GF using ASTM C 311 and ASTM C 593. The activation temperature in this test was 60°C. Three GF replacement levels by CH were used, that is 10, 20, and 30% CH.

B. Sodium metasilicate ($Na_2SiO_3.9H_2O$) activator

Sodium silicate activator is one of the well-known activators used in the activation of slag and fly ash. Sodium meta-silicate consisting of 22% Na_2O, 21% SiO_2, and 57% H_2O was used. The silica modulus (Ms = SiO_2/Na_2O) is a crucial factor that affects its activation capacity. Available literature indicates that Ms = 0.75 is the best ratio for this purpose; however, other ratios were used (0.33 and 0.97). Different SiO_2 and Na_2O concentrations calculated with respect to GF total mass were used. Consequently, different Ms ratios with different Na contents were investigated.

3.12.7 Binary activator

Different binary mixtures of inorganic activators were tested for their efficiency to activate different GF paste mixtures with water-to-binder ratio of 0.35 and at an activation temperature of 60°C for an 18 hour period of activation.

A. $Ca(OH)_2$ and Na_2CO_3 –based system

The efficiency of this binary activator was also tested at an activation temperature of 60°C. The aim of using this activator depends on the reversible reaction that gives NaOH as the target activator, which is obtained indirectly through the reaction of $Ca(OH)_2$ and Na_2CO_3, as follows:

$$Ca(OH)_2 + Na_2CO_3 \leftrightarrow 2NaOH + Ca\,CO_3 \qquad (3.1)$$

The molar ratio of Na_2CO_3 to $Ca(OH)_2$ that was used in this test was 1.122. This molar ratio was formulated in such a way that it gives 1.5% Na_2O with respect to GF content.

B. $Ca(OH)_2$ and NaOH –based system

A mixture of 20% $Ca(OH)_2$ and NaOH equivalent to 1.5% Na_2O with respect to GF content was tested. This mixture is very important as it shows the competence between the formation of both of NaF and CaF_2 minerals in the formed paste. The temperature of activation was also 60°C. As well, other mixtures of 20% $Ca(OH)_2$ and NaOH with concentrations of 2 and 5% Na_2O were tested at 80°C to investigate the effect of the abundant presence of $Ca(OH)_2$.

C. NaOH and Na_2CO_3

A binary mixture of both NaOH and Na_2CO_3 was used to activate GF in such a way that their sum equals approximately 1.5% Na_2O and where the Na_2O content coming from Na_2CO_3 equals to 0.5 % Na_2O in terms of total percentage with respect to GF content.

D. NaOH and Na_2SO_4

A binary mixture of both NaOH and Na_2SO_4 was used to activate GF in such a way that their sum equals approximately 1.5% Na_2O with respect to total mass of GF. The dosage of Na_2SO_4 was calculated to give 0.5% Na_2O with respect to the total mass of GF.

E. $Ca(OH)_2$ and K_2CO_3 –based system

The efficiency of this binary activator was evaluated during this part of the study. The aim of using this binary activator depends on the reversible reaction that gives KOH as the target activator, which is obtained indirectly through the reaction of $Ca(OH)_2$ and K_2CO_3, as follows:

$$Ca(OH)_2 + K_2CO_3 \leftrightarrow 2KOH + CaCO_3 \qquad (3.2)$$

The molar ratio of K_2CO_3 to $Ca(OH)_2$ used in this test was 1.16. This molar ratio was formulated in such a way that it results in K_2O, which is equivalent to 1.5% Na_2O with respect to GF weight, while the w/GF ratio was 0.35.

F. $Ca(OH)_2$ and $CaCO_3$ –based system

A mixture of $Ca(OH)_2$ and $CaCO_3$, each with a dosage of 2.5% with respect to the total mass of GF by addition, was used. The w/GF ratio was also 0.35. This low concentration of $Ca(OH)_2$ was chosen to ensure the activity of GF at low concentration of $Ca(OH)_2$.

G. $Ca(OH)_2$ and Na_2SO_4 –based system

A binary mixture of 20% $Ca(OH)_2$ and Na_2SO_4 with a dosage equivalent to 1.5% Na_2O, was used. The equation shown below was taken into account. Therefore, this mixture can be considered as a quaternary mixture (containing the reactant and product of this reaction).

$$Ca(OH)_2 + Na_2SO_4 \leftrightarrow CaSO_4 + 2NaOH \qquad (3.3)$$

3.12.8 Ternary mixture

One ternary combination of activators was used to assess the effect of combining more than two activators on the development of the compressive strength.

A. $Ca(OH)_2$ -Na_2SO_4 - NaOH–based system

A ternary mixture of 20% $Ca(OH)_2$, Na_2SO_4, and NaOH equivalent to 1.5% Na_2O was investing. The dosage of Na_2SO_4 was formulated in molar ratio so that half of $Ca(OH)_2$ reacts with the entire quantity of Na_2SO_4 to from anhydrite.

3.12.9 Mortars

A. Sample preparation and mixing method

This mortar is prepared in the same way as the paste was prepared in the previous part, except for the sand, for which Ottawa sand was added directly after 30 seconds of adding GF to the

activator-containing mixing solution. The total mixing time was kept at 6 minutes as with the aforementioned paste part. The mixer used is shown in Figure 3.9

B. NaOH-activator

In this part of the study, a series of mortars made up of glass frit, Ottawa sand, and NaOH activator were tested. An activation temperature of 60°C and a concentration of 3% Na_2O were chosen as both values were found to be optimum based on the results of testing. Different GF-to-sand ratios were evaluated, as shown in Table 3.6. The reference flow value was taken to be about 25 ± 5 (as that used with ASTM C 227) and any sample that gave higher than this limit was rejected.

TABLE 3.6 COMPOSITION OF TESTED MORTARS

Mixtures	(GF/(GF+sand))%
M0.5	66.67
M1	50.00
M1.5	40.00
M2	33.33
M2.5	28.57

C. $Ca(OH)_2$ activator

Different amounts of portlandite (CH), with respect to total mass of GF, were added to GF. It is important to mention that CH was added to, and did not partially replace, GF. Two activation temperatures, i.e. 30 and 50°C, three CH addition values, and three w/GF ratios, because of the addition of three different CH dosages, were chosen, as shown in Table 3.7.

TABLE 3.7 COMPOSITION OF TESTED MORTARS

Sand/GF	(GF/(GF+sand)) (%)	CH (%)	w/GF
M1.5-1	40	10	0.445
M1.5-2	40	20	0.474
M1.5-3	40	30	0.506

3.12.10 Concrete

A. Materials

The physical and chemical properties of binders, activators, chemical admixtures, and the type and properties of fine and coarse aggregates were outlined earlier in this chapter.

B. Mixture proportions

The mix design of these mixtures is based on the mixtures used in studying the alkali-silica reaction in concrete according to CSA A23.1-14A, with some modifications required to simulate field concrete whereas the mix design used is shown in Table 5.9.

C. Samples preparation and mixing method

An ordinary rotating tilting drum concrete mixer was used to prepare the activated concrete, as shown in Figure 3.9. NaOH activator is dissolved in a bucket containing the whole amount of mixing water, while in the case of portlandite, it is pre-weighed with GF powder. The fine aggregate is added first to the drum mixer, followed by the coarse aggregate during the rotation of the drum, within 30 seconds after that, half the amount of mixing water was added followed by the binder for 2.5 minutes where the drum remained under rotation. During this time the second half of water was added. It was then stopped for another 2.5 minutes, after which it was left to rotate for 4 minutes. At this moment, the concrete is ready for fresh properties measurements.

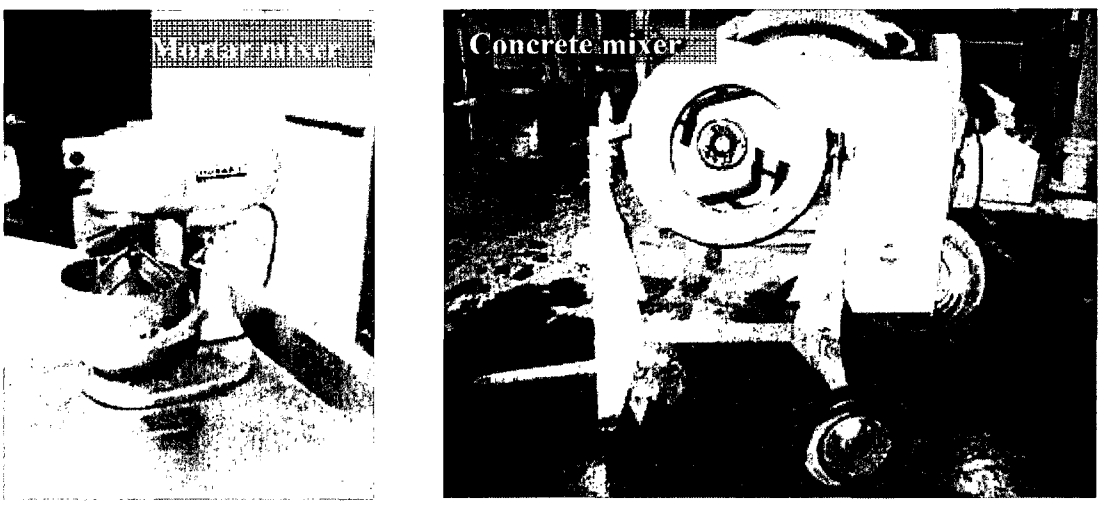

Figure 3.9 Two mixers used for mortar and concrete fabrication

3.13 Alkali-silica reaction studies on glass frit-containing mortar and concrete

3.13.1 Tests on mortars

A. Testing method

In this part, the effect of the presence of GF, with and without other mineral admixtures, on the linear expansion of mortar mixtures was investigated according to different specifications the following: CSA 23.2-25A, ASTM C227, and ASTM C1260.

B. Materials

Five types of aggregates were used: Ottawa, Aimé Côté, and LG sands, and Spratt and Mirabel aggregates. As well, different cement mixtures were used. The grading proportions used for preparing the mortar bars throughout this part of the study (for Aimé Côté sand and Mirabel and Spratt aggregates), are shown in Table 3.8.

St. Lawrence GU cement was the main cement used, which was partially replaced (% of mass) by different mineral admixtures according to the mix desig used. Commercial Canadian condensed silica fume (CSF) cement was also used in one test to show the effect of superplasticizer on the expansion of ternary mixtures containing silica fume.

TABLE 3.8 GRADING PROPORTION FOR THE AGGREGATE USED IN MORTAR BAR TEST (CSA A23.2-25A)

Sieve size		
Passing	**Retained**	**Mass %**
5 mm	2.50 mm	10
2.5 mm	1.25 mm	25
1.25 mm	630 μm	25
630 μm	315 μm	25
315 μm	160 μm	15

TABLE 3.9 WATER-TO-BINDER RATIOS ACCORDING TO THE SPECIFICATION USED

Specification	Water-to-binder ratio (w/b)
ASTM C227	That gives flow of mortar of 105-120
CSA A23.2-25A	0.44 for natural fine aggregate 0.5 for crushed coarse aggregates

C. Proportion of mortar

The dry materials for the test mortar were proportioned using 1 part cement and 2.25 parts graded aggregate by mass, w/c equal to 0.44 by mass for natural fine aggregates (Aimé Côté, and Ottawa sand), and 0.5 for the crushed coarse aggregate (Spratt and Mirabel aggregates). The flow table was also used to establish the required amounts of mixing water, where the flow value was to be in between 105-120 (according to ASTM C227 specification), as in Table 3.9. A test series is comprised of three mortar bar specimens measuring 2.54 X 2.54 X 28.5 cm. Samples are identified by a number indicating the percentage of each cementitious material, as well as by a symbol, for example S for slag, SF for silica fume, FA for fly ash, and finally GF for glass frit. The letters B, T and Q stand for binary, ternary, and quaternary mixtures, respectively. For example, T20GF5SF stands for a ternary mixture with 20% GF and 5% SF.

The following mortars were tested:

i- Binary mortars (cement plus either GF, slag, fly ash, or silica fume);

ii- Ternary mortars (cement + GF and either slag, fly ash or slica fume against commercial ternary cements);

iii- Quaternary mortars (ciment plus GF and silica fume plus either slag or fly ash).

The most important mixtures in this part of the study are the two main quaternary cements that were tested without any change in their compositions, as follows:

i- Quaternary cement – fly ash (25% GF, 20% fly ash, 5% silica fume);

ii- Quaternary cement – slag (25% GF, 30% slag , 5% silica fume).

D. Curing conditions

- 38°C, 100% R.H. (ASTM C227)
- 80°C , 1N NaOH (CSA A23.2-25A)

E. Linear expansion measurement

The length change can be calculated at any age using a length comparator in accordance with ASTM C490, as shown in Figure 3.10, as follows:

$$L = \frac{(Lx - Li)}{G} * 100 \qquad (3.1)$$

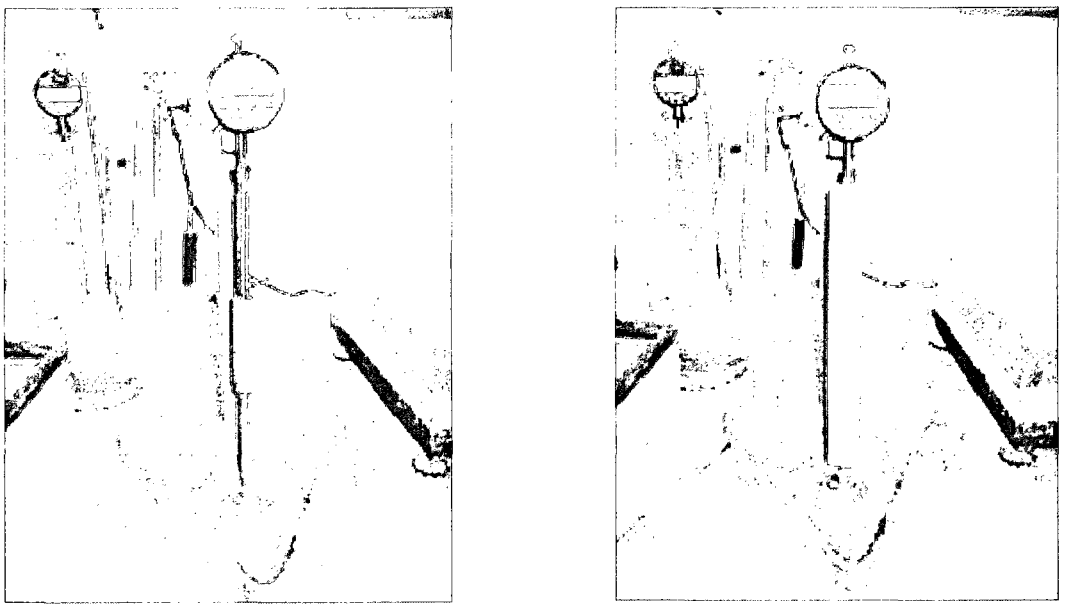

Reference bar Test bar

Figure 3.10 Length comparator and re-zero before reading

F. Storage of mortar bar containers

There are two types of mortar bar containers, as shown in Figure 3.11, depending on the type of specification used. For the accelerated mortar bar test, the bars were immersed in 1N NaOH

solution at 80°C, while for ASTM C227 the mortar bars were stored in containers lined with wicking material to ensure 100% R.H. and then stored at 38°C.

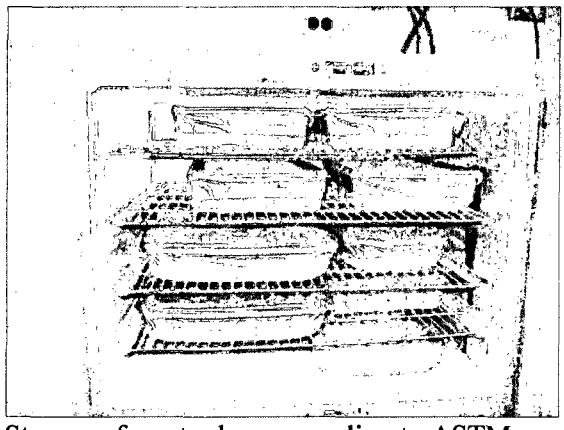

Storage of mortar bars according to ASTM CSA A23.2-25A (ASTM C 1260)

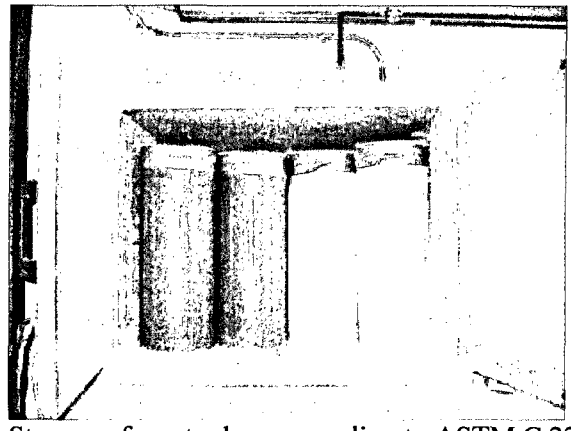

Storage of mortar bars according to ASTM C 227

Figure 3.11 Curing of different mortar mixtures according to type of specification used

G. Evaluation method

According to ASTM C 227 and C 33, when linear free expansion of mortar bar at 90 and 180 days is less than 0.05% and 0.1%, respectively, no harmful alkali aggregate reaction (AAR) would occur in concrete. As well, according to CSA A23.2-2A, accelerated mortar barexpansion of less than 0.15% at 16 days after casting is indicative of innocuous behaviour in concrete. Mortar bar tests are important tests that provide valuable information about the nature of interaction between GF and different types of mineral admixtures. In addition, these data could provide the compositions of the pessimum mixtures of GF with other mineral admixtures.

3.13.2 Tests on concrete

In this part of the study, CSA A23.2-14A specification was followed to study the effect of the presence of GF, with and without other mineral admixtures, on the linear expansion behaviour of the concrete prism of mixtures cured at 38°C and 100 % R.H. This specification is a long-term test, from which significant data were obtained after one year.

A. Materials

i) Cement and NaOH

St. Lawrence GU cement with a total Na_2O_{eq} alkali content of 0.86% was used. The total alkali content was calculated as:

$$Na_2O + 0.658\ K2O = Na_2Oeq \qquad (3.2)$$

Reagent grade NaOH was added to the concrete mix water to increase the alkali content of the cement used, expressed as Na_2O equivalent, to 1.25% by mass of cement.

ii) Aggregates

A non-reactive fine aggregate was used (Ottawa sand), while the coarse reactive aggregate (Spratt aggregate) was sieved into three equal parts using four sieves. The size fractions used were 20-14 mm, 14-10 mm, and 10-5 mm. The grading machine works in a way that sieving was conducted under continuous shaking process, as shown in Figure 3.12. Oversize and undersize grades were discarded.

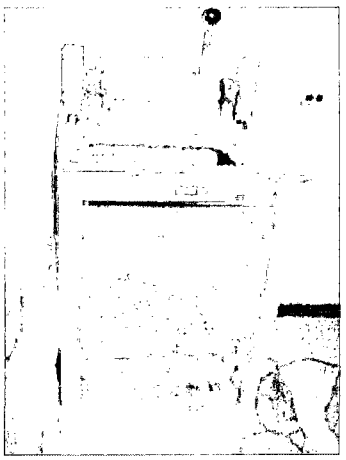

Figure 3.12 Sieving machine for Spratt aggregate

B. Concrete mixture proportions

A total of 19 concrete mixtures were proportioned as shown in Tables 3.10 with the following requirements:

- Cement content of 420 kg/m^3 of concrete;

- Coarse to fine aggregate ratio of 60:40 by mass;
- Effective water to binder ratio in the range of 0.42-0.45;
- NaOH was dissolved in mixing water to obtain total alkali content (Na_2Oeq) of 1.25 by mass of cement.

The mixtues made consisted of the following:
- Control cement concrete composed of 100% GU cement. Both Ottawa and Aimé Côté sands were used separately with Spratt aggregate to study the effect of Ottawa and Aimé Côté sands on ASR expansion. These samples were identified as Control (CO, control Ottawa), Control+(CO-Na), Control-A+(CA-Na, Control-Aimé Côté), where "Na" or "+" represents added alkali.

- Binary cement concrete mixtures composed of OPC partially replaced by 25 and 50% GF with and without added alkali. They were identified using the following symbols: B25GF, B25GF-Na, B50GF, and B50GF-Na, where Na denotes added alkali, which is sometimes, represented using the "+" sign. Ottawa sand and Spratt aggregate were the only aggregates used in these mixtures.

- Ternary cement concretes composed of OPC partially replaced by GF and silica fume in the presence or absence of both added alkali and SP. They were identified using the following symbols: T20GF5SF, T20GF5SF-Na, T20GF5SF-SP, and T20GF5SF-Na-SP, where Na denotes alkali, which is sometimes, represented using the "+" sign and where SP stands for PNS superplasticizer. Ottawa sand and Spratt aggregate were used in this part.

- Quaternary cement concretes composed of GU cement partially replaced by GF, silica fume, and slag or fly ash in the presence or absence of SP. In this part, Ottawa sand and Spratt aggregate were the only aggregates used and their mixture compositions are identified by Q25GF30S5SF+, Q25GF30S5SF, Q25GF30S5SF+SP, Q25GF30S5SF-SP, Q20GF25FA5SF+, Q20GF25FA5SF, Q20GF25FA5SF-SP, and Q20GF25FA5SF+SP. The "+" sign represents added alkali while "SP" represents added superplasticizer.

TABLE 3.10 MAIN MIX PROPORTIONS FOR CONCRETE PRISM MIXTURES WITH AND WITHOUT ADDED ALKALI

19 Concrete mixtures	w/c	SP (PNS)	Added alkali	Mix composition of tested concretes (Kg/m^3)							
				Cement	Slag	Fly ash	Silica fume	Glass frit	Ottawa sand	Aimé Côté sand	Spratt agg.
CO	0.45	-	-	420	-	-	-	-	712	-	1070
CO+		-	+	420	-	-	-	-	712	-	1070
CA+		-	+	420	-	-	-	-	-	712	1070
B25GF		-	-	315	-	-	-	105	709	-	1064
B25GF+		-	+	315	-	-	-	105	709	-	1064
B50GF		-	-	210	-	-	-	210	709	-	1064
B50GF+		-	+	210	-	-	-	210	709	-	1064
TSF		-	-	315	-	-	21	84	707	-	1060
TSF+		-	+	315	-	-	21	84	707	-	1060
TSF-SP+		+	+	315	-	-	21	84	707	-	1060
TSF-SP		+	-	315	-	-	21	84	707	-	1060
QFa		-	-	210	-	105	21	84	698	-	1050
QFa+		-	+	210	-	105	21	84	698	-	1050
QFa-SP+		+	+	210	-	105	21	84	698	-	1050
QFa-SP		+	-	210	-	105	21	84	698	-	1050
QS		-	-	168	126	-	21	105	702	-	1054
QS+		-	+	168	126	-	21	105	702	-	1054
QS-SP+		+	+	168	126	-	21	105	702	-	1054
QS-SP		+	-	168	126	-	21	105	702	-	1054

C. Storage of concrete prism

The concrete prisms were cured according to CSA 23.2-14A, in a vertical position inside a 25-L plastic container, then in a temperature-controlled cabinet, as shown in Figures 3.13 and 3.14, respectively.

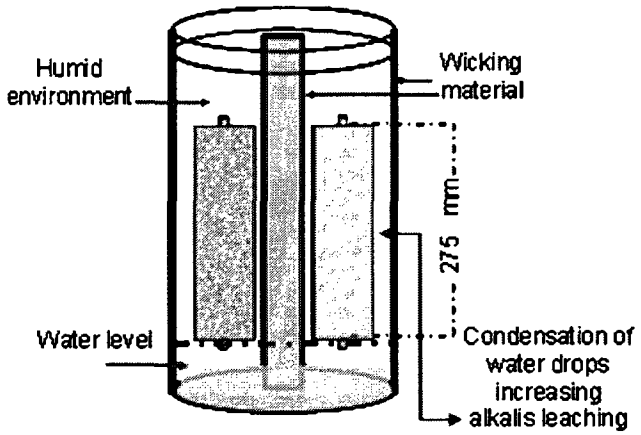

Figure 3.13 Mortar bar and concrete prism curing container set-up

Figure 3. 14 Curing chamber for concrete prism test adjusted at 38°C

D. Calculation of length change

The change in length of each prism is based on the initial measurement. The difference between the initial and each successive measurement is calculated and expressed as a percentage of the initial effective length, adjusted to reflect the fact that the effective length is the distance between the inner ends of the steel measuring studs and not the overall length [CSA 23.2-14A], as shown in Figure 3.15.

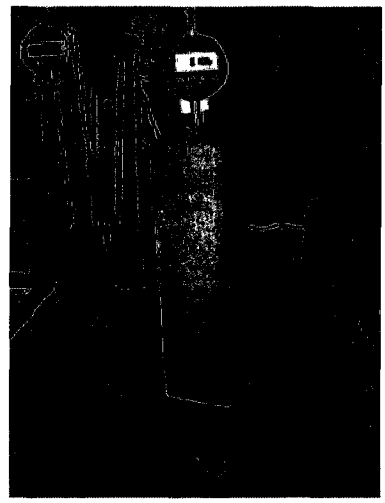

Figure 3.15 Length comparator for concrete prism samples

Samples of concrete cylinder with dimension of 100 X 200 mm were cured under the same test conditions and were tested for compressive strength after 2 years, to correlate the final expansion with final compressive strength.

3.14 Pore solution chemistry, micro-pores, and microanalysis

3.14.1 Pore solution chemistry

The expressed pore solution analysis was also undertaken. In this part of the study, pastes containing the same cementitious matrix and a water-to-binder ratio of 0.50, as shown in Table 3.11, were fabricated and cured at 38°C in a closed system to prevent evaporation or acquiring of humidity in order to prevent interaction with the surrounding environment.

TABLE 3.11 MIXTURE COMPOSITIONS OF THE MOST FREQUENTLY USED CEMENTITIOUS SYSTEMS

Mixtures	Symbol	Composition (%)
Control	**C10**	100% cement (0.9% Na_2O_{eq})
B25GF	**B25**	75% cement + 25% glass frit
B50GF	**B50**	50% cement + 50% glass frit
T20GF5SF	**TSF**	75% cement + 20% glass frit + 5% silica fume
Q25GF30S5SF	**Qs**	40% cement + 25% glass frit + 30% Slag + 5% silica fume
Q20GF25FA5SF	**QFa**	50% cement + 20% glass frit + 25% fly ash + 5% silica fume

Two pressure cycles were used; the first cycle was under squeezing pressure of 200kN, which was followed by release of the pressure, and the second cycle of the pressure was then applied under squeezing pressure of 1MN. The mixtures containing GF (B25 and B50) needed more pressure, where a squeezing pressure of 1.4 MN was applied to get the same volume of extracted water as from the control sample. When using the same pressure, the extracted pore water from Gf samples was nearly half of that given by the control; therefore, extrapressure was applied to get as much volume of pore water as possible.

A series of microstructural and micro-pore analyses was also carried out on these systems. The paste samples were prepared and placed in sealed plastic containers, and cured at 38°C for 3, 7, 28, and 180 days. At the time of each test, the data were obtained by squeezing the pore solutions from the blended cement pastes with an appropriate pore solution expression device, as shown in Figure 3.16, immediately followed by chemical analysis of the clear solution. The chemical analysis included the determination of Na^+, K^+, Ca^{+2}, and OH^- ions concentrations, as well as pH. The micro-pore analysis was conducted at 3, 7, 28, and 180 days of curing. The electrical conductivity of the extracted solutions was also determined at the same time as the chemical analysis using pH and conductivity meter.

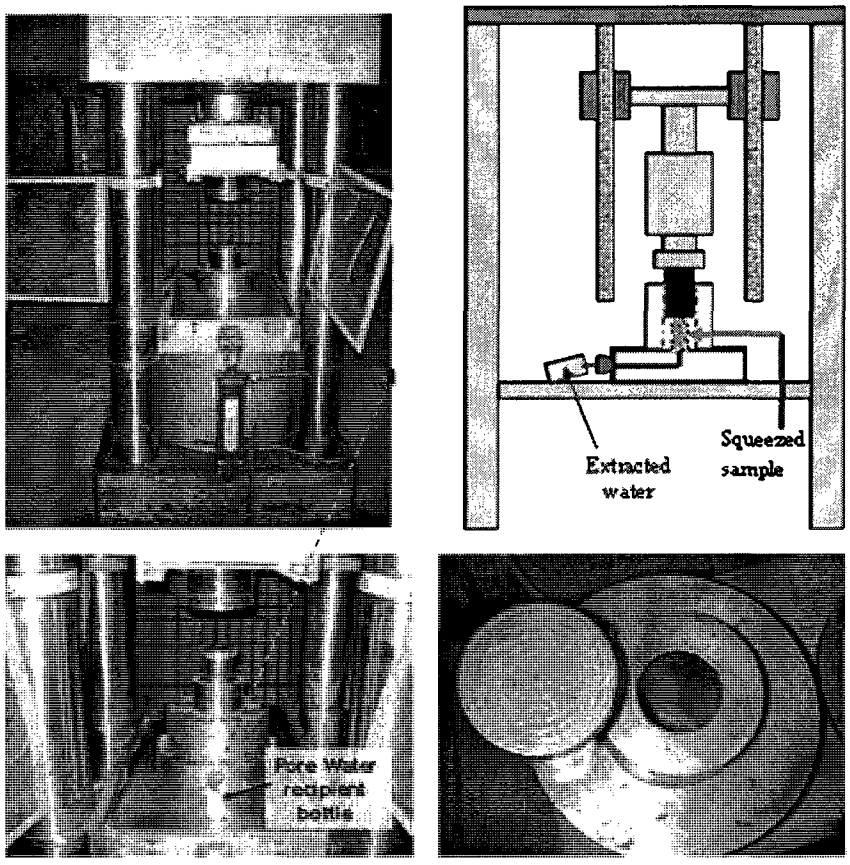

Figure 3.16 Pore solution expression device set-up

3.14.2 Pore size distribution analysis

Different control, binary, ternary and quaternary paste mixtures were tested for change in pore size distribution due to the change in their cementitious matrices after 28-day curing at 38°C. Different cement-to-water ratios were investigated in different control and ternary mixtures, in addition to two quaternary mixtures. The compositions of the cementitious mixtures tested are shown in Table 3.12. Some of these mixtures were used with superplasticizer at 0.8% as a dry extract with respect to cement content. Each mixture was tested three times and each curve represents the average of three results, as will be shown later in Chapter 6.

TABLE 3.12 MIXTURE COMPOSITIONS OF DIFFERENT CEMENTITIOUS SYSTEMS

Mixtures	W/C	SP, % Dry extract
Control	0.4	-
Control	0.45	-
Control	0.5	-
B25GF	0.5	-
B50GF	0.5	-
T20GF5SF	0.35	0.8
T20GF5SF	0.5	-
T25GF15S	0.35	0.8
T25GF15S	0.45	-
T20GF15FA	0.35	0.8
T20GF15FA	0.40	-
Q20GF25FA5SF	0.5	-
Q25GF30S5SF	0.5	-

The Pascal 240 porosimeter operates in the classic range from atmospheric pressure up to 200 MPa, as shown in Figure 3.17. This unit is a versatile, high-pressure porosimeter.

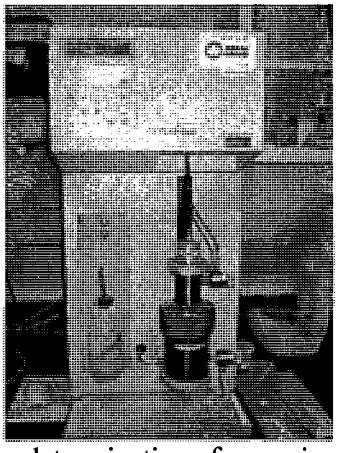

Figure 3.17 Pascal 240 porosimeter for determination of pore-size distribution

3.14.3 Microstructure analysis

Use of scanning electron microscope (SEM) is of great significance as it provides deep insight into microstructural changes between different cementitious systems, water-to-binder ratio, and curing time. The importance of the analyzing unit EDS, which is attached to the SEM, was attributed to its ability to carry out X-ray elemental spot analysis, mapping, and area

analyses. Jeol SEM is the device generally used in this part of study, as shown in Figure 3.18. Samples were fixed on an aluminum sample holder with carbon-based adhesive tape, which is coated with Au-Pd. Samples were observed using a JEOL JSM-840A scanning electron microscope, as well as with a Hitachi S-3400N scanning electron microscope, as shown in Figure 3.19. High resolution Hitachi FEG-SEM S-4700 was also used during this study (Figure 3.20). The S-4700 has a snorkel objective lens and achieves high resolution of 2.1 nm at low voltage of 1 kV and short working distances that are preferred for high-resolution work.

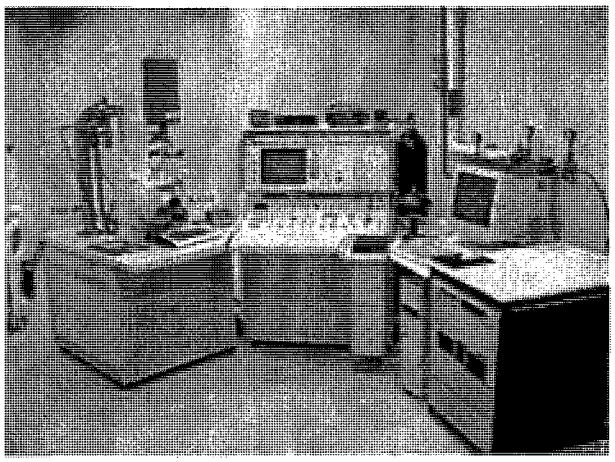

Figure 3.18 JEOL JSM-840A scanning electron microscope with EDXA unit

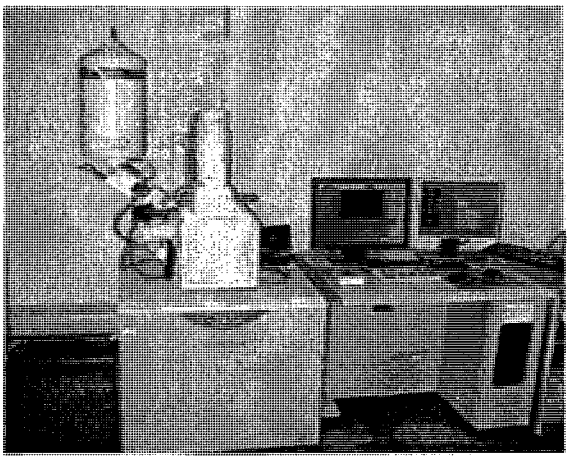

Figure 3.19 Hitachi S-3400N scanning electron microscope

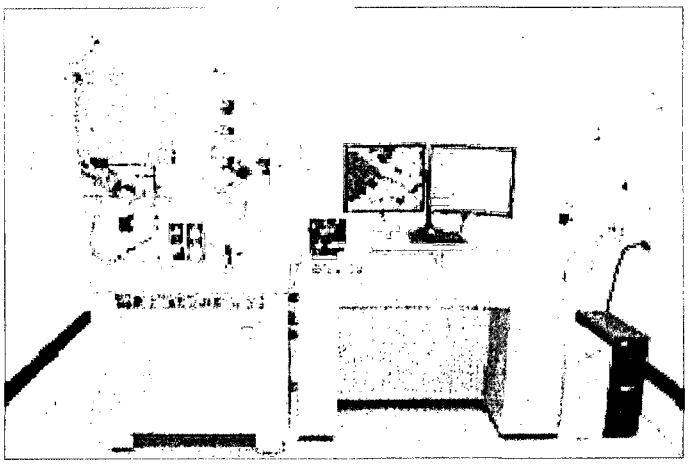

Figure 3.20 High resolution Hitachi FEG-SEM S-4700

A. Samples preparation for SEM analysis

The hardened paste samples are placed in a plastic mould. Epoxy resin was then cast into the mould and cured overnight at room temperature. The following day, the sample was removed and cut using an Isomet Buehler low speed saw equipped with a low concentration diamond wavering blade, as shown in Figure 3.24. The lubricant used during the cutting process was ISO Cut Fluid. The cross-section obtained was then polished using a Struers polishing machine (Model DAP-7, from Beta Diamond Products Inc.), as shown in Figure 3.24. Each paste was used with a separate Struers polishing cloth to avoid contamination. The sample was polished twice with each diamond paste at two different speeds (250 and 125 rpm) for 5 min. Following each polishing process, the sample was immersed in methanol, which is kept under ultrasonic vibration for at least 5 min before being sputtered under vacuum with gold/palladium (Au-Pd), and analyzed using the JEOL SEM, Model JSM-840A and the Hitachi SEM Model S-3400N at 20 kV.

3.15 Rheological studies

Four paste mixtures including control and binary mixtures containing 25, 50, and 75% GF were prepared in 500 mL containers and mixed using a kitchen blender. A quantity of 200 g of cement or GF-blended cements was mixed with cold water, at 5°C, and at water-to-cement ratio of 0.5 to compensate for heat generation resulting from the mixing action. The temperature of the paste was 22 ± 2 °C after mixing.

After 5 min from initial water and cement contact, consistency of the pastes was measured using a mini-slump cone. A plexiglass mini-slump cone was used to determine slump flow. It had an upper diameter of 19 mm, a bottom diameter of 38 mm, and a height of 57 mm. The tests were made on a plexiglass plate. The spread diameter or slump flow was obtained by the mean of two diagonal diameter measurements.

Following the slump flow determination, plastic viscosity and yield stress of the pastes were then determined using a co-axial rotating cylinder viscometer. The co-axial rotating cylinder viscometer (Chandler 3500) used for the determination of rheological properties had an outer cylinder radius of 18.42 mm, as shown in Figure 3.21. The height of the bob was 38 mm and

the gap between the bob and rotor was 1.17 mm. A paste sample of 350 ml was used for each test. The cylinder and the bob were kept within the paste prior to test for 20 seconds to allow the paste to fill the gap between the cylinder and the bob. The speed of the rotating cylinder was increased from 0 rpm to 300 rpm (510 s^{-1}) in 4 steps (3, 60, 100, and 300 rpm). The speed was then reduced to 3 rpm (5.1 s^{-1}) again stepwise, and measurements were taken at each of the following speeds: 300, 200, 100, 60, and 3 rpm (corresponding to 510, 340, 170, 10.2, and 5.1 s^{-1}, respectively). Each step continued for 20 sec, and the dial reading of the viscometer was recorded at the end of this period. The dial reading was converted to shear stress (in Pa) by multiplying the values with a coefficient of 0.511 which was supplied by the manufacturer of the viscometer. A linear fit (modified Bingham model) was used to estimate plastic viscosity and yield stress by regression analysis of the shear stress-shear rate data obtained from the descending curve. Apparent viscosity was expressed as the ratio of the shear stress to shear rate at any given shear rate using the descending curve again. The reason why the rheological measurements were made using the descending curve is that the behaviour of the pastes is dependent on their shear history. If the paste is not sheared before the test, the pastes will have different degrees of structuring. Shearing the paste under high speed at the end of the up-curve causes structural break-down and creates uniform conditions before testing.

Figure 3.21 Chan 35 Viscometer Model 3500 Chandler Engineering

3.16 Compressive strength machine

The compressive strength machine for mortar was adjusted at a loading rate of 2500 lb/10 s for all tested samples, as shown in Figure 3.22-a. This machine was mainly used in the

determination of the compressive strengths of the activated paste and GF mortar samples. The concrete samples were tested using the compressive strength machine shown in Figure 3.22-b with a loading rate of 1800N/s. Compressive strength normally represnts the average of three samples, which is approximated to the nearest integer value. This value is written over the curve or the histogram representing the compressive strength.

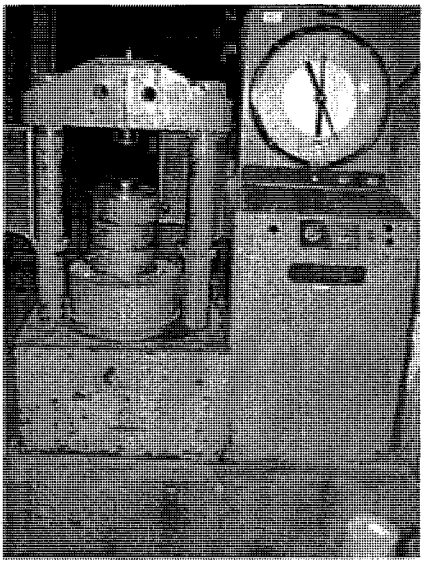

a-Compressive strength machine for mortar

b-Compressive strength machine for concrete

Figure 3.22 Compressive strength machines used during the study

3.17 Other instrumental devices

The devices used in this part of the study are of great importance and are available at the laboratories of the Université de Sherbrooke. These devices include XRD diffraction, scanning electron microscope with analyzing XRD probe (SEM-EDS), laser granulometry, pycnometer for density, and cutting and polishing machine.

3.17.1 X-ray diffraction (XRD)

Tested paste samples were manually grinded using an agate mortar to obtain sufficiently fine particles to avoid preferred orientations, which could affect results. The measurements were performed on PANalytical's version X-ray diffractometer, Model X'Pert Pro, implementing the following experimental parameters: Tension, 45 kV; Current 40 mA; Goniometer, Theta/Theta; Soller Slit, 0.04 rad., and Mask, 10mm with CuKα radiation working, as shown

in Figure 3.23. The readings were collected in the range of 2θ of 5-60°, with scanning rate of 0.04°/second.

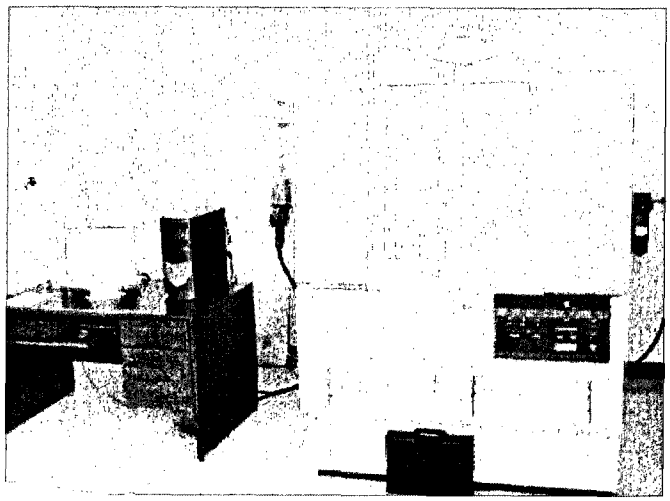

Figure 3.23 Philips X-ray diffraction device used for XRD analysis

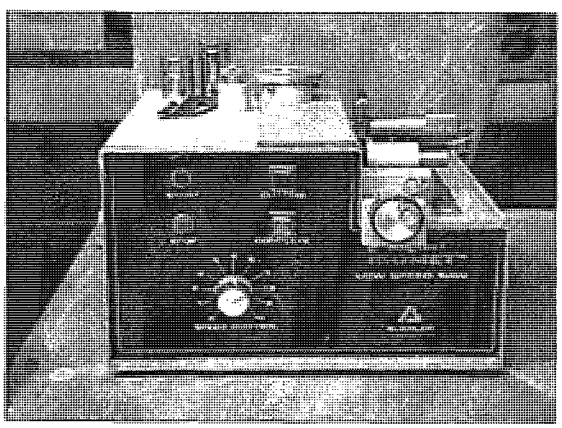

Cutting machine

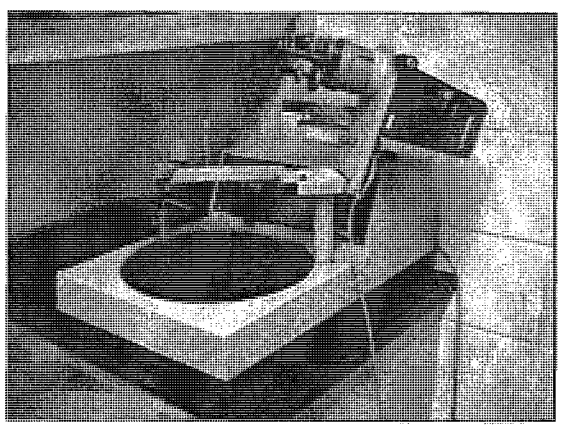

Polishing machine

Figure 3.24 Cutting and polishing machines for preparation of samples used in SEM analysis

The sputter coater uses an electric field and argon gas. The sample is placed in a small chamber that is at a vacuum, as shown in Figure 3.25. Argon gas and an electric field cause an electron to be removed from the argon, making the atoms positively charged. The argon ions then become attracted to a negatively charged gold/palladium foil. The argon ions knock gold/palladium atoms from the surface of the gold/palladium foil. The gold/palladium atoms

fall and settle onto the surface of the sample producing a thin gold/palladium coating of a thickness of 20 nm.

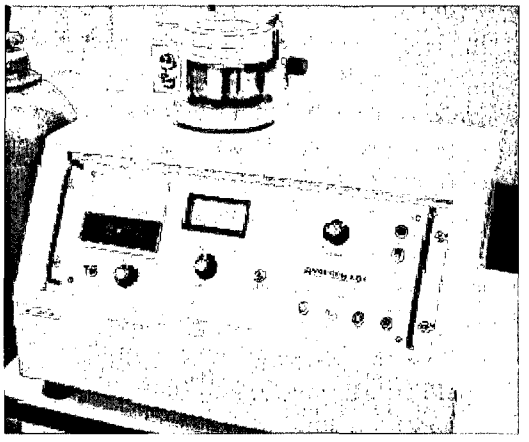

Figure 3.25 A sputter coater coats the sample with gold atoms

3.17.2 Particle size and density analyzers

The particle size analyzer used in this part of the study was a FRITSCH analysette22, while a Quantachrome multipycnometer was used for density throughout this study, as shown in Figure 3.26 and 3.27, respectively.

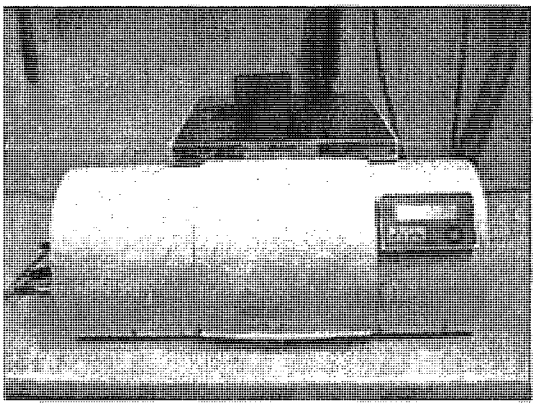

Figure 3.26 Laser granulometry

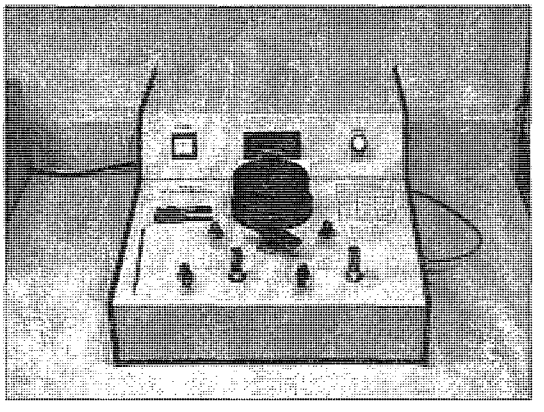

Figure 3.27 Pycnometer for density of powder samples

CHAPTER 4

CHARACTERIZATION OF GF AND OTHER MINERAL ADMIXTURES

4.1 Introduction

The characterization of GF and other mineral admixtures is important. The whole study is largely based on the results obtained from this part. The main physical and chemical properties of glass frit (GF) were obtained and compared with other cementitious materials (cement, CSF, Pfa and slag). The pozzolanic, hydraulic, mechanical, and some rheological properties of GF were studied.

4.2 Chemical analysis

The chemical analysis of GF and other cementitious materials is shown in Table 4.1, from which some parameters such as the lime-silica ratio, the basicity ratio, and the hydraulic index could be obtained. These parameters are very helpful in predicting the reactivity of GF and comparing it with other materials. Data obtained from this analysis are decisive from the ASR- and alkaline-activation points of view. Alkali content is critical and a matter of great concern in terms of ASR studies, while the hydraulic index is a good indication of the possibility of alkaline-activation. The use of spot analysis carried out with a scanning electron microscope (SEM-EDS) is extremely important to emphasize the chemical analysis as well as in calculating of C/S ratio in the overall C-S-H formed in different cementitious matrices.

4.3 Physical properties

Table 4.1 shows various physical properties, while the rest of the physical properties such as particle-size distribution, X-ray diffraction patterns, and microstructure, are shown in Figures 4.1 to 4.9, respectively.

TABLE 4.1 PHYSICAL AND CHEMICAL PROPERTIES OF CEMENTITIOUS MATERIALS

Oxide composition (%)	GF	OPC	Slag	PFa	CSF	Cem-SF
SiO_2	33.8	22.0	37.6	48.1	95.94	26.2
Al_2O_3	25.10	3.93	10.79	23.43	0.48	3.77
Fe_2O_3	3.40	3.76	1.37	17.53	0.15	3.77
CaO	14.6	63.3	42.45	2.24	0.63	56.4
MgO	0.76	1.91	7.03	0.86	0.33	1.9
Na_2Oeq	10.12	0.90	0.53	2.54	0.74	0.92
CaF_2	12.1					
SO_3		2.47	0.42	0.42	0.23	3.7
*Lime silica ratio	0.63	2.95	1.13	0.17		
**Basicity ratio	0.40	2.51	1.02	0.04		
***Hydraulic index	1.20	3.15	1.60	0.55	0.01	2.36
Loss on ignition (%)		<1	0.99	0.14	0.97	2.43
C_3S	N/A	58.76	N/A	N/A	N/A	N/A
C_2S	N/A	18.64	N/A	N/A	N/A	N/A
C_3A	N/A	4.05	N/A	N/A	N/A	N/A
C_4AF	N/A	11.44	N/A	N/A	N/A	N/A
Density	2.68	3.15	2.89	2.53	2.22	3.0
Fineness (m^2/kg)	419	420	410	410	17500	580
Specific surface, BET(m^2/kg)					20250	
Passing 45μm (%)	95	95	N/A	90	100	N/A
Time to initial set (min)	N/A	180	N/A	N/A	N/A	N/A
Time to final set (min)	N/A	365	N/A	N/A	N/A	N/A
Compressive strength (MPa)	N/A		N/A	N/A	N/A	
3 days		20.4				N/A
7 days		27.7				

*Lime silica ratio = CaO/SiO_2

**Basicity ratio = $(CaO + MgO)/(SiO_2 + Al_2O_3)$

***Hydraulic index = $(CaO + MgO + Al_2O_3)/SiO_2$

4.4 Particle-size distribution

The particle-size distribution of the three main cementitious materials is given in Figure 4.1, from which it can be observed tha. GF and slag had comparable particle-size distributions and are both finer than fly ash.

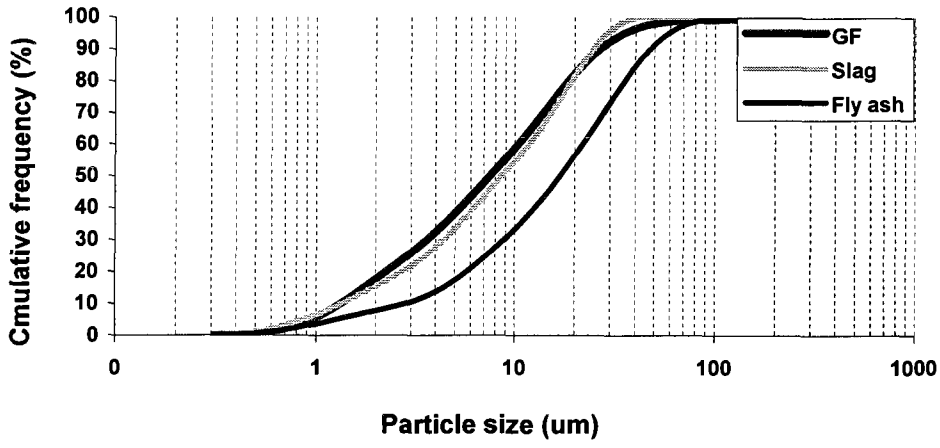

Figure 4.1 Particle-size distributions for GF, Pfa and slag

4.5 SEM-EDS analysis

This part of the study concerns the microstructural investigation of all of the mineral admixtures used, with special emphasis on GF as the main target of the study. GF was analyzed using micro- and nano-microprobe analyzers. The main elements found in the chemical analysis shown in Table 4.1 were confirmed by micro and nano-analyses, as shown in Figures 4.2 and 4.3.

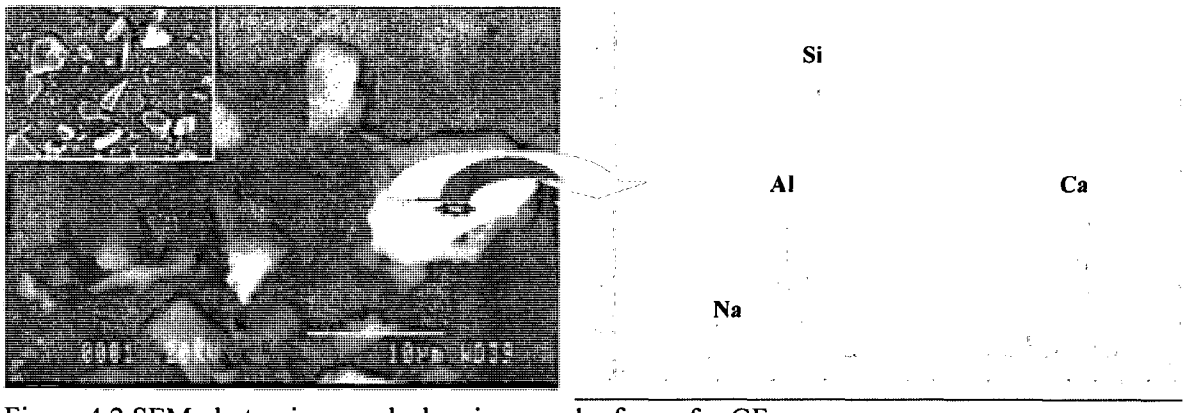

Figure 4.2 SEM photomicrograph showing angular forms for GF

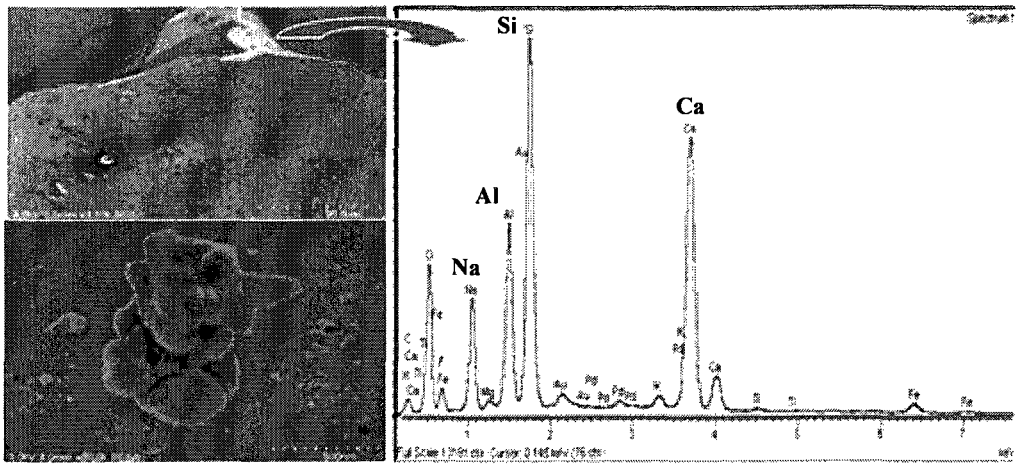

Figure 4.3 SEM Photomicrograph of glass frit powder (nano-scale)

Both GF and slag particles are irregular and angular in shape, while those of fly ash are spherical, and those of condensed silica fume appear in the shape of very fine particles and condensed in lump forms, as shown in Figure 4.4 and 4.5. These physical forms are important in the interpretation and analysis of results.

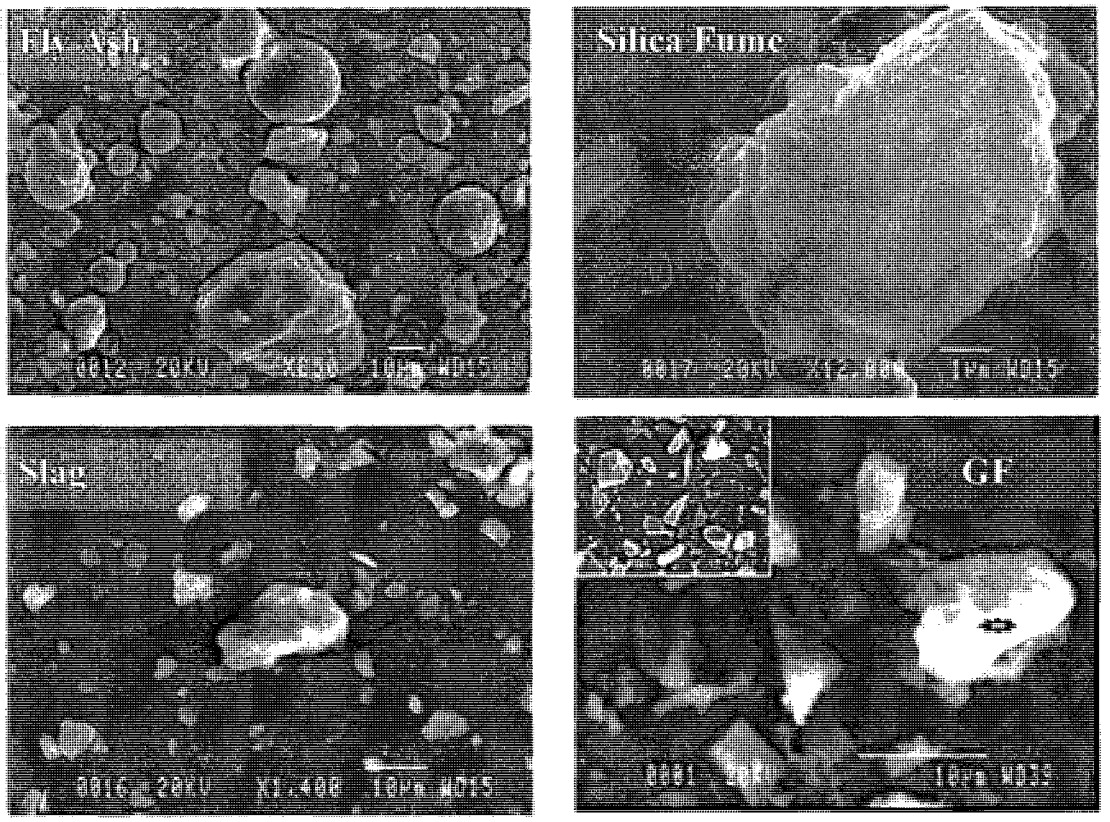

Figure 4.4 Photomicrograph of the four mineral admixtures used

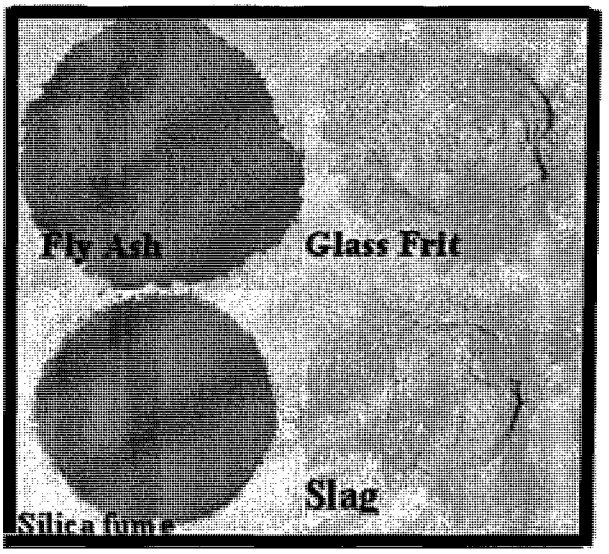

Figure 4.5 Powder state of the four mineral admixtures used

4.6 X-ray diffraction analysis

The X-ray diffraction patterns showed that GF is nearly 100% amorphous material, very comparable to silica fume and slag; these are classified as non-crystalline materials, as shown in Figures 4.6 to 4.9. The hump of GF is of intermediate intensity between slag and condensed silica fume. GF is then more amorphous than slag and less than that of condensed silica fume, as shown in Figures 4.6 to 4.8. XRD patterns of fly ash are completely different, where fly ash is mainly glassy (amorphous) with some crystalline inclusions of mullite (Mul), hematite (Hem), magnetite (Mag) and quartz (Qz).

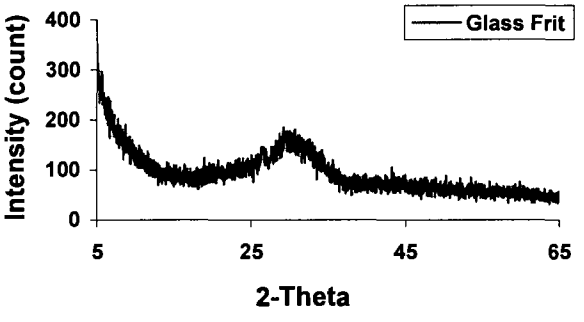

Figure 4.6 X-ray diffraction patterns for GF powder

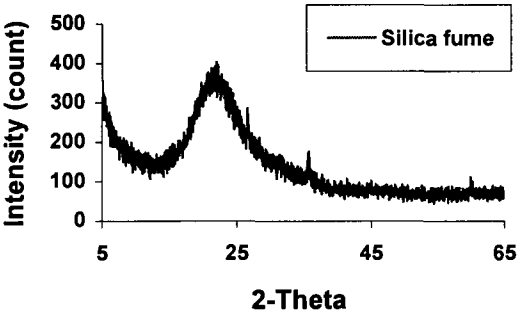

Figure 4.7 X-ray diffraction patterns for silica fume powder

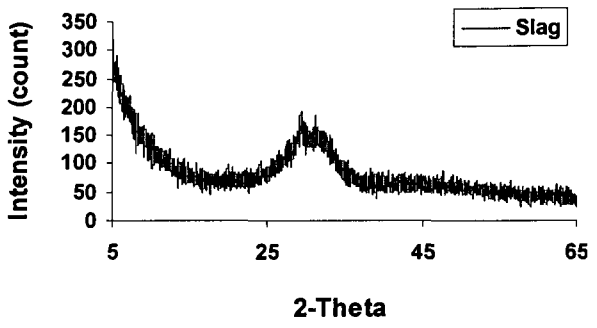

Figure 4.8 X-ray diffraction patterns for slag powder

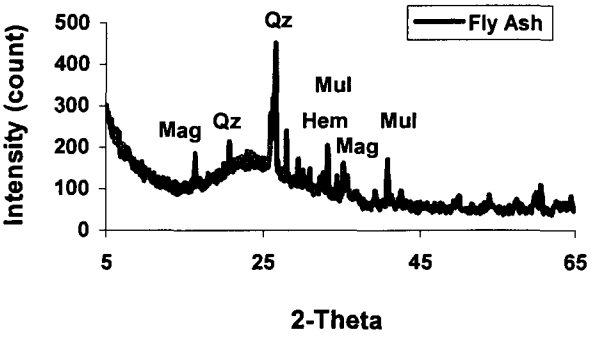

Figure 4.9 X-ray diffraction patterns for fly ash powder

Therefore, according to the hump of amorphicity given by XRD analysis (under the same conditions) of the three mineral admixtures and GF, these admixtures can be arranged, in a descending order, as follows:

Silica fume > GF > Slag > Fly ash

Hence, it is expected according to this preliminary test that fly ash has slow reactivity with respect to other mineral admixtures used. As well, it is expected that its thermal activation needs more energy to overcome the energy barrier because of the crystalline compounds.

4.7 Chemical reactivity of GF

The chemical reactivity of GF, especially its reactivity with acids and bases, is of great significance. Comparative laboratory observation of the reactivity of mineral admixtures with different acids and bases has been summarized and shown in Table 4.2. Comparison between GF, slag, and fly ash was carried out to investigate the chemical behavior of GF with respect to other well-known mineral admixtures. The data derived from Table 4.2 and Figure 4.10 show that GF is an amphoteric material with a dual nature reacting with acids as a base and with base as an acid. The reactivity with acids is a type of decomposition reaction, which can be taken as a benefit for acid activation or structure changes by acidic modification depending on the chemical composition of the rest of the material.

TABLE 4.2 CHEMICAL REACTIVITY OF GF, PFA, AND SLAG WITH DIFFERENT ACIDS AND BASES

Observation		Glass frit	Slag	Fly Ash, class F
Acidity	NaOH	+ (- ΔT)	+ (+ ΔT)	+ (- ΔT)
	$Ca(OH)_2$	+ (- ΔT)	+ (+ ΔT)	+ (- ΔT)
	Na_2CO_3	+ (- ΔT)	+ (+ ΔT)	+ (- ΔT)
	Na_2SiO_3	+ (expansion, cracks)	+ (shrinkage, cracks)	-
Basicity	HCl	-	+ (+ ΔT)	-
	HNO_3	+ (+ ΔT)	+ (+ ΔT)	+ (+ ΔT)
	H_2SO_4	-	+ (+ ΔT)	-

+ = +ve reaction, - = -ve reaction, +ΔT= exothermic reaction, and -ΔT= endothermic

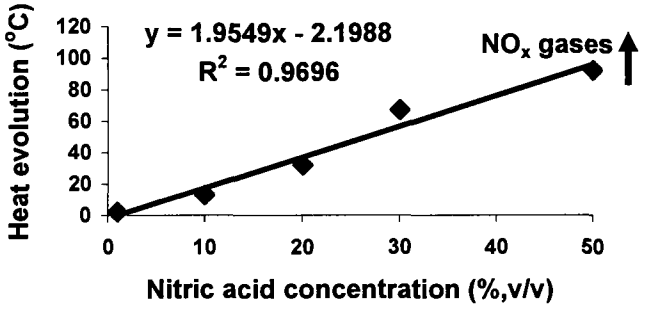

HNO3 (%, v/v)	$T_{initial}$ (°C)	T_{final} (°C)	ΔT
1	23	25	2
10	23	36	13
20	23	55	32
30	23	90	67
50	23	115	92

Figure 4. 10 Reactivity of GF with different concentrations of nitric acid

The reactivity of GF in alkaline media is essential and considered as the basis for the activation of GF into clinkerless binder (Chapter 5). In the current chapter, the hydraulic and pozzolanic properties of GF were explored and assessed, paving the way for real application of clinkerless-activated GF cement.

4.8 Investigation of the pozzolanic and hydraulic activity of GF

4.8.1 Pozzolanic activity

A. ASTM C311

ASTM C311 specification was used to evaluate the strength activity index of GF with Portland cement. In the test mixture, 25% cement used in the control mixture was replaced by the same mass of GF powder, instead of 20% GF as recommended in ASTM C311. The use of 25% GF as cement replacement is suggested because 25% GF is the actual dosage that was

used in the alkali-silica reaction studies. The mixture proportion was 1:2.75 for cement or blended cement and the standard graded sand, respectively. The water-to-cement ratio was 0.484 for the control mixture, while for the GF-cement mixture, 0.482 helped maintain the same flow. After casting 50-mm cubes and demoulding them according to ASTM C 109, the cubes were stored in lime-saturated water, and compressive strengths were determined at 1, 7 and 28 days of age. The strength activity index with Portland cement was determined as follows:

$$\text{Strength activity index} = (A/B)^* 100 \qquad (4.1)$$

where: A = average compressive strength of test mixture cubes (MPa), and B = average compressive strength of control mixture cubes (MPa).

Another mixture with the same composition was prepared at the same time, but after demoulding, the cubes were heat-cured by immersion in hot water, at 80°C in a sealed container. The strength activity indices of each mixture at different curing times are shown in Table 4.3 and Figures 4.11 and 4.12.

TABLE 4.3 STRENGTH ACTIVITY INDEX FOR 25% GF AT DIFFERENT CURING TEMPERATURES

	Strength activity index		
	1d	7d	28d
21 ± 2°C	84.08	91.84	114.56
80 ± 2°C	91.36	86.22	103.26

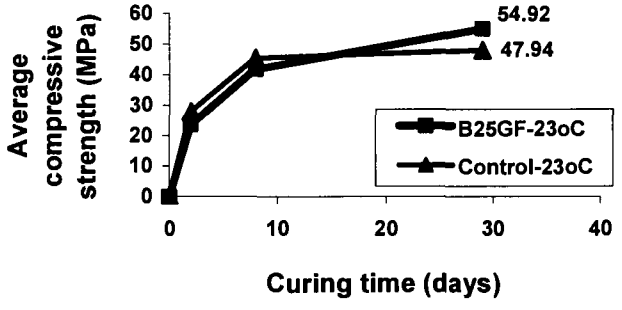

Figure 4.11 Compressive strength of 25% GF binary mortar mixture cured at normal temperature

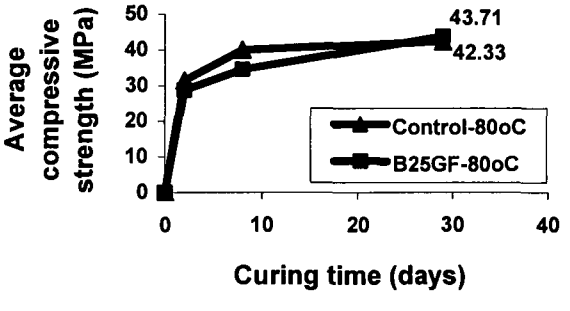

Figure 4.12 Compressive strength of 25% GF binary mortar mixture cured at 80°C

The results showed that 25% GF replacement contributed to the development of compressive strength. The mixture containing 25% GF resulted in higher compressive strength than the control mixture after 28 days under normal curing conditions. The same trend was also observed with heat curing. The heat-cured mixtures gave lower compressive strength than those cured under normal curing conditions, as shown in Figures 4.11 and 4.12.

B. ASTM C593

This test is intended to qualify pozzolans for use with lime. The pozzolanicity of GF with lime at 55°C was determined according to ASTM C593, and the mixture design is shown in Table 4.4. The compressive strengths should be calculated after 7 days according to ASTM C593, but they were determined at 1, 3, and 7 days. The results showed that the compressive strength at 1 day is about 25 MPa, whereas at 7 days the compressive strength reached 32 MPa, as shown in Figure 4.13. Therefore, GF has substantial pozzolanic properties according to ASTM C593, which recommended a minimum compressive strength of 4.1 MPa.

TABLE 4. 4 POZZOLANIC REACTIVITY OF GF WITH LIME

Constituents	Values used
Hydrated lime (CH)	33.33%
GF	66.67%
Graded Ottawa sand/(GF+lime)	2.74
Water/(GF+lime)	0.59

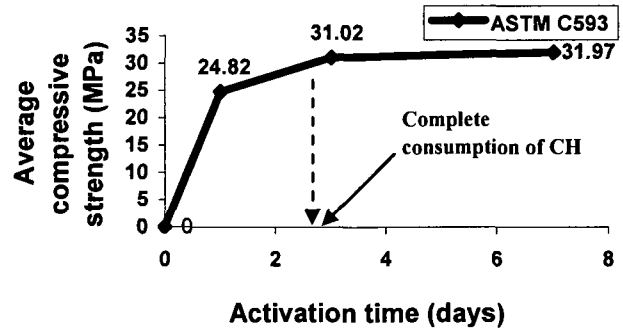

Figure 4.13 Compressive strength of GF mortar activated by lime according to ASTM C593

4.8.2 Hydraulic activity

A. ASTM C1073

The hydraulic activity of GF and slag by reaction with alkali was also determined according to ASTM C 1073. Instead of normal mixing water, a reagent of sodium hydroxide solution at 20% concentration and a solution/binder ratio of 0.45 by volume of solution and mass of binder with a curing temperature of 55°C were used. The calculated quantities of the materials were mixed in one batch to prepare the test specimens, as shown in Table 4.5. There is no test limit has been recommended by ASTM C1073 specification.

TABLE 4.5 CONSTITUENTS TO BE USED IN THE HYDRAULIC ACTIVITY INDEX TEST

Constituent	Mixture
Graded standard sand (g)/ test sample (g)	2.75
NaOH solution (20%), (mL)/ test sample(g)	0.45
Average compressive strength (MPa) for slag	19 MPa
Average compressive strength (MPa) for GF	31 MPa

The hydraulic activity is the average of the compressive strengths of three cubes at 24 hours. It was found that the hydraulic activity of slag with NaOH at 55°C is 19 MPa, while that of GF is 31 MPa. Therefore, according to ASTM C 1073 specification, that did not recommend a specific limit, slag has a hydraulic activity index of about 61% of that obtained with GF. According to ASTM C 593 and C 1073, NaOH activator is more effective than a $Ca(OH)_2$ activator. NaOH activator gave a compressive strength at 24 hours equal to what was given by $Ca(OH)_2$ after 7 continuous days under activation condition.

4.8.3 Compressive strengths

The development of compressive strength due to the addition of GF, which partially replaced cement used in fabricating mortar mixtures at different conditions, was investigated. The importance of this test is that it reflects the direct effect of the pozzolanic reactivity of GF on the development of compressive strength with time.

In this test, mortar cubes measuring 5 X 5 cm were fabricated using Ottawa sand to ensure the absence of any side effect due to ASR reactivity of aggregates used, which may affect the evolution of compressive strength with time. The cubes were cured in lime-saturated water at 21±1°C. The compressive strength development with time was determined until 2 years. Figure 4.14 shows the effect of incorporating 25% GF partially replaced GU cement used in this test. The binary mixture with 25% GF shows higher compressive strength from 28 days until 2 years, as an indication of the continuous pozzolanic reactivity and the stability of such binary system with time.

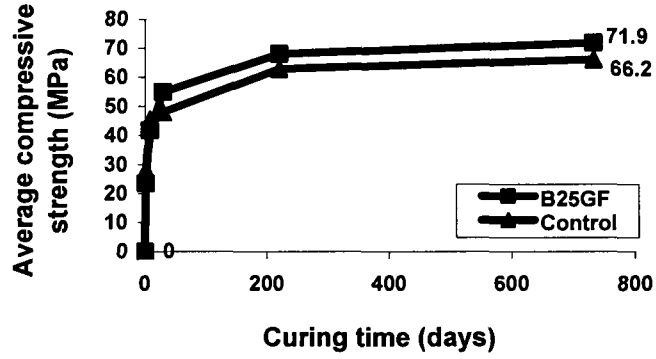

Figure 4.14 Long-term compressive strength of 25% GF binary mortar mixture cured at normal temperature

4.9 Resistance to sulfate attack

4.9.1 Expansion due to sulfate attack

Sulfates are widespread in soil, ground water, and seawater. Damage caused by sulfates has been observed particularly in foundations, sewage systems, and marine structures. The long-established explanation of sulfate attack is that sulfate reacts with calcium hydroxide, $Ca(OH)_2$, to form gypsum. The gypsum may then react with tricalcium aluminate C_3A in the concrete to form ettringite and monosulfoaluminate. These reactions result in substantial increase in volume with subsequent cracking. ASTM C1012 was employed to evaluate the inhibiting effect of binary mixtures containing GF to sulfate attack on cement mortar. The test consists in preparing three mortar prisms (25.4 X 25.4 X 279.4 mm) using Ottawa sand with a special pin cast in both ends of the specimen to facilitate length change measurement. The water-to-binder ratios for the control, 25% GF, and 50% GF mixtures were, 0.485, 0.459, 0.436, respectively. The specimens were cured in limewater until they achieved strength of 20

MPa, and were then placed in the sodium sulfate solution. The change in length was monitored using a length comparator at designated test times. The cement binder is considered sulfate-resistant if the expansion does not exceed a pre-selected value, of 0.1%, after 6 months for moderate sulfate resistant binder or a year for high sulfate-resistant binder. At 6 months, the control mixture (made with the type GU cement of Table 4.1) has surpassed the specification limit at about 3 months, while the 25% GF mixture approaches the borderline of the specification limit. The mixture with 50% GF, for its part, is still far from the specification limit and it can be said that it did not react with the sulfate solution, which is a good indication of the high sulfate resistivity of this mixture, as shown in Figure 4.15.

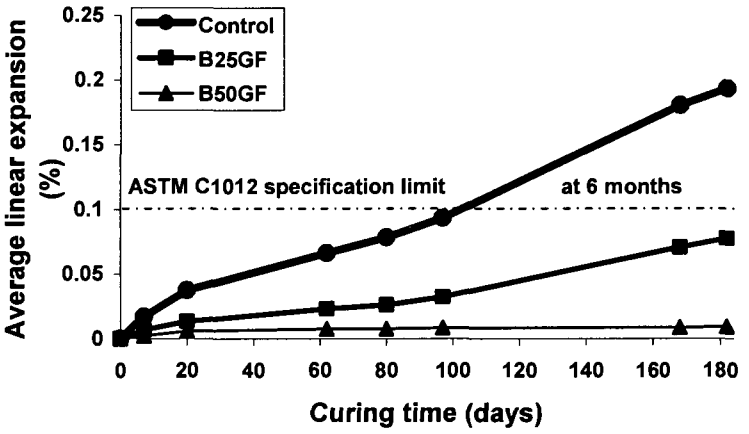

Figure 4.15 Resistance to sulfate attack at 6 months

4.9.2 Effect of sulfate attack on compressive strength

The compressive strength of 5 X 5 X 5 cm cubes made of the same mortar according to ASTM C1012 specification was investigated with time. The importance of this study is that it shows the effect of sulfate attack on the expansion of mortar containing different dosages of GF, as well as the effect of such attack on the development of compressive strength of the same mortar with time. Figure 4.16 shows that the binary mixture with 50% GF is still acquiring compressive strengths with time whereas, the binary mixture with 25% GF and the control stopped acquiring compressive strength at earlier times. This result is in accordance with other test results obtained in the next chapters of the present study. It is worth mentioning that the binary mixture containing 25% GF suffered remarkable disintegration at 1 year, as shown in Figure 4.17

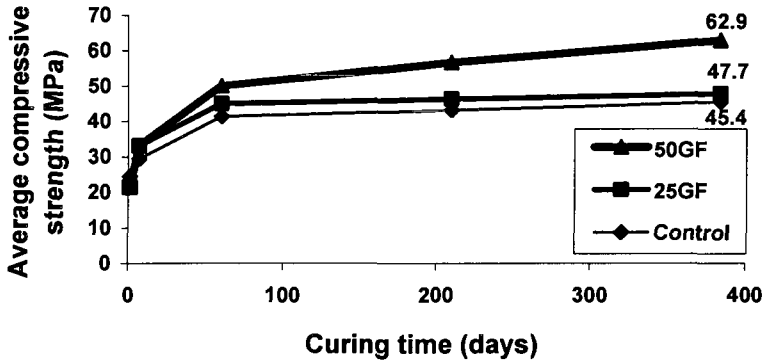

Figure 4.16 Progress of compressive strength in sulfate attack environment

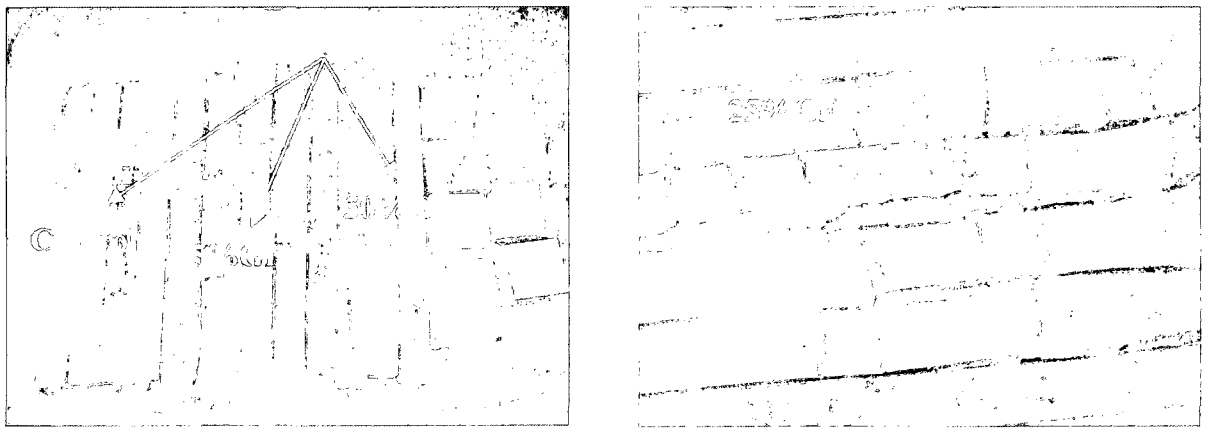

Figure 4.17 Effect of sulfate solution after 2 years immersion, binary mixture containing 25% GF was damaged by sulfate solution

4.10 Rheological studies

4.10.1 Mini-slump test

This test is a multi-purpose test that was carried out on GF binder pastes. The effect of water-to-cement ratios, as well as the effect of the partial replacement of cement by GF-based binders, on the flowability of the corresponding pastes was determined. The compatibility of these binders with superplasticizer was also investigated. Different systems including binary, ternary, and quaternary mixtures were studied. These systems were also tested for ASR expansion, as shown in Chapter 6.

The most important cementitious systems used in this part of the study are listed in Table 4.6. These mixtures were used in mortar and concrete. Some of the mixtures in Table 4.6 have

been mechanically tested by [LALDJI AND TAGNIT-HAMOU, 2006; 2007; TAGNIT-HAMOU, LALDJI, 2004] and were chosen for their satisfactory results.

TABLE 4.6 MIXTURE COMPOSITIONS OF THE MOST FREQUENTLY USED CEMENTITIOUS SYSTEMS

Mixes	Composition (%)
Control	100% cement (0.9% Na_2O_{eq})
B25GF	75% cement + 25% GF
B50GF	50% cement + 50% GF
B75GF	25% cement + 75% GF
T25GF15S	60% cement + 25% GF + 15% Slag
T25GF15FA	60% cement + 25% GF + 15% fly ash
T20GF5SF	75% cement + 20% GF + 5% silica fume
Q25GF30S5SF	40% cement + 25% GF + 30% Slag + 5% silica fume
Q20GF25FA5SF	50% cement + 20% GF + 25% fly ash + 5% silica fume

Different control mixtures were made using different water-to-binder ratios of 0.4, 0.45, and 0.5 to compare with the ternary mixtures containing GF, slag, fly ash, and silica fume, while the binary, ternary, and quaternary mixtures containing GF were used with water-to-binder ratio of 0.5. The effect of GF replacement level on the flowability of its mixtures is clearly shown in Figure 4.18, where the mixture containing 25% GF gives more flowable consistency than the other mixtures, including the control. Therefore, 25% GF decreases the water demand in the paste, and as the water-to-binder ratio was kept constant, an increase in flowability is expected. On the other hand, replacement levels of 50 and 75% GF decreased the flowability, as shown in Figure 4.18. The reduction in flowability by increasing GF dosage was attributed to the viscosity of the mixture containing this dosage of GF, as proven by the reduced viscosity measurements mentioned in this chapter (refer to 4.10.2).

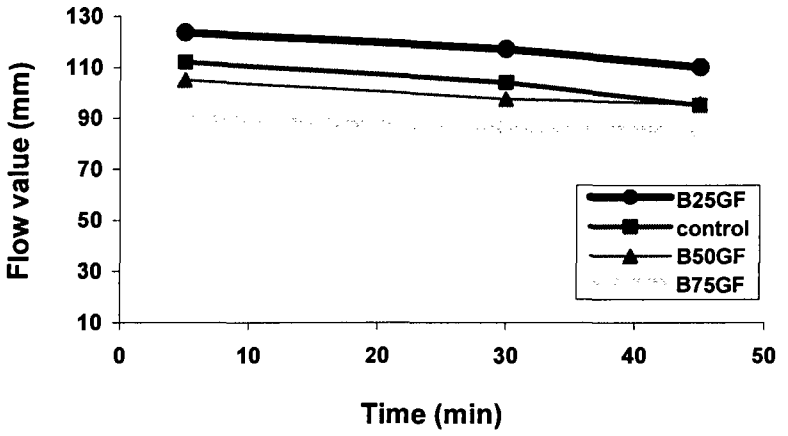

Figure 4.18 Flow value of different binary mixtures

By comparing the mixtures to each other, which are control, B25GF, B50GF, T20GF5SF, Q25GF30S5SF, and Q20GF25FA5SF at constant water-to-cement ratio of 0.5, an expected behavior was observed, as shown in Figure 4.19. That is to say, the mixtures containing silica fume gave very low flowability and the ternary mixture of T20GF5SF gave zero flow from the beginning until the end of the test. The Q20GF25FA5SF quaternary mixture was slightly better, as it gave relatively poor flowability after 5 minutes and 30 minutes, but reached zero reading at 45 minutes; The other Q25GF30S5SF quaternary mixture has lost its flowability after 5 minutes where it gave zero reading at 30 minutes. On the other hand, the control and the three binary mixtures, B25GF, B50GF, and B75GF are still flowable until 45 minutes, as shown in Figure 4.18. These curves show the effect of GF in presence of other mineral admixtures on the flowability of mixtures containing these binders.

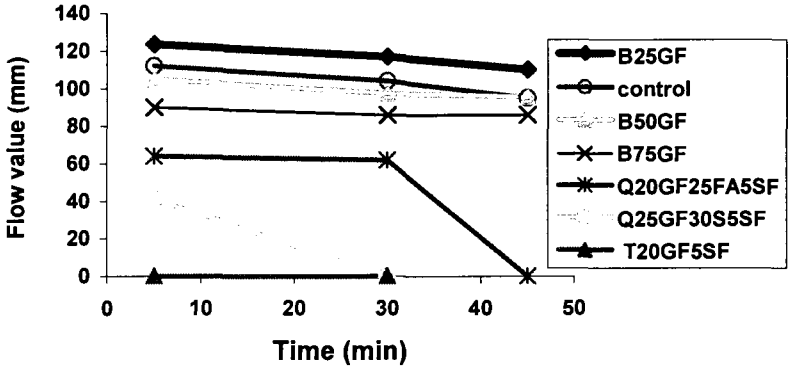

Figure 4.19 Flow value of the main cementitious mixtures

4.10.2 Viscosity by rheometer

In this part of the study, the effect of GF addition on the rheology of different pastes was investigated. The plastic viscosity for each of the four binary mixtures containing GF with replacement levels of 0, 25, 50, and 75%, was calculated from the slope of the rheogram shown in Figure 4.20 and the results given in Table 4.7. The slopes of these curves were obtained from modified Bingham model where the points fit the second order equation.

$$\tau = \tau_o + \mu_p.\dot{\gamma} + c\dot{\gamma}^2$$

where τ is the shear stress (Pa), τ_o is the yield stress (Pa), μ_p is the plastic viscosity, c is insignificant constant, and finally $\dot{\gamma}$ is the shear rate (s^{-1}). As $c\dot{\gamma}^2$ is very small, it can be neglected. The plastic viscosity was obtained from the second order equation. It is important to remember that:

$\tau = \theta * 0.511$, where θ is the angle of deflection, and γ = speed (rpm)*1.7

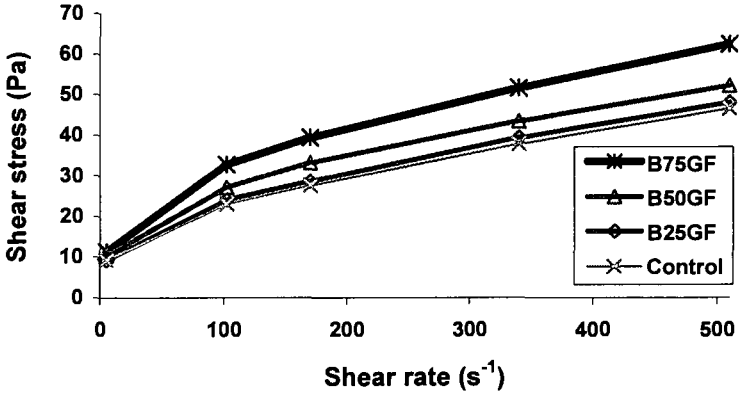

Figure 4.20 Rheogram for cement paste made with different GF replacement levels

TABLE 4.7 PLASTIC VISCOSITY AND YIELD STRESS OF THE FOUR PASTE MIXTURES

Mixtures	Plastic viscosity (Pa.s)	Yield stress (Pa)	R^2
Control	0.1197	9.804	0.99
B25GF	0.1270	9.871	0.99
B50GF	0.1491	11.042	0.99
B75GF	0.1818	12.539	0.98

The relationship between flow and yield stress is shown in Figure 4.21. The flow of different mixtures containing GF is inversely proportional to yield stress, the initial stress needed to cause these mixtures to move. As the viscosity of the mixtures increases with increase in GF content, the flow value decreases and yield stress increases. It is important to note that the mixture containing 25% GF had a higher flow value than that of the control, and both mixtures had nearly the same yield stress. This finding was supported by the mini-slump test, which showed that the mixture containing 25% GF gave higher flowability than the control mixture at the same water-to-cement ratio.

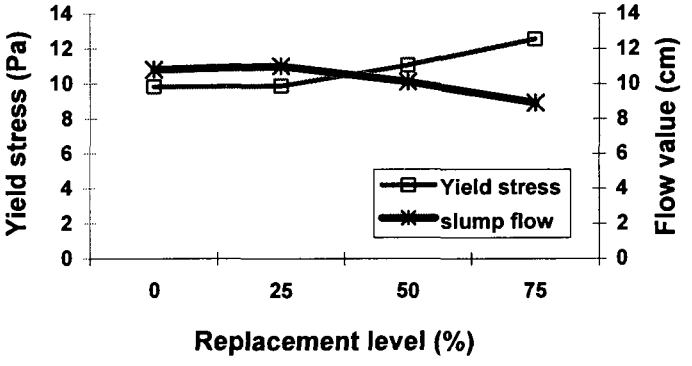

Figure 4.21 Relation between yield stress and mini-slump flow

4.11 Electrical conductivity and heat evolution

The electrical conductivity of cement paste can be used as an effective means of studying the progress of cement hydration and for monitoring structural changes occurring within the paste. Five binary mixtures were studied in this part of the study. This binary mixtures are 25 and 40% slag (B25S and B40S), 25% fly ash (B25Fa), 25% GF (B25GF) and 5% silica fume

(B5SF). Figure 4.22 shows that the electrical conductivity of the binary mixture with 5% SF is higher than all mixtures at the beginning, due to its fineness. As well, Figure 4.23 shows that ternary mixture of GF with slag is the highest among the other ternary with fly ash and silica fume, as an indication of its higher reactivity at the beginning of the reaction. On the other hand, the ternary mixture of GF with silica fume is the most reactive mixture as it has the lowest electrical conductivity.

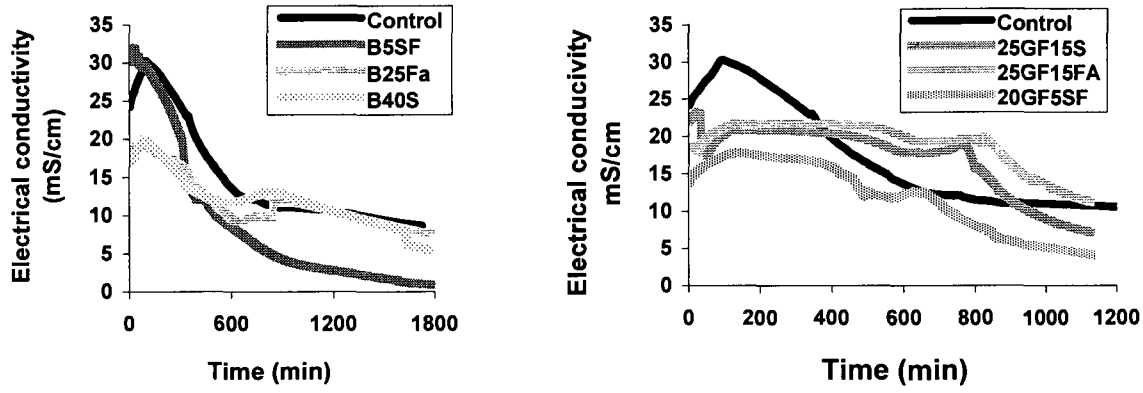

(a) Binary mixtures

(b) Ternary mixtures

Figure 4.22 Electrical conductivity of different binary and ternary mixtures

Heat of hydration is another important property, which reflects the reactivity of the blended cement mixture with respect to the control mixture. Generally, the addition of mineral admixtures decreases the heat of hydration. As silica fume is much finer than GF, slag, and fly ash, its binary mixture develops higher temperature than the other binary mixtures, as shown in Figure 4.23(a). As well, B25S develops silghtly higher temperature than that B25GF mixture, as shown in Figure 4.23(a). Accordingly, 20GF5SF ternary mixture (20% GF and 5% SF) is more reactive than the ternary of 25% GF with 15% slag or 15% fly ash (25GF15S and 25GF15Fa), which can also be attributed to the difference in the replacement levels. Due to its slow pozzolanic reactivity, the ternary mixture with GF and fly ash gives lower heat of hydration due to the lower reactivity of fly ash, as shown in Figure 4.23(b).

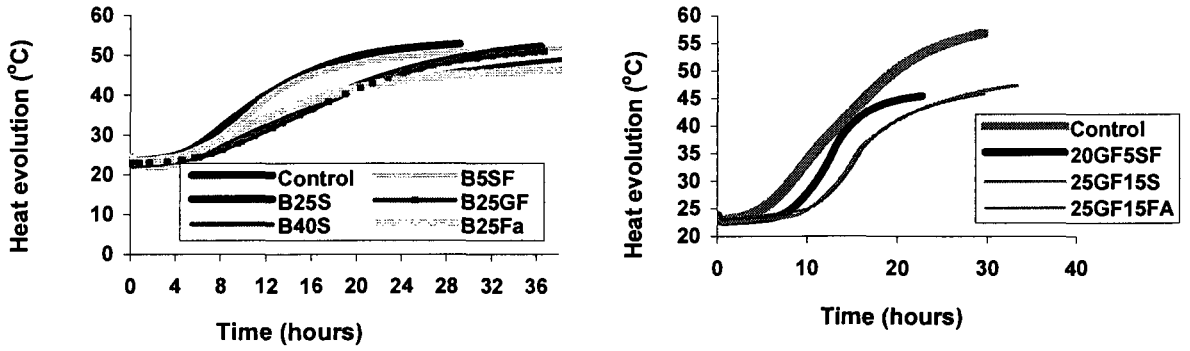

(a) Binary mixtures (b) Ternary mixtures

Figure 4.23 Heat evolution as a function of time

In conclusion, GF is an amorphous material. GF reacts with hydrated lime and sodium hydroxide as both pozzolanic and hydraulic material. The addition of 50% GF prevents the deterioration due to sulfate attack. The rheoligical properties of GF pastes are highly affected by GF content. The flowability of GF pastes decreases by increasing GF content from 25 to 50%.

CHAPTER 5

ALKALI-ACTIVATED GF CEMENT (AAGFC)

5.1 Introduction

The construction industry has made considerable strides forward over the last decade with regards to the use of many pozzolanic materials, in particular slag, fly ash, and metakaolin. These materials possess excellent latent hydraulic properties that could be highlighted by the addition of certain types of activators, resulting in a series of new binders. Some of these binders are strong enough to produce clinker-free concrete that can compete with normal concrete.

Today, most concrete producers worldwide recognize the value of pozzolanic enhancements to their products and, where they are available, they are even becoming a basic routine concrete ingredient. Most pozzolans used today are by-products from other industries, such as slag and fly ash. As such, there has been relatively little work done with regard to recycled, optimized, and engineered pozzolanic materials, which are specifically intended for use in Portland cement-based formulations. Glass frit (GF) is one example of such materials that originates from the aluminium industry. In the present study, glass frit has been used as a clinker-free binder and evaluated in pastes, mortars, and concretes.

The work described in this chapter is the first to be carried out on such material, and has been conducted and planned in order to answer the following questions:

- Can glass frit be activated?
- What are the best activators?
- What is the best method of activation?
- At what concentration should they be used?
- What are the conditions of activation?
- What about incompatibility between GF and some activators?
- What are the main problems with activation?
- What is the best application?
- Can the mechanical properties be improved by mixing glass frit with low replacement levels of both slag and fly ash?

A wide variety of NaOH concentrations was tested and the effect of each on the development of mechanical and microstructural properties was assessed. As well, other activators were tested. The success of the GF-activating trial mixtures has facilitated the current work and led to a realistic prediction of the results throughout this research. In fact, the results obtained showed the real potential of GF conversion into a binder after 18 hours of activation at different activation temperatures of 50, 60 and 80°C. The activation time of 18 hours was chosen as the optimum time for activation, as after this time undesirable thermal effects including swelling and cracks formation begin to appear. The tested samples were then 100% humid cured for 28 days.

5.2 Development of NaOH activator: effect of concentration, and temperature

5.2.1 Activation temperature of 50°C

Figure 5.1 shows the compressive strength development of 10 activated GF mixtures using 10 different concentrations of NaOH expressed as a percentage of the total mass of GF, i.e. 0.5 to 5% Na_2O with incremental increase of 0.5, as shown in Table 3.4 (p.81). Figure 5.1 presents the average compressive strength results for each mixture with time until 28 days. Other histograms at curing time of 1 and 7 days are presented in Figure 5.A1 (Appendix A). Figure 5.1 shows that compressive strength increases as NaOH concentration increases for all mixtures at 1 day, while this behavior changed with 7 and 28-day tests. Two observations could be made: the first is related to the effect of temperature, where the tested samples after 24 hours gave a continuous increase in compressive strength, while the second is related to the effect of curing time. After 7 and 28 days, compressive strength increases from the initial concentration (C0.5) to a concentration of C2, while at C3 the compressive strength begins to decrease, then increase again with cracks appearing at the surface. From Figure 5.1, it is apparent that the best concentrations at later ages are 5, 4.5 and 1.5% Na_2O. There is a big gap between the samples activated at 0.5% Na_2O and those activated at 1% Na_2O. This means that 1% Na_2O is enough to activate GF to give a binder with significantly higher compressive strength. It also means that there is a pessimum concentration of NaOH, at which the system acquires improved properties. From this observation, it could be concluded that there exists optimum temperature and concentration of NaOH after which undesirable cementitious

properties may be obtained. As the final aim of this chapter is to create a cementitious material that is suitable for concrete applications, it was determined that, according to the results obtained on the group of pastes activated at 50°C, GF could be appropriate for the fabrication of precast concrete elements. For this reason, and to determine the feasibility of this application, activation temperatures of 60 and 80°C were also investigated in the experimental program. The 7-day test is very critical, as it reflects the initial effect of curing conditions on the stability of the cementitious products formed.

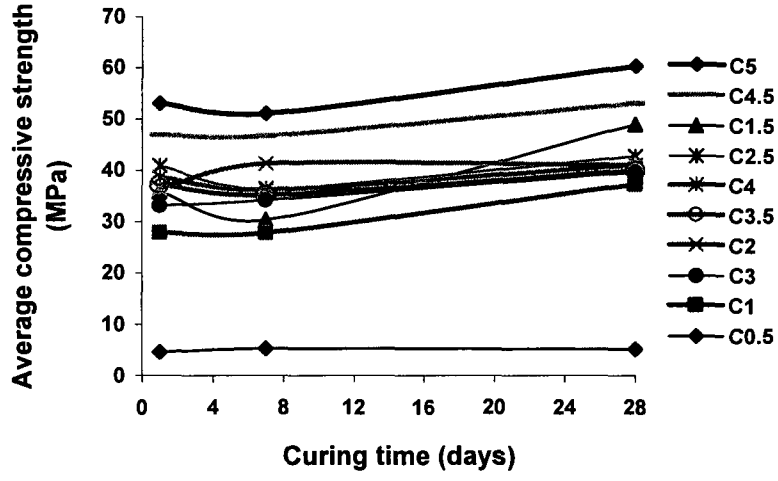

Figure 5.1 Compressive strengths of 1, 7 and 28-day samples activated at 50°C

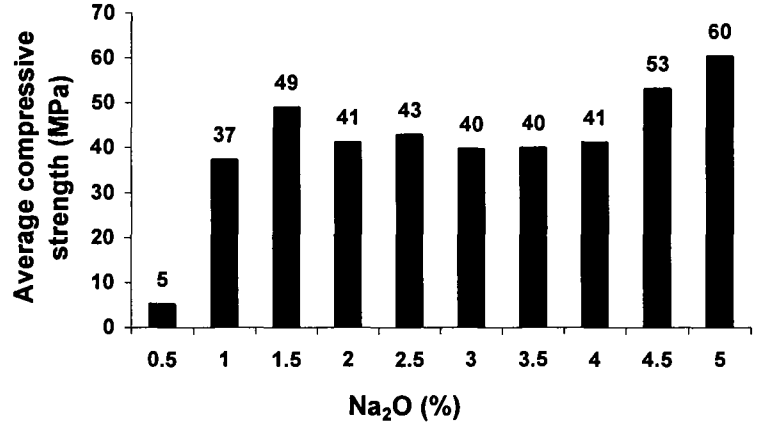

Figure 5.2 Compressive strengths of 28-day samples activated at 50°C

5.2.2 Activation temperature of 60°C

As was done with the samples activated at 50°C, the compressive strength development of 10 activated GF mixtures at 60°C using 10 different concentrations of NaOH expressed as a

percentage of the total mass of GF, i.e. 0.5 to 5% Na_2O with incremental increase of 0.5 was investigated; the results are presented in Figure 5.3 and Table 3.4. As well, compressive strengths at 1, 7, and 28 days are presented in Figures 5.4 and 5.A2 (Appendix A). At 60°C, the activated samples showed different behaviors, which can be classified into two groups. The first group starts at 0.5% Na_2O and ends at 3% Na_2O, while the second group starts at 3.5% Na_2O and ends at 5% Na_2O, as clearly shown in Figures 5.4 and 5.2A (Appendix A). This behavior is evident at testing times of 1 and 7 days, while at 28 days, the samples activated at high concentrations of 3.5% to 5% Na_2O showed a reduction in compressive strength. In other words, compressive strength decreases as NaOH concentration increases at later ages and under this specific temperature of activation, as shown in Figure 5.4. Figure 5.A2 (Appendix A) showed the presence of a large gap between the samples activated at 0.5% and 1% Na_2O, and this gap is larger than the gap found between those samples activated at 50°C by more than 39%, as calculated from Figures 5.A1 and 5.A2 (Appendix A). The best results were obtained from the samples activated by 3.5, 4, and 1% Na_2O, respectively.

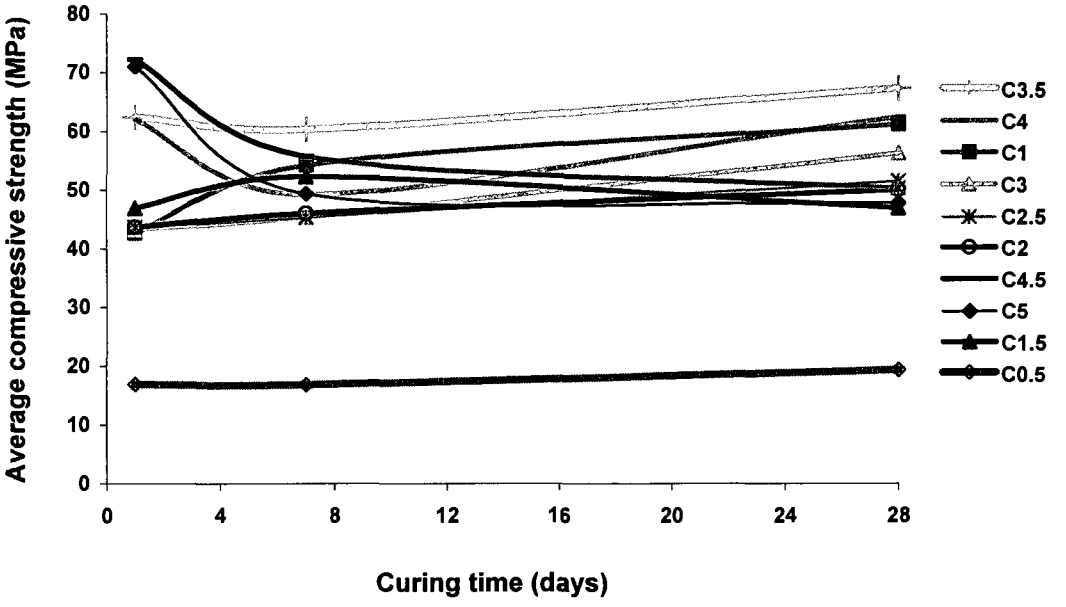

Figure 5.3 Compressive strength of 1, 7, and 28-day samples activated at 60°C

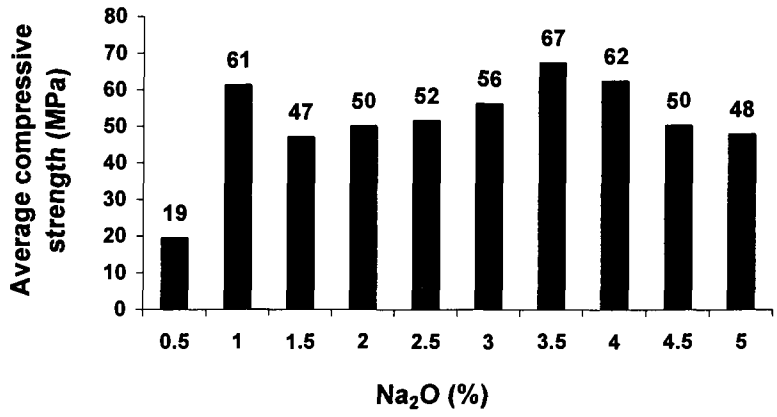

Figure 5.4 Compressive strength of 28-day samples activated at 60°C

5.2.3 Activation temperature of 80°C

At a temperature of 80°C, we suggested the use of superplasticizer (SP) with critical concentrations to adjust the workability, as shown in Table 3.5. A naphthalene sulfonate-based superplasticizer was used with samples activated with concentrations of 1 and 3% Na_2O where these concentrations were critical, as shown in the samples activated at 50 and 60°C. The average compressive strengths of 5 activated GF mixtures at 80°C using 5 different concentrations of NaOH expressed as a percentage of the total mass of GF, that is 1 to 5% Na_2O with incremental increase of 1, are presented in Figure 5.5. The effect of temperature of activation has been demonstrated in this part. At the age of 1 day, there is no significant difference in compressive strength, and unlike those cured at 50 and 60°C, this can be attributed to the effect of higher temperatures, as shown in Figure 5.6. The gain in compressive strength is directly proportional to the concentration of the activator. However, at curing ages of 7 and 28 days the tested samples start to show the same behavior of loss in compressive strength, as shown in Figure 5.A3 (Appendix A), similar to previous experiments. These samples can be separated into two groups. The first group begins at 1% and ends at 2% Na_2O, while the second group begins at 3% and ends at 5% Na_2O, as shown in Figures 5.6 and Figure 5.A3 (Appendix A). It is evident that the samples containing superplasticizer showed higher compressive strengths than the same samples without superplasticizer, likely due to the dispersing effect of superplasticizer, making more particles available for the reaction. Therefore, superplasticizer plays an important role in improving the durability of such activated samples by affecting the microstructure of the formed phases.

Figure 5.5 shows that the samples activated with 1% Na_2O (C1) with superplasticizer give the best compressive strength, as does the sample activated by 2% Na_2O (C2) at 28 days. In addition, the samples activated by 1% Na_2O without superplasticizer give equivalent strengths with time, while the other samples show a reduction in compressive strength with time, as shown in Figures 5.5, and 5.3A (Appendix A) The critical concentration yielding the lowest strength is still at 3% Na_2O. This suggests that there exists a midpoint concentration before and after which there is substantial change in the essence and nature of the newly formed cementitious structure. It is worth noting that the samples activated by concentration of 5% Na_2O had shown a considerable reduction in compressive strength from around 90 MPa at 1 day to lower than 50 MPa at 28 days. It was attributed to the formation of NaF mineral, which is a very soluble mineral and its presence was confirmed by XRD analysis, as shown later. The reduction in compressive strength was attributed to the cracks and splitting formation at the surface due to formation of soluble mineral, which was expected to be villiaumite.

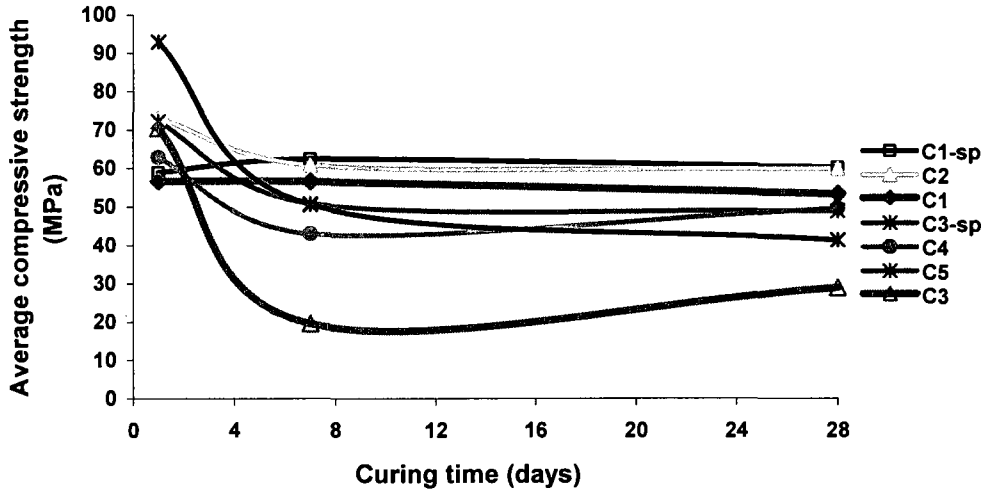

Figure 5.5 Compressive strength of 1, 7 and 28-day samples activated at 80°C (sp=superplasticizer)

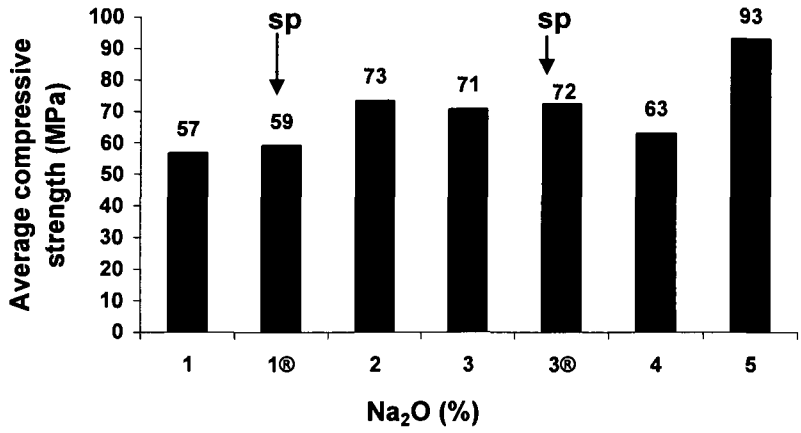

Figure 5.6 Compressive strength of 1-day samples activated at 80°C (sp= superplasticizer)

5.2.4 Comparison between the activation temperature and concentration of activator

At a curing age of 1 day, the compressive strength increases with increase in temperature at the same activator concentration, as well as compressive strength generally increases as the concentration of activator increases. The higher compressive strengths are obtained at the higher concentration, as shown in Figure 5.7. At 7 days, the optimum concentration of activator seems to be at 2% Na_2O concentration at a temperature of activation of 80°C, whereas the optimum concentration at 60°C is 1% Na_2O and that at 50°C is 5% Na_2O, as shown in Figure 5.8. There are two optimal concentrations at a curing age of 28 days and a temperature of 60°C, which are 1 and 4% Na_2O, while at 50°C there is only one optimal concentration at 5% Na_2O. At 28 days and at 80°C, there is also only one optimal concentration at 2% Na_2O, as shown in Figure 5.9. This part of the activation process using NaOH as an activator, is accompanied by SEM-EDS analysis to investigate the effect of NaOH concentration and temperature on GF particles, as shown later.

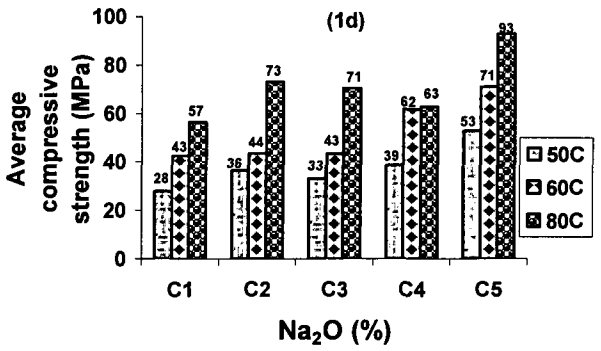

Figure 5.7 Comparison between samples activated at different temperatures and concentrations of activator at 1 day

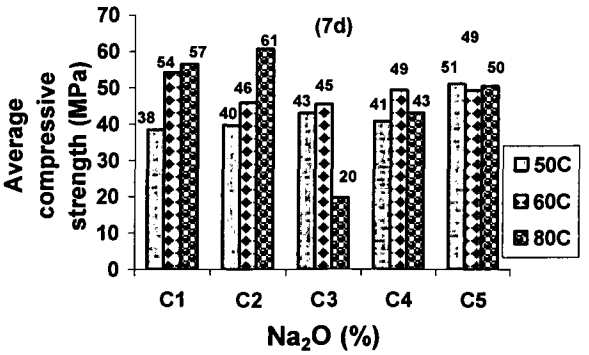

Figure 5.8 Comparison between samples activated at different temperatures and concentrations of activator at 7 days

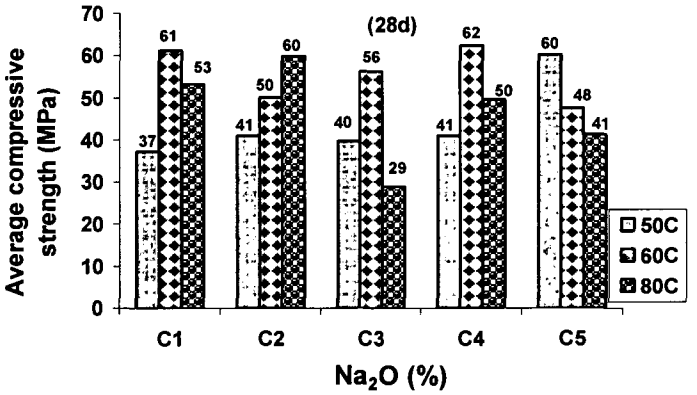

Figure 5.9 Comparison between samples activated at different temperatures and concentrations of activator at 28 days

5.2.5 Simple analysis

A statistical analysis was carried out with the previously mentioned results to calculate the rate of gain in compressive strength with temperature increase at constant concentration and curing age. The analysis was conducted using results obtained from activated samples at a curing age of 1 day at 50, 60, and 80°C. Both 1 and 5% Na_2O concentrations have the same rate of gain in compressive strength with temperature. The rate of gain in compressive strength due to these two concentrations is very low at high temperature. This behavior can be interpreted as follows, and as shown in Figure 5.A4 (Appendix A):

i) At high temperature and low concentration, there are enough GF particles and low concentration of activator to activate these GF particles.

ii) At high temperature and high concentration of activator, there is sufficient concentration but fewer GF particles, so that the rate is accelerating with temperature until it reaches complete dissolution of GF particles, after which the rate begins to slow down.

The rate of gain in compressive strength at concentrations of 2 and 3% Na_2O increases with the increase in temperature, as shown in Figure 5.A5 (Appendix A). This trend is the reverse of what was obtained at 1 and 5% Na_2O. This can be interpreted the same way, as there are enough GF particles and sufficient concentration of activator to dissolve these particles. However, the rate of gain in compressive strength at a concentration of 4% Na_2O has shown the same trend as that of 1 and 5% Na_2O, as shown in Figure 5.A6 (Appendix A). From regression and best-fit line analysis of the curves obtained from Figures 5.A4-5.A6 (Appendix A), the following equations could be obtained, as shown in Table 5.1:

TABLE 5.1 EQUATIONS FOR BEST FIT LINES OF COMPRESSIVE STRENGTH-TEMPERATURE RELATION

Concentration	Best fit equations, R^2~1
C1	$Fc_1 = -0.026 * T^2 + 4.3435 * T - 124.16$
C2	$Fc_2 = 0.025 * T^2 - 2.0232 * T + 75.16$
C3	$Fc_3 = 0.0112 * T^2 - 0.2108 * T - 15.6$
C4	$Fc_4 = -0.0511 * T^2 + 7.9493 * T - 231.18$
C5	$Fc_5 = -0.0236 * T^2 + 4.3923 * T - 107.7$

Fc stands for compressive strength, C stands for concentration, and T for temperature used

By taking the first derivative of these equations with respect to the applied temperature and then substituting in the resulting equations by each temperature value, the following data could be derived, as shown in Table 5.2:

TABLE 5.2 CHANGE IN RATE OF COMPRESSIVE STRENGTH GAIN WITH ACTIVATOR CONCENTRATION

Temperature(°C)	Rate of compressive strength gain (MPa/ °C)				
	C1	C2	C3	C4	C5
50	1.74	0.48	0.91	2.84	2.03
60	1.22	0.98	1.13	1.82	1.56
80	0.18	1.98	1.58	-0.23	0.62

From Table 5.2, the following curves representing the change in rate of compressive strength gain with the activator concentration can be obtained, as shown in Figures 5.10 to 5.12. The change in rate of compressive strength gain for mixtures activated at 50 and 60°C can be demonstrated, as in Figure 5.10 and 5.11, where there is one peak for each temperature; which stands around 4-4.5% Na_2O at 50°C and 3.5-4% Na_2O at 60°C, while at 80°C, the peak stands around 2.5% Na_2O, as shown in Figure 5.12. These results are in accordance with the previously mentioned results, as shown in Figures 5.2, 5.4, and 5.A.3. It is important to note the effect of temperature change on optimal activator concentration, which flips to lower concentration value in the direction of applied temperature, as shown in Figure 5.13.

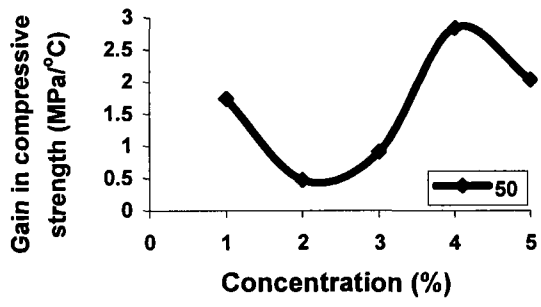

Figure 5.10 Change in the rate of compressive strength gain at 50°C and different activator concentrations

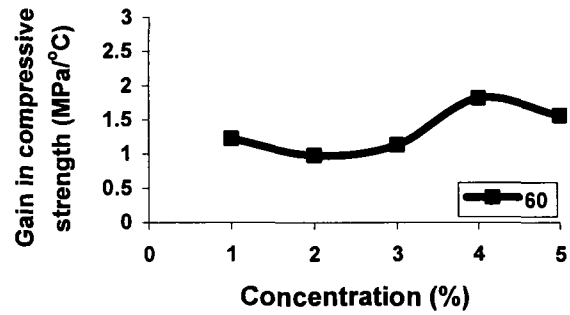

Figure 5.11 Change in the rate of compressive strength gain at 60°C and different activator concentrations

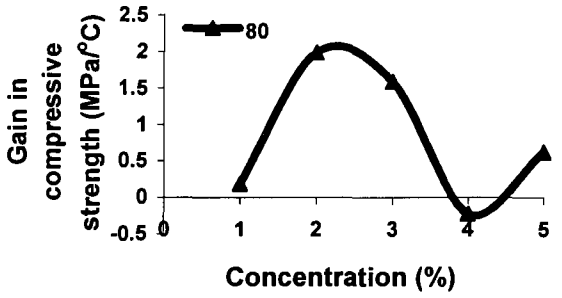

Figure 5.12 Change in the rate of compressive strength gain at 80°C and different activator concentrations

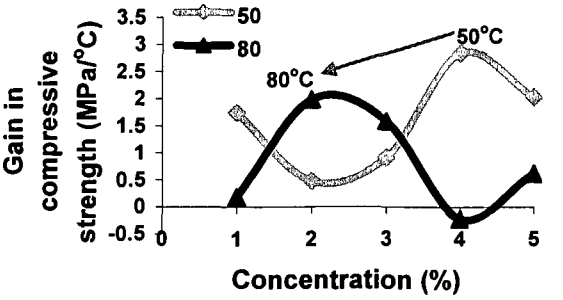

Figure 5.13 Difference between change in the rate of compressive strength gain at 50 and 80°C and different activator concentrations

The explanation as to why at 80°C and higher NaOH concentration, compressive strength experiences an abrupt drop was attributed to the formation of villiaumite mineral (NaF), as shown in SEM-EDS and XRD analyses.

5.2.6 XRD analyses

A series of XRD and SEM-EDS analyses were undertaken to interpret the mechanism of activation. XRD analysis obtained from samples activated using 1, 4 and 5 % Na_2O at 80°C and a curing age of 1 day, as shown in Figure 5.14. XRD analysis showed the presence of villiaumite (NaF), which is very soluble with respect to fluorite (CaF_2) mineral [BEKMURATOV AND DOBRYNINA, 1971; CATHERINE AND JOSEPH, 1986; CATHERINE, 1987; PAUL AND SEIKO, 1991; MORALES et al., 2007] and can lead to instability of the cementitious system formed. Villiaumite formation increases with Na_2O concentration. It is evident that the fluoride originated from the composition of GF. This also explains previously mentioned results obtained from the group of samples activated at high concentrations of Na_2O and at 80°C, which were accompanied by cracks and cleavage at the surface and were attributed to a high rate of formation of NaF. This unstable mineral leads to instability in the activated system and results in a reduction in compressive strength due to formation of different planes of cleavage that leads to splitting and failure in strength. Figure 5.14 shows the formation of villiaumite with increasing NaOH concentration. As well, Figure 5.15 shows the formation of other newly formed phases that are responsible for the bonding force of the cementitious system. Zeolite-like materials are the major phases that formed during the activation process, which are responsible for the bonding force.

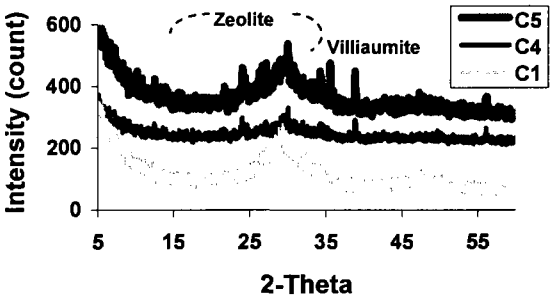

Figure 5.14 XRD patterns of paste samples activated by 1, 4 and 5% Na_2O at 80°C for 24 hours

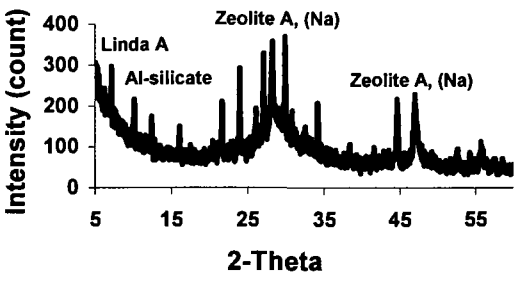

Figure 5.15 XRD patterns of C4 sample activated at 80°C with 4% Na_2O

The negative effect of villiaumite formation was overcome by adding $Ca(OH)_2$ activator (refer to 5.5.2), which competes with NaOH to form fluorite mineral (CaF_2), which is more stable than NaF.

5.2.7 SEM analysis

Figures 5.16 to 5.23 show the effect of NaOH concentration on GF particles. At low concentration of NaOH, namely 0.5% Na_2O, there is initial formation of reaction rims around the GF particles, which are responsible for the weak binding capacity in this system. At higher concentration, the rim thickness increases, as shown in Figures 5.16 and 5.18. Consequently, the binding force increases and the compressive strength increases as a result. Figures 5.16 and 5.18 explain the gap found between the compressive strength of the samples activated by 0.5 and 1 % Na_2O. The thickness of the reaction rim in the mixture containing 1% Na_2O can be inferred from the compressive strength difference. As well, the intensities of the SEM-EDS spectra are directly proportional to the concentration used, as shown in Figures 5.17 and 5.21, as an indication for the existence of internal rearrangement and reconcentration of the silicate layers at the surface, as shown in Figures 5.19 and 5.20. Therefore, NaOH is a selective activator prone to react with silicate compounds, thus opening their structures and facilitating their recrystallization into new cementitious phases, as shown in Figures 5.19 and 20 (rectangular crystals).

In this part of the analysis, the paste activated by 0.5 % Na_2O showed that GF particles started to stick to each other and pack themselves in a very condensed way, as shown in Figure 5.16. The SEM total area analysis showed the presence of silicon, calcium, aluminium, sodium, and potassium elements, which are the main components of GF particles, as shown in Figure 5.17. It is very important to trace the intensities of these elements to evaluate their concentrations on the surface of GF particles due to the activation reaction.

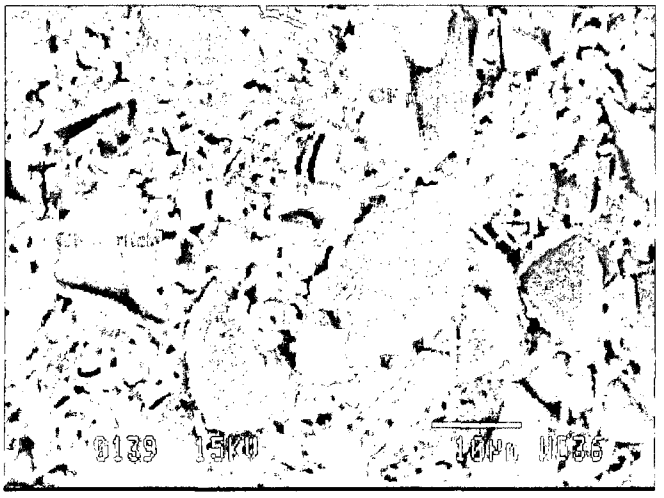

Figure 5.16 SEM image of paste activated by 0.5% Na_2O at 50°C, at 1 day

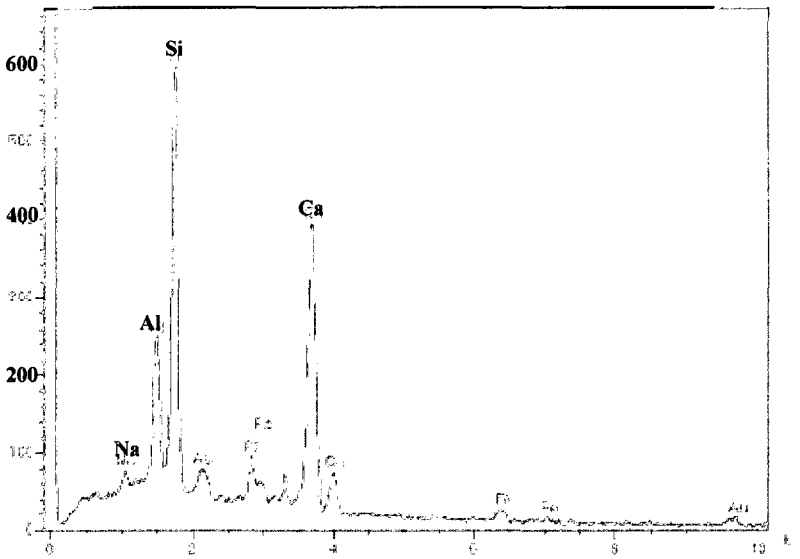

Figure 5.17 SEM elemental spot analysis of paste activated by 0.5% Na_2O at 50°C, at 1 day

As the concentration of NaOH increases along with the reaction rims around GF particles, this may lead to more binding capacity between the GF particles, as shown in Figure 5.18. NaOH begins the reaction with the surface of GF particles leading to dissolution of the surface with formation of reaction rims around GF particles, which was followed by de-polymerization of the amorphous system, as clearly shown in Figure 5.18.

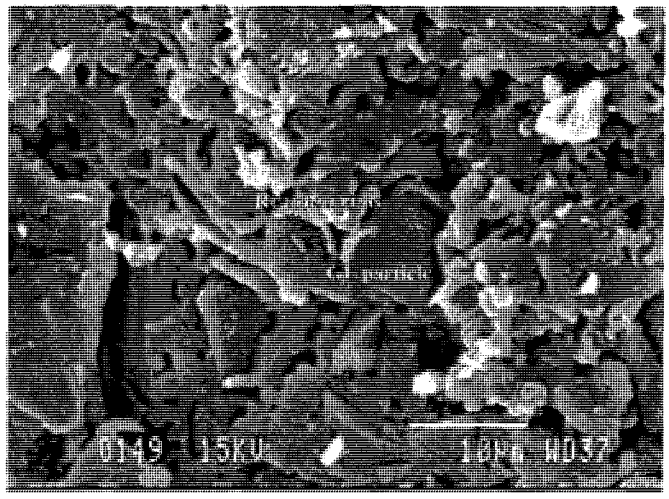

Figure 5.18 SEM image of paste activated by 1% Na_2O at 50°C, at 1 day

As the concentration of NaOH increases, the reaction rims increase, and as the dissolution of GF particles increases, as the ease of formation of new phase crystals. These crystals formed as a result to an increase in the interaction between GF parfticles and NaOH leading to rearrangement and polymerization of the de-polymerized GF particles, as shown in Figure 5.19-5.21.

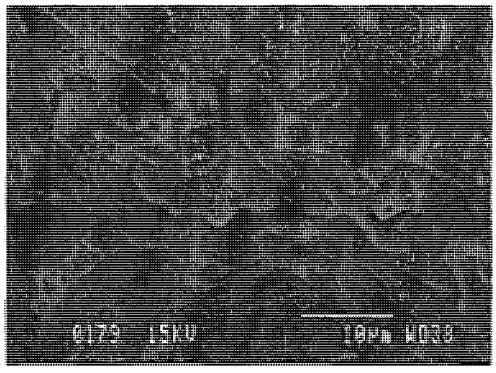

Figure 5.19 SEM image of paste activated by 5% Na_2O at 50°C, for 24 hour

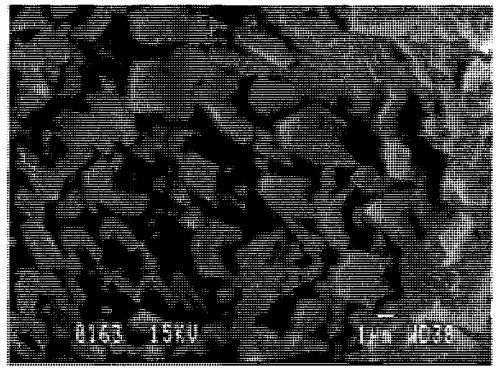

Figure 5.20 SEM image of paste activated by 5% Na_2O at 50°C, for 24 hours (different place)

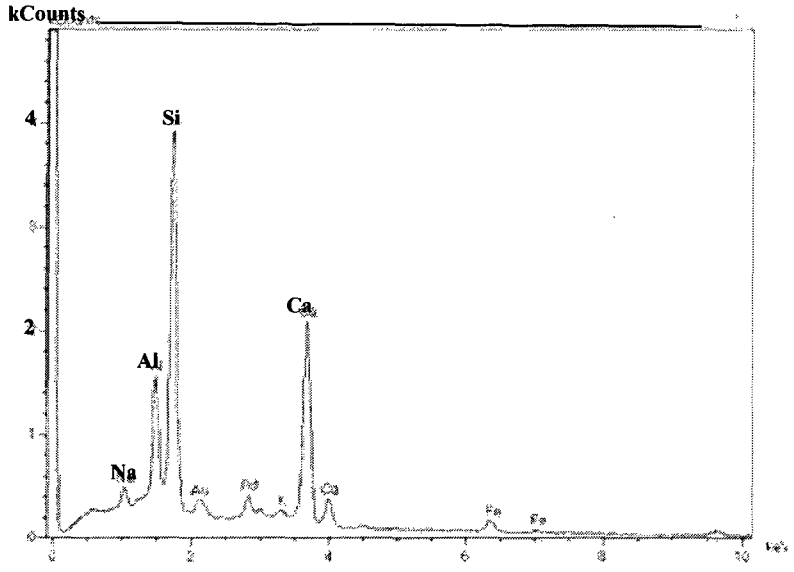

Figure 5.21 SEM elemental spot analysis of paste activated by 5% Na_2O, at 50°C for 24 hours

The intensities of the SEM-EDS spectra are directly proportional to the activator concentration used: low intensity at low concentrations and high intensity at high concentrations, as an indication of the reformation of the silicate layers, i.e. polymerization at the surface, as shown in Figures 5.17 and 5.21. The relation between the intensity of the silicate phase and the concentration of NaOH used is shown in Figure 5.A7 (Appendix A). NaOH can be considered a selective activator, which reacts with silicate compounds dissolving their structures and easing their crystallization to form new phases with new geometrical structures (rectangular), as shown in Figures 5.19 and 5.20.

As the concentration of 3% Na_2O is the intermediate concentration that showed good results, it was therefore chosen for study by SEM-ED analysis at 60°C. Figures 5.22 and 5.23 showed that as the temperature increases, the system becomes more structured and more compact. The effect of increasing activation temperature is evident, as there is formation of a mix of rectangular and spherical crystals, indicating the effect of heat on GF particles. Therefore, increase in temperature produces quite enough energy to induce the rapid formation of different types of crystals, as shown in Figures 5.22 and 5.23.

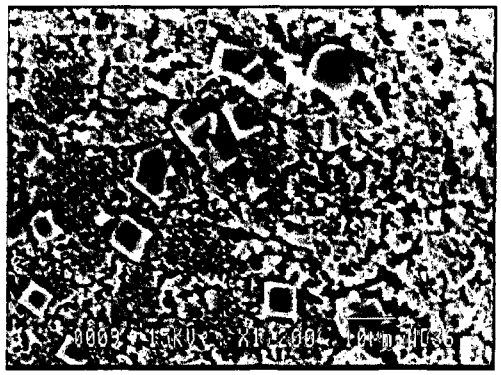

Figure 5.22 SEM image of paste activated by 3% Na_2O at 60°C, for 24hours

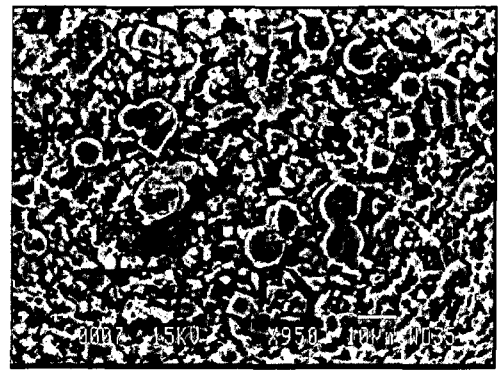

Figure 5.23 SEM image of paste activated by 3% Na_2O at 60, for 24 hours

These figures show that the resulting phases are mainly sodic zeolite-based alumino-silicate compounds (geo-polymers), as confirmed by XRD analysis, which is shown in Figure 5.24.

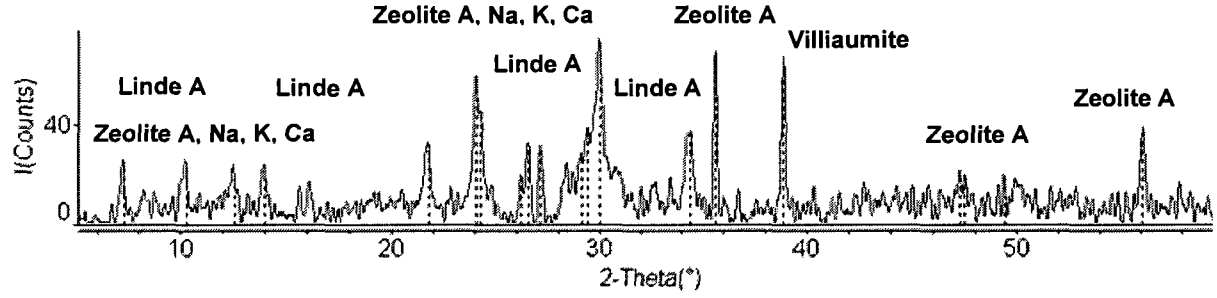

Figure 5.24 XRD analysis for paste activated by 3% Na_2O at 60, for 24 hours

These minerals, as confirmed by XRD analysis, have quasi-crystalline structure due to their low intensities. Therefore, based on previously mentioned results, the following hypotheses could be postulated:

i) The effect of NaOH is extremely vital in creating the appropriate environment that promotes disintegration of the alumino-silicate structure of the GF by rupturing the weak bonds in that structure;

ii) Increased temperature facilitates their rupture and accelerates the disintegration of the network of this structure;

iii) Once there are available reacting species in the system, a process of de-polymerization and re-polymerization, along with the alkaline condition, promote the formation of geopolymeric structures;

iv) These structures mainly consist of sodium alumino-silicate hydrate compounds as the major mineral, while the minor minerals are a mixture of alumino-silicate, calcium alumino-silicate, and calcium silicate hydrates;

v) The presence of Na^+, K^+ and Ca^{2+} is needed because of their charging balance and catalytic role. The alkali ions are found in two states:
   a- entrapped inside the cementitious system and ionically bound in the structure;
   b- trapped around the polymeric structure, where they are free in the system to guarantee the stability condition of the formed structure, as visualized and demonstrated in Figure 5.A8 and 5.A9.

5.3 $Ca(OH)_2$ activator (CH)

CH was previously investigated in Chapter 4, in which the pozzolanic activity of GF with portlandite at 55°C was evaluated. The pozzolanic activity of GF with hydrated lime was evaluated, and it was found that its activity increases with temperature. The change in GF activity with change in CH dosage can be followed by tracking the major peaks of portlandite using XRD analysis. Table 5.3 shows that the water demand increases with increasing CH content. On the other hand, compressive strength decreases with an increase in CH dosage, as shown in Figure 5.25. The concentration of 10 % CH seems to be the optimum concentration, after which there is remarkable reduction in compressive strength, because of the presence of extra free and unreacted hydrated lime, as shown in Figure 5.25. The most important observation here is that there is gradual progress in compressive strength with time, which indicates that the temperature of activation of 60°C was not adequate to facilitate the pozzolanic reactivity of GF to consume most of CH rapidly.

TABLE 5.3 MIX DESIGN AND WATER DEMAND

GF (%)	CH (%)	Water/(GF+CH)
90	10	0.359
80	20	0.400
70	30	0.435

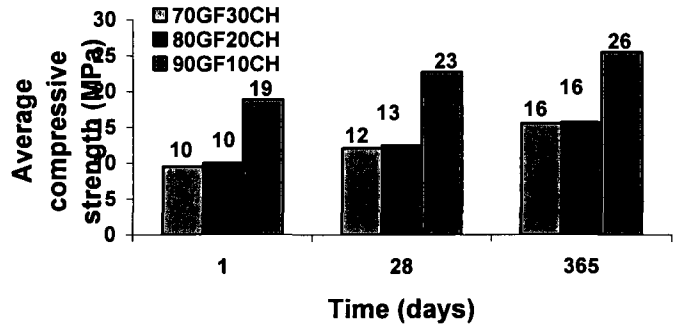

Figure 5.25 Compressive strength of GF-based mixes with different CH contents (60°C)

The intermediate mix of 80% dry GF powder and 20% CH was selected, based on results shown in Figures 5.13 and 5.25, for monitoring by XRD analysis. This XRD analysis was used to quantify the pozzolanic activity of GF with CH based on the major peaks of CH. This combination was mixed with water (GF-to-water ratio was 0.40) and the paste was cast in molds measuring 50 × 50 × 50 mm and cured under accelerating conditions of 80°C and 100% R.H. for 18 hours in the curing chamber. After curing, the moulds were removed from the curing chamber and covered with a thermal insulator to cool down slowly. The samples were then tested for compressive strength. The compressive strength was the average of 3 tested samples. Paste hydration was also monitored by X-ray diffraction (XRD) analysis. X-ray diffraction analysis has effectively shown that after 18 hours of hydration, the lime was largely consumed, as shown in Figure 5.26 and Appendix 5.B. This test showed the strong pozzolanic behavior of GF. Figure 5.26 has also shown the formation of fluorite (CaF2). Fluorite is a stable mineral. Although, part of the lime was used in fluorite formation, the pozzolanic behavior of GF is still predominant because the average compressive strength of the paste was found to be about 16 MPa after 18 hours.

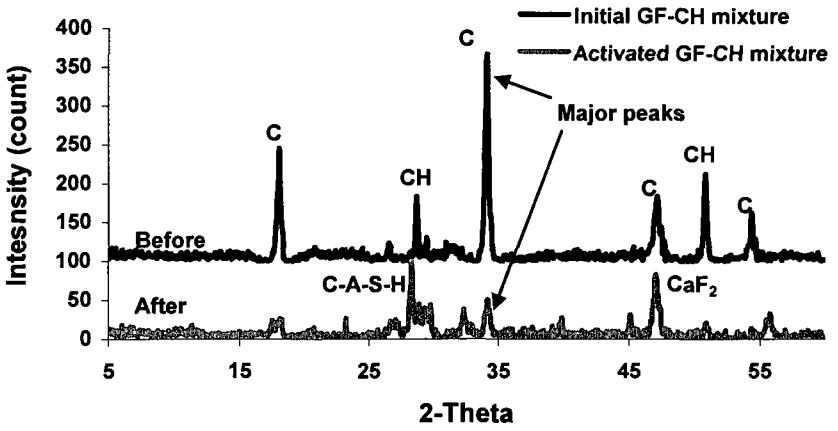

Figure 5.26 XRD analysis of activated GF paste with 20% CH activated at 80°C

Moreover, the identification of the newly formed phases such as calcium alumino-silicate hydrate (C-S-A-H) and fluorite (CaF_2) minerals is of great significance that confirms the formation of fluorite. As a result, this part of the study can be used as a fruitful introduction to the chemistry of this system and prove the way for further study.

5.4 Sodium metasilicate activator (SMS)

The properties of this activator were given in Chapter 3. This activator has been tested with different silica moduli (Ms = SiO_2/Na_2O = 0.319, 0.75, and 0.97) by changing its Na_2O content. The main problem with SMS activator is its solubility, where it was used in powder form. The silica modulus (M_s) was changed using NaOH pellets, and by recalculating their molar ratio to each other, different M_s could be obtained. Silica modulus of 0.75 was first used in such a way that Na_2O concentrations were 2 and 3% Na_2O. The temperature of activation was 60°C. The results are shown in Table 5.4 and Figure 5.27.

TABLE 5.4 MIXTURE CHARACTERISTICS OF SAMPLES TESTED AT CONSTANT M_S AND AT 60°C

Na_2O %	M_s	GF/w ratio	Remarks
2	0.75	0.35	**Surface swelling and scaling**
3	0.75	0.35	**Water silica is very insoluble**

The main difficulty with this M_s is swelling, cracking and/or scaling at the surface of the activated samples, as shown in Figure 5.27.

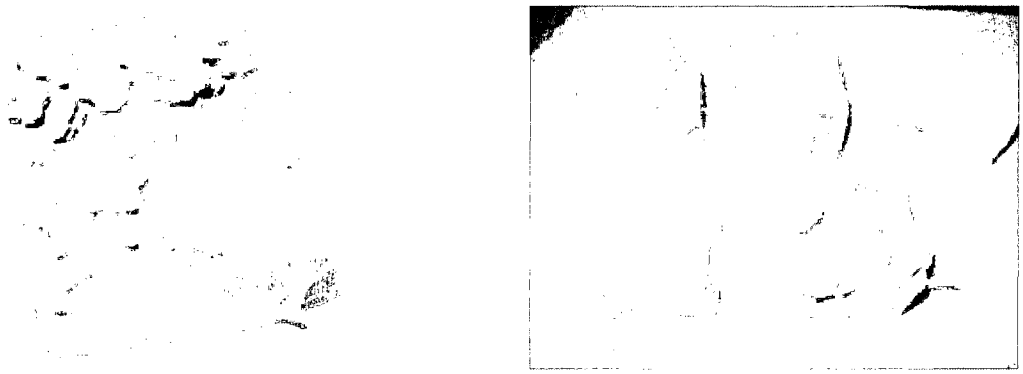

Figure 5.27 Surface swelling, cracks, and scaling

Therefore, this M_s modulus from literature does not function well with GF. For this reason, new M_s formulations were conducted, as shown in Table 5.5 and 5.6. The first formulation was designed in such a way that M_s equals to 0.97 and Na_2O content changes from 1 to 2%. The formulation with this M_s did not show any effective reaction, as shown in Table 5.5 and Figure 5.28.

TABLE 5.5 MIXTURE CHARACTERISTICS OF SAMPLES TESTED AT CONSTANT M_S AND AT 60°C

Na_2O %	M_s	GF/w ratio	Remarks
1	0.97	0.35	**No setting**
1.5	0.97	0.35	**No setting**
2	0.97	0.35	**No setting**

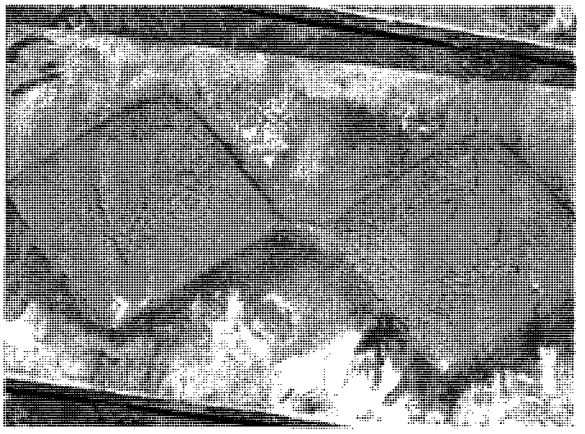

Figure 5.28 Negative reaction with deteriorated surface (no setting)

Therefore, another formulation was conducted with low M_s equal to about half of the first formulation presented in Table 5.4, as shown in Table 5.6. The formulation with this M_s was characterized by two regions of efficiency, as shown in Figure 5.29. In first region, for a concentration of Na_2O equals 2.94%, where the final products show no signs of deterioration; however, in the second region, where the concentration of Na_2O is higher than 4.41%, there is clear formation of cracks and early deterioration. Despite that, the compressive strengths given by the latter concentrations were higher than that given by 2.94% Na_2O with no cracks, as shown in Figure 5.30.

TABLE 5.6 MIXTURE CHARACTERISTICS OF SAMPLES TESTED AT CONSTANT M_S AND AT 60°C

Na_2O %	M_s	GF/w ratio	Remarks
2.94	0.329	0.35	Good setting
4.41	0.329	0.35	Surface cracks
5.87	0.329	0.35	Surface cracks

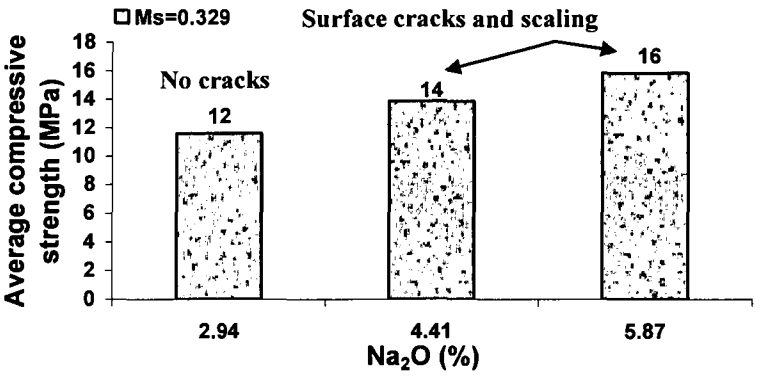

Figure 5.29 Effect of SMS concentration as a function of Na_2O content on the development of compressive strength

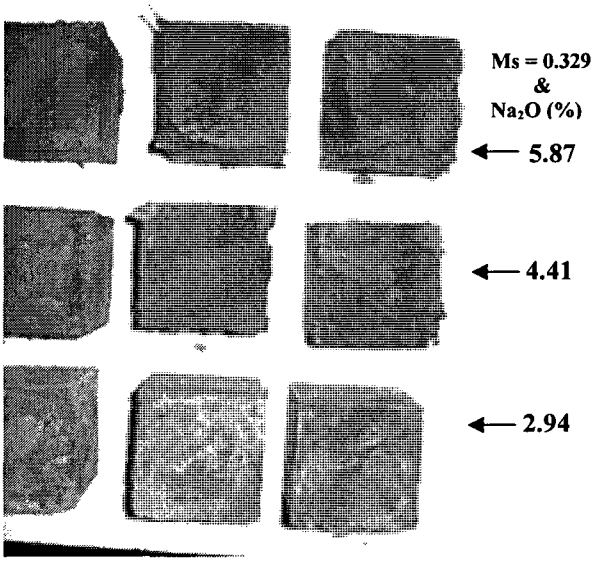

Figure 5.30 Appearance of final product as a function of M_s concentration

A clear relation could be drawn between M_s and Na_2O concentration, as shown in Figure 5.31. Different regions of SMS efficiency are clearly shown, where the most efficient region is that with low M_s and moderate Na_2O concentration, as demonstrated in Figure 5.30.

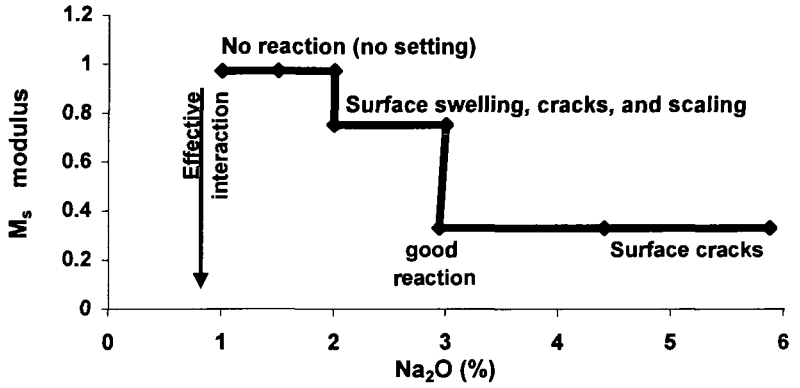

Figure 5.31 Effect of Na_2O content of SMS on final product appearance and durability

5.5 Binary activators

5.5.1 $Ca(OH)_2$ and Na_2CO_3 -based system (CH-NC)

Both $Ca(OH)_2$ and Na_2CO_3 are basic compounds that synergistically interact to form calcite and NaOH, as follows:

$$Ca(OH)_2 + Na_2CO_3 \leftrightarrow 2NaOH + Ca\,CO_3 \qquad (5.1)$$

Their interaction indirectly pumps NaOH into the system with a given concentration according to their molar ratio. A slight quantity of $Ca(OH)_2$ (CH) or Na_2CO_3 (NC) may remain in the system and react with GF particles. A mixture of NC and CH with a molar ratio of NC to CH of 1.12 was thus formulated in a such way to supply free NaOH with concentration of 1.5 % Na_2O. The efficiency of this binary activator was evaluated under a temperature of activation of 60°C.

The results obtained show that this dosage of $Ca(OH)_2$ is not sufficient to initiate reasonable strength, as shown in Figure 5.32. Therefore, addition of further CH is recommended, as well as extra heat input. Moreover, Figure 5.32 shows that strength gradually increases with time.

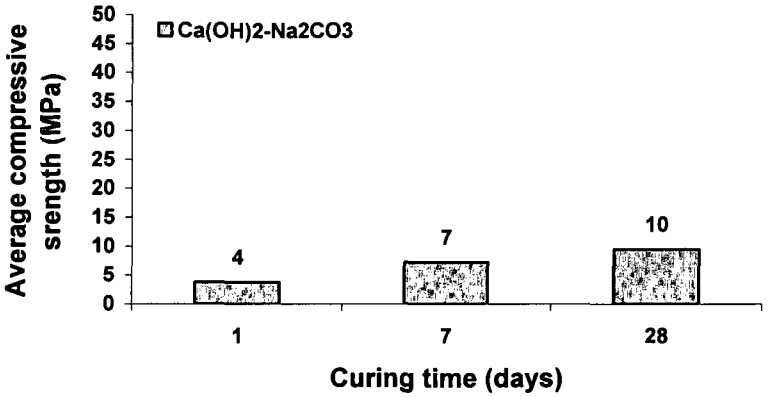

Figure 5.32 Development of compressive strength by CH-NC binary activator

5.5.2 $Ca(OH)_2$ and NaOH-based system (CH-NH)

This system has a double advantage. First, it decreases the formation of NaF, villiaumite mineral, and second, the activated system acquires the advantages of the presence of NH and CH. A mixture of 20% CH with exact amount of NH equivalent to 1.5% Na_2O (1.5NH20CH) with respect to GF content was tested at 60°C. The combination of CH and NH shows their synergetic interaction to form the stable CaF_2 mineral at the expense of unstable NaF mineral in their cementitious matrix. The results shown in Figure 5.33 support the supposition of decreasing the formation of villiaumite by the addition of $Ca(OH)_2$, which guarantees steady compressive strengths with time without any detectable deterioration. As well, the mixtures of 20% $Ca(OH)_2$ and NaOH with concentrations of 2 and 5% Na_2O (2NH20CH and 5NH20CH) with respect to GF were tested at 80°C to investigate the effect of the abundant presence of $Ca(OH)_2$ in the prevention of NaF formation. Figure 5.33 shows the stability of compressive strength with time even at higher concentration of NH (5% Na_2O) in presence of 20% CH, contrary to what was found with NH alone, as previously shown in Figure 5.8 and 5.9.

In comparison with CH-NC activator, CH-NH activator imparts the system with approximately 12 times more compressive strength than that provided by CH-NC activator. As well, compressive strength is nearly stable with time, as shown in Figure 5.33. CH-NH binary activator with different ratios is highly recommended, as it gives promising results. The abundant presence of CH assists the formation of CaF_2 (stable mineral) and prevents NaF mineral formation even at higher NH concentration (5% Na_2O), as confirmed in Figure 5.34. The SEM-DS analysis of 5NH20CH has shown the formation of nano-sized and well-oriented

fiber-like structures with a width smaller than 50 nm, as shown in Figure 5.35. Two structural forms were observed, spherical and cubic. The only difference between both structures is the sulfur content, where sulfur was detected only in the spherical structure, as shown in Figure 5.36. There is an indication of the continuous transformation of the cubic form into a spherical one, as indicated by the abundant presence of spherical forms, as shown in Figure 5.37.

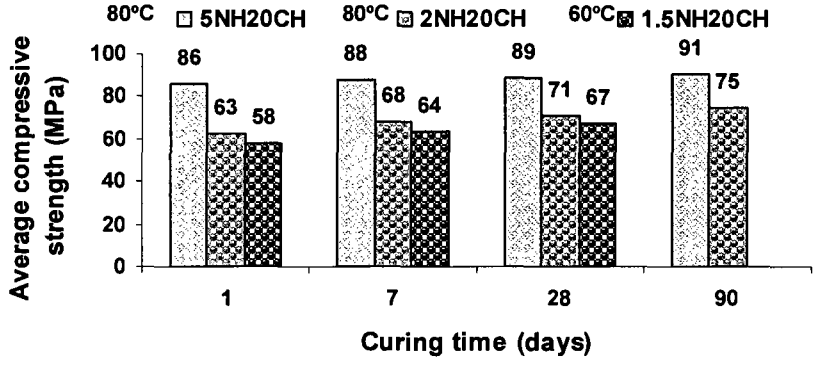

Figure 5.33 Development of compressive strength by NH-NC binary activator

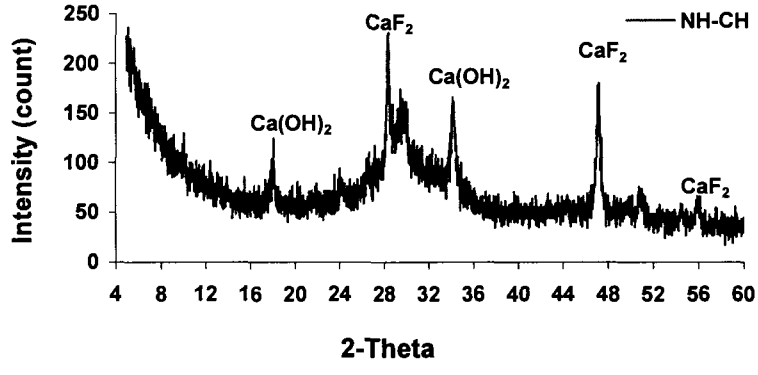

Figure 5.34 XRD patterns of the interaction of GF with 5NH20CH after 24 hours at 80°C

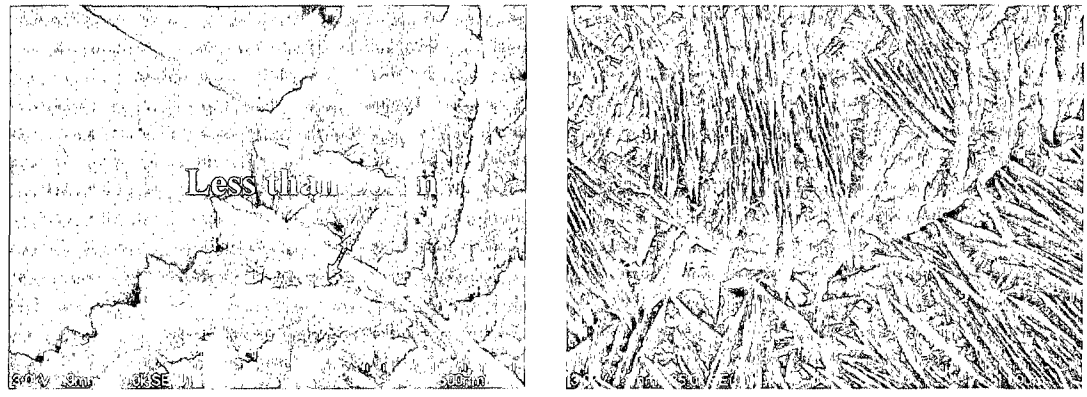

Figure 5.35 Zeolitic nano fibre-like structure formed due to interaction of GF with 5NH20CH after 24 hours at 80°C.

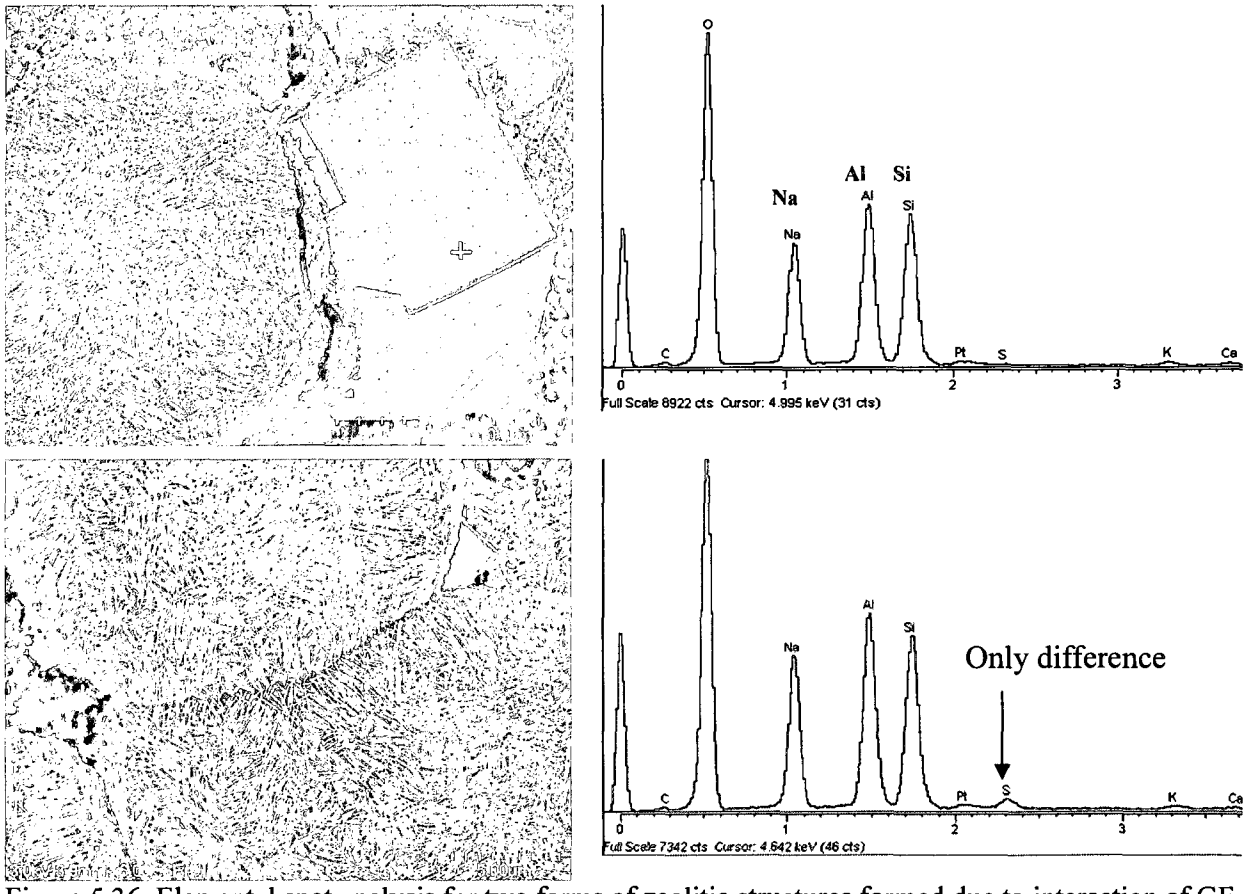

Figure 5.36 Elemental spot analysis for two forms of zeolitic structures formed due to interaction of GF with 5NH20CH after 24 hours at 80°C.

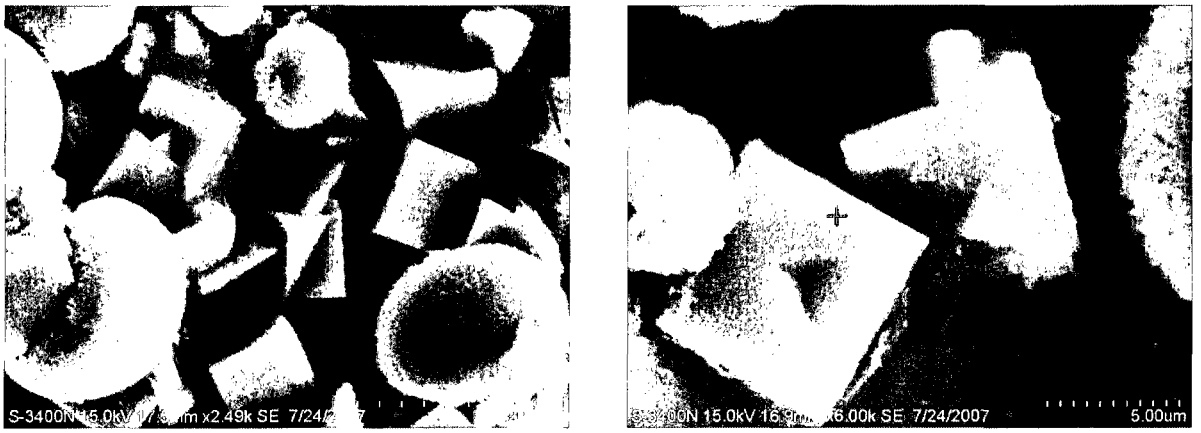

Figure 5.37 Zeolitic structures formed due to GF-NH-CH interaction

5.5.3 NaOH and Na_2CO_3 -based system (NH-NC)

A binary mixture of both NaOH and Na_2CO_3 was used to activate GF in a way that their sum equals approximately 1.5% Na_2O. The part of Na_2O content obtained from Na_2CO_3 equals 0.5% with respect to GF total mass. The temperature of activation was 60°C. The results of the compressive strength of pastes obtained using NH-NC activator are shown in Figure 5.38. The presence of calcite was suggested as a result of the reaction of gradually liberated calcium from the opened-GF structure, due to the presence of low NH concentration at 60°C, with the free carbonate radical provided by Na_2CO_3 salt, according to the suggested reaction:

$$Na_2CO_3 + Ca^{+2} + 2OH^- \rightarrow 2NaOH + CaCO_3 \qquad (5.2)$$

The progress of compressive strength development after 24 hours is very slow. Accordingly, steady state was reached during the activation process. Consequently, invariable compressive strengths were noticed with time, as clearly shown in Figure 5.38.

In comparison with CH-NH and NH-NC activators, NH-NC activator gave compressive strength of half what was given by CH-NH activator. This result was expected as NC is soluble and may react with Ca^{+2} ions, which may be gradually liberated from GF particles in a long-term reaction, as previously suggested by Equation 5.2

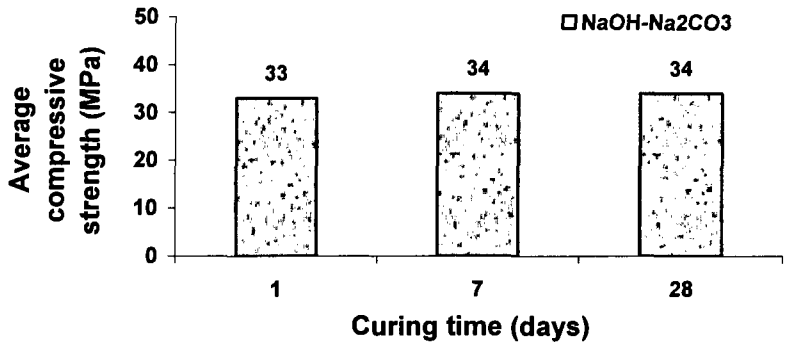

Figure 5.38 Development of compressive strength by NH-NC binary activator

5.5.4 NaOH and Na_2SO_4-based system (NH-NS)

A binary mixture of both NaOH and Na_2SO_4 (NS) was used to activate GF in a similar way to NH and NC, where their sum equals approximately 1.5% Na_2O with respect to GF total mass. The part of Na_2O content obtained from NS equals 0.5% with respect to GF mass. The temperature of activation was 60°C. The gradually liberated calcium ions from the opened-GF structure reacts with the free sulfate radical released by NS salt to form anhydrite (CS) according to the following reaction:

$$Na_2SO_4 + Ca^{+2} + 2(OH)^- \rightarrow 2NaOH + CaSO_4 \text{ (anhydrite)} \qquad (5.3)$$

The anhydrite (CS) may hydrate with time to give hemihydrates or even gypsum that may take part in the development of compressive strength with time, as confirmed later and as shown in Figure 5.39.

In comparison with CH-NC, CH-NH, and NH-NC activators, NH-NS is actually efficient, as it gave higher compressive strength. However, its strength is lower than that given by CH-NH activator. This result was attributed to the alkali content of NH-NS, which was higher than that used in NH-NC, as well as to the efficiency of NH activator which is higher than that of CH and to the formation of anhydrite, which may form under the activation conditions, as explained by Equation 5-3.

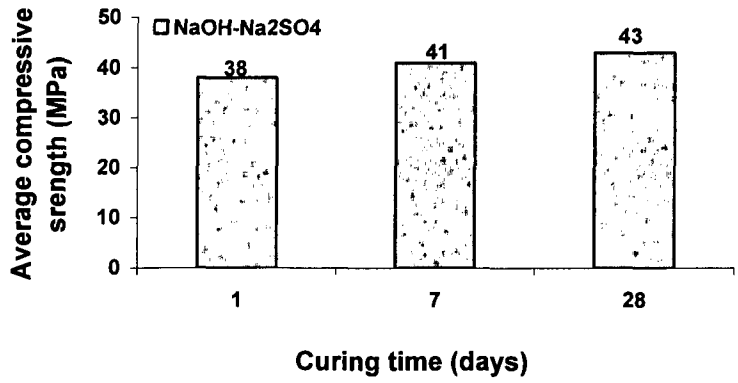

Figure 5.39 Development of compressive strength by NH-NS binary activator

5.5.5 $Ca(OH)_2$ and K_2CO_3-based system (CH-KC)

The efficiency of this binary activator was tested at a temperature of activation of 60°C. The efficiency of this activator depends on the reversible reaction that gives KOH as the target activator, which can be obtained indirectly through the reaction of $Ca(OH)_2$ and K_2CO_3, as follows:

$$Ca(OH)_2 + K_2CO_3 \leftrightarrow 2KOH + CaCO_3 \qquad (5.4)$$

The molar ratio of K_2CO_3 to $Ca(OH)_2$ used in this test was 1.16. This molar ratio was formulated in such a way that it results in K_2O equivalent to 1.5% Na_2O with respect to GF weight, while the w/GF ratio was 0.35. Figure 5.40 shows that the development of compressive strength with time was very slow and the compressive strength obtained was very low in comparison to CH-NC activator, therefore KOH obtained during this reaction, as shown in equation 5-4, is not as efficient as NaOH.

Kinetic studies have indicated that recombination of K-ion with OH-ion is about 30% faster than Na-ion with OH-ion [CHELLIAH et al., 2002], and this perhaps is the primary reason for the effectiveness of NaOH over that of KOH.

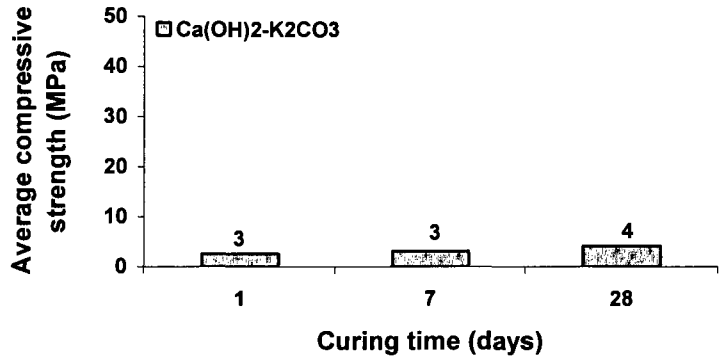

Figure 5.40 Effect of CH-KC binary activator on compressive strength

5.5.6 $Ca(OH)_2$ and $CaCO_3$-based system (CH-CC)

A mixture of 2.5% each $Ca(OH)_2$ and $CaCO_3$, with respect to GF weight at a temperature of activation of 60°C, was used. The w/GF ratio was also 0.35. This low dosage of $Ca(OH)_2$ was chosen to confirm the reactivity of GF at low dosage of $Ca(OH)_2$. Figure 5.41 shows that there is a gradual development in compressive strength with time comparable to CH-KC and CH-NC activators. The strength obtained was low in comparison to the results attained with the other combinations of activators.

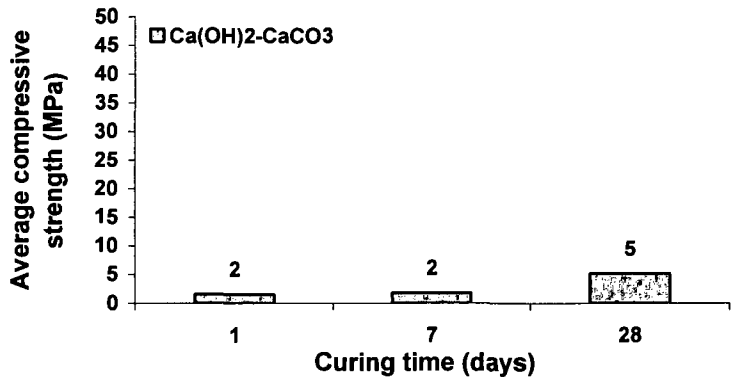

Figure 5.41 Effect of CH-CC binary activator on compressive strength

5.5.7 $Ca(OH)_2$ and Na_2SO_4-based system (CH-NS)

A binary mixture of 20% $Ca(OH)_2$ and a definite amount of Na_2SO_4 equivalent to 1.5% Na_2O were used. Equation 5-5, shown below, was taken into account. For that reason, this mixture can be considered as a quaternary mixture of activators (containing the reactants and products of Equation 5-5 at the same time). The temperature of activation was 60°C.

$$Ca(OH)_2 + Na_2SO_4 \leftrightarrow CaSO_4 + 2NaOH \qquad (5.5)$$

Figure 5.42 shows CH-NS activator is highly efficient, and as expected, resulted in high compressive strength of about 32 MPa at 1 day and 40 MPa at 28 days. Compressive strength development, in comparison to the other mixture, is comparatively faster. It is important to note that this activator gave comparable results to what was obtained with NH-NS, as a good indication of the presence of NH in the mixture during the activation process. Therefore, Equation 5-5 is correct and correctly expressed the reaction occurring during the activation process.

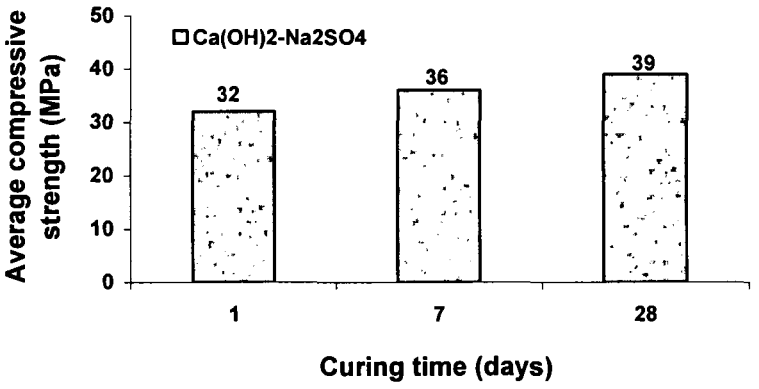

Figure 5.42 Effect of CH-NS binary activator on compressive strength

5.6 Ternary activators

5.6.1 $Ca(OH)_2$-NaOH-Na_2SO_4-based system (CH-NS-NH)

A ternary mixture of $Ca(OH)_2$, Na_2SO_4, and NaOH (CH-NS-NH), as designed in such a way that NaOH was equivalent to 1.5% Na_2O and $Ca(OH)_2$ content was 20% with respect to the total mass of GF by addition. Na_2SO_4 was formulated in molar ratio so that half of the $Ca(OH)_2$ theoretically reacts with the entire dosage of Na_2SO_4 to form anhydrite. The

temperature of activation was 60°C and the w/b ratio was 0.35. To confirm the formation of anhydrite (CS), the activated pastes were tested after 18 hours of activation by XRD analysis (Figure 5.43). The results obtained are shown in Figure 5.43. According to Equation 5-5, this ternary activator can be considered a quaternary activator with CH-NS-NH-CS composition. The compressive strengths are significantly higher than those obtained with the other activators. The formation of CS was confirmed by XRD analysis, as shown in Figure 5.44. The development of compressive strength was fast, it was monitored at 2.5 hours and 18 hours where compressive strengths reached were about 8 and 64 MPa, respectively. While under humid curing, the compressive strength at 7 and 28 days were about 69 and 75 MPa, respectively. The existence of a trace of CH, confirmed by XRD analysis after 18 hours of activation, was believed to be responsible for the gradual increase in compressive strength noticed at later ages, as shown in Figure 5.43.

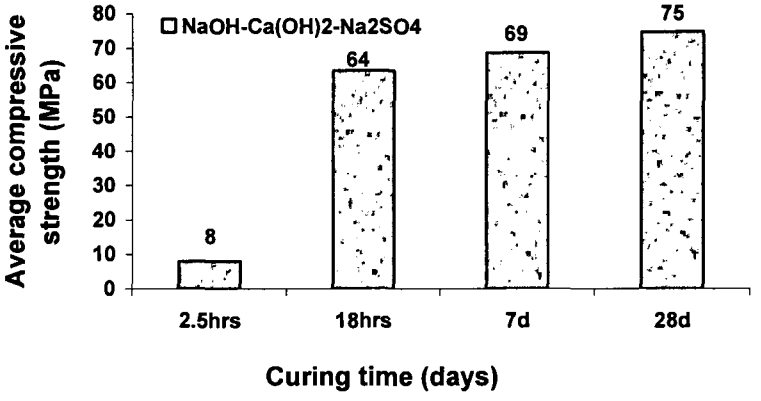

Figure 5.43 Effect of CH-NS-NH ternary activator on compressive strength

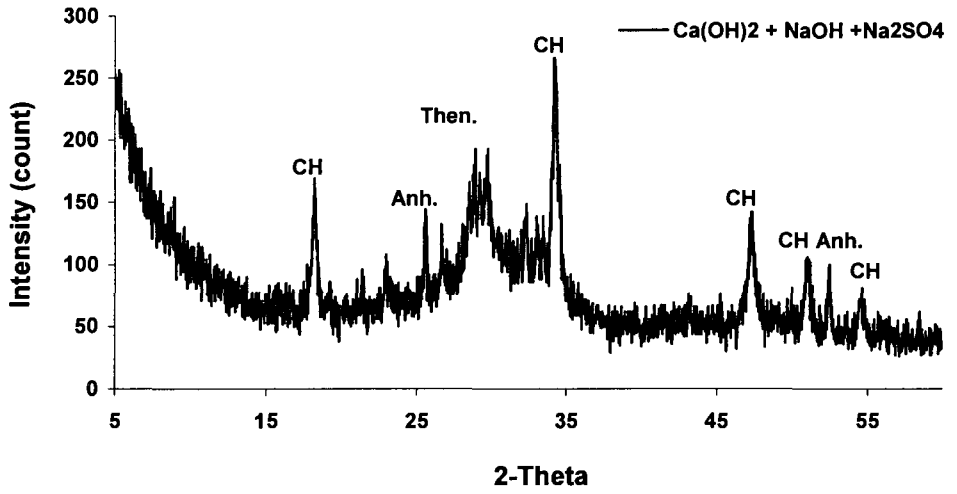

Figure 5.44 XRD patterns of the reaction of CH-NS-NH ternary activator and GF after 18 hours

Figure 5.44 shows that there is formation of anhydrite mineral (Anh.), which is calcium sulfate (CS), as expected, especially since thermal treatment (60°C) used prevents the formation of gypsum or hemihydrates [FREYER, VOIGT, 2003]. As well, there is clear evidence for the formation of thenardite mineral (Then.), mainly in the form of sodium sulfate, which is a soluble mineral. Higher thenardite content is not preferable, as it affects the durability of the formed paste. Therefore, a higher portlandite content is recommended to compete with the formation of thenardite and to lead to anhydrite mineral formation.

5.7 Comparison between different activator combinations

This comparison illustrates the effect of different binary and ternary activators on the activability of GF due to the direct effect of such combinations on GF particles, as shown in Figure 5.45. In comparison with NH as a reference activator with a concentration of 1.5% Na_2O, the binary activators can be divided into two groups. The first group comprises different combinations of NH with NC, KC, and CC, which gives lower compressive strength that can be attributed to the chemically inactive CO_3 radical. While the second group of binary activators comprises different combinations of NH with CH and NS, which gives higher compressive strength with respect to NaOH activator. This also can be attributed to the active SO_4 and OH radicals. The best combinations of activators are those containing NH and CH or NH and NS or any of their binary or ternary mixtures, as previously shown in this part of the study and in Figure 5.45.

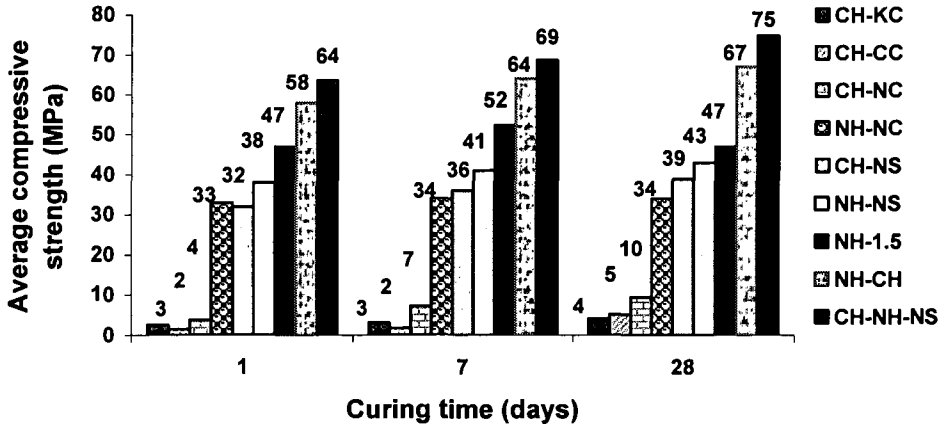

Figure 5.45 Comparison between different combinations of activators at 60°C

5.8 Activated binary cementitious system

5.8.1 Activated GF system with slag

Different replacement levels of slag to GF were used to study the effect of slag replacement on the activability of GF. NaOH was used as the main activator in this part of the study with two concentrations of 1.5 and 3 % Na_2O and with w/b ratio of 0.35 at 60°C for 18 hours. A series of slag replacement levels of 5, 10, 20, and 30% were tested up to 28 days activated by 1.5 and 3% Na_2O. The results of the first series activated by 1.5% Na_2O are shown in Figure 5.46, from which the replacement level of 10% slag can be considered as the optimal replacement level. In addition, Figure 5.47 shows that all replacement levels of slag activated by 3% Na_2O gave better and comparable compressive strengths at later age of 28 days.

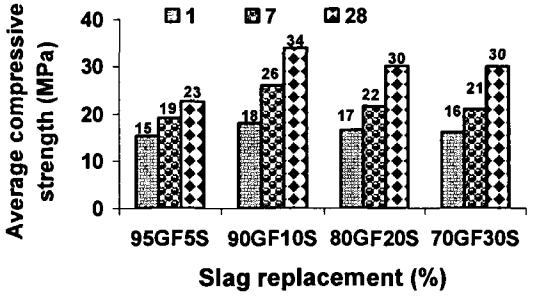

Figure 5.46 GF pastes partially replaced with slag and activated by 1.5% Na_2O at 60°C

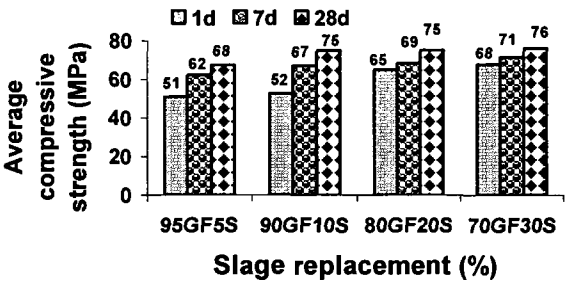

Figure 5.47 Partially replaced GF mixtures with slag and activated by 3 % Na_2O at 60°C

5.8.2 Activated GF system with fly ash

According to the literature review [GUTIERREZ et al., 1993; KOUKOUZAS et al., 2006] and mineralogical composition of fly ash shown in Figure 4.9, it can be realized that fly ash contains significant proportion of crystalline compounds. Therefore, it needs higher activator concentration and temperature of activation to open and disintegrate its crystalline structure. For this reason, an initial concentration of 3% Na_2O and a temperature of activation of 60°C were chosen. The results show that compressive strength increases with time, however, there is notable reduction in compressive strength with an increase in fly ash replacement level, as shown in Figure 5.48. To avoid such behavior, either the concentration of NaOH or the temperature of activation must be increased with the increase in fly ash replacement level to compensate the effect of replacement. The replacement level of 10% fly ash can be considered as the optimal dosage, which gives higher compressive strength with respect to the other mixtures. The result of this replacement level is comparable to that given by 10% slag replacement, as shown in Figures 5.47 and 5.48.

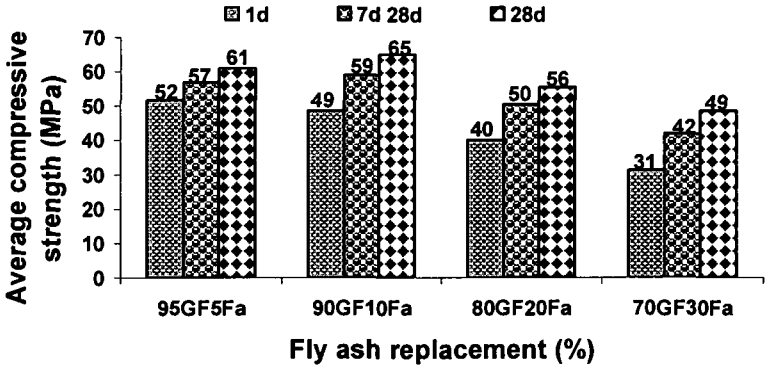

Figure 5.48 GF mixtures partially replaced with fly ash and activated by 3 % Na_2O, at 60°C

5.8.3 Comparison between GF-slag and GF-fly ash systems

These two systems are very promising as they provide an easy solution for the recycling of by-products in a sustainable system. The two systems of slag and fly ash activated by 3% Na_2O at 60°C were compared to each other at 1, 7, and 28 days. The addition of slag always increases compressive strength, while the addition of fly ash always decreases compressive strength due to its crystalline structure that needs extra energy input or higher activator concentration as opposed to that of slag, which needs less energy, as shown in Figure

5.49. The compressive strength of GF system with higher replacement level of slag is double that with fly ash, as shown in Figure 5.49. Therefore, partially replacing GF with slag is better than with fly ash at low NH concentration and temperature of activation.

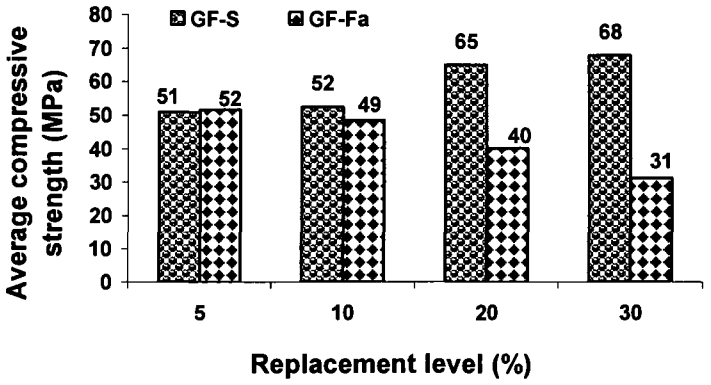

Figure 5.49 Comparison between 1-day activated GF either with slag or fly ash 3% Na_2O at 60°C

5.9 Activated-GF mortars

5.9.1 NaOH activator

This part of the study is a complementary test to the hydraulic properties of GF, as shown in Chapter 4 (characterization). This test depends mainly on the fineness of GF and activator concentration. In this part, a series of mortars were made using GF, Ottawa sand, and NaOH activator, as shown in Table 5.7. A temperature of activation of 60°C was used along with 3% Na_2O activator concentration. Both values are considered as optimal temperature and concentration, as shown in the previously mentioned part of the study on paste. The reference flow value was taken as 25 ± 5 (as that used with ASTM C227) and any sample whose value was higher than this limit was rejected.

A. Mixtures preparation

These mortars were prepared in the same way as the paste was prepared in the previous part, except for sand, with Ottawa sand being added directly 30 seconds after GF addition to the activator-containing mixing solution. The total mixing time was kept at 6 minutes, as with the previously mentioned study on paste. This part is critical, since the optimum GF-to-sand ratio was determined. This ratio is important in formulating GF-to-aggregates ratio in concrete, as shown in Table 5.7 and Figure 5.50. The optimum sand-to-GF ratio was found to be 1.5, the

w/GF ratio was 0.348 and the molar concentration of NaOH as Na_2O was 1.39 molar. Figure 5.50 shows that the effect of sand-to-GF ratio can be easily visualized. This relation reflects the effect of this ratio on the binding capacity between the newly formed cementitious phases and aggregates.

TABLE 5.7 MIXTURES CHARACTERISTICS OF THE MORTAR SAMPLES TESTED AT 60°C

Sand/GF	(GF/(GF+sand))%	w/GF	Na_2O	Na_2O Molar	Flow* (cm)
0.5	66.67	0.343	3	1.41	30.0
1.0	50.00	0.344	3	1.41	28.5
1.5	40.00	0.348	3	1.39	26.0
2.0	33.33	0.365	3	1.32	21.5
2.5	28.57	0.415	3	1.17	22.0

* Target flow = 25 ± 5 cm

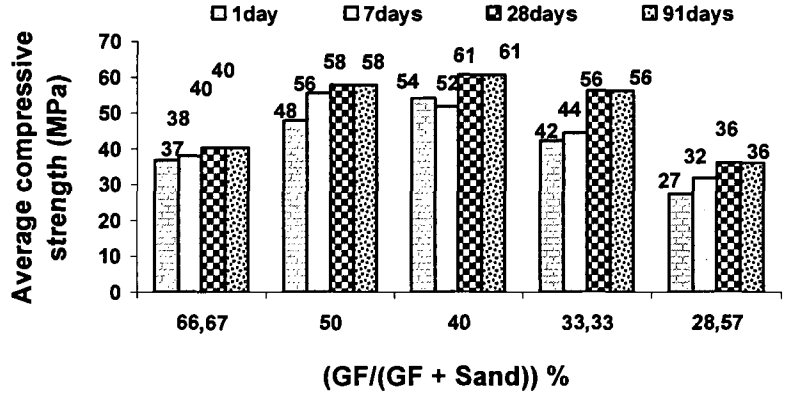

Figure 5.50 Compressive strength of mortar for 1, 7, 28 and 91 days, activated at 60°C

5.9.2 $Ca(OH)_2$ activator

Different additions of portlandite (CH) were added to GF. The effect of CH addition, as well as the effect of temperatures has been investigated. With CH activator, two temperatures of activation, three CH addition values, and three w/GF ratios were chosen based on data from the work done with NaOH. The effect of temperature, the percentage of added activator, and the concomitant w/GF ratios have been investigated, as shown in Table 5.8 and Figures 5.51 and 5.52. Compressive strength increases with both temperature and with an increase in the percentage of CH added. The development of compressive strength can be attributed to the

solubility of CH, which increases with temperature where CH becomes more soluble, and consequently more OH ions are available, resulting in an increase in the pH of the system. The higher the pH, the greater the dissolution of the silicate network is. As well, the more CH is added, the more OH ions become available. This results in the formation of calcium-alumino silicate compounds and increase in compressive strength. By increasing the temperature from 30 to 50°C, compressive strength increases to more than 250%. Therefore, these results indicate the effect of heat and concentration on adjusting desired compressive strength.

TABLE 5. 8 MIXTURE CHARACTERISTICS OF MORTAR SAMPLES TESTED AT 30 AND 50°C

$Ca(OH)_2$	Sand/GF	(GF/(GF+sand)) (%)	w/GF	CH (%)	Flow* (cm)
10	1.5	40	0.445	10	30
20	1.5	40	0.474	20	28.5
30	1.5	40	0.506	30	25.5

* Target flow = 25 ± 5 cm

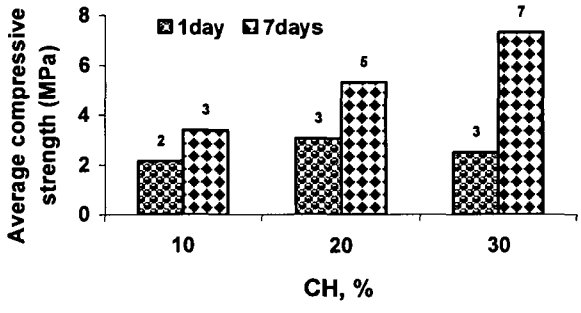

Figure 5.51 Compressive strength of mortar for 1 and 7 days, activated at 30°C

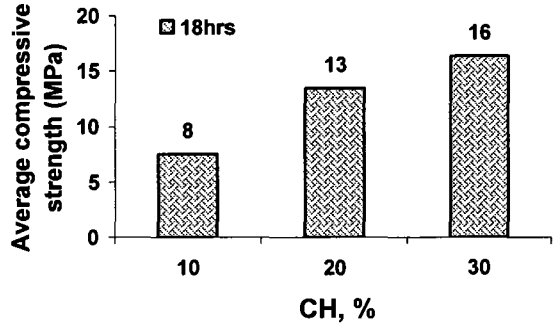

Figure 5.52 Compressive strength of mortar for 18 hours, activated at 50°C

5.10 Development of alkali-activated GF concrete (AAGFC) mixtures and some engineering properties

Five concrete mixtures have been activated using two types of activators, namely, NH and CH. These concrete mixtures were activated at 70°C for 21 hours. The compressive strengths of these mixtures were then followed at different curing ages to assess the stability of these mixtures with time.

5.10.1 Scope of work

The aim of this part of the study is to investigate the possibility of creating concrete mixtures using AAGFC. Assessing the stability of the resulting concrete, by testing compressive strength with time, is of great interest. The most convenient application for this type of concrete was found to be precast concrete. Therefore, the aims can be summarized as follows:

i. Study of mechanical properties;
ii. Study of the effect of single and double activators such as NH and CH;
iii. Study of the effect of w/b ratio;
iv. Study of the effect of GF-to-aggregate ratio.

5.10.2 Mixture proportions and results

The mix design of these mixtures is based on those used in studying the alkali-silica reaction in concrete, according to CSA A23.1-14A, with some modifications required to simulate field concrete, as given in Table 5.9

Two groups of concrete mixtures with two different GF-to-aggregate ratios were used. The first group of concrete included mixtures C1, C2, and C3, while the second group of concrete included mixtures C4 and C5. The compositions of the two groups are presented in Table 5.9. Mixtures C1, C2, and C3 were tested for compressive strength until more than 50 days to assess the early age stability of these mixtures, as shown in Figure 5.53. As well, the later age stability of these mixtures was assessed for up to more than 800 days, and it was found that these mixtures are very stable at early and later ages, as shown in Figures 5.53 and 5.54.

TABLE 5.9 MIX DESIGN FOR DIFFERENT ACTIVATED CONCRETE MIXTURES

Concrete mix design (1 m^3)						
Materials	**Density g/cm^3**	**C1**	**C2**	**C3**	**C4**	**C5**
Glass Frit (kg)	2.85	451.2	451.2	427.36	451.2	451.2
Water (kg)	1.00	168.0	178.0	206	203.04	203.04
W/B	-	0.37	0.39	0.39	0.45	0.45
Aimé Côté Sand (kg)	2.69	712	712	712	712	712
Aimé Côté aggregate (kg)	2.69	1100	1070	894	1001.57	1001.57
Added alkali, Na_2O (%)	-	2.0	3.46	-	1	3.46
CH (%)	2.24	0.18	0.55	24.5	-	0.18
SP, dry extract (%)	-	0.12	0.08	0.71	0.12	0.12

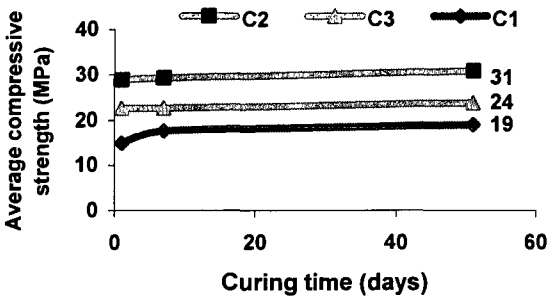

Figure 5.53 Average compressive strength of concretes up to 51 days

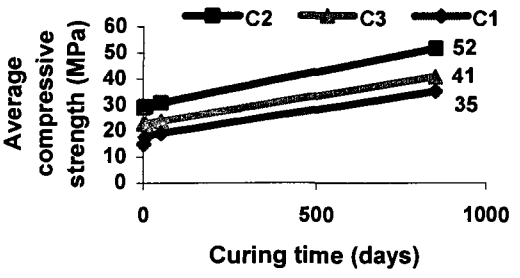

Figure 5.54 Average compressive strength of concretes up to more than 2 years

It is worth mentioning that the C2 concrete mixture gave the best strength development characteristics of the first group; consequently, concentration of 2% Na_2O seems more efficient than 3.46% Na_2O. As well, NH activator is more efficient than CH activator, as shown in Figure 5.54.

The second group of concrete mixtures, C4 and C5 contain lower GF-to-aggregate ratio (higher W/B) than that used in first group and was tested up to 28 days, as shown in Table 5.9 and Figure 5.55. Changing GF-to-aggregate ratio reduced compressive strength. This can be observed with mixture C5, which had the same composition as mixture C2 except for its low GF-to-aggregate ratio. As well, reducing NH concentration with this lower GF-to-aggregate ratio has notably reduced compressive strength, as shown in Figure 5.55. It is worth noting that the low concentration of NH (1% Na_2O) was not efficient enough to provide C4 concrete mixture with adequate strength to be tested at early ages, as shown in Figure 5.55.

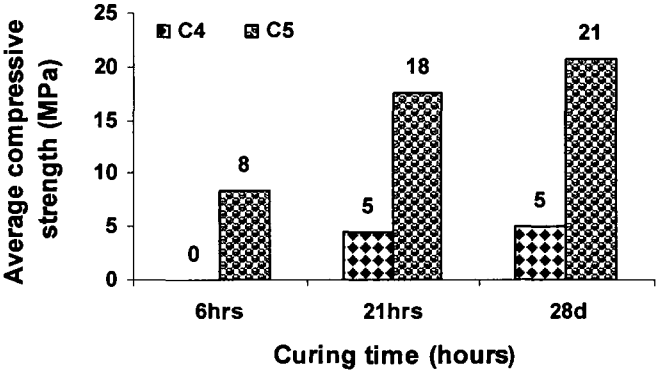

Figure 5.55 Average compressive strength at 6 and 21 hours of activation and 28 days of curing

The results showed that NH is confirmed as the best activator and its efficiency is greater than that of CH. It is not recommended to use a high percentage of CH, as compressive strength is not supported at higher CH dosages. The mixing method is critical and it has a remarkable effect on compressive strength. Concrete mixture has to be well homogenized in order to ensure good distribution of the activator and binder around the aggregates. Figure 5.A10 (Appendix A) shows some photos taken for the activated concrete mixture in the humidity chamber during curing time. Generally, the effect of type and concentration of activator, water-to-binder ratio, and GF-to-aggregate ratio have substantial effect on the final compressive strength and durability of the concrete and must be tested in detail in the future.

5.11 Development of alkali-activated GF system at ambient temperature

In this part of the study, four new non-traditional and confidential activators were proportioned and tested for their efficiency to activate 1:1 combination of GF and slag mixtures at ambient temperature without input heat. These activators are given different identifications such as ANH, TA, TCA, and QA, and they are created from definite combinations of different activators. The results of the activated mortars are shown in Figures 5.56 and 5.57. Sand-to binder ratio of 2.25 was used with mortars fabricated with TA, ANH, and TCA, as shown in Figures 5.56.

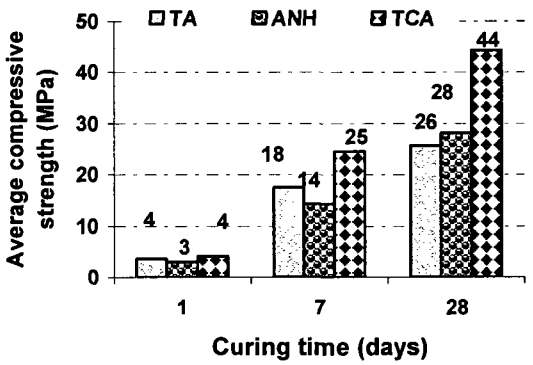

Figure 5.56 GF-S activated mortars at ambient temperature using new activators

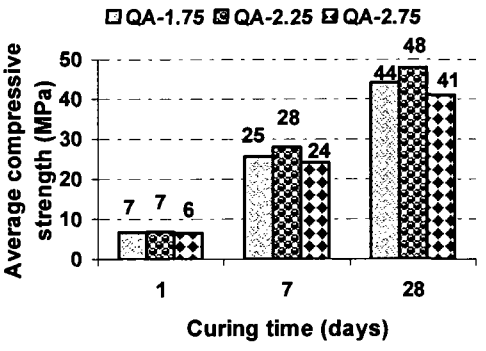

Figure 5.57 GF-S activated mortars at ambient temperature using compound activator

TCA is the best activator, as it gives compressive strength nearly double of what are given by ANH and TA, as shown in Figure 5.56. According to these results, QA activator was formulated based on the results and compositions of ANH, TA, and TCA shown in Figure

5.57. The effect of sand-to-binder ratio was tested using QA activator. Three sand-to binder ratios of 1.75, 2.25, and 2.75 were tested. Figure 5.57 shows that the sand-to-binder ratio of 2.25 is the best. Therefore, TCA and QA can be considered as the best activators capable of activating GF-S combinations at ambient temperature with a high strength. This part of the study will be started in separate project and large scale, as an extension to this work.

5.12 Hypothetical studies

5.12.1 Hypothesis for alkali-activated GF according to collision theory

A. Kinetics and Arrhenius Equation

- Collisions between reacting species create an unstable state, which is required to initiate the disintegration of GF network.
- By changing the surrounding environment to conditions favoring the formation of unstable state (alkaline), GF particles are excited to a state of higher energy.
- The number of collisions increases with increasing temperature.
- Heterogeneous reactions (geochemical) involve more than one phase formation.

Accordingly, the reaction of GF with NH and CH can be represented by the following equation:

$$nNaOH + GF\ (Si, Al, Ca, F) \longrightarrow Na\text{-}Al\text{-}Si + Na\text{-}Al\text{-}Ca\text{-}Si + NaF \quad (5.6)$$

$$nCa(OH)_2 + GF\ (Si, Al, Ca, F) \longrightarrow Na\text{-}Al\text{-}Si + Na\text{-}Al\text{-}Ca\text{-}Si + CaF_2 \quad (5.7)$$

As the reaction is a function of [OH] concentration, the reaction rate can be represented by the following equation:

$$\frac{d[OH]}{dt} = -k[OH]^n \quad (5.8)$$

$$\int d[OH] = \int -k[OH]^n dt \quad (5.9)$$

When n = 0, the reaction is zero order, and the following equation can be obtained by rearranging and solving the integral

$$[OH] = [OH]_o - kt \qquad (5.10)$$

Where k is the reaction rate constant and t stands for time. When n = 1, the reaction is first order and the following equation can be obtained by rearranging and solving the integral

$$\ln[OH] = \ln[OH]_o - kt \quad \text{or} \quad [OH] = [OH]_o e^{-kt} \qquad (5.11)$$

B. Effect of temperature on reaction rates

Experimentally, it has been found that reaction rates increase with temperature rise. This increase can be formulated as follows:

$$k = Ae^{\left(-\frac{Ea}{RT}\right)} \qquad (5.12)$$

This relationship is called the Arrhenius equation, where R is the gas constant, A is the pre-exponential frequency factor, and Ea is the activation energy representing the energy barrier needed, as shown in Figure 5.58. Consequently, the relationship between k and T is as follows:

$$\ln k = \ln A - \frac{Ea}{RT} \qquad (5.13)$$

A straight line should be produced by a plot of lnk versus 1/T, with the slope equal to:

$$\frac{Ea}{R} \quad \text{or} \quad \frac{d(\ln k)}{d\left(\frac{1}{T}\right)} = \frac{Ea}{R} \qquad (5.14)$$

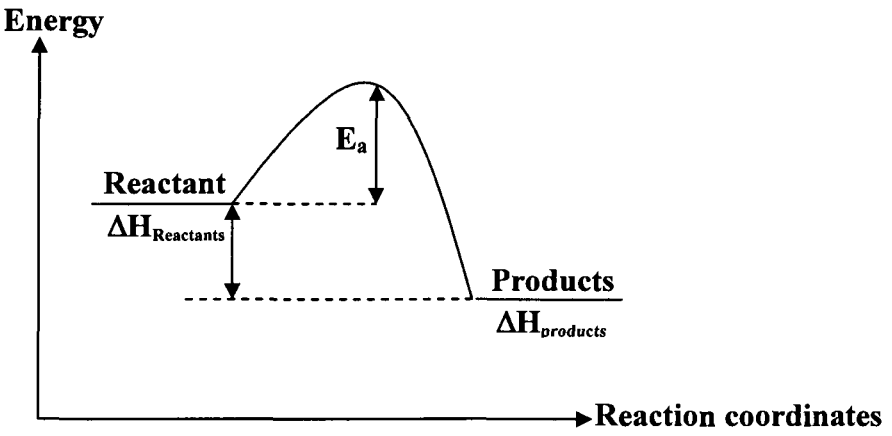

Figure 5.58 Activation energy and enthalpy of chemical reaction

Activation energy, is the driving force for a chemical reaction to take place, and is therefore experimentally defined as the slope multiplied by –R, the intercept on the lnk axis is ln A. A is the pre-exponential factor, or frequency factor, that is thought to relate to the entropy of the activated complex. A is assumed to be a constant that does not vary with temperature.

Only a fraction of molecules has sufficient energy to react at a specified temperature. The distribution of kinetic energy amongst molecules and the required energy for molecules to react give rise to the activation energy. The activation energy quantitatively describes the effect of temperature on reaction rates.

C. Confirmatory tests needed

The main variable parameters are temperature, pressure, OH-concentration, OH/GF ratio, w/GF ratio, time of activation, and finally, grain-size distribution effect. During each test, pressure could be considered as a fixed parameter that depends on the temperature used. Therefore, the change in OH-concentration could be determined with time while keeping temperature, GF content, and w/GF ratio constant during the test. Changing the temperature, while keeping the other parameters constant, is the next step. These confirmatory tests will be done as an extension to this thesis, to widen the scope of the study.

5.13 Stoichiometry of GF and calcium hydroxide

The stoichiometry of the reaction between GF having a simplified empirical formula of $NC_{2.55}S_{3.45}A_{1.5}$ derived from the complex formula of $N_{7.67}C_{12.24}S_{26.44}A_{11.55}\overline{F}_{7.28}F$ and calcium hydroxide (CH) was tested. The symbol $\overline{F}$ denotes fluorite mineral (CaF_2), where fluoride ions are present in the chemical composition and calculated as fluorite presented in its chemical composition, as shown in Table 4.1 (Chapter 4).

According to the simple GF empirical formula, the reaction of one mole of GF and unkown moles of CH can be written as follows:

$$\mathbf{NC_{2.55}S_{3.45}A_{1.5}} + aCH + bH \rightarrow 3.45N_{0.29}\mathbf{C_nSA_{0.43}}H_m \qquad (5.15)$$

where a = 1.32(3.45n – 2.55), b = 3.45m-0.243a, and n = C/S. Then m = 4.554(C/S) + 0.29b

The reaction of GF and CH was previously studied in Chapter 4, as well as here in Chapter 5 (refer to 5.3) where 20% CH was considered the optimum value that can react completely with 80% GF; that is 80 g of GF reacts completely with 83% of 20 g (16.6 g) of CH, as shown in Figure 5.35. Therefore, after transferring these values into molar ratios, 1 mole of GF reacts with about 1.6 moles of CH, and "a" = 1.6 (knowing that 80 g of GF equals 0.142 mol GF and 16.6 g of CH equals 0.223 mol CH). This latter value is comparable to what was found in the reaction of slag with CH as examined by RICHARDSON [2002]. As well, n can be calculated from SEM of the activated mixture of GF and CH, which was estimated as 1.29. Therefore, m = 4.45-0.29b. It can be concluded from Table 5.3 that "b" depends on GF/CH ratio and temperature of activation, consequently m is a b-dependent variable. Therefore, the above equation can be written as follows:

$$NC_{2.55}S_{3.45}A_{1.5} + 1.6CH + bH \rightarrow 3.45N_{0.29}\mathbf{C_{1.29}SA_{0.43}}H_m \qquad (5.16)$$

The variable 'm' can be calculated from the free water determined by drying and combined water determined by ignition, or by subtracting the free water from total added water.

5.14 Stoichiometry of GF and sodium hydroxide

The stoichiometry of the reaction between GF and NaOH (N) was intensively tested in this chapter. Therefore, many data can be used to imitate the reaction of GF and N and to establish a scientific basis to model the reaction of GF and N. The following equation was supposed:

$$NC_{2.55}S_{3.45}A_{1.5} + aNH + bH \rightarrow 3.45N_hC_nSA_{0.43}H_m \qquad (5.17)$$

where a = 1.29(3.45h – 1), b = 3.45m-0.225a, and n = C/S, then m = 0.225(C/S) + 0.29b

From the work done on alkali-activated GF, the optimum N concentration was estimated to be 1.5% with respect to total weight of GF. Therefore, 1 mole of GF reacts with 4.72 moles of N, then a = 4.72, consequently h = 1.35. From SEM the average C/S equal 0.62 where it ranges from 0.55 to 0.67. The average water-to-GF ratio equals 0.322, then the empirical coefficient b equals 47.7, consequently m equals 13.97, which means approximately 14. Therefore, the above-mentioned equation can be written as follows:

$$NC_{2.55}S_{3.45}A_{1.5} + 4.72NH + 47.7H \rightarrow 3.45N_{1.35}C_{0.62}SA_{0.43}H_{14} \qquad (5.18)$$

In hydration products, the S/A, silica modulus, and C/S ratios are 2.32, 0.74, and 0.62, respectively. These ratios are important in modeling the hydration of cement in presence of GF. Therefore, this part can be considered as an introduction to hypothetical studies of hydration of cement in presence of GF, as well as the activation process of GF in presence of different activators.

5.15 Conclusions

GF is a highly amorphous material, which has a great potential for conversion into cementitious binder. This chapter has concentrated on choosing different inorganic activators with different combinations capable of performing safe GF activation. The best optimal activator concentrations were chosen. Different temperatures of activation were investigated. The best GF-to-sand ratio was found and different concrete mixtures were made. NaOH

activator and the temperature of 60°C were chosen as the best activator and optimal temperature of activation, respectively.

Different inorganic activators have shown dissimilar behavior with GF. Sulfate-based activators have synergistically reacted with GF forming stable sulfate compounds, as confirmed by XRD-analysis. The presence of other mineral admixtures, such as slag and fly ash, improved the mechanical properties of the binders obtained. Therefore, partial replacement of GF with small amounts of these admixtures can results in great changes in physical and mechanical properties of the binders obtained.

The mechanism of GF activation reaction with NaOH was assumed and confirmed by SEM-EDS analysis. It has been shown that the outer particle surface of GF was attacked first by NaOH solution. Thereafter, melting of the particle's surface has taken place, which fused the particles together, forming the initial binding effect. Finally, rearrangement with recrystallization took place to produce the last cementing solid form.

5.16 Future research

The following are proposed for future research:

i- Kinetics of the activation process and determination of activation energy according to ASTM C 1074;

ii- Improving the efficiency of the new activator capable of activating GF at ambient temperature;

iii- Intensive work on the fabrication of concrete and determination of the parameters affecting the fabrication process, including w/b , sand-to-coarse aggregates, and GF-to-total aggregate ratios;

iv- Durability studies of these types of activated concretes including scaling, freezing and thawing, permeability, and porosity of the system.

CHAPTER 6

ALKALI-SILICA REACTION STUDIES ON MORTAR AND CONCRETE CONTAINING GF

6.1 Introduction

The use of supplementary cementitious materials to counter alkali-silica reactions in concrete is well documented in North America, where pioneering research in this area has been performed [CSA 23.2-27A and 28A; Bouzoubaâ and Fournier, 2005]. As previously mentioned, the alkali content of GF is approximately 10% Na_2O_{eq}. This alkali content is a matter of concern, making it the main issue when using GF in concrete. To fully investigate the effect of the alkali content of GF on expansion due to the alkali-silica reaction (ASR), different strategies have been considered. The main strategy in this chapter was to determine what effect the incorporation of different levels of GF in mortar and concrete, without any other mineral additives, has on ASR expansion. It was expected that this amount of alkalis would cause harmful expansion if higher replacement levels were used. The second strategy was to assess the effect of different ternary and quaternary mixtures on ASR expansion, and then choose the optimum mixtures for future work as recommended mixtures. Different as-is (normal), modified, accelerated, and long term-Canadian and American specification tests were used. Samples containing GF were subjected to normal, medium, and aggressive media in order to study the effect of such media on ASR expansion. Synergistic mixtures of GF with fly ash, slag, and silica fume were tested to set up a database of synergistic mixtures from which the best concrete mixtures could be formulated. Values observed from both the longer and accelerated tests show consistent results. A proposal for a new standard from the work done on the modified ASTM C227 to establish an accelerated test lasting less than one month, instead of the current length of 6 months, is presented.

This part of the study is divided into two main tests: mortar bar and concrete prism tests, using Canadian (CSA) and American (ASTM) specifications. Mortar bar tests are subdivided into normal mortar bar (ASTM C227) and accelerated mortar bar (ASTM C 1260/CSA A23.2-25A) tests. A few modifications were made to these tests in order to study their effect on ASR expansion.

The most important cementitious systems used throughout this work are listed in Table 6.1. These mixtures were used in mortar and concrete in addition to other mixtures presented in the forthcoming sections that are not listed in Table 6.1. LADJI et al. [2004], LALDJI and TAGNIT-HAMOU [2006; 2007], and TAGNIT-HAMOU and LALDJI [2007] have mechanically tested the mixtures shown in Table 6.1, which were chosen for their satisfactory results.

TABLE 6.1 MIXTURE COMPOSITIONS OF THE MOST FREQUENTLY USED CEMENTITIOUS SYSTEMS

Mixtures	Symbol	Composition (%)
Control	**CO**	100% cement (0.9% Na_2O_{eq})
B25GF	**B25GF**	75% cement + 25% glass frit
B50GF	**B50GF**	50% cement + 50% glass frit
T20GF5SF	**TSF**	75% cement + 20% glass frit + 5% silica fume
Q25GF30S5SF	**Qs**	40% cement + 25% glass frit + 30% Slag + 5% silica fume
Q20GF25FA5SF	**Qfa**	50% cement + 20% glass frit + 25% fly ash + 5% silica fume

6.2 Mortar Bar Test (ASTM C 227)

This test was performed according to the American specification ASTM C227, which recommends that tested bars be left in their containers for up to 6 months (100% R.H., at 38°C). The containers were previously shown in Figure 3.13. The length change measurements were monitored for three to six months and compared with the control sample. The specification limit is 0.1% linear expansion after 6 months. Two well-known types of aggregates representative of a range of effect from innocuous to deleterious were used, namely Ottawa sand and Spratt aggregate, respectively, in addition to moderately reactive aggregate, namely Aimé Côté sand (as shown in Chapter 3).

6.2.1 Mortar mixtures using Spratt aggregate

A. GF binary mixtures

Two replacement levels of 25 and 50% GF-binary systems made from CSA GU cement were used. The physical and chemical properties of the cement were given in Chapters 3 and 4. The readings were taken as the average of three bars. The control and binary mixtures containing

25% GF gave comparable results, placing them at the border of the specification limit, while the mixture containing 50% GF is still well below the specification limit. Based on the pozzolanic properties of GF, those results may be interpreted as follows: the GF-containing mixture is reacting with the released portlandite, which decreases the amount of leaching taking place. As a consequence, the GF-containing samples have the ability to maintain more alkali ions than the control samples, which suffer portlandite leaching that always contains alkalis. Therefore, portlandite leaching generally decreases the alkali content, especially in the control samples. As a consequence of alkali leaching, the effect of alkalis appeared to be less important than in the mixture containing 25% GF. The replacement level of 25% GF is not the optimum replacement level that should be used, as will be shown in this chapter. The results obtained from the 50% GF mixture confirm this interpretation. If the alkali content of GF were the main element responsible for the results obtained with 25% GF, a higher expansion with 50% GF replacement would be expected. However, this was not the case. The higher the GF content, the higher the reduction in the ASR expansion obtained. This may also be due to the replacement effect. As the cement is replaced by half of the amount, the alkali content of cement has been reduced by half and therefore the expansion is reduced by half, as clearly shown in Figure 6.1. The expansion values of the 50% GF samples are nearly half of what was obtained for the control samples. This takes place only when GF is an inert material that does not supply the system with potentially deleterious alkali. This could also be taken as another proof that alkali content of GF is not available over the testing period (6 months). The unavailability of alkalis has been confirmed by accelerated and concrete prism tests, at approximately more than 2 years, as will be shown later in this chapter.

B. GF-SF ternary mix

Due to its extreme fineness and high glass content, condensed silica fume (CSF) is a very efficient pozzolanic material. The high specific surface area of CSF results is increasing water demand, which was compensated by using GF, which decreases water demand in mortar mixture. In this part of the study, a ternary mixture containing 20% GF and 5% silica fume (20GF5SF) was tested and compared with control and binary mixtures containing 25%, and 50% GF. The effect of silica fume addition has revealed the importance of ternary mixtures and the synergistic effect among different supplementary cementitious materials (SCMs) that

improve the mitigating action against ASR expansion. The expansion of 20GF5SF mixture with time is lower than the binary mixture containing 25% GF, however, it gave slightly higher expansion than the binary mixture containing 50% GF. This implies that 50% GF results in lower expansion than the equivalent ternary mixture containing silica fume, as shown in Figure 6.1. These results suggest that the 20GF5SF ternary mixture is not the optimum mixture that should be used, especially that the rate of expansion of the bars is such that the 0.10% limit may be reached within the next few months of testing.

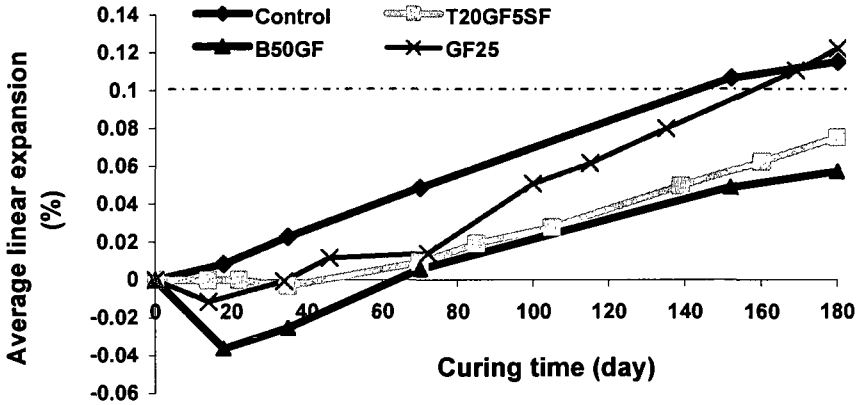

Figure 6.1 Mortar bar test (according to ASTM C227) for GF binary and ternary mixtures (38°C, 100% R.H.)

C. GF-Pfa-CSF and GF-Slag-CSF quaternary mixtures (Qfa and Qs)

The vast majority of fly ash used in concrete is low-calcium ash (ASTM class F), as was used in this mixture. Both physical and chemical properties of fly ash and slag are given in Chapter 4. In this part of the study, two quaternary mixtures made up of slag and class F fly ash, were used, identified as Qs and Qfa, respectively, as shown in Table 6.1. These two quaternary mixtures were found to efficiently control ASR expansion in the test specimens (i.e. expansion < 0.02% at 6 months), as shown in Figure 6.2. Again, the synergistic effect of such SCMs, referred to as co-additives (author's preference), is shown to be highly effective.

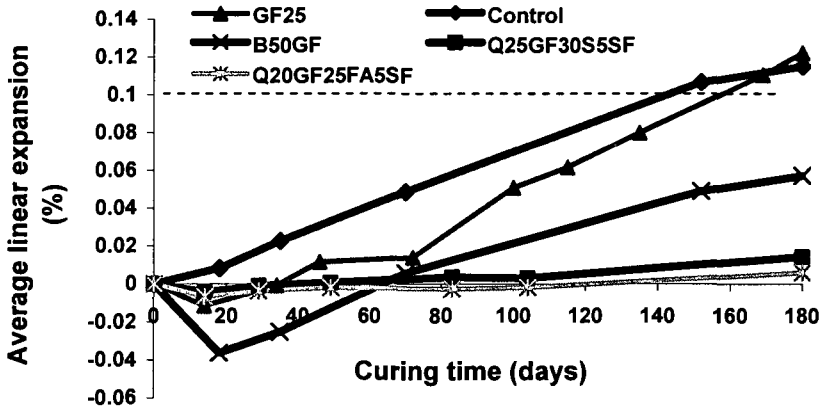

Figure 6.2 Mortar bar test (according to ASTM C227) of quaternary systems using Spratt (38°C, 100% R.H.)

From the above-mentioned Figures 6.1 and 6.2, it can be concluded that a binary system of GF with replacement levels of more than 25% could be effective in mitigating the alkali-silica reaction (ASR). The same also applies to the ternary and quaternary mixtures investigated. However, the ternary mixture is slightly less effective than the binary with 50% GF, which is consequently less effective than the two quaternary mixtures.

6.2.2 Mortar mixtures using Aimé Côté sand

A. Control and GF binary mixtures

Aimé Côté sand is river-bed sand that is less reactive than Spratt aggregate. Its physical properties were presented in Chapter 3 (Materials). According to ASTM C227, Aimé Côte sand is a non-reactive aggregate whose reactivity is approximately 4 times less than that of the Spratt, as can be easily concluded from Figures 6.2 and 6.3. However, according to ASTM C1260, the accelerated mortar bar test (AMBT), Aimé Côté sand is a reactive aggregate, as will be shown in the accelerated test (section 6.4). The expansion values of both the control and the binary mixtures with 25% GF are well below the specification limit (0.10% expansion), as shown in Figure 6.3. However, the expansion value of the binary with 25% GF mixture at 180 days is equal or even slightly higher than that of the control. The same argument that applies to the Spratt aggregate can be applied in this case: alkali leaching in control sample is also higher than that of the binary with 25% GF.

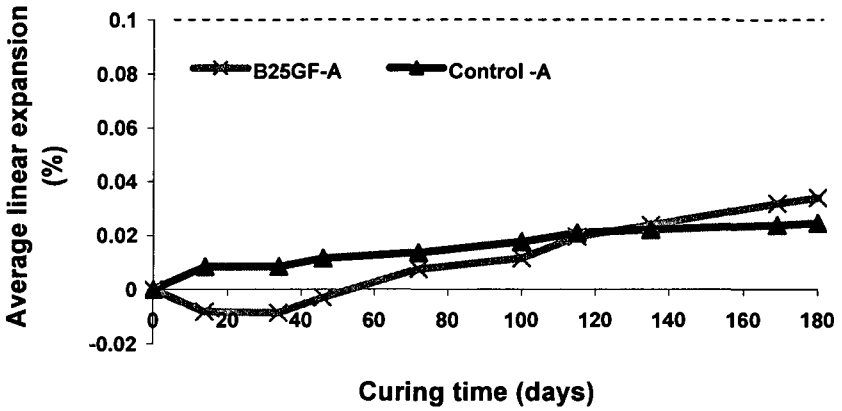

Figure 6.3 Mortar bar test (according to ASTM C227) for GF binary systems using Aimé Côté sand(38°C, 100% R.H.)

6.2.3 Mortar mixtures using Ottawa sand

Ottawa sand has been used as an innocuous aggregate and as reference aggregate, according to ASTM C109. Its physical properties and grain-size distribution were given in Chapter 3.

A. GF binary and ternary (GF-CSF) mixtures

It was expected that all mixtures containing Ottawa sand would give expansion values much lower than the ASTM expansion limit. This is due to the non-reactive character of such aggregate. The same mixtures that had been used with Spratt aggregate were used in this part, except that the Spratt aggregate was replaced by Ottawa sand. The expansion of the control mixture is higher than the binary mixture, which is slightly higher than that of the ternary mixture. This follows the same expansion trend as that of the Spratt aggregate, except for the actual expansion levels that have been observed.

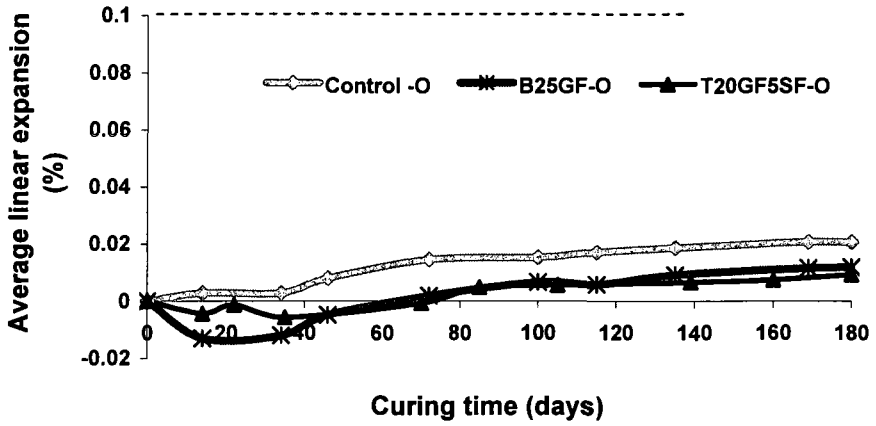

Figure 6.4 Mortar bar test (according to ASTM C227) of the ternary system using Ottawa sand (38°C, 100% R.H.)

B. Binary and quaternary glass frit systems

The same two quaternary mixtures that were made using Spratt aggregate were used in this part, except that the Spratt aggregate was replaced by the Ottawa sand. According to the non-reactivity of he Ottawa sand, there is no major difference among the ASR expansion values of binary, ternary, and quaternary mixtures. This test is applicable and recommended for reactive aggregate in order to assess the combination of reactive aggregate and blended cements. Therefore, the presence of GF with non-reactive aggregate shows no relevant effect that requires full evaluation. The same applies to the use of the ternary and quaternary mixtures, as their effectiveness is highly remarkable in the case of the use of reactive aggregate only. If any alkali is released from GF, it will be very difficult to notice it when an innocuous aggregate is used. The small difference between the binary and two quaternary mixtures using the Ottawa sand is irrelevant, as expected. However, the control sample shows higher expansion than the other mixtures. The innocuity of Ottawa sand is not a given, as will be shown in the accelerated test (section 6.4).

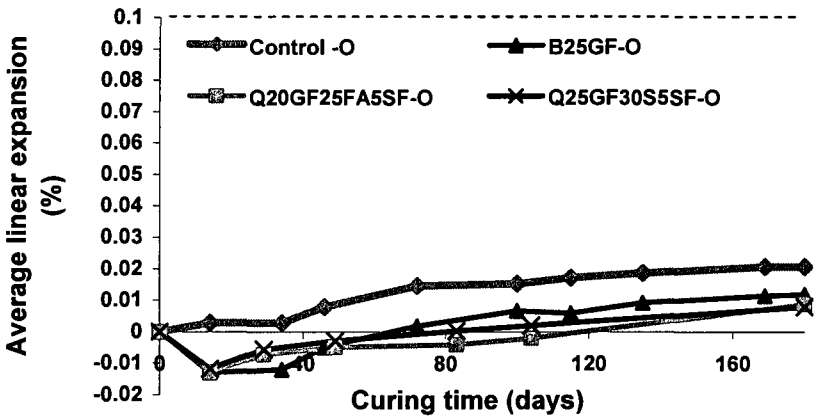

Figure 6.5 Control, binary and quaternary mortar bar mixtures using Ottawa sand (38°C, 100% R.H.)

From Figures 6.4 and 6.5, it can be concluded that due to the absence of non-reactive constituents, most of the cementitious systems give comparable results that could be attributed to the non-reactivity of Ottawa sand.

The drawback of this test is the leaching of alkalis due to the leaching of portlandite [RANC et al., 1994; WIGUM et al., 1997; MALVAR et al., 2002]. ROGERS and HOOTON (1991) showed that higher expansion always takes place when mortar bars are stored in containers without wicking material. However, when excessive condensation of water takes place on specimen surfaces, alkalis are removed from the concrete and the rates of reaction and expansion are reduced [RIVARD et al., 2003]. As a consequence, the expansion of control samples seems to be less than what it should be. As the active additives react with portlandite, its leachability decreases, and as a result, so does the leachability of alkalis. Therefore, active additive-containing mixtures seem to give higher expansion values compared to the expansion values of the control samples that undergo leaching of alkalis. The alkali content in the control samples should be increased by the external addition of alkalis, exactly as is done in the concrete prism test. This increase in alkali content could also be adjusted to reach 1.25% Na_2O_{eq} or higher of total alkalis content in the mortar mixture based on the alkali content of the cement used. Therefore, an increase in Na_2O_{eq} concentration can compensate alkali leaching.

6.3 Modified ASTM C227 mortar bar test using Spratt aggregate (accelerated test)

Expansion due to ASR increases with the increase in alkalis concentration, pessimum grain size, and change in surrounding environment, such as temperature and humidity [SHAYAN et al., 1996; OBERHOLSTER AND WESTRA, 1981; GUDMUNDSSON et al., 1998]. Based on the literature and these facts, the reactivity has been increased according to changes in these parameters. The grade size proportions of Spratt aggregate, stated in Table 3.10, were modified in order to increase fine constituents. A mixture composed of two grade sizes: the first passed through a sieve of 316 μm and retained on a sieve of 160 μm , while the other grade passed through a sieve of 1.25 mm and retained on a sieve of 630 μm, were proportioned to 1:1. The water-to-binder ratio was 0.5. The binder-to-aggregate ratio remained the same as in ASTM C227, i.e. 1:2.25. The alkali content was changed through NaOH addition to the mixing water to increase its total content to 1.25 and 2.5% Na_2O_{eq} for both the control (CO-1.25 and CO-2.5) and binary mixtures containing 50% GF (GF-1.25 and GF-2.5). As well, the curing temperature was changed from 38 to 60°C. These modifications clearly demonstrate the effect of curing temperature and leaching rate on expansion of the control mixtures containing those two alkali concentrations. The results of this test are shown in Figure 6.6.

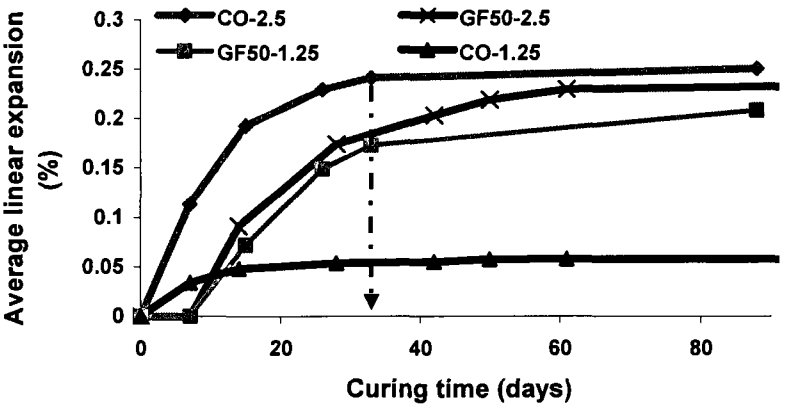

Figure 6.6 Binary 50% GF mixture according to modified ASTM C227 using Spratt (60°C, 100% R.H.)

Figure 6.6 shows that the leaching effect in the control sample with an alkali content of 1.25% Na_2O_{eq} (CO-1.25) is much greater than that in the control sample with an alkali content of 2.5% Na_2O_{eq} (CO-2.5). As well, expansion of the binary mixture containing 50% GF with an

alkali content of 2.5% Na_2O_{eq} is much higher than the control mixture with an alkali content of 1.25% Na_2O_{eq}. There is therefore a threshold value, after which the leaching effect has no significant effect on expansion. It can also be concluded that GF blended cement having the same alkali content as the control has a greater ability to retain alkalis. The control sample with an alkali content of 2.5% Na_2O_{eq} gave expansion values higher than the binary mixture containing 50% GF and the same alkali content. This means that GF has the ability to retain alkalis in a non-harmful way. In other words, it consumed alkalis by forming new cementitious phases in which alkalis are part of the structure (chemically entrapped inside their structure), as confirmed in Figure 6.6 and later in this chapter. To demonstrate this assertion, the expansion values of the GF samples with 1.25 and 2.5% Na_2O_{eq} are very comparable to each other and still lower than the control with 2.5% Na_2O_{eq}. It is noted that maximum expansion was reached at 33 days. Therefore, these modifications could be extended as a proposal for a new specification based on the modifications made to ASTM C227. When using ASTM C227, it is highly recommended to use the modifications carried out on reactive aggregate and Portland cement through by its alkali content through external alkalis addition. To accelerate the reaction rate, high curing temperatures, as well as high ASR reactive surface area by increasing the fine constituents of the reactive aggregate, are recommended.

6.4 Accelerated Mortar Bar Test (AMBT) CSA A23.2-25A

This test method is commonly used for assessing the potential reactivity of aggregates, as well as the effectiveness of the cementitious materials. However, this method does not replace other similar lengthier test methods. This test was carried out in accordance with CSA A23.2-25A (equivalent to ASTM C1260), in which the mortar bar samples have to be immersed in 1N NaOH at 80°C; expansion data of the mortar can be obtained within as little as 16 days. The test method was developed because of the shortcomings of ASTM C227 and ASTM C289. It is the most popular test used today. In this part of the study, five aggregates were used (Spratt, Aimé Côté, Ottawa, Mirabel, and LG aggregates). First, a comparison was made between different replacement levels of glass frit, and then between different mineral admixtures. Thereafter, a series of binary, ternary, and quaternary mixtures were prepared to determine the synergistic effect of GF with different mineral admixtures.

6.4.1 Mortar mixtures using Spratt aggregate

A. Binary GF mixtures

GF mixtures were tested to investigate the effect of different replacement levels of GF on ASR expansion. Replacement levels of 25, 50, 75, and 90% GF have shown that expansion decreases when the replacement level is increased. This result is in phase with the results obtained using ASTM C227, as shown in the following Figures 6.7 and 6.8.

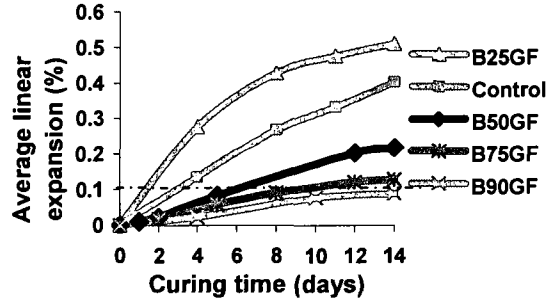

Figure 6.7 Effect of different GF replacement levels on ASR expansion (80°C, 1N NaOH)

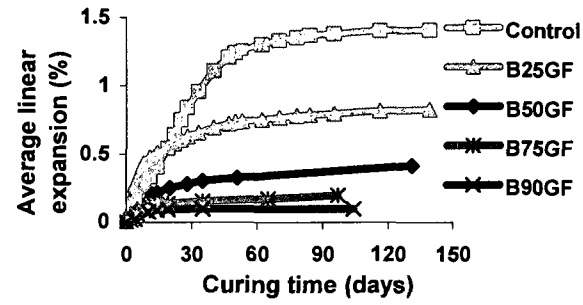

Figure 6.8 Effect of different GF replacement levels on long-term ASR expansion (80°C, 1N NaOH)

This is further proof that the alkali content of GF is not deleterious; the incremental increase in GF content does not enhance ASR expansion. The difference between expansion of the control and 25% GF binary mixture can be attributed to either the optimized quantity of GF that should be used or other inherent properties that contributed to expansion, as shown later in this chapter. Accordingly, 25% replacement level of GF is not the optimum dosage of GF that should be used; the mortar bars containing this dosage react as if they only contained 75% cement and kept the same w/c ratio. Therefore, at early age, they are more porous and less compact than the control samples containing 100% cement, as confirmed later by pore analysis. Figure 6.8 shows that the 25% GF curve intersects with the control curve at about 19 days, and then the expansion rate starts to slow down as an indication of the beginning of the mitigating action for this replacement level. The other replacement levels show lower expansion values at the beginning. This indicates the presence of a pessimum replacement value before which, there is a reverse action that negatively affects the microstructure of this system. It is worth noting that 90% GF-containing mortar bars are rigid enough to withstand

the severe conditions of this accelerated test. This is yet another proof that GF reacts as a cementitious binder and that the cement used (10%) has acted as an activator.

Another test has been done on mortar bars containing 75% cement, with the remaining 25% being replaced by innocuous Ottawa sand to compare it with that containing 25% GF. If the expansions of these mixtures are co-parallel with little difference, then the previously mentioned explanation is correct. It is expected that the two mixtures will have a similar expansion trend. The results obtained show that the expansion behavior of the mixture containing 75% cement and 25% Ottawa sand is indeed similar to that containing 25% GF and 75% cement, as shown in Figure 6.9. The main difference between the two curves can be attributed to the presence of Ottawa sand (25%), which may be responsible for decreasing the expansion values to be slightly lower than that with 25% GF. Nevertheless, in general, the trend of both expansion curves seems to be similar. This may be due to the effect of Ottawa sand that hinders and decreases the expansion of that mixture in a similar way, but earlier than the effect of 25% GF. This test confirms the above-mentioned discussion concerning the drawback effect of 25% GF at early ages, as well as its mitigating action against ASR expansion at later ages.

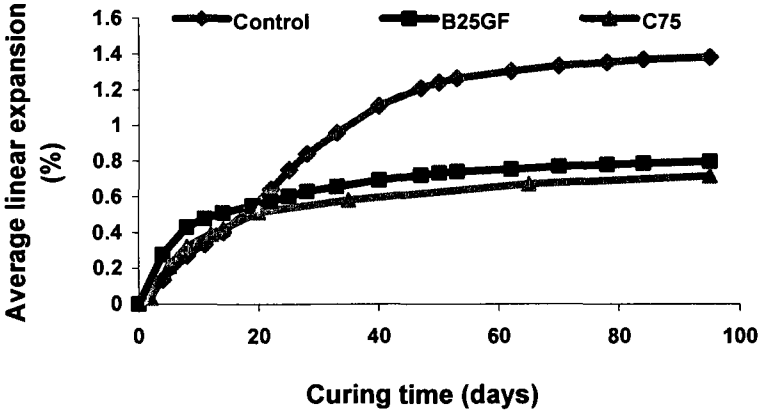

Figure 6.9 ASR expansion for a mortar mix with 75% cement and 25% GF or Ottawa sand Using Spratt (80°C, 1N NaOH)

B. Specific weight gain

The specific weight hange with time, the weight change in gram over the volume change in cubic centimeter of the mortar bar samples of the control and three binary mixtures containing

25, 50, and 75% GF, was determined. The results are shown in Figure 6.10, from which it can be concluded that the specific weight gain change for the Spratt control mixture is higher than that of the other binary mixtures. The specific weight gain change with time for these mixtures decreases with an increase in GF content. The reduction in specific weight change can be arranged according to the gain values, as follows:

Control>B25GF>B50GF>75GF

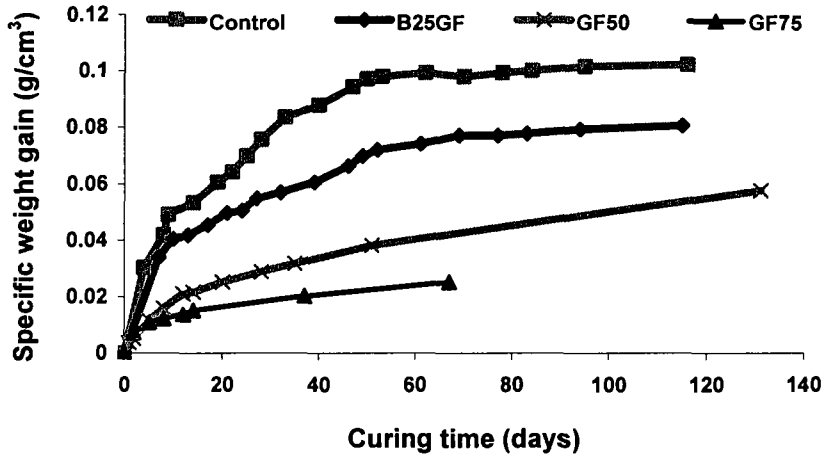

Figure 6.10 Specific weight gain for mortar mixtures with different GF levels using Spratt (80°C, 1N NaOH)

These results are entirely in accordance with corresponding expansion results. Therefore, this method needs to be verified using other mixtures, and if successful, it can be recommended as a helpful means of verifying the expansion data. The importance of Figure 6.10 lays in the supposition that there may be a threshold value, which can be taken as a reference, after which the tested sample can be considered as potentially deleterious compared to, and in accordance with, AMBT results.

C. Simple analysis of GF-binary mixtures results

Expansion values at 14 and 28 days for each GF replacement level were plotted, and the points that fit the linear curve were used to obtain lines presenting the best fit, as well as their equations. The two linear lines obtained intersected at a given point at which the expansion at 14 days is equal to the expansion at 28 days. This point is obtained by solving the two

equations of best-fit lines at 14 and 28 days. This point has a replacement level of 91.8% GF at which the expansion value at 14 days is theoretically equal to that at 28 days. Experimentally, at a replacement level of 90% GF, the expansion value at 14 days was 0.089% while at 28 days it was 0.094%. The difference between the two expansion values is only about 5%, as shown in Figure 6.11

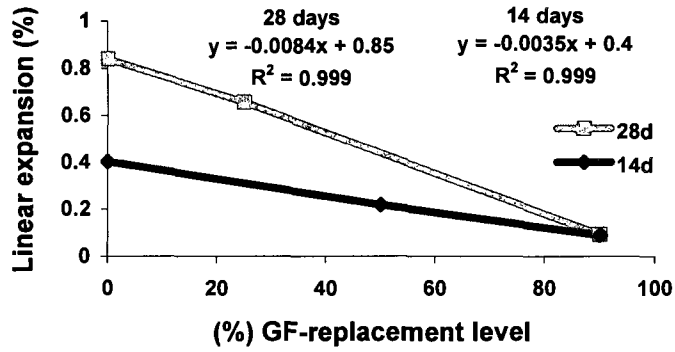

Figure 6.11 Linear expansions against GF replacement levels using Spratt (80°C, 1N NaOH)

It is worth mentioning that the binary mixture containing 75% GF was excluded from the above calculation to serve as a verifier of calculation correctness. By substituting 75% into the first equation of 14-day expansion and into the second equation of 28-day expansion to predict expansion at these ages, the obtained values were 0.1374 and 0.2198%, respectively. The experimental expansion values of the mixture containing 75% GF corresponding to the same ages are 0.129 and 0.2044%, respectively. Therefore, the difference between the expected values and the predicted ones at 14 and 28 days are 6.5 and 7.5%, respectively. Therefore, the above equation gives reliable results.

6.4.2 Comparison between the binary mixtures using Spratt aggregate

A. GF against SF system

A comparison between binary mixtures containing different GF contents with that containing condensed silica fume (CSF) at 14 days was conducted, and the efficiency sequence was determined, as shown in Figure 6.12:

$$12\%\ CSF \geq 90\%\ GF > 75\%\ GF > 10\%\ CSF > 5\%\ CSF > 50\%\ GF > control > 25\%\ GF$$

Therefore, the expansion of the binary mixture containing 90% GF is comparable to that of the binary containing 12% CSF, while the expansion of the binary mixture containing 75% GF is comparable to that of the mixture containing 10% CSF.

At later ages (28 days), the sequence shown in Figure 6.13 was:

90% GF > 75% GF> 12% CSF > 50% GF >10% CSF >5% CSF > 25% GF > control

Based on the 28-day expansion value, the binary mixtures containing 90 and 75% GF are more effective in reducing ASR expansion than the binary mixtures containing 10 and 12% CSF; therefore, it was expected to obtain efficient ternary mixtures containing GF-CSF.

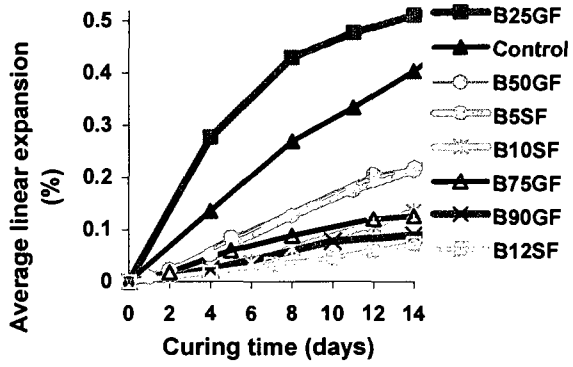

Figure 6.12 Comparison between binary mixtures made from GF andCSF systems at 14 days (80°C, 1N NaOH)

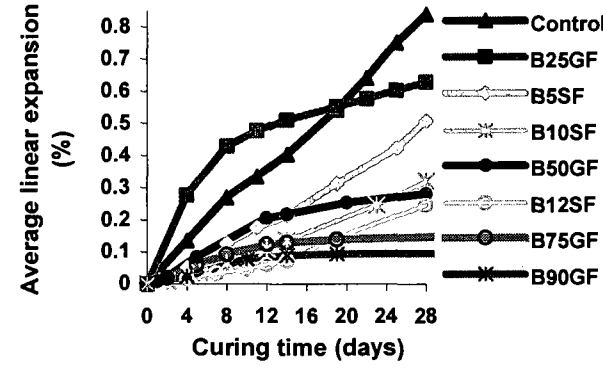

Figure 6.13 Comparison between binary mixtures of GF and CSF system at later ages (80°C, 1N NaOH)

B. GF against fly ash (Pfa) system

Comparing binary mixtures containing GF with those containing Pfa at 14 days, the efficiency sequence shown in Figure 6.14 was found to be:

25% Pfa > 90% GF > 50% GF > control > 25% GF

Therefore, among these mixtures, 25% Pfa is the most effective mixture at early age, while at later ages the sequence shown in Figure 6.15 was found to become:

90% GF > 25% Pfa > 50% GF > 25% GF > control

The mixture containing 25% Pfa is known to be effective in controlling ASR expansion at early ages in the test; however, at later ages, the efficiency of 90% GF is greater than that of 25% Pfa. Therefore, it was expected to obtain synergistic ternary mixtures of GF-Pfa at lower combination contents.

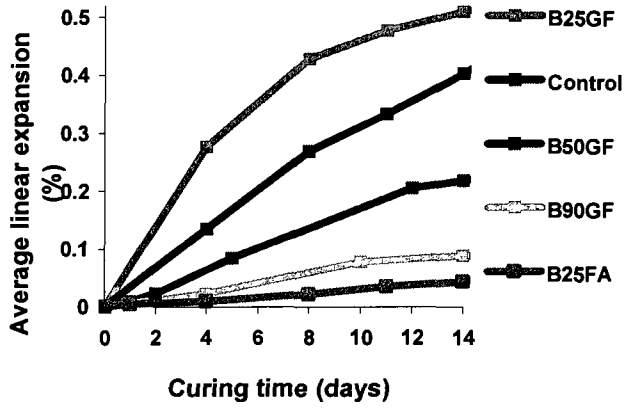

Figure 6.14 Comparison between binary mixture made from GF or Pfa systems at 14 days

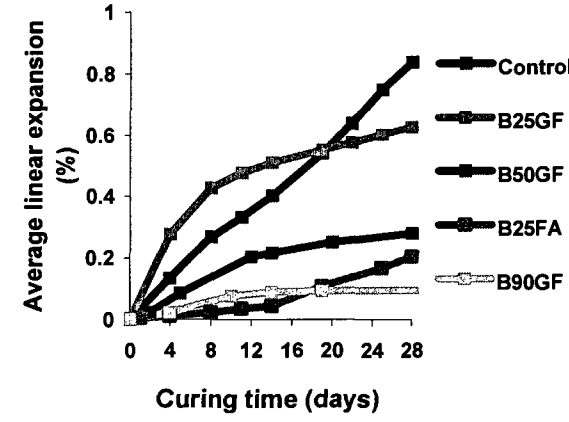

Figure 6.15 Comparisons between binary mixtures of GF or Pfa systems at 28 days

C. GF against slag system

Comparing binary mixtures of GF with those containing slag at 14 days, the efficiency sequence shown in Figure 6.16 was found to be:

$$50\%\ \text{slag} = 90\%\ \text{GF} > 50\%\ \text{GF} > \text{control} > 25\%\ \text{GF}$$

Therefore, the efficiency of 50% slag equals that of 90% GF at early ages, while at later ages, the sequence shown in Figure 6.17 was found to become:

$$90\%\text{GF} > 50\%\ \text{slag} > 50\%\text{GF} > 25\%\text{GF} > 25\%\text{GF} > \text{control}$$

The efficiency of slag is substantial at high replacement levels (i.e. ≥50%), however, at later ages the efficiency of 90% GF is higher than that of 50% slag. Therefore, it was expected to

obtain efficient ternary mixtures containing GF-slag at higher dosages, which is not recommended.

It is worth mentioning that the binary mixture containing 25% slag gave an expansion somewhat similar to that of the binary mixture containing 25% GF at later ages. Therefore, GF is an effective admixture at later ages. Although the binary mixture containing 25% GF showed undesirable results at early ages, it reversed its chemical behavior at later ages, as shown in Figure 6.17. The efficiency of the binary mixtures containing 25, 50, and 90% GF is persistent at later ages, as shown in Figure 6.8, as opposed to these binary mixtures containing CSF, Pfa, and slag, which seem to show increasing expansion with time.

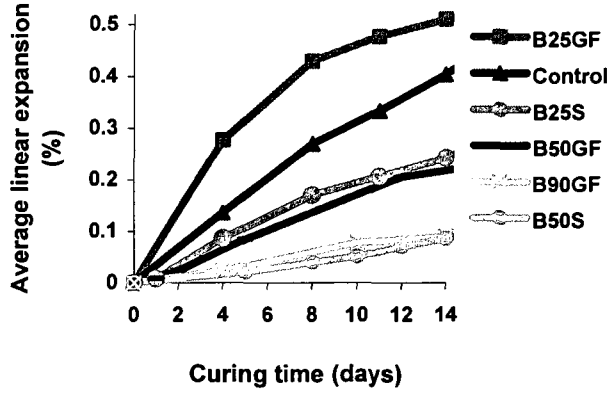

Figure 6.16 Comparison between binary mixtures containing GF or slag systems at 14 days

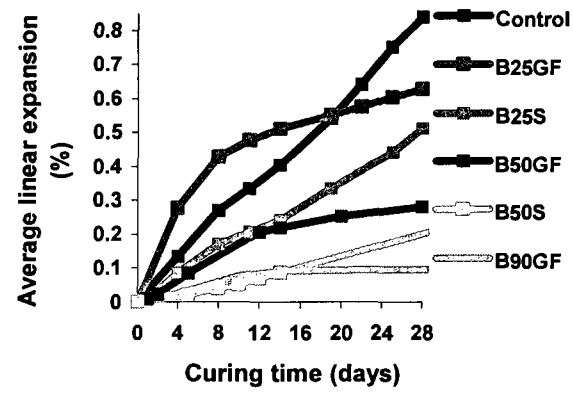

Figure 6.17 Comparison between binary mixtures containing GF or slag systems at 28 days

D. Overall comparison of GF-CSF-Pfa-slag binary systems

It has been found that 25% Pfa at 14 days is the most effective mixture among other mineral admixtures, as shown in Figure 6.18. The order of effectiveness of such mixtures is as follows:

25% Pfa>50% S>90% GF>75% GF>10% CSF>5% CSF>50% GF>25% S>control>25% GF

However, when comparing the same mixtures at 28 days, as shown in Figure 6.19, the order of effectiveness changes to become:

90% GF >75% GF>50% S>25% Pfa>50% GF>10% CSF>5% CSF>25% S>25% GF>control

All GF-containing mixtures moved to a higher effectiveness order with respect to the control; this means that the effectiveness of GF increases both with an increase in its replacement level and with time. GF seems to react and show its effectiveness at later ages, as shown in Figures 6.18 and 6.19.

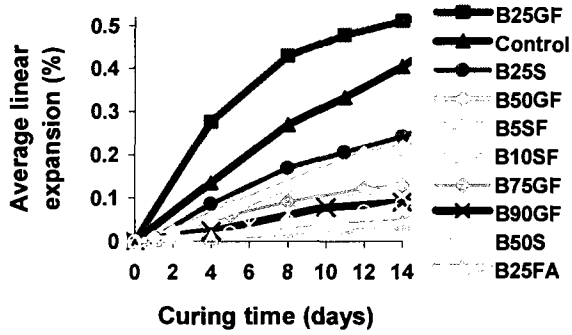

Figure 6.18 Comparison of different binary mixtures containing different mineral admixtures

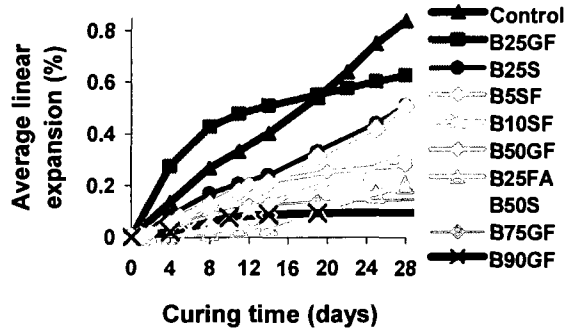

Figure 6.19 Comparison of different binary mixtures containing different mineral admixtures

The advantages of such binary mixtures are significant in designing different synergistic ternary and quaternary combinations. Such mix design depends mainly on knowing the pessimum percentage of each mineral admixture and taking advantage of such values when designing the synergistic diagrams of each ternary combination, as shown later in this chapter.

6.4.3 Comparison between binary and ternary mixtures

It is important to note that Spratt aggregate is one of the most reactive aggregates and it has been used as standard reactive aggregate in evaluating the effectiveness of many active additives in mitigating ASR expansion [CSA A23.2-14A]. Some ternary mixtures containing GF, CSF, Pfa, and slag were studied and compared with their binary mixtures over the short and long term.

A. GF-CSF ternary mixtures

Different ternary GF-CSF mixtures were tested at 14 days and at later ages to evaluate the effectiveness of GF-CSF ternary mixtures in controlling ASR expansion. A polynaphthalene-based superplasticizer (SP) was used and expressed in percentage with respect to binder content, more specifically at 0.35% (dry extract). At fixed (5%)CSF and variable GF contents, expansion increases with the increase in GF content up to 35%. The presence of superplasticizer also increases expansion. These results are in accordance with results reported by [PERRY, GILLOT, 1985], [BONEN, DIAMOND, 1992], and [DIAMOND, 1997], where Diamond showed that silica fume can induce ASR rather than mitigate it, especially when used with alkali-based sulfonated superplasticizer such as our SP. In the case of SP, the sulfonated group of the superplasticizer is neutralized by alkalis. These alkali ions remain in the pore solution when the superplasticizer polymer chains are adsorbed into the cement hydration products. Hence, increase in OH^- ion concentration results in an additional increase in expansion, with respect to the mixtures without superplasticizer. These observations require that other mixtures be evaluated to explain the reasons for such behavior. To interpret the effect of SP, the following procedure was proposed: the addition of 25% GF in mortar mixture decreases water demand, as shown in Chapter 4, and the addition of CSF increases water demand, they may thus adversely affect each other. As a result, any addition of superplasticizer increases pore formation, which decreases the impermeability of the system. This leads to a notable difference in their expansions. It may also be attributed to the condensed form of CSF (see Figure 4.4) that may be difficult to disperse by such quantity of SP. Thus, CSF lumps work as new centers of reactivity, leading to an increase in ASR expansion. The ternary system containing GF and CSF was expected to give the most efficient system in mitigating ASR expansion. Other mixtures were made to assess this system. A dosage of 5% CSF was chosen as fixed, a value that causes no significant workability loss. It is therefore very important to choose other replacement levels. As a preliminary observation, the 5% CSF that was mixed with different replacement levels of 20 and 35% GF seems to result in unoptimized ternary mixtures. The results of these mixtures are discussed in the following two points:

1- At 14 days, results show that the mixture containing 35% GF and 5% SF (35GF5SF) gave an expansion slightly lower than that of the corresponding binary containing 5% SF, while the mixture containing 20% GF and 5% SF gave an expansion value that is slightly lower than the corresponding binary of 10% CSF. It is worth noting that the addition of superplasticizer to the latter mixture (20GF5SF-SP) increased expansion with respect to the same mixture without superplasticizer, as shown in Figure 6.20.

2- At later ages, the results show that the mixture with a high GF content gave the lowest expansion values. These results are in accordance with the previously mentioned results in 6.4.2. It is also worth mentioning here that both ternary mixtures of 20 and 35% GF and 5% CSF gave comparable results at later ages, while the ternary mixture of 20% GF and 5% SF with SP gave much higher expansion value. All mixtures at later ages have surpassed the Canadian and American limits of 0.1 at 14 days, as shown in Figure 6.21.

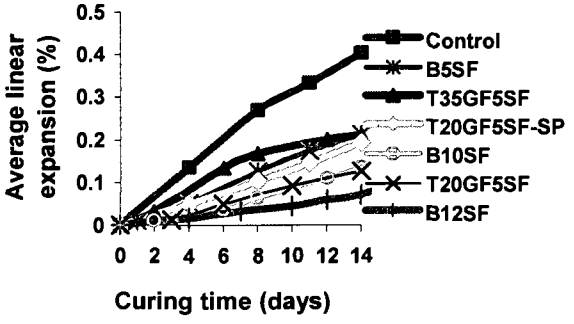

Figure 6.20 Comparison between different binary and ternary mixtures made using GF-SF systems

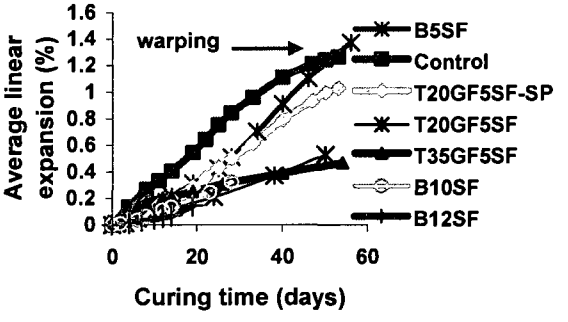

Figure 6.21 Comparison among different binary and ternary mixtures containing GF-SF system at later ages

In addition to the previously mentioned explanation, another binary mixture containing 5% CSF and the same amount of SP was prepared and tested for ASR expansion to verify the effect of SP and to investigate if the expansion is due to CSF or due to the presence of GF. This binary mixture is commercially available binary blended cement on the Canadian market, which contains nearly the same CSF replacement (5%). It was labeled Cem-SF, and its chemical composition is shown in Table 4.1. Cem-SF has been tested with and without the same percentage of SP, and results were compared with each other. It has been observed that the commercial binary cement (Cem-SF) without SP gave similar expansion values to those

obtained with the binary mixture containing 5% CSF (B5SF), while the other mixture with SP (Cem-SF-SP) gave a higher expansion value than the same commercial mix without SP, as shown in Figure 6.22. The difference in expansion is nearly the same as the difference obtained with the mixtures of 20GF5SF with and without superplasticizer. Thus, SP is mainly responsible for increasing expansion, so that this problem can be attributed to the presence of superplasticizer, as shown in Figure 6.22. This behavior, as previously discussed, has been reported by [PERRY, GILLOT, 1985], [MATSUKAWA, 1991], and [DIAMOND, 1997], who have attributed such behavior to the sulfonated groups of SP that are neutralized by alkali ions. The alkali ions derived from the superplasticizer remain in the solution when the superplasticizer polymer chains are absorbed into cement hydration products. Depending on the dosage, a considerable increase in the OH- ion concentration of the pore solution can be produced, leading to an increase in ASR expansion.

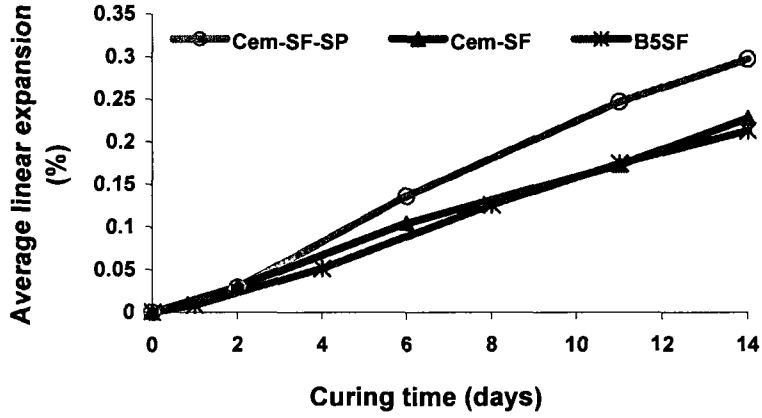

Figure 6.22 Commercial binary cement containing about 5% CSF with and without superplasticizer

The importance of the other ternary GF-CSF mixture is to investigate the synergistic properties of this system. A large variation in the replacement values of both GF and CSF was used. Three ternary mixtures containing 40, 50, and 60% GF with corresponding dosages of 8, 7, and 4% silica fume were tested, respectively. The most efficient mixture is that containing 50% GF and 7% silica fume, which gives a 95% reduction in expansion with respect to the control mixture, as shown in Figure 6.23. Therefore, to assess the GF-CSF ternary system, it is recommended to use a variety of replacement levels. The other mixtures are also efficient, but their efficiency is lower than the optimal mixture, as shown in Figure 6.23. As a general

comparison of the different mixtures in the GF-CSF ternary system tested, and from Figure 6.23, two different groups of GF-CSF ternary mixtures can be differentiated. The first group is characterized by a GF content equal to or lower than 35% with expansion values higher than the Canadian specification limit (> 0.10%). The second group is characterized by GF content higher than or equal to 40% that in combination with CSF contents ranging between 4 to 8%, gives ASR expansion values lower than the Canadian specification limit, as shown in Figure 6.24. This means that there is a threshold value for GF under which undesired results will be obtained. This value seems to be around 40% GF, as previously indicated.

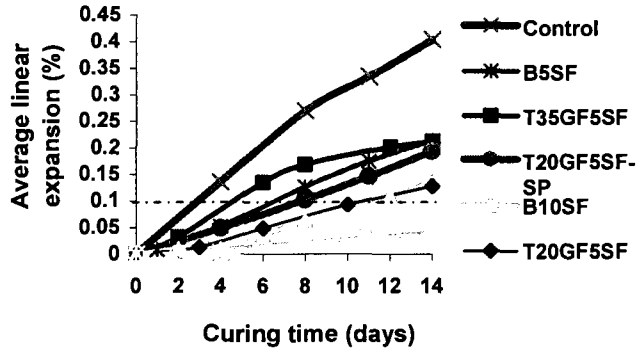

Figure 6.23 Comparison among different binary and ternary mixtures in the GF-SF system at 14 days (80°C, 1N NaOH)

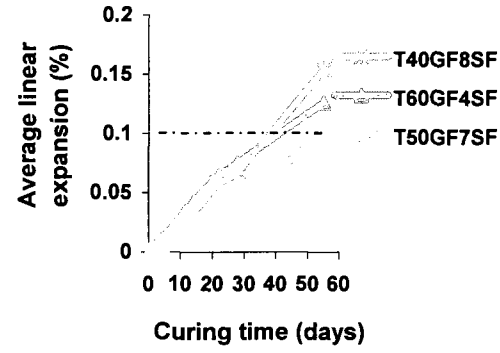

Figure 6.24 Comparison between the most efficient ternary mixtures in the GF-SF systems at later ages (80°C, 1N NaOH)

It is highly recommended to use GF content higher than or equal to 40% with any CSF content that may vary from 4 to 8%. Such optimized combinations of GF and CSF can result in efficient mixtures that can control ASR expansion, even in the long term (28 days in the AMBT), as shown in Figure 6.24.

B. GF-Pfa ternary mixtures

The first ternary mixture of GF (30%) and class F fly ash (20% Pfa) was tested and compared with the other binary mixtures containing both GF and Pfa. It was found that this ternary mixture, T30GF20FA, yields comparable results to the binary mixture with 90% GF, which are still lower than the CSA specification limit (0.10% at 14 days). The expansion value of this ternary mixture at 14 days is still much lower than the binary mixture containing 50% GF. This ternary mixture has shown the synergistic effect of the ternary GF-Pfa system, especially

when compared to the binary mixture containing 25% GF, as shown in Figure 6.25 and 6.26. This ternary system resulted in a reduction in expansion of about 76% with respect to the control mixture, while the reduction in expansion in the binary mixture containing 25% Pfa, with respect to the control sample, is about 89%. This means that this ternary mixture has a lower efficiency than the binary mixture with 25% Pfa. For this reason, other ternary mixtures of variable dosages were formulated and tested. These ternary mixtures are 40% GF with 20% Pfa, 45% GF with 15% Pfa, and 40% GF with 15% Pfa, all of which are effective in controlling ASR expansion. The mixture containing 40% GF and 20% Pfa has shown itself to be the most efficient at early and later ages, as shown in Figures 6.27 and 6.28. It results in a reduction in expansion of approximately 88% with respect to the control. These results are similar to those found with the binary mixture containing 25% Pfa at early ages. It is worth noting that the binary mixture containing 25% Pfa gives large expansion at later age, while the ternary mixtures maintain a more stable level of expansion, as shown in Appendix.

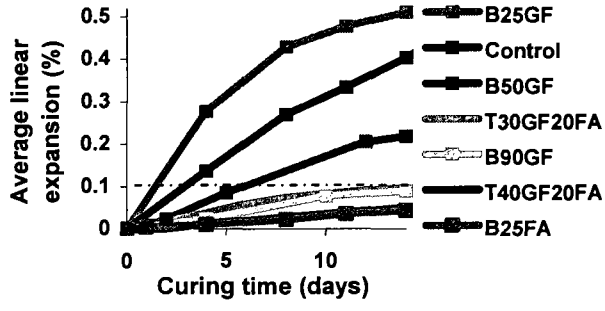

Figure 6.25 Comparison between different GF and Pfa binary and GF-Pfa ternary mixtures

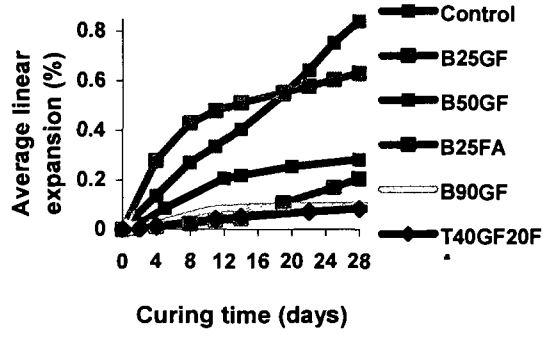

Figure 6.26 Comparison between different GF and Pfa binary and GF-Pfa ternary mixtures at later ages

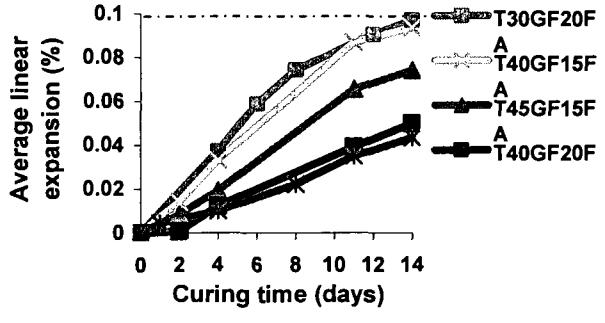

Figure 6.27 Comparison between different GF-Pfa ternary mixtures

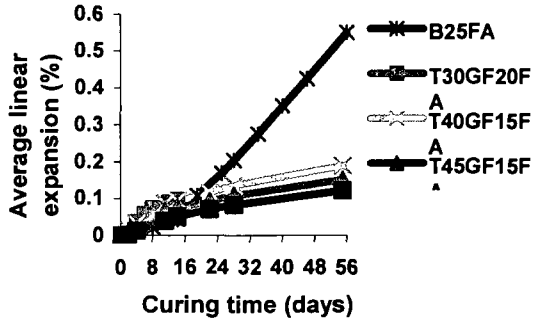

Figure 6.28 Comparison between different GF-Pfa ternary mixtures at later ages

C. GF-slag ternary mixtures (GF-S)

Four ternary GF-slag mixtures (25% GF with 15% S, 15% GF with 25% S, 40% GF with 20% S, and 30% GF with 30% S) were tested and compared to the binary mixtures of GF and slag. It was found that, at 14 days, the T25GF15S ternary mixture containing 25% GF gave higher expansion values than the ternary mixture containing 15% GF (T15GF25S), while at later ages, the reverse was observed; therefore this suggests that, GF reacts at later ages while at early ages slag reacts faster than GF. Thus, the higher the GF and the lower the slag contents, the higher the expansion values at early ages and the lower the rate of expansion at later ages. As well, reversing the process will produce the opposite effect (higher expansion at later ages), as shown in Figures 6.29 and 6.30. The T30GF30S and T40GF20S ternary mixtures give lower expansion at early ages of 14 days, which is, however, higher than the binary B50S mixture with 50% slag. However, at later ages of more than 56 days, the T40GF20S ternary mixture gives the lowest expansion values. It is worth noting that, the B50GF binary mixture gives comparable expansion values to the T30GF30S ternary mixture at later ages, as shown in Figure 6.30.

Figure 6.30 shows that the efficiency of the binary mixture containing 50% slag is higher at both early and later ages. However, when comparing all of these mixtures (binary and ternary) with the binary mixture of 50% GF, it was found that the B50GF binary mixture of 50% GF and the T40GF20S ternary mixture are the best mixture at later ages. Thus, the ternary mixtures of GF-slag can be used to formulate effective mixtures at both early and later ages.

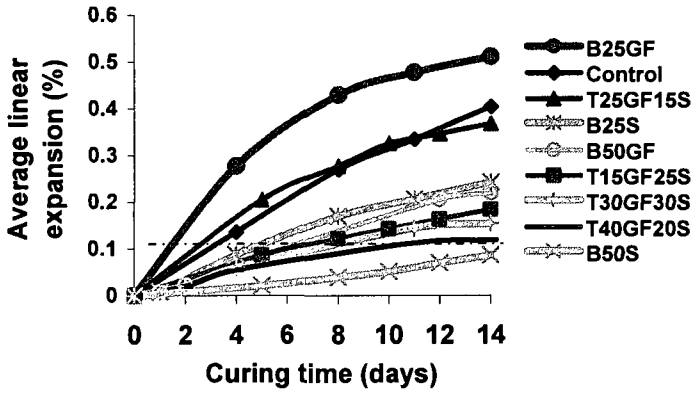

Figure 6.29 Comparison between different binary and ternary mixtures containing GF-Slag systems

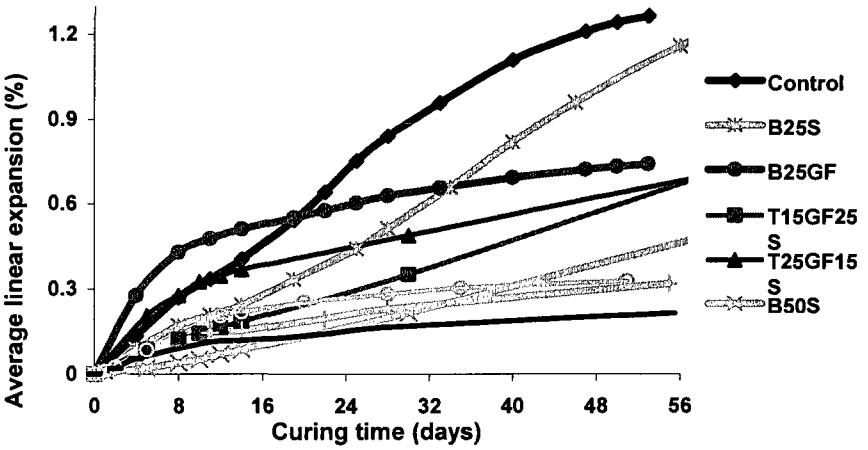

Figure 6.30 Comparison between different GF and slag binary mixtures with GF-slag ternary mixtures at later ages

6.4.4 Synergistic diagrams

Mixtures containing a single mineral admixture require high levels of replacement. The importance of drawing synergistic diagrams for ternary mixtures is to help formulate the best proportions for different ternary mixtures containing GF, CSF, Pfa, and slag in a way that ensures mechanical and ASR resistant mixtures that is to say durable mixtures. Three different ternary mixtures containing GF-CSF, GF-Pfa, and GF-slag were presented to show the effect of each combination on ASR expansion. Therefore, the efficient mixtures of each ternary system can be visualized in a practical way. An expansion of 0.10% at 14 days is selected as the decisive point to determine fail or pass criterion for the test in the case of the ternary mixtures containing GF-SF and GF-Pfa. However, in case of the ternary mixture using the GF-slag system, an expansion of 0.15% is selected as the decisive value, as all of the ternary GF-S mixtures have surpassed the 0.10% expansion limit. The GF-S ternary mixtures tested are not efficient enough to mitigate ASR expansion due to the need for higher replacement levels, which are impractical. Circles were chosen for mixtures passing the test while squares represent mixtures that failed the test; this representation is used throughout this part of the study.

A. GF-CSF system

ASR expansion readings for different GF-CSF binary and ternary mixtures at 14 days were taken and plotted to obtain the ternary synergistic mix diagram, as shown in Figure 6.31. As

previously mentioned, this diagram is very important in designing efficient concrete mixtures against ASR. The obtained synergistic diagram shows two important curves. The first curve (plain curve) represents the line between the lowest ellective replacement levels for each individual SCM, i.e GF and CSF. The second curve (dotted curve) represents the synergistic effect of these SCMs when used internary blends, which is above the theoretical combination of the GF-CSF line. The area between the theoretical effective line and the synergistic effective curve represents the area in which any ternary mixture will give an expansion lower than 0.10%, as shown in Figure 6.31. As the synergistic effective curve is above the theoretical effective line, this means that the effective combination of GF-CSF is attained either at high replacement levels of GF and CSF or in the intermediate region in this area, under the synergistic effective curve. For example, the mixture identified as T50GF7SF is an example of the most effective ternary blend of GF and CSF, as it results in a reduction of nearly 95% in expansion with respect to the control sample at 14 days. Figure 6.31 shows that the ternary mixtures containing between 7 and 8% CSF with GF replacement levels more than 30% are efficient. Therefore, the effective use of CSF with GF can lead to the formation of a series of effective ternary mixtures containing GF-CSF that can greatly diminish the problem of ASR expansion, as shown in Figure 6.31. The order of effectiveness of the effective GF-CSF ternary mixtures investigated is as follows:

T50GF7SF > T40GF8SF > T60GF4SF > T25GF9SF

This ternary system is effective and must be completely assessed by adding more points in the area under the synergistic effective curve and above it.

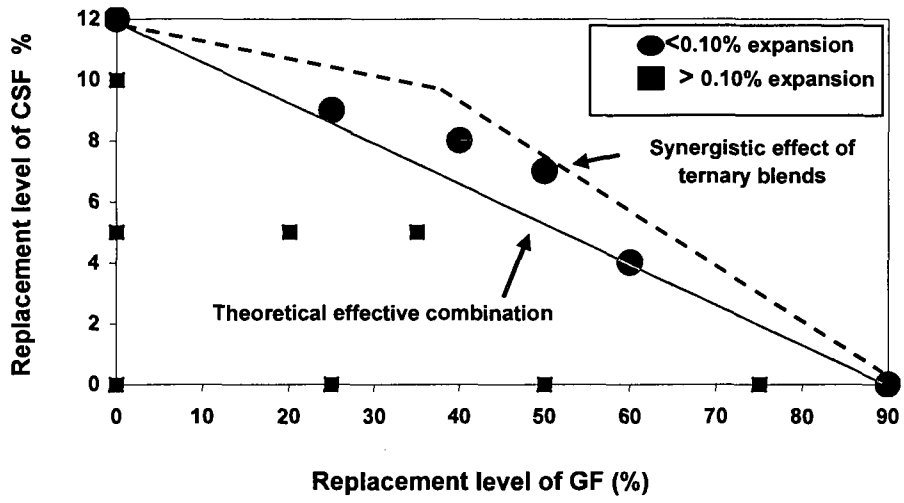

Figure 6.31 Performance of ternary blend combinations of GF-CSF system

THOMAS and BLESZYNSKI (2000) have performed similar work on the efficacy of ternary combinations of silica fume and slag with Spratt aggregate, as mentioned in the literature review. The most effective mixture found among the combinations they investigated was 25% slag and 8% SF, which gives an expansion of 0.025%. This represents a 95.4 % reduction in expansion with respect to the control. Comparing this result with what was obtained in this part of the study, it was found that the most effective ternary combination of GF and silica fume is 50% GF and 7% SF, which gives an expansion of 0.019%, which represents a 95% reduction in expansion. The main difference with this mixture and others is the replacement level of GF, which is nearly double that of slag. As previously shown, the effective binary mixture containing GF has a replacement level of about 90% while the effective replacement level of slag is approximately 50% or more. Therefore, the GF replacement level is approximately twice that of slag and this explains the difference in the efficiency of their comparable replacement level.

B. GF-Pfa system

The GF-Pfa system trend is similar to that of the GF-CSF system, where the curve of synergistic effect of GF-Pfa ternary blends is above the theoretical effective combination line. The most important thing to notice here is that the summation of replacement levels of GF and Pfa is around 55%, which is very practical in comparison with 75% GF for short and long term. The synergistic effective curve is located above the theoretical effective combination

line, identical to what was found in the GF-CSF system, as shown in Figure 6.32. The most effective combination is that composed of 40% GF and 20% Pfa (written as T40GF20FA), which resulted in approximately 88% reduction in expansion with respect to the control sample. The order of effectiveness of the effective ternary mixtures investigated is as follows:

T40GF20FA > T45GF15FA > T40GF15FA > T30GF20FA

Figure 6.32 shows the potential of attaining an effective ternary mixture (i.e. against ASR) of GF and Pfa with a total replacement level lower than 50% summation of GF and Pfa. Also, this figure shows the synergistic interaction between GF and Pfa, which can be taken as a guideline for the formulation of any GF-Pfa ternary concrete mixture presenting lower concerns about the occurrence of ASR expansion. More points inside the area of effectiveness under the theoretical effective curve, to verify the feasibility of this diagram, are needed. As well, some concrete mixtures are also recommended to test these mixtures inside the diagram.

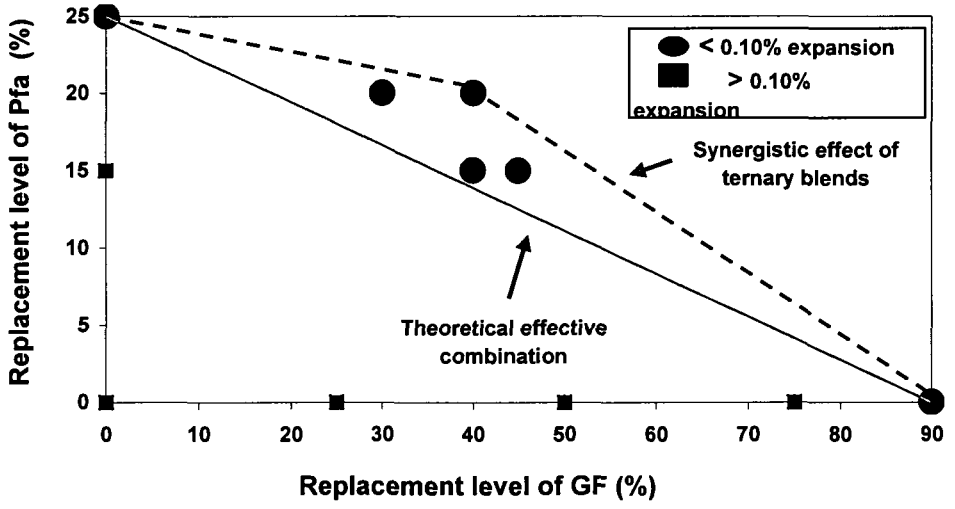

Figure 6.32 Performance of ternary blend combinations made using the GF-Pfa system

C. GF-Slag system

The effective replacement levels of both GF (90%) and slag (50%) are quite high in their binary mixtures. Therefore, and as expected, this system is characterized by higher total replacement levels corresponding to the summation of GF and slag in their ternary mixtures. It is anticipated that efficient ternary mixtures will require high replacement levels that may be

impractical from an early durability point of view. Also, the Canadian specification limit of 0.10 could not be applied where all of these mixtures surpassed this limit. For this reason, the American specification limit of 0.15% was taken as the limit for assessing these ternary mixtures, as shown in Figure 6.33. The effective ternary mixture in this diagram is composed of 40% GF with 20% slag (T40GF20S), which represents a total replacement level of 60% of the summation of GF and slag. The reduction in expansion due to use of this mixture is about 92%. The order of effectiveness of the GF-S ternary mixtures is as follows:

T40GF20S > T30GF30S > T15GF25S > T25GF15S

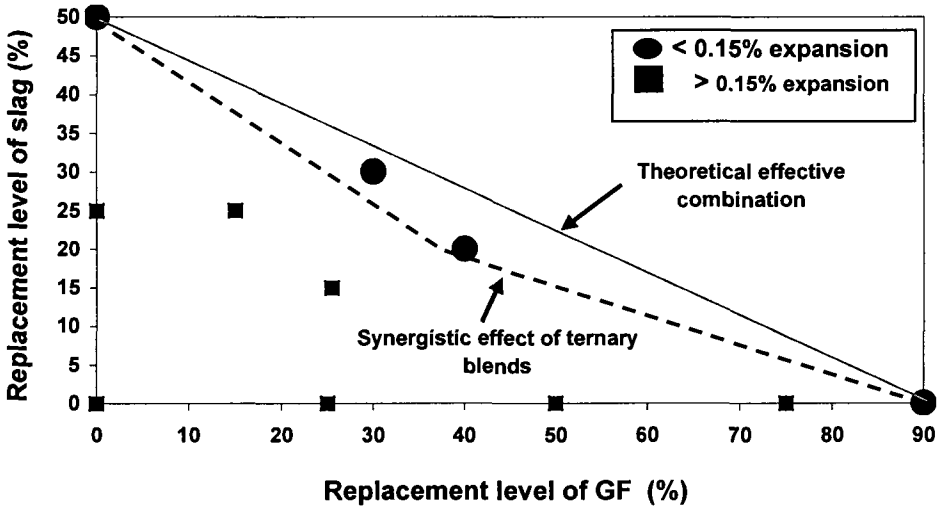

Figure 6.33 Performance of ternary blend combinations made using the GF-slag system

6.4.5 Comparison between different quaternary systems using Spratt aggregate

Two quaternary cementitious systems were used, identified as Q20GF25FA5SF and Q25GF30S5SF. The composition of the first cementitious system was 20% GF with 25% Pfa and 5% CSF, while the composition of the second cementitious system was 25% GF with 30% S and 5% CSF. These systems were studied using ASTM C227 specification (refer to 6.2) and have been selected as promising mixtures where they present effective mitigation against ASR expansion, the AMBT results of the system are shown in Figures 6.34 and 6.35. It can be shown in Figure 6.34 that the two quaternary mixtures produced lower expansion than the binary mixture containing 90% GF at 14 days. However, at later ages of over 100 days, the binary mixture containing 90% GF mitigated ASR expansion as opposed to the two

quaternary mixtures, which expand with time surpassing the CSA specification limit (0.1%), as shown in Figure 6.35.

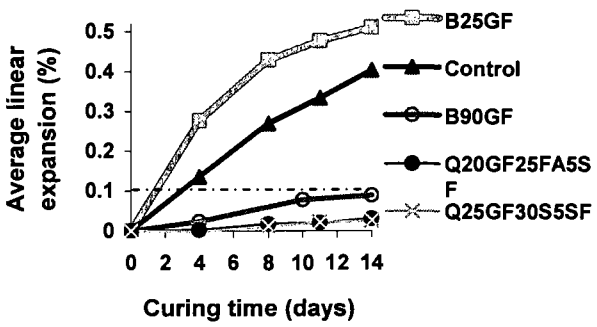

Figure 6.34 Performance of the quaternary systems at 14 days

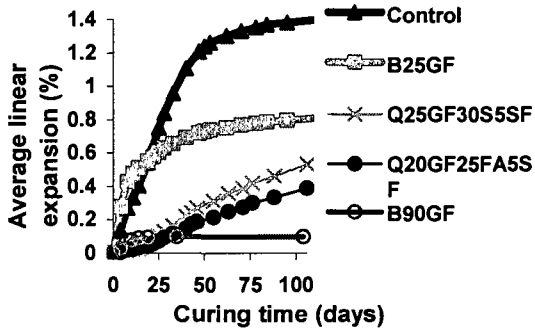

Figure 6.35 Performance of the quaternary systems at later ages

6.4.6 Comparison between different systems using Ottawa sand

A. Binary and ternary systems

The physical properties of Ottawa sand were previously shown in Chapter 3. This type of sand is well known for the innocuousness of its ASR reaction. Therefore, it is expected that any mixture containing the Ottawa sand will result in low ASR expansion values at 14 days. The lon-term reactivity of the Ottawa sand in the AMBT conditions was also tested. The results are shown in Figures 6.36 and 6.37, from which it can be seen that Ottawa sand is not resistant for longer time under the severe conditions of the accelerated test. The curves' behavior show the same trend as that previously shown with Spratt aggregate. Ottawa sand is showing low ASR expansion at 14 days. Expansion of the binary mixture containing 25% GF is slightly higher than that of the control with the Ottawa sand, with nearly equal ratio as that found between the comparable mixtures using Spratt aggregate. Therefore, this difference may not be due to ASR reactivity, but to another phenomenon that should be further investigated. At early ages, there was very low expansion; the ternary mixture containing 20% GF and 5% CSF showed effectiveness in suppressing even further that very low ASR expansion, as clearly shown in Figure 6.36. However, at later ages, there was substantial expansion in the control and ternary mixtures, while expansion was mitigated by the binary mixture containing 25% GF. Figure 6.37 indeed shows that the ternary mixture containing 20% GF and 5% SF (T20GF5SF) surpassed the CSA specification limit of 0.1% after 80 days in the severe

conditions of the accelerated test (AMBT). Nevertheless, the binary mixture containing 25% GF performed well under these severe conditions and maintained a stationary expansion of about 0.05% until 140 days.

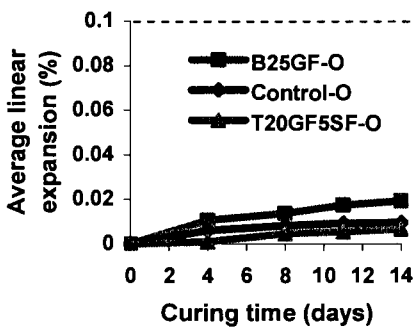

Figure 6.36 Comparison between GF-binary and ternary mixtures

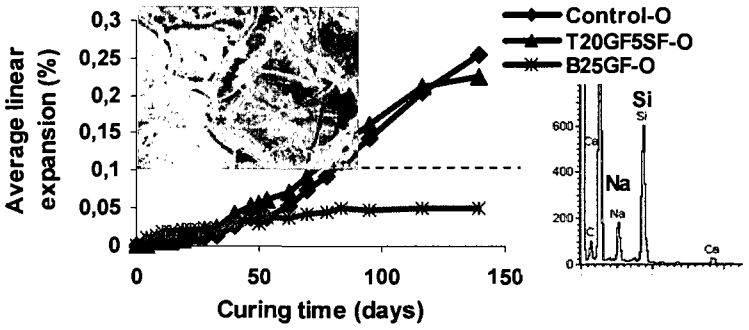

Figure 6.37 Comparison between GF-binary and ternary mixtures at later ages (silica gel formation confirmed with EDS

B Binary, ternary, and quaternary systems

The behavior of all mixtures containing the Ottawa sand depends on many factors, as the reactivity of aggregate at early ages is nearly negligible. There is no significant difference between the binary system of 25% GF, the quaternary of 20%GF25%Fa5%SF or the other mixtures in the short term, as shown in Figure 6.38. The most important factor for evaluating the mixture containing Ottawa sand is the long-term results. As mentioned above, the Ottawa sand results in much longer notable expansion at later ages. The sequence of the efficiency of the mixtures at 14 days, according to Figure 6.38, is as follows:

25GF30S5SF > T20GF5SF > control > Q20GF25Fa5SF > B25GF

It is worth noting that the Ottawa sand shows remarkable expansion in the long-term under the severe conditions of the accelerated test. Therefore, it is expected to result in a different efficiency order as that mentioned above. The order of efficiency at later ages is as follows:

Q20GF25Fa5SF > B25GF > Q25GF25S5SF > T20GF5SF > control

From this sequence, it can be concluded that 25% GF is effective at later ages. The expansion value of the binary mixture containing 25% GF is located between the two quaternary expansion curves and shows stability with time, as shown in Figure 6.39.

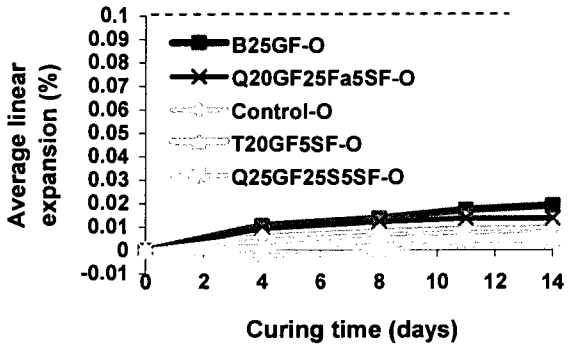

Figure 6.38 Comparison between GF-binary, ternary, and quaternary mixtures at 14 days using Ottawa sand

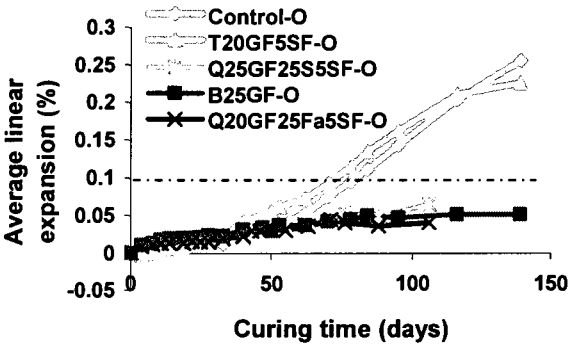

Figure 6.39 Comparison between GF-binary, ternary, and quaternary mixtures at later ages using Ottawa sand

6.4.7 Comparison between binary and ternary systems using Aimé Côté sand

The physical properties of Aimé Côté sand were previously shown in Chapter 3. This type of sand is known for its moderate ASR reactivity level. Therefore, it was expected that noticeable ASR expansion values would be found for any mixture with Aimé Côté sand at 14 days. The ASR resistivity of Aimé Côté sand with time was also tested. The results are shown in Figures 6.40 and 6.41, from which it can be seen that Aimé Côté sand gives comparable expansion results to those found using Spratt aggregate at 14 days, but a lower value for the long-term test. It is worth noting that the addition of 25% GF decreased expansion to about 58% and maintained the expansion slightly above the CSA specification limit, while the ternary mixture of 20% GF and 5% CSF lowered the expansion to the innocuous area of the graph (expansion < 0.10% at 14 days). At later ages, the expansion of 25% GF is still lower, as with the other mixtures such as those containing Spratt or Ottawa aggregates. Therefore, the results are in accordance with each other.

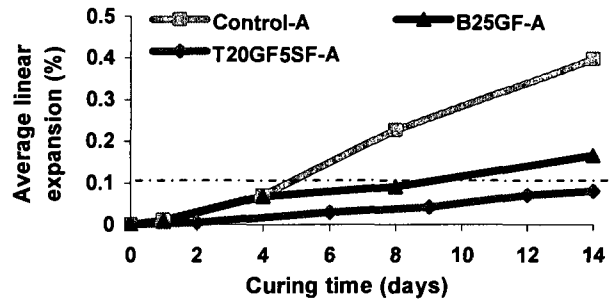

Figure 6.40 Comparison between GF-binary and ternary mixtures using Aimé Côté sand

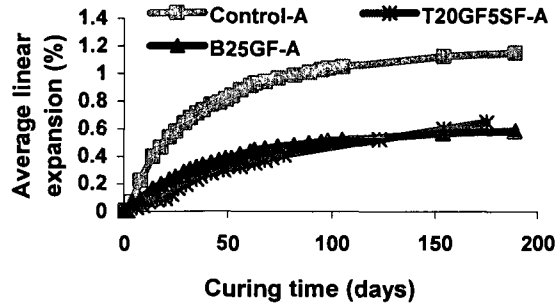

Figure 6.41 Comparison between GF-binary and ternary mixes at later ages using Aimé Côté sand

6.4.8 GF systems containing Mirabel aggregate

The physical properties of Mirabel aggregate were previously given in Chapter 3. This type of aggregate is known for its moderate reactivity against ASR reaction. The ASR resistivity of Mirabel aggregate with time was tested, as well as the effectiveness of GF with Mirabel aggregate. Four mortar mixtures were tested: the control, two binaries containing 25 and 50% GF, and a ternary mixture (20% GF and 5% SF). The results are shown in Figures 6.42 and 6.43, from which it can be seen that the control mixture containing Mirabel aggregate results in an expansion above the CSA specification limit. Also, the binary mixture containing 25% GF gave an expansion value slightly higher than that of the control, while at later ages it resulted in slightly lower expansion values than that of the control, in accordance with other results. On the other hand, the binary mixture containing 50% GF gave an expansion value of nearly 0.10% at 14 days and the ternary mixture gave an expansion value below 0.10%. The ASR reaction decreases with an increase in replacement level of GF. These results are accordance with each other and support the previously mentioned results.

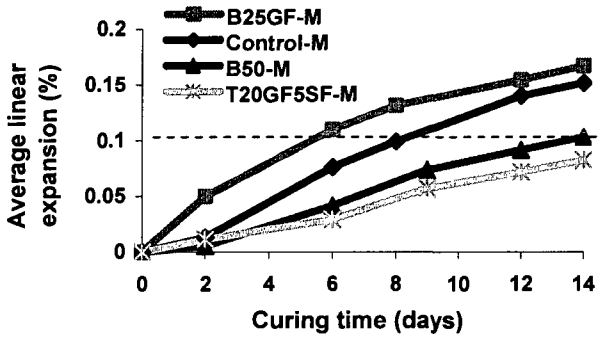

Figure 6.42 GF-binary and ternary mixtures containing Mirabel aggregate

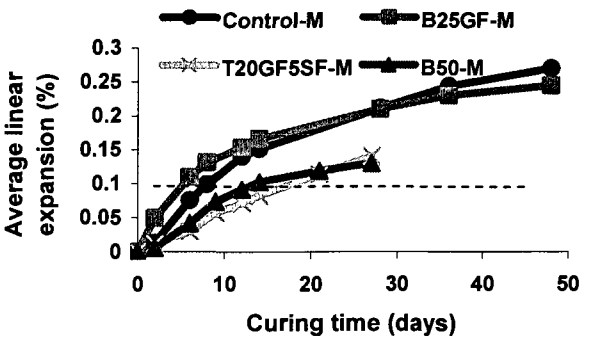

Figure 6.43 GF-binary mixture containing Mirabel aggregate at later ages

6.4.9 GF systems containing LG aggregate

LG sand is a fine aggregate that has been classified as a non-reactive aggregate. However, its reactivity is about 4 times that of Ottawa sand. Its physical properties were given in Chapter 3. The same mixtures used with Mirabel aggregate were also used with LG aggregate, that is the control, two binaries containing 25 and 50% GF, and a ternary mixture of T20GF5SF (20% GF and 5% SF), as shown in Figure 6.44. The control and the binary containing 25% GF were superposed and the expansion values (of approximately 0.037%) are much lower than the specification limit, but still higher than those of the binary mixture containing 50% GF and the ternary mixture containing 20% GF and 5% CSF. As well, the expansion of the binary mixture containing 50% GF is slightly higher than that of the ternary mixture. Therefore, the binary mixture containing 50% GF and the ternary mixtures containing 20% GF and 5% CSF may have the same effectiveness at 14 and 28 days, as shown in Figures 6.44 and 6.45. Expansion results in the presence of different replacement levels of GF using LG aggregate show the same trend as that of the same GF mixtures containing different aggregates.

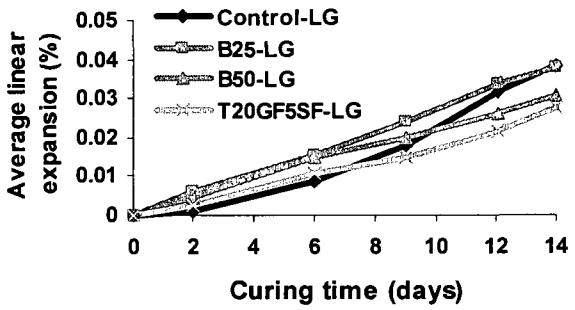

Figure 6.44 GF-binary and ternary mixtures containing LG aggregate at 14 days

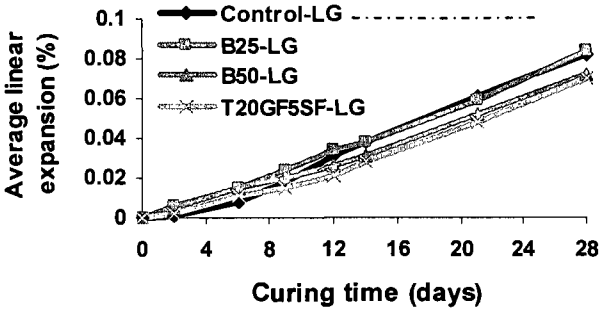

Figure 6.45 GF-binary and ternary mixtures containing LG aggregate at 28 days

6.4.10 Comparison between 25% GF binary mixtures containing different aggregates

The behavior of the binary mixture containing 25% GF depends on the type of aggregate used, as illustrated in Figures 6.46 and 6.47. From Figure 6.46 (.e. for expansions up to 14 days), three categories can be easily classified according to the expansion values. For an expansion of less than 0.10%, four mixtures (belonging to Ottawa and LG aggregates) are classified according to their ASR expansion reactivity, which is less than 0.10%, as follows:

B25GF-LG > Control-LG > B25GF-O > Control-O

The 25% GF binary mixture containing LG aggregate (B25GF-LG) is higher than its control without GF. The same trend was found when Ottawa sand (B25GF-O) was used. The expansion of LG aggregate is higher than that of Ottawa sand in all of their mixtures.

For an expansion between 0.10 and 0.20%, three mixtures (belonging to Aimé Côté and Mirabel aggregates) are classified according to their ASR expansion reactivity, which is higher than 0.10% and lower than 0.20%, as follows:

B25GF-M > B25GF-A > Control-M

Altogether, the 25% GF binary mixtures containing both Mirabel and Aimé Côté aggregates, B25GF-M and B25GF-A, respectively, have similar expansion value, while the control mixture containing Mirabel aggregate had a slightly lower expansion than above binary mixtures, as shown in Figure 6.47.

In the last category, three mixtures were found (belonging to Aimé Côté and Spratt aggregates), which are characterized by expansion values above 0.40% and lower than or equal to 0.50%. These mixtures are classified according to their ASR expansion reactivity, in the following order:

B25GF > Control > Control-A

The most important thing to notice here is that the control containing Aimé Côté aggregate (Control-A) has nearly the same expansion value as that of the control containing Spratt aggregate, the opposite of what was obtained according to ASTM C227. This can also be taken as another drawback of ASTM C227 specification.

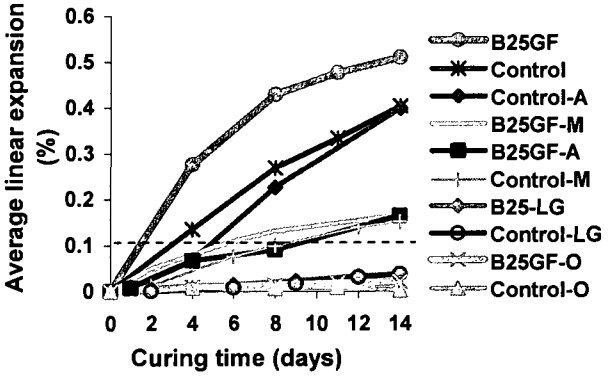

Figure 6.46 Comparison between different types of aggregates containing 25% GF at 14 days

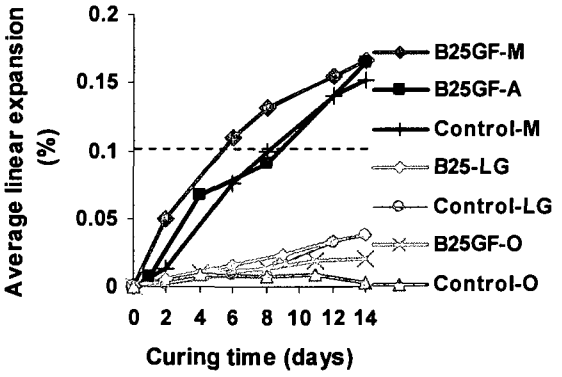

Figure 6.47 Comparison between different types of aggregates containing 25% GF without Spratt aggregate at 14 days

Based on the he 28-day expansion values, all binary mixtures containing 25% GF resulted in expansion values lower or similar to those corresponding to the controls made with the same type of aggregate, as shown in Figures 6.47 and 6.48. For example, the 25% GF binary mixture with Spratt aggregate has lower expansion value than that of the control with Aimé Côté at later ages.

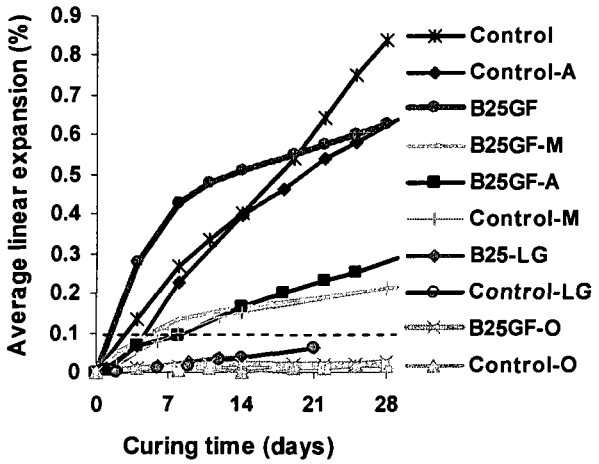

Figure 6. 48 Comparison between different types of aggregates containing 25% GF at 28 days

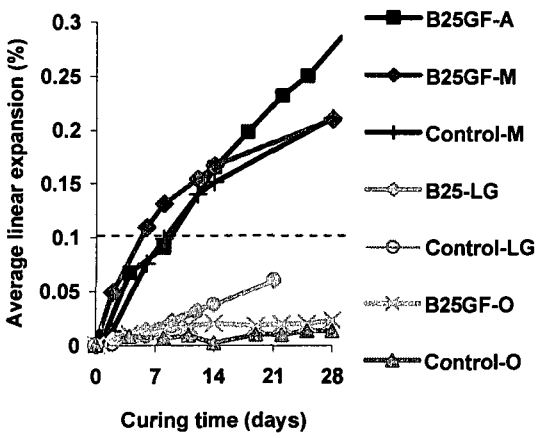

Figure 6. 49 Comparison between different types of aggregates containing 25% GF without Spratt aggregate at 28 days

6.4.11 Comparison between 50% GF binary mixtures containing different aggregates

In this comparison, three types of aggregates, which are characterized by high, moderate, and low reactivity, were selected. These aggregates were Spratt, Mirabel and LG aggregates, respectively, as shown in Figure 6.50. As it was mentioned previously that 25% GF is not the optimum replacement level that should be used, therefore the expansion of all mixtures with all types of aggregates made with 25% GF gave higher expansions than the control mixtures made with the corresponding aggregates. The expansion values of the binary mixture containing 50% GF with all types of aggregate are lower than their corresponding control mixture. Therefore, the expansion value decreases with an increase in GF replacement level. It is important to note that the difference between the expansion value of the binary mixture containing 50% GF and its control mixture increases with an increase in reactivity of the aggregate used in these mixtures, as shown in Figure 6.50.

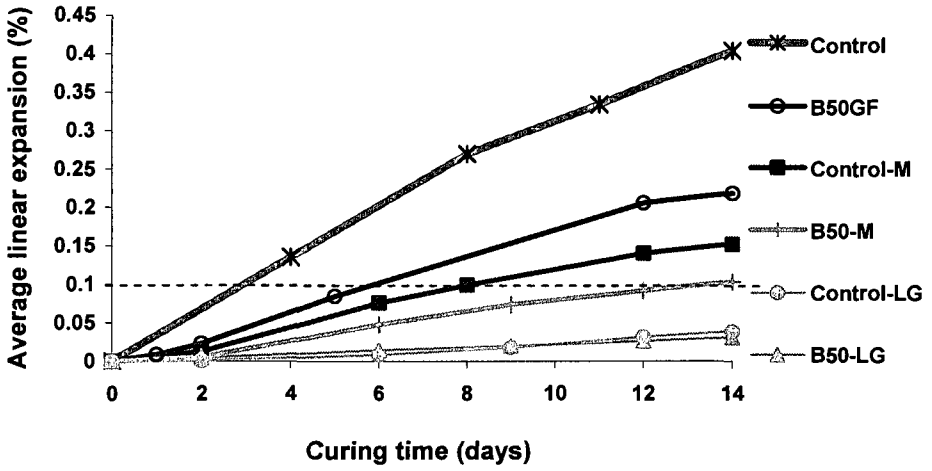

Figure 6.50 Comparison between three types of aggregates containing 50% GF

6.4.12 Comparison between 20%GF5%SF ternary mixtures containing different aggregates

The ternary mixture containing 20% GF and 5% SF show the same trend shown by the binary mixture containing 50% GF binary mixtures using the same aggregates. The expansions of the ternary mixtures containing all types of aggregates are lower than those of the corresponding control mixtures, as shown in Figure 6.51. The expansion of the ternary mixture containing Spratt aggregate gives comparable results to the control mixture containing Mirabel aggregate. As well, the expansion of the ternary mixture containing Mirabel aggregate gives comparable expansions as the ternary mixture containing Aimé Côté aggregate. The control mixture containing LG aggregate also gives comparable results to the ternary mixture with the same aggregate. The difference in expansion between the ternary mixture and the control mixture with the different tested aggregates increases with an increase in reactivity of the aggregate used, as shown in Figure 6.51. The expansion value of the ternary and the control mixtures containing Ottawa sand are the same.

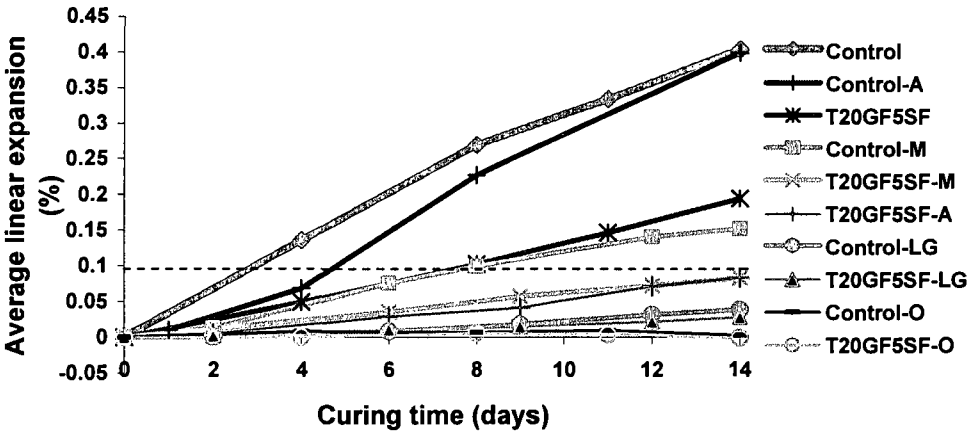

Figure 6.51 Comparison between different types of aggregates containing the ternary binder of 25% GF and 5% SF (T20GF5SF)

6.5 Simple analysis

The following data, which represent reduction in expansion due to the presence of GF with and without supplementary cementitious materials, SCMs (CSF, Pfa, and slag), were calculated from the previous results and classified into the parts described in the following paragraphs.

6.5.1 Different binary GF systems

The effect of different GF replacement levels on reduction in expansion due to ASR reaction, at different curing times, was investigated. It was found that all replacement levels at all curing times increased the reduction in expansion, except for the replacement level of 25% GF at 14 days, as shown in Figure 6.52. This anomaly has been attributed to the porosity of the system that seems to be more porous at 14 days than the control itself, whereas at later ages the pozzolanic and hydraulic reactions contribute to reducing this porosity. Thus, once these reactions become more effective, the residual expansion decreases, therefore the expansion rate decreases with respect to the control and finally the reduction in expansion becomes more significant, as seen in Figure 6.52. These results only confirm the innocuousness of GF in mortar. According to specified limit of 0.10% for the AMBT test when used to evaluate the efficacy of SCMs against ASR (CSA A23.2-27A), the reduction in expansion required to pass this test limit is 75.2%. Figure 6.52 shows that the binary mixture containing 90% GF has

passed this limit at both the 14- and 28-day period test, while the binary mixture containing 75% GF has passed this limit at 28 days only.

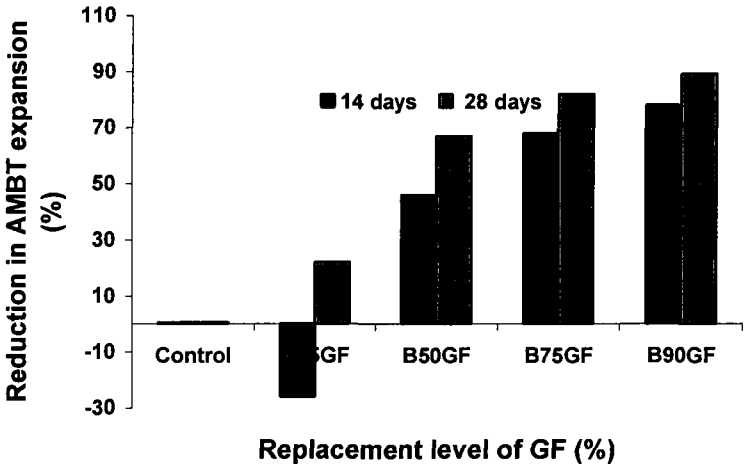

Figure 6.52 Reduction in ASR expansion at 14 and 28 days and at different GF replacement levels

6.5.2 Different ternary GF-CSF systems

The higher efficiency of these systems is attributed to CSF due to its extreme fineness and high glass content, which are responsible for its high pozzolanic reactivity at early ages. GF-CSF are the most efficient systems, resulting in a higher reduction in expansion due to ASR reaction, where the maximum reduction obtained is 95% at 14 and 28 days, as shown in Figures 6.53 and 6.54. Also, the different combinations of these systems give stable reduction in expansion with time contrary to the GF-slag systems. It can also be observed that the minimum recommended replacement level of GF in these systems (based on the limited numbers of combinations tested) is no less than 40% GF. The maximum total replacement level in these systems is 64%, which is composed of 60% GF and 4% CSF and which gives 90% reduction in expansion at 14 and 28 days. However, the mixture containing 50% GF and 7% CSF results in 95% reduction in expansion at 14 and 28 days, which is very comparable with the mixture that is composed of 40% GF and 8% CSF that results in 92% reduction in expansion at 14 days. Therefore, the most recommended mixture from these systems is that with 40% GF and 8% CSF, which has a much lower replacement level of 48%.

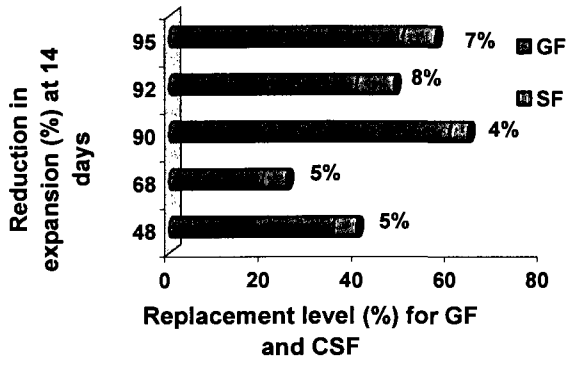

Figure 6.53 Reduction in ASR expansion at 14 days and at different GF-SF replacement levels

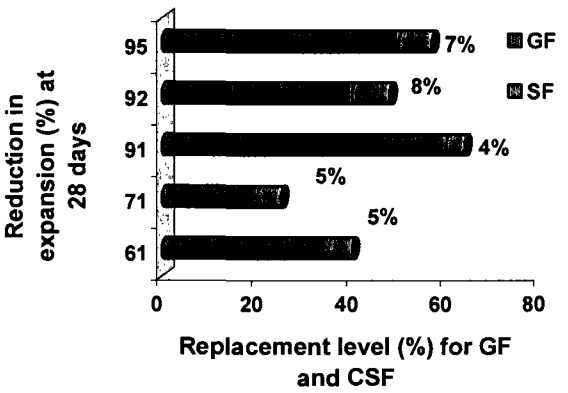

Figure 6.54 Reduction in ASR expansion at 28 days and at different GF-SF replacement levels

6.5.3 Different ternary GF-Pfa systems

The presence of Pfa with GF in their ternary systems greatly affected the reduction in expansion due to ASR reaction. The synergistic interaction between GF and Pfa is the main reason for such a phenomenon. Most of the GF-Pfa ternary mixtures are very efficient in reducing ASR expansion. Figures 6.55 and 6.56 show the effect of varying the replacement level of both of GF and Pfa on reducing expansion due to ASR reaction. The most effective mixture in this ternary system, which is composed of 40% GF and 20% Pfa, is comparable with the 90% GF binary mixture at 14 and 28 days. Moreover, the efficiency of this ternary mixture in reducing ASR expansion increases with time. All of these ternary mixtures passed the 14-day CSA specification limit (0.10%), which corresponds to a 75.2% reduction in expansion with respect to the control, as shown in Figures 6.55 and 6.56.

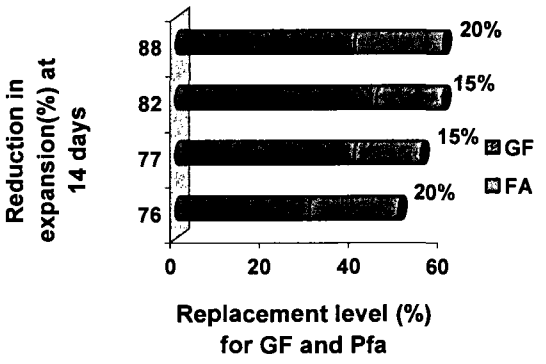

Figure 6.55 Reduction in ASR expansion at 14 days and at different GF-Pfa replacement levels

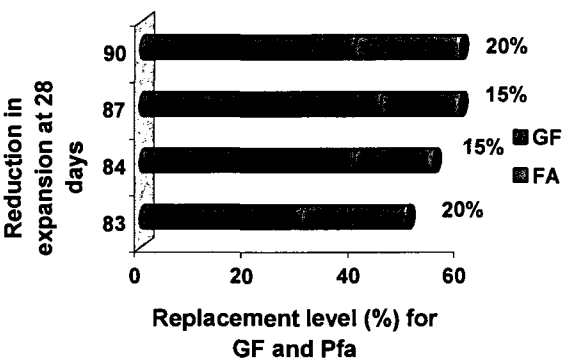

Figure 6.56 Reduction in ASR expansion at 28 days and at different GF-Pfa replacement levels

6.5.4 Different ternary GF-slag systems

The main drawback of these systems is that the effective binary mixture of both GF and slag is significantly high in replacement levels compared to Pfa and CSF. Therefore, it was expected that the efficient mixtures derived from the combination of these systems would require much higher replacement levels to produce a comparable reduction in expansion. Figures 6.57 and 6.58 show the effect of varying the replacement level of both of GF and slag on reducing expansion due to ASR reaction. The most effective mixture in this ternary system, that passed the proposed limit (0.15%), is composed of 40% GF and 20% slag, and is comparable to the effective mixture in the GF-Pfa ternary systems at 14 and 28 days. However, the efficiency of this ternary mixture in reducing ASR expansion decreases with time contrary to the GF-Pfa systems. In general, the efficiency of these systems increases with an increase in replacement level, especially that of the GF. The maximum reduction in expansion produced by the most efficient mixture in this system is 92% at 14 days and 80% at 28 days, as shown in Figures 6.57 and 6.58, respectively.

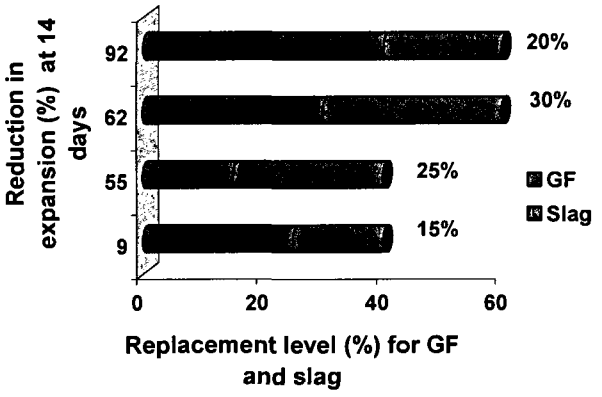

Figure 6.57 Reduction in ASR expansion at 14 days and at different GF-slag replacement levels

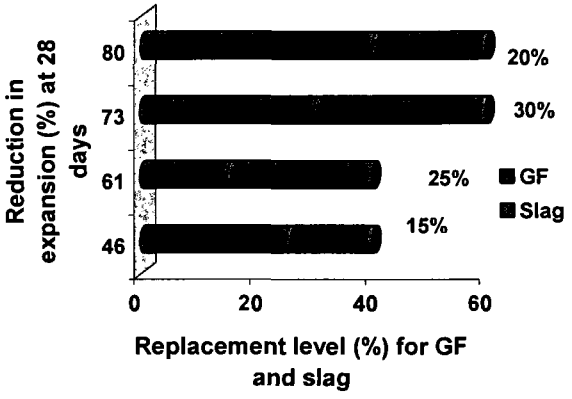

Figure 6.58 Reduction in ASR expansion at 28 days and at different GF-slag replacement levels

6.6 General comparison between some of the most important tested systems

In this comparison, different binary, ternary, and quaternary systems were compared with each other to highlight the efficiency of each mixture in reducing ASR expansion. Figure 6.59 shows that the most effective mixtures in this comparison are the binary mixture containing

25% Pfa, the binary containing 90% GF, and the main quaternary systems of Q25GF305SF and Q20GF25FA5SF which give comparable results to each other at both 14 and 28 days. The efficiency of 50% slag decreases with time while that of 50% GF increases with time, therefore they can complement each other in their mixtures

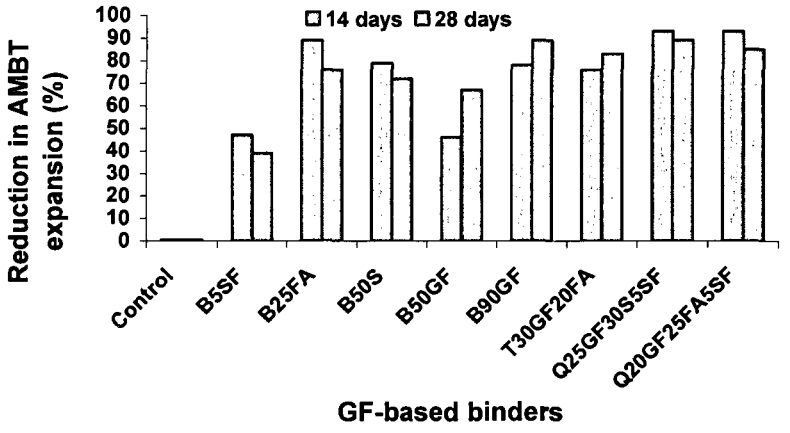

Figure 6.59 Reduction in ASR expansion at 14 and 28 days for different systems

6.7 Conclusions on mortar bar testing

Based on the results reported before, the following conclusions can be derived:

ASTM C227 has many drawbacks, including long period of time to obtain results, alkali leaching in the control mixture due to humidity of the testing conditions and to the small cross-sectional area of the tested mortar bars. All of these factors lead to an overall low expansion value from the control mixtures compared to the blended mixtures. It is also highly recommended, when planning to use ASTM C227, to increase the amount of alkali to an extent that guarantees a sufficient level of alkalis in the cementitious system to disregard alkali leaching. The recommended percentage of alkali in cement is above 1.25%, according to the previously mentioned results in this part of the study.

The increase in surface area of the reactive constituent, as well as alkali concentration when ASTM C227 specification test is applied, increases the rate of the reaction. Thus, this modification has led to a contraction of testing time from 180 days to about 33 days, as shown in the modified ASTM C227 test. This modification can successfully lead to a proposal for a new standard, as a new modification to ASTM C227.

CSA A23.2 25A (equivalent to ASTM C1260) is a highly recommended test for evaluating the effectiveness of any cementitious material. According to this test, the addition of GF decreases the ASR expansion, despite its high alkali content. The negative effect of the binary containing 25% GF with respect to the control in the case of Spratt aggregate use was attributed to the disturbance in the permeability of the system, as proven later in this chapter. This test is suggested to continue until the stability of the expansion with time or at least up to 28 days instead of 14 days.

The long-term preventive action of GF is evident and can be taken as a benefit in case of use of ternary mixture of GF and silica fume to synergistically interact as a dual mixture that works at early and later ages. Therefore, the mixture of GF and silica fume can form synergistic mixtures in a way that guarantees short- and long-term ASR reaction prevention.

A replacement value of about 91% GF is the measured and calculated optimum binary GF replacement level that should produce the same lower ASR expansion value at both 14 and 28 days.

The successfully obtained synergistic ternary diagrams of GF with silica fume, fly ash, and slag are very promising. The ternary mixtures of GF and slag are impractical due to their higher effective replacement levels. For this reason, the American specification limit of 0.15% concerning ASR expansion was chosen instead of the Canadian specification limit of 0.1%.

The importance of the synergistic ternary diagrams resides in their use as a guide for designing different ternary GF-based concrete binder to ensure minimum risk of the occurrence of ASR expansion. A synergistic quaternary diagram was suggested to be carried out to see how it will look like, as a proposal for a new research work.

6.8 Concrete Prism Test (CPT) CSA A23.2-14A

This test has been conducted according to CSA A23.2-14A (in 100% R.H. at 38°C, equivalent to ASTM C1293) from which ASR expansion results in a 2-year period were obtained and the

specification limit of 0.04% for expansion after two years of testing was applied. The use of CPT for SCMs is covered by CSA A23.2-28A, which specifies the use of 14A for CPT with SCMs. CSA A23.2-14A specification is also a popular test, as is the accelerated mortar bar test. According to CSA A23.2-27A, the results from accelerated mortar bar test (AMBT) is not sufficient and it has to be supported with CPT results. As well, the CPT specification limit is much more important than the specification limit of AMBT.

This test is the most reliable and realistic test and has been used for several years. Different combinations of reactive aggregates and cementitious systems were prepared in a way similar to actual concrete. This test is categorized as a long-term test. It extends over two years in order to evaluate any cementitious system in combination with reactive aggregates, while it extends over one year for evaluating an aggregate. As previously mentioned in Table 6.1, the most important cementitious systems were tested and the results are given in this part of the study. These cementitious systems were investigated using the CPT test to obtain further confirmation of what has already been done using the accelerated mortar bar test (AMBT), to determine the compatibility and type of relation between the AMBT and CPT tests. The importance of this test originates from its similarity with real concrete used in the field. It can also be classified as a decision-making-based test from which any concrete mixture can be excluded from any future use according to test results obtained.

In this part of the study, one coarse aggregate (Spratt) and two fine aggregates (Ottawa and Aimé Côté sands) were used. For this reason, there are two identification for their control samples, CO and CA stand for the control mixtures with Ottawa and Aimé Côté sands, respectively. The symbol "Na" stands for alkali added to cement to increase its alkali content to 1.25% Na_2O_{eq}. Aimé Côté sand was used only with one control mixture to compare its expansion with the other control mixtures containing Ottawa sand. The mixture composition of the binary, ternary, and quaternary binder compositions are the same as those binders used in the accelerated mortar bar test, as mentioned earlier in this chapter in Table 6.1.

The mix design of the concrete mixtures tested in this part has been described in detail in Chapter 3. According to CSA A23.2-14A, the concrete samples were made using Spratt

aggregate as coarse aggregate and Ottawa sand as fine non-reactive aggregate, as well as another control mixture made up of Spratt coarse aggregate and Aimé Côté sand, as previously mentioned. The physical properties of these aggregates were given in Chapter 3.

It is worth mentioning here that when calculating the amount of NaOH that must be added to the concrete mix water, it was assumed that GF is free of any alkalis. Therefore, the amount of added alkali was calculated with respect to the amount of cement used, in such a way that 0.86% Na_2O_{eq} of the cement was increased to 1.25% Na_2O_{eq}. Each concrete mixture was done twice, one with added free alkali and the other without any alkali except for that of the cement itself, in order to determine the effect of the alkali of GF alone apart from any added free alkali. Therefore, the number of tested mixtures was doubled. The mixtures containing CSF were also divided into two groups: one with SP superplasticizer (with and without alkali) and the other without SP (with and without alkali). Hence, the mixtures containing CSF were quadrupled. The CPT was extended to two years according to CSA specification. Therefore, the mixtures used with both added alkali and superplasticizer are identified by "Na" and "SP", respectively. The ternary and quaternary mixtures are identified by T and Q, respectively. Qfa and Qs are used when either fly ash or slag is used in the quaternary mixtures, respectively. The binary mixtures with 25 and 50% GF are identified as GF25 and GF50, respectively.

In the AMBT test results, it has been shown that the binary mixture containing 25% GF gives a higher expansion than the control made up of Spratt, Mirabel or even Ottawa aggregates. It has also been concluded that, as Ottawa sand is innocuous and nearly inert at early ages under AMBT test conditions, therefore, the expansion of the 25% GF mixture containing Ottawa sand cannot be attributed to ASR reaction, but to another phenomenon that was discussed in detail in the AMBT test using Spratt aggregate. Moreover, it was expected that the binary mixture containing 25% GF using Spratt aggregate in concrete mixture would give lower expansion than the control (in this case the expectation was correct). This expectation was attributed to the difference in the total size between mortar bar and concrete prism, as well as to the test conditions. Moreover, the major effect of porosity on the expansion of mortar bar is a minor effect in case of concrete prism. In fact, the CPT test has confirmed the expectation, as will be shown in this part of the study.

6.8.1 Comparison between different GF binary mixtures

Two GF replacement levels were tested to study the effect of replacement level on ASR expansion. The two replacement levels of GF were 25 and 50% (with and without added free alkali). It was found that GF mixtures give lower expansion values than those of the control mixtures, as shown in Figure 6.60 and Figures 6A.1-6.A3 (Appendix 6.A). This indicates the suppressing effect of GF against ASR reaction. Expansion decreases with the addition of GF in a similar way to what was found in the AMBT test. Therefore, the replacement level of 25% GF could be used in manufacturing of concrete. Figure 6.60 shows that the 25 and 50% GF binary expansion curves surpassed the CSA specification limit (0.04% after 2 years); however, they still give lower expansions than that of the control mixtures, indicating the absence of a deleterious effect of GF with time at up to 2 years. It is worth noting that the binary mixtures containing 50% GF give lower expansion than that containing 25% GF, as shown in Figure 6.60 and Figure 6.A3 (Appendix 6.A). Therefore, the efficiency of GF against ASR expansion increases with an increase in GF content in a similar way to these results obtained in mortars.

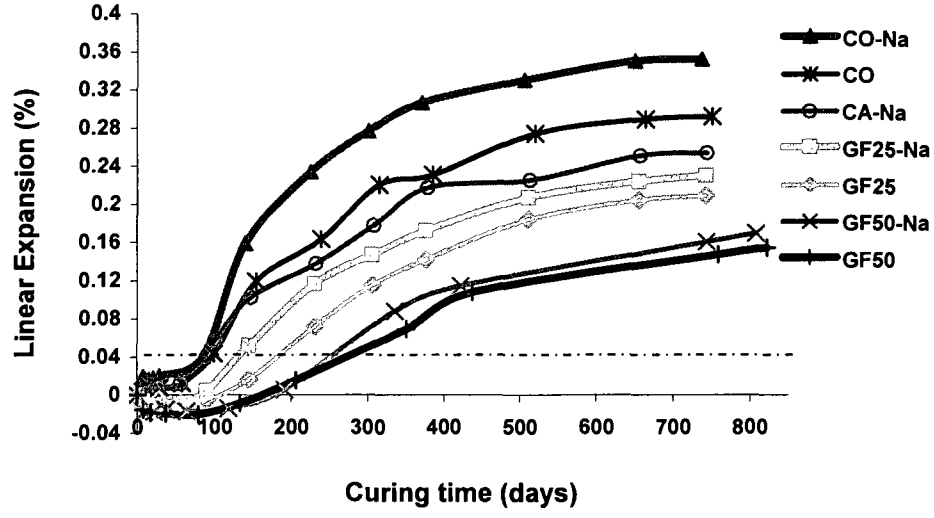

Figure 6.60 Binary concrete mixture after 2 years containing 25 and 50% GF, with and without alkalis (Spratt aggregate and Ottawa sand)

6.8.2 Comparison between different GF ternary mixtures

Because of its extreme fineness and high glass content, CSF is a very efficient pozzolanic material that, when properly formulated in ternary mixtures with GF, can give valuable results. This ternary system includes 5% CSF and 20% GF with and without added alkali, as well as with and without SP superplasticizer, forming a set of four groups, as shown in Figure 6.61 and Figures 6.A4-6.A7 (Appendix 6.A). The role of superplasticizer is to disperse CSF in the mix and thus increase its efficiency. However, results obtained were the opposite of what was expected with respect to the positive role of superplasticizer, where the addition of superplasticizer to the ternary mixture of GF and CSF increased expansion. This unexpected behavior has been discussed previously under the AMBT test heading. It was shown that CFS is responsible for such behavior. Therefore, the presence of GF does not explain such behavior, whether in mortar or concrete. The behavior of the concrete mixtures (with and without alkali, and with and without SP) was tested and compared to each other up to 2 years, as shown Figure 6.61 and Figures 6.A4-6.A7 (Appendix 6.A) . There is a direct correlation between the results obtained from the AMBT test and the CPT test, and the curves from both tests show similar trends. As previously discussed in the synergistic diagrams for GF-CSF systems, the 20% GF and 5% CSF mixture is located under the theoretical effective combination line in the negative interaction area indicating the inadequateness of this ternary mixture. Therefore, the other ternary GF-CSF mixtures will be covered in an extended part of this research, as recommended future work. The importance of this research is that the effect of added alkali was tested by comparing the mixture with added alkali to that mixture without added alkali. In this way, the effect of added alkali could be estimated. The effect of both added alkali and SP was studied in the ternary and quaternary concrete mixtures as will be shown in the following part of the study.

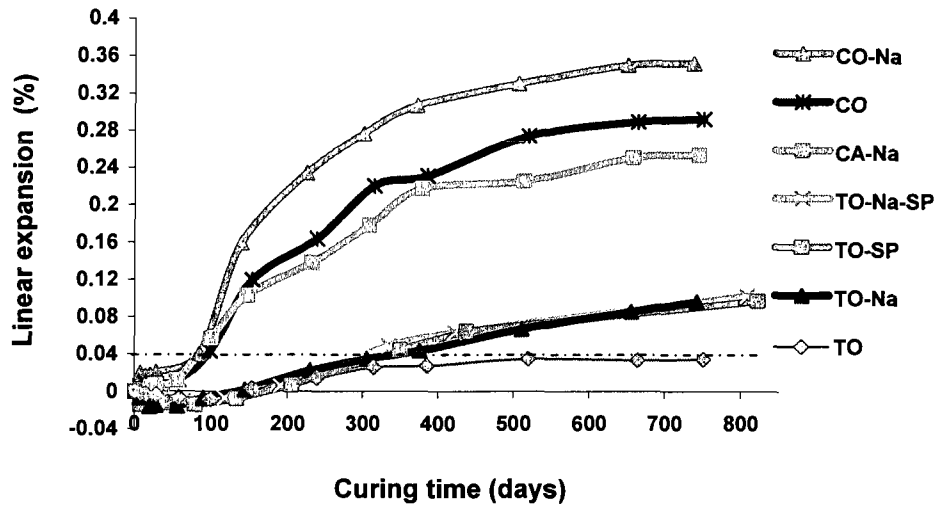

Figure 6.61 Comparison between control and GF-ternary concrete mixtures with and without alkali (Spratt aggregate and Ottawa sand)

It is worth mentioning that the effect of SP is noticeable after one year,as shown in Figure 6.A6 (appendix 6.A), while at two years, the two ternary mixtures containing SP have almost equal expansion values, greater than the Canadian specification limit (0.04% after two years), as shown in Figure 6.A7 (Appendix 6.A).

6.8.3 Comparison between different GF-quaternary mixtures

Quaternary systems are amongst the best solution for many of the concerns related to durability. The use of quaternary mixtures has shown promises as one of the most effective solutions for the recycling of by-products while resolving potential durability concerns, in both the short and long terms. In this part of the study, the efficiency of the GF-Pfa and GF-Slag quaternary mixtures was investigated. The compositions of the two cementitious systems are the same as those tested using the AMBT test, which were identified as Q20GF25PFa5SF and Q25GF30S5SF. Therefore, the importance of this part is not only to show the efficiency of these quaternary mixtures but also to show the similarities between results for the two tests (AMBT and CPT tests), as well as to assess the compatibility between each after one and two years.

A. Comparison between different GF-Pfa quaternary mixtures

As mentioned before, the composition of this quaternary cementitious binder is identical to the one used in the AMBT test, which is 20% GF, 5% SF, and 25% Pfa. This system has shown results supporting those obtained from the AMBT test, thus confirming compatibility between the two tests (AMBT and CPT tests). Figure 6.62 and Figures 6.A8-6.A11 (Appendix 6.A) show the difference between the control and quaternary mixtures with and without both alkali and superplasticizer. The effect of superplasticizer is obvious where the samples containing superplasticizer and added alkali give almost no expansion after two years, while those without superplasticizer and added alkali give very low expansion values that are still well below the CSA specification limit (slow expansion rate), as shown in Figures 6.A8-6.A11 (Appendix 6.A). These results can be ascribed to the synergistic interaction between the components of the quaternary system that diminish the negative effect of SP on CSF. Figures 6.A10 and 6.A11 (Appendix) also shows the effect of superplasticizer after the one and two-year tests with respect to the control curves. The mixtures containing SP with and without added alkali still give undetectable expansion values and the readings are below zero, which indicates the presence of shrinkage in the first year, as shown in Figure 6.A10 (Appendix 6.A). After two years, expansion starts to become detectable in the mixtures with added alkali, while the mixture with SP and without added alkali still reads zero, as shown in Figure 6.62 and Figure 6.A11 (Appendix 6.A).

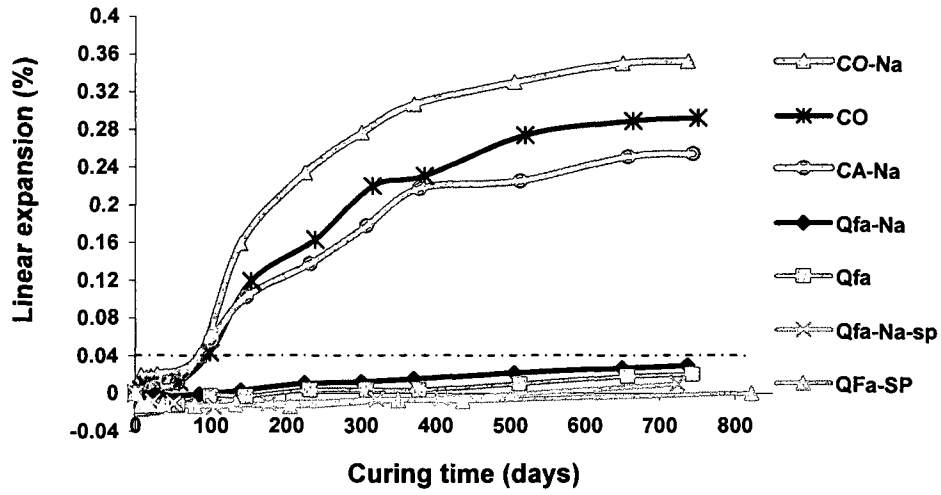

Figure 6.62 Comparison between control and GF-Pfa quaternary concrete mixtures with and without alkali after two years (Spratt aggregate and Ottawa sand)

B. Comparison between different GF-slag quaternary mixtures

As mentioned before, the composition of this quaternary cementitious system is identical to the one used in the AMBT test that is 25% GF, 30% slag, and 5% CSF. Figure 6.63 and Figures 6.A12-6.A15 (Appendix 6.A) show the difference between the control and quaternary mixtures with and without both added alkali and superplasticizer. This system has also shown supporting results to those obtained in the AMBT test, in a way similar to the GF-Pfa quaternary system. This system seems to be slightly more efficient than the GF-Pfa quaternary system where it gives lower expansion values after one and two years, as shown in Figures 6.A14 and 6.A15 (Appendix 6.A). The samples containing superplasticizer give slightly higher expansion values than the system with fly ash. This phenomenon can be attributed to the reactivity difference between fly ash and slag in long-term reactions, as well as to the total replacement level of slag system, which is 60%, while that of fly ash is 50%. The GF-slag quaternary system is characterized by its high alkali tolerance and large capacity to intake the free alkalis in the system. From the experimental work presented earlier in the document, it has been shown that both GF and slag can be easily activated using alkalis to form new cementitious products that have improved properties. These systems have been shown to solve many problems related to concrete durability by changing their composition and their ratios with respect to each other, this assertion will be verified in future research. The results show that the quaternary samples with and without alkali give a lower expansion that is well below the CSA specification limit. The quaternary mixtures with and without both alkali and superplasticizer give almost no expansion in a steady state starting from one year to up to two years, as well-illustrated in Figures 6.A14 and 6.A15 (Appendix 6.A). The mixtures with and without added alkali and with superplasticizer give nearly no expansion at one year while at up to two years the mixture with both alkali and superplasticizer shows a small expansion that is still comparable to the mixtures that do not contain any superplasticizer. It is important to note that the expansion given by the mixtures from this quaternary system is still far from the CSA specification limit (0.04%). Comparing this system with that of fly ash, it could be concluded that the quaternary system with slag tested is slightly more efficient than that with the fly ash system tested. It is to be noted, however, that the total SCMs contents were different, i.e. 60% for QS and 50% for Qfa..

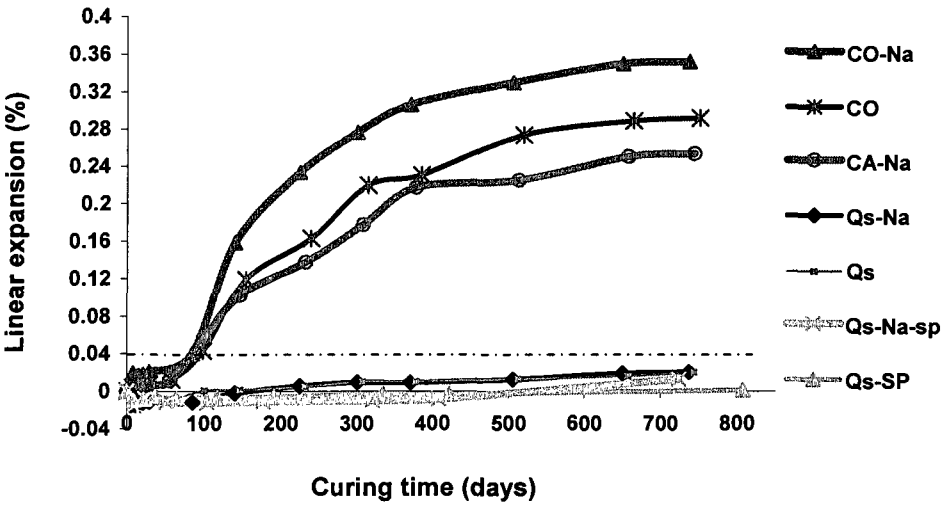

Figure 6.63 Comparison between GF-slag quaternary concrete mixtures with and without both alkali and superplasticizer after two years (Spratt aggregate and Ottawa sand)

This part of the study has shown the importance of using a well-formulated quaternary system on the ASR expansion at short and long terms. Therefore, for alkali-bearing systems, the well-formulated quaternary mixture seems to be a good solution to any concern related to their alkali content. Consequently, the use of quaternary system is highly recommended. It is then important to evaluate this system in much more detail.

6.8.4 Comparison of 19 concrete mixtures after one and two years

Table 6.2 shows the main difference between the concrete mixtures tested according to CSA CPT specification conditions. These mixtures vary from different control mixtures containing Spratt aggregate as an essential component, which represents coarse aggregate (reactive ingredient), to either Ottawa or Aimé Côté sands, which represent the fine non-reactive aggregates. However, in reality, Aimé Côté sand is much more reactive than Ottawa sand; hence it is possible that the mixtures containing Aimé Côté sand, will have more reactive sites, and will then give lower expansion values than the mixtures with Ottawa sand and this expectation can be more or less confusing. To interpret this expectation, the following was used to prove results. It is worth mentioning that the CSA specification considers this test reliable if the expansion of the control sample after one year is between 0.12 and 0.23% and between 0.15 and 0.29% after two years. Table 6.2 shows that the expansion results of the control mixture containing Ottawa sand (0.301%) are higher than those of the control mixture

containing Aimé Côté sand (0.209%). Since the ASR reaction is clearly a surface-area-dependent phenomenon, one would first think that the ASR expansion would increase linearly with aggregate fineness. However, there exists an aggregate size at which maximum expansion occurs; this is called the pessimum size. From the above-mentioned results and from the fact that Aimé Côté sand is more reactive than Ottawa sand, it is found that the concrete mixture with Aimé Côté sand likely contains more reactive sites while maintaining the same alkali content, undergoing what is called a dilution effect. This effect takes place when the surface area of the reactive species increases to a certain value, after which there is no significant effect caused by any addition of alkalis due to the higher surface-to-alkali ratio, which suppresses expansion. In the case of Ottawa sand, the reverse is true, this means that the surface area of the reactive sites is lower. This leads to a concentration of alkalis around the Spratt aggregate, exacerbating expansion. Such phenomenon was reported in the literature [GRATTAN-BELLEW et al., 1998; ZHANG et al., 1999; KURODA et al., 2000; RAMYAR et al., 2005]. Therefore, many factors affect ASR expansion such as, the surface area of the reactive species, the SiO_2/Na_2O ratio formed in ASR gel products, humidity and curing temperature, the presence of SCMs, and many other factors. Another explanation may be that the reactive silica-to-alkali ratio (SiO_2 /Na_2O) is quite high at the reaction sites (dilution effect) and the total quantity of gel likely to be formed is so small that it is not able to swell in the same way as when the SiO_2/Na_2O ratio is low. The widely distributed reaction sites tend to limit expansion both by altering the composition of the gel and by distributing the gel almost homogeneously in the concrete so that the swelling effect is weakened.

Table 6.2 summarizes the expansion values recorded from the CPT test after one and two years. It shows the main differences between tested mixtures, as well as the effect of SP superplasticizer on different mixtures after one and two years. It is clear that the addition of SP has no detrimental impact on expansion for the ternary and quaternary concrete mixes tested, with the exception of the T20GF5SF mixture.

TABLE 6.2 CPT TEST RESULTS FOR 19 CONCRETE MIXTURES AFTER ONE AND TWO YEARS

Concrete mixtures	CPT expansion (%)				Concrete mixes with SP
	Without SP		With SP		
	1yr	2yrs	1yr	2yrs	
Control-A+	0.209	0.248	-	-	-
Control+	0.301	0.348	-	-	-
Control	0.218	0.283	-	-	-
B25GF+	0.157	0.226	-	-	-
B25GF	0.129	0.205	-	-	-
B50GF+	0.095	0.157	-	-	-
B50GF	0.072	0.141	-	-	-
T20GF5SF+	0.042	0.094	0.0527	0.092	**T20GF5SF+**
T20GF5SF	0.026	0.033	0.046	0.086	**T20GF5SF**
Q25GF30S5SF+	0.010	0.020	0.0097	0.013	**Q25GF30S5SF+**
Q25GF30S5SF	0.009	0.020	0.0061	0.001	**Q25GF30S5SF**
Q20GF25FA5SF+	0.015	0.028	0.0072	0.010	**Q20GF25FA5SF+**
Q20GF25FA5SF	0.004	0.020	0.0062	0.0004	**Q20GF25FA5SF**

CPT = concrete prism test, (+) for added alkali, SP stands for superplasticizer
Control-A+ = Control mixtre with Aimé Côté sand and added alkali
Control-+ = Control mixtre with Ottawa sand and added alkali

6.8.5 Compressive strengths after two years for some concrete mixtures

Concrete cylinders were cast for compressive strength determination for some of the concrete mixtures made a part of this study. They were cured under the same conditions of concrete prism test (38°C and 100% R.H.) and were set aside for two-year compressive strength test (average of 3 samples). Test results are shown in the following histogram shown in Figure 6.64, in which compressive strength trend results are to some extent comparable to expansion results, which help judge the precision of CPT test results. The two quaternary mixtures with either slag or fly ash gave higher compressive strengths than the other mixtures (binary, ternary and control). It was planned to extract the pore solution, but due to difficulty in extracting pore solutions from these concrete samples after two years, a series of paste mixtures with the same binder compositions was fabricated for pore solution analyses, as will be shown.

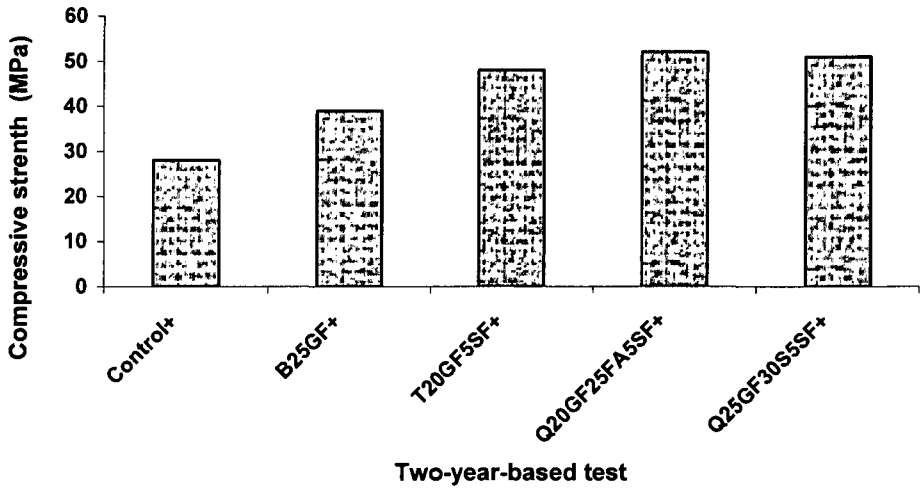

Figure 6.64 Compressive strengths of the main cementitious system-based concretes at two years

6.9 Comparison between accelerated mortar bar and concrete prism tests

A brief comparison is shown in Table 6.3 in which results of the CPT test after one and two years, as well as results of the AMBT test after 14 and 28 days, are presented. Expansion levels of less than 0.10% at 14 days were used to evaluate effective mortar mixture combinations, while a threshold expansion level of 0.040% at 2 years was used to evaluate concrete mixture effectiveness. A good correlation was established between the AMBT test at 14 days and the long-term CPT test using the Canadian reactive Spratt aggregate, as shown in figure 6.65. As expected, and as discussed in this chapter, the expansion of the binary mixture containing 25% GF in the AMBT test is not due to the presence of GF. Therefore, a series of GF mixtures with different GF replacement levels were made to confirm the mitigating action of GF. It was however confirmed that the presence of 25% GF in concrete did not enhance ASR expansion but rather suppresses it, as shown in the above-mentioned Figure 6.60. Figure 6.65 showed the correlation between CPT results at 2 years and AMBT test results at 14 days. Compared with Figure 6.66, showing CPT results at 2 years and AMBT test results at 28 days, it can be observed that all points were shifted to the right (higher expansion). However, the two quaternary mixtures are still located in the innocuous region (under the specification limits of the CPT and AMBT tests).

TABLE 6.3 MIXTURE COMPOSITIONS AND EXPANSION RESULTS FOR MORTAR BAR AND CONCRETE PRISM TESTS AT DIFFERENT CURING AGES

Mixtures	Glass Frit (%)	Silica Fume (%)	Slag (%)	Fly Ash (%)	Alkali Loading (kg/m^3)	Expansion (%)			
						Concrete Prism (1 yr)	Concrete Prism (2 yrs)	Mortar Bar (14 days)	Mortar Bar (28 days)
Control+	0	0	0	0	**5.25**	0.301	**0.348**	0.403	**0.839**
Control	0	0	0	0	**3.61**	0.218	**0.283**		
B25GF+	25	0	0	0	**3.94**	0.157	**0.226**	0.510	**0.656**
B25GF	25	0	0	0	**2.71**	0.129	**0.205**		
B50GF+	50	0	0	0	**2.62**	0.095	**0.141**	0.218	**0.280**
B50GF	50	0	0	0	**1.80**	0.072	**0.157**		
T20GF5SF+	20	5	0	0	**3.94**	0.042	**0.094**	0.127	**0.329**
T20GF5SF	20	5	0	0	**2.71**	0.026	**0.033**		
Q25GF30S5SF+	25	5	30	0	**2.10**	0.010	**0.020**	0.026	**0.092**
Q25GF30S5SF	25	5	30	0	**1.44**	0.009	**0.020**		
Q20GF25FA5SF+	20	5	0	25	**2.63**	0.015	**0.028**	0.030	**0.092**
Q20GF25FA5SF	20	5	0	25	**1.81**	0.004	**0.020**		

+ stands for added alkali

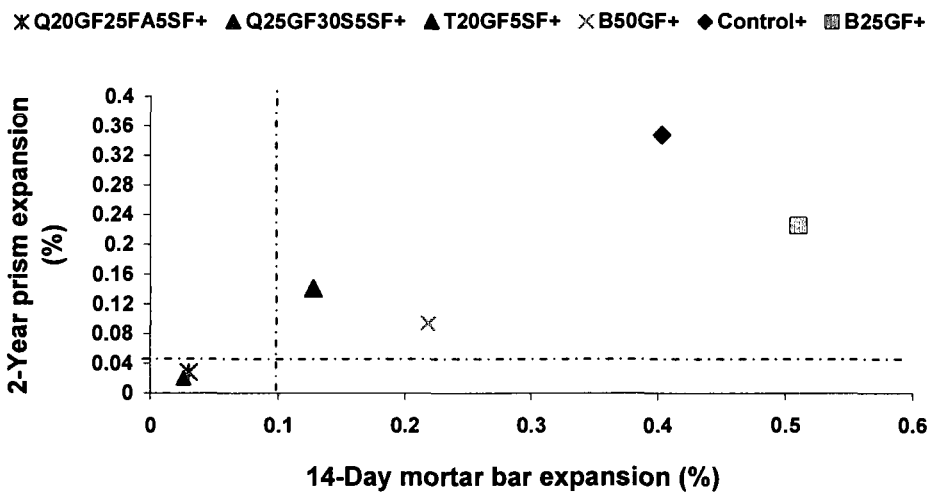

Figure 6.65 Comparison of 14-day mortar bar expansion and 2-year concrete prism expansion

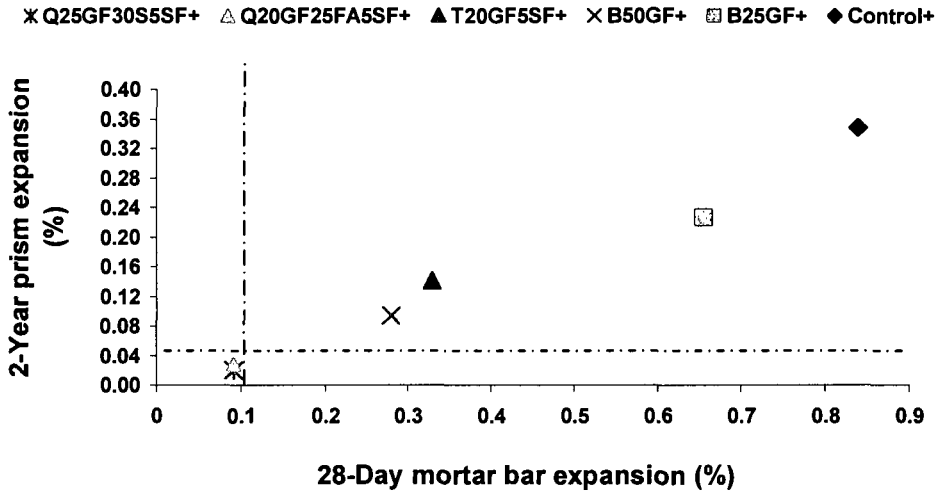

Figure 6.66 Comparison of 28-day mortar bar expansion and 2-year concrete prism expansion

6.10 Comparative analysis

The effect of added alkali on concrete mixtures, as well as the effect of different replacement levels on each system has been assessed. The derived data were obtained from Table 6.3 from which the reduction in expansion for each concrete mixture with respect to the control mixture was calculated, as shown in Table 6.4. This analysis, showed the effect of replacement level on reduction in expansion due to cement replacement by GF-based supplementary cementitious material (GF-based SCMs). The effect of alkali added to the cement to increase

the equivalent alkali content to 1.25% with respect to GU cement used according to CSA specification, was clearly shown in this part of the study.

A. Effect of replacement level and added alkali on ASR expansion

Table 6.4 represents the reduction in expansion due to cement replacement by GF-based systems (binary, ternary, and quaternary GF systems). It is interesting to note that Table 6.4 shows the combination effect of different elements: effect of replacement level, effect of added alkali, effect of superplasticizer, and finally the effect of time on ASR expansion. The maximum reduction was obtained for both quaternary systems at one and two years. Nearly no effect of the presence of both alkali and SP can be seen. The ternary mixture without alkali was affected by SP where the reduction in expansion after two years, without SP, was 88% while with SP, it was 70%. In the presence of alkali, the presence or absence of SP produces no effect, as shown in Figures 6.67 to 6.69.

TABLE 6.4 REDUCTION IN CPT EXPANSION IN PRESENCE AND ABSENCE BOTH OF ALKALI AND SP

Different GF-based SCM with and without alkali	Reduction in expansion (%)			
	Without SP		With SP	
	1 year	2years	1 year	2years
B25GF	41	27	-	-
B25GF+	48	35	-	-
B50GF	67	50	-	-
B50GF+	68	55	-	-
T20GF5SF	88	88	85	70
T20GF5SF+	86	73	85	73
Q25GF30S5SF	96	93	102	100
Q25GF30S5SF+	97	94	103	96
Q20GF25FA5SF	98	93	103	100
Q20GF25FA5SF+	95	92	102	97

+ stands for added alkali

Figure 6.67 Reduction in expansion of the main cementitious system-based concretes at 1 and 2 years, in presence of SP

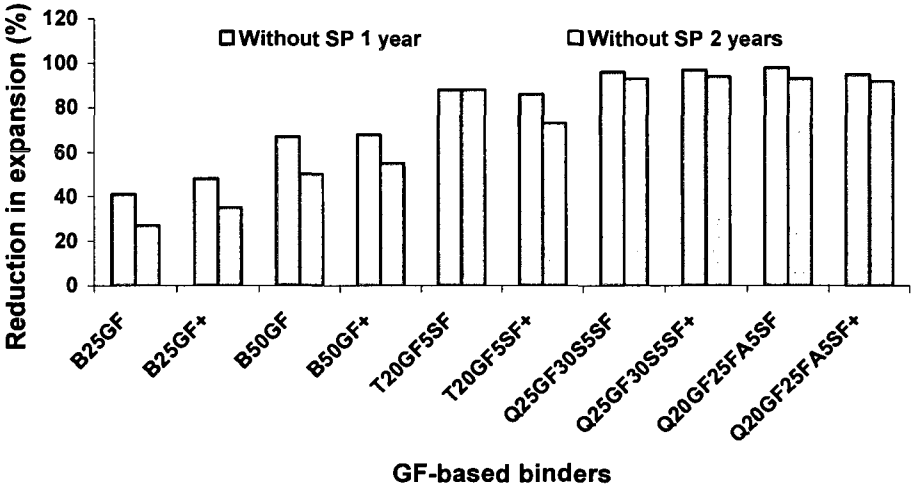

Figure 6.68 Reduction in expansion of the main cementitious system-based concretes at 1 and 2 years, in absence of SP

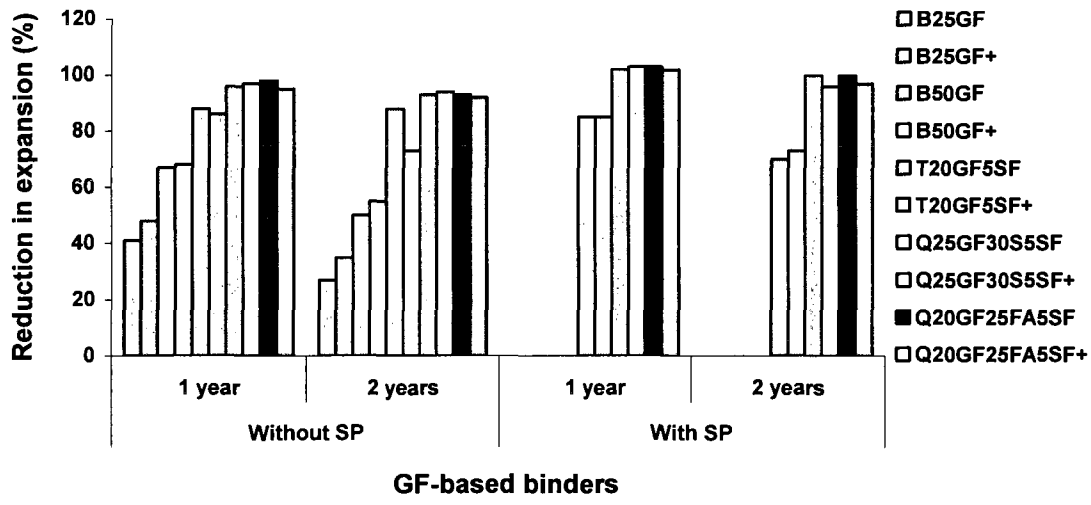

Figure 6.69 Reduction in ASR expansion measured using the CPT test at one and two years, in presence and absence of SP

Alkali addition has an accelerating effect on expansion of concrete and its effect varies considerably according to the cementitious system used. Significant differences between the binary, ternary, and quaternary systems can be seen, though in many systems with slag, added alkali has an insignificant effect, which seems instead to diminish the effect of alkali, that is it reduces ASR expansion (consumption of alkali in the alkali-activated slag reaction).

6.11 Specific mass changes

The specific weight changes of the concrete prisms of different cementitious systems, which are control, 25, and 50% binary mixtures, were determined. As the volumes of the tested concrete prism samples were determined (as a function in measured length and cross-sectional area), the change in weight of each concrete prism was also determined at the same moment for expansion of concrete prisms. Therefore, change in the specific mass can be easily followed during each testing time. Specific mass change (S_m) in the concrete prisms is very low compared with that in the mortar bars due to the large difference in volume of each type of sample, where the concrete prism has a volume about 12 times that of the mortar bar. The significance of this suggested test is attributed to its ability to show the total change in specific mass (mass/volume) of the tested concrete prism during the entire test. The results obtained from this test are promising, as seen in Figure 6.70, where the trend of S_m curves for the control, 25, and 50% GF binary mixtures are identical to these curves shown in Figure 6.60.

Therefore, this test monitors both the change in mass and volume of the tested sample during the entire test period.

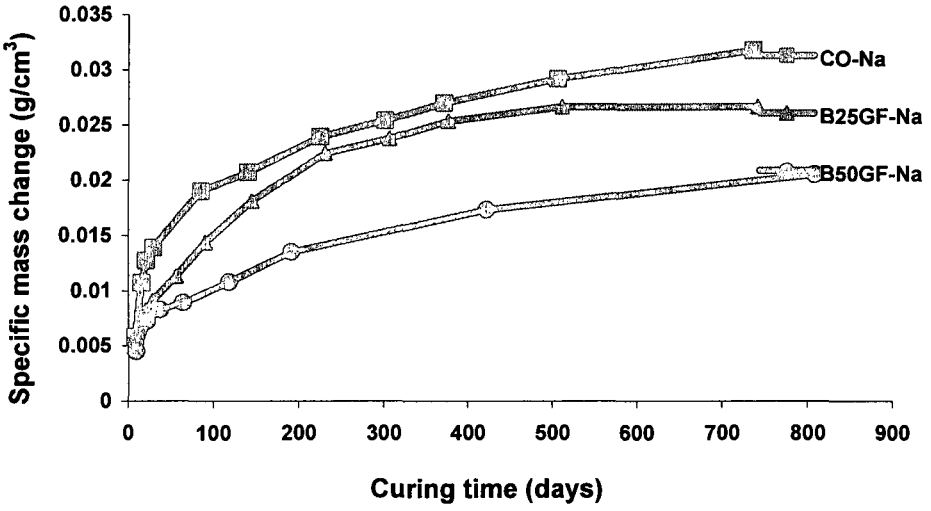

Figure 6.70 Specific mass changes of concrete prisms under CPT test conditions

6.12 Pore solution chemistry

As a well-established fact, the alkali aggregate reaction is essentially a reaction between the hydroxyl ions in the pore solution of a mortar or concrete and the siliceous (or other alkali-susceptible) minerals in the aggregate. Study of the pore solution chemistry of mature cement pastes, mortars, and concretes has been possible in recent years through the development of pore solution-expression techniques, as that shown in Figure 3.17. The study of the pore solution chemistry of cement pastes, mortars, and concretes is still at an early stage. However, the data accumulated so far are already able to help explain some of the phenomena associated with alkali aggregate reactions and also to suggest questions to be answered by further work. In addition, the information yet to be determined in order to tie the pore solution data directly to the problems of alkali-aggregate reactions, is the level of hydroxyl ion concentration necessary to cause damaging alkali-aggregate reactions with different aggregates and combinations of aggregates. Therefore, different pastes were mixed to simulate the environment of the pore solution in different cementitious systems. These cementitious systems, identical to those used in concrete, were used to investigate the relation between the pore chemical composition and the corresponding expansion in the corresponding concrete prism.

6.12.1 Chemical analysis of pore water

The same curing temperature of 38°C and water-to-binder ratio (w/b) of 0.5 were used. The samples were prepared and placed in sealed plastic containers and cured for 3, 7, 28 and 180 days. At the time of each test, samples were squeezed to extract pore solutions out of the blended cement pastes with an appropriate pore solution expression device as shown in Figure 3.17, followed immediately by chemical analysis of the clear solution. The chemical analysis included determination of Na^+, K^+, Ca^{+2}, and OH^- (by acid-base titration) ions concentrations, as well as pH, as described in detail in Chapter 3. The results are shown in Figures 6.71-6.74.

The compositions of the cementitious mixtures were shown in Table 6.1. It is also worth noting that the volume of extracted pore solution depends on the type of cementitious system used. As a general observation, the binary mixture containing 25% GF gives the minimum volume of extracted solution, while the quaternary mixture Qs (25GF30S5SF) gives the maximum volume. This volume is more than double that given by 25% GF mixture, at all testing ages. Figure 6.71 shows K-ion concentration in each tested mixture. The difference in K-ion concentration is due to replacement level, which reduces the concentration of K-ions, and the reduction in concentration was directly proportional to the replacement level used. Therefore, the sequence of the K-ion concentrations in descending order is as follows:

$$C10 > B25 > Tsf > B50 > Qfa > Qs$$

The volume of extracted solution decreases with time, which is also responsible for the gradual increase in concentration with time noted in Figure 6.71. Also, this gradual increase can be attributed to continuous hydration and release of K-ions from cement grains.

On the other hand, Na-ion concentration behaves in a different way, whereas, the mixtures containing GF give much higher Na-ion concentration than the control mixture, as shown in Figure 6.72. The mixtures containing 25% and 50% GF give the highest Na concentration. The sequence of Na-ion concentration in each mixture is as follows, in descending order:

$$B25 > B50 > Tsf > Qs > Qfa > C10$$

The previous concrete prism test (CPT) results for the same binders showed that the binary mixtures with 25 and 50% GF with and without added alkali have lower expansion than the control with and without alkali. Concrete prism expansion results showed that all the mixtures containing GF give lower expansion than the control mixture, as shown in Figure 6.70. Therefore, Na-ions are not available, to the same extent, in the pore solution of the GF-containing mixtures, as it is in control pore solution during the concrete prism test (2 years). The volume of extracted solutions from the binary mixtures with 25 and 50% GF is lower by half that of the control, despite the fact that extra pressure was applied to recover as much pore solution as possible from the sample. Accordingly, due to the high squeezing pressure, some amount of the GF internal Na-ion may be squeezed out, which was estimated to be about 6.5% in the case of the binary mixture containing 25% GF. This estimated value is lower in the other mixtures. The estimation method used to calculate the amount of alkali depends on the volume of extracted solution, original volume, amount of cement, and the amount of alkali in GF.

Figures 6.72 and 6.74 clearly show that Na released from GF maintain pH level higher than the threshold value required to control expansion with Spratt aggregate and this explains the lower efficacy of B25GF, B50GF, and T20GF5SF

Comparison between volumes of extracted solution from each mixture was carried out. It was observed that the extracted volumes were not equivalent, where the mixtures containing 25 and 50% GF give the minimum pore solution volumes, nearly half, under the same pressure and even higher, as shown in Figure 6.75 and 6.76. Therefore, and as mentioned previously, significant difference in Na-ion concentration in the mixtures containing 25 and 50% GF and in the control mixture can be attributed to the difference in extracted pore volumes, as well as to the applied squeezing pressure. Moreover, it was observed that the volume of extracted solution from the binary mixture containing 25% GF at 6 months is nearly half of that extracted from Qs and Qfa mixtures, as well as the control. This test can also be taken as concrete proof of the degree of fixation of alkalis in GF structure.

OH-ions originate from the hydrolysis of Na and K oxides, as well as from the partial hydrolysis of $Ca(OH)_2$. Therefore, the concentration of OH-ion is comparable to the

summation of Na- and K-ions, as shown in Figure 6.73. The pH was affected by the difference in OH-ion concentration, as shown in Figure 6.74.

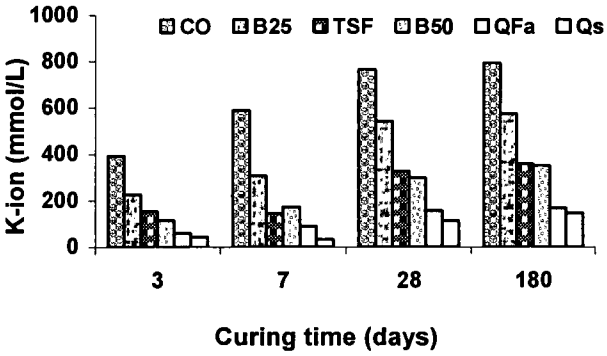

Figure 6.71 Expression pore solution analysis for K-ion (mmol/L) from cement paste

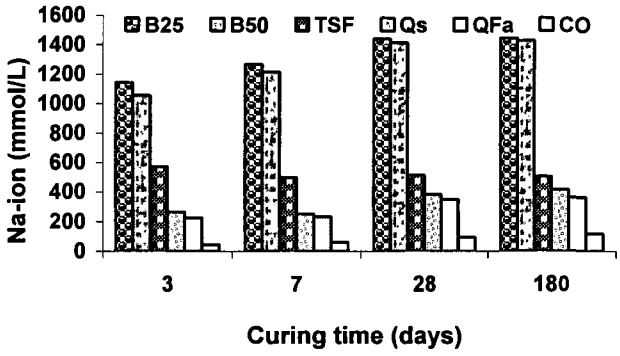

Figure 6.72 Expression pore solution analysis for Na-ion (mmol/L) from cement paste

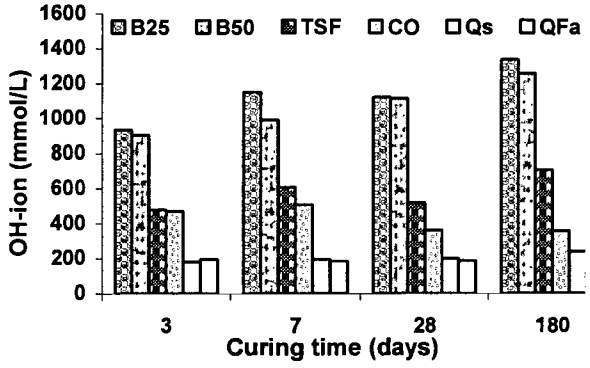

Figure 6.73 OH-ion concentration of the expressed pore solution from cement paste

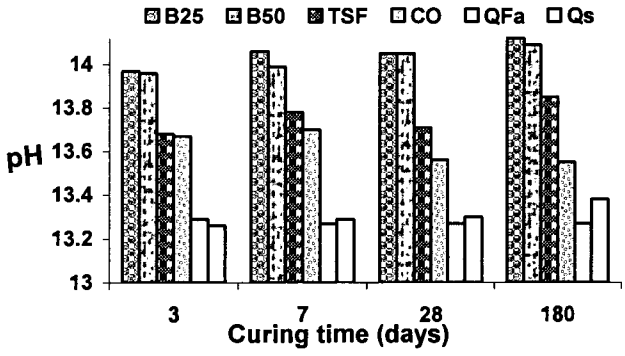

Figure 6.74 Measured pH of the expressed pore solution from cement paste

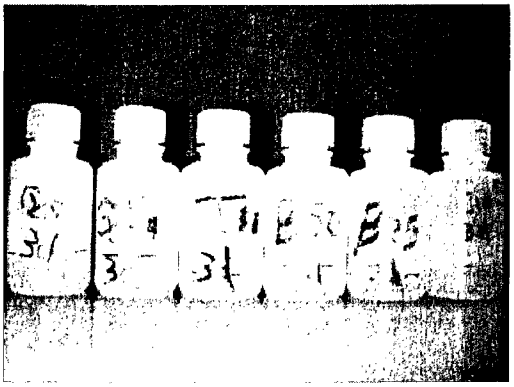

Figure 6. 75 Expressed pore solution after 3 days curing at 38°C from cement paste

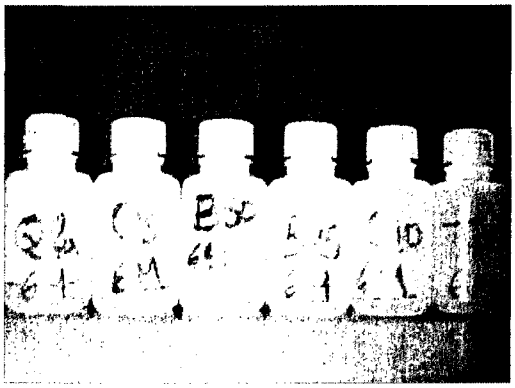

Figure 6. 76 Expressed pore solution after 6 months curing at 38°C from cement paste

6.12.2 Conductivity of expressed pore solution

The electrical conductivity of each extracted pore solution was measured and plotted against curing time. In accordance with previous results, the conductivity of B25GF, B50GF, and Tsf mixtures is higher than that of the control mixture, which is also higher than that of Qfa and Qs quaternary mixtures, as shown in Figure 6.77. Therefore, the two quaternary mixtures are the best among these mixtures. The conductivity results are not only influenced by the concentration of the soluble ions in the squeezed pore solutions, especially the mono-valence ions, but are also influenced by the volume of pore water extracted.

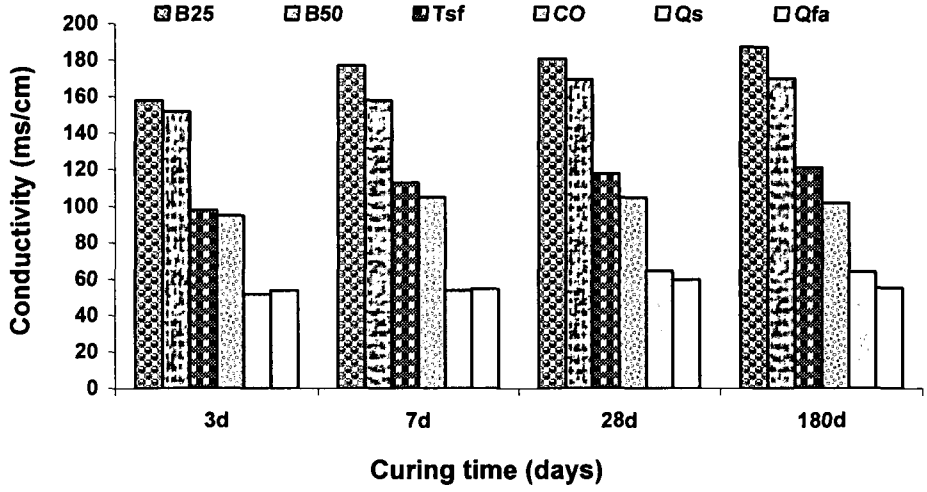

Figure 6.77 Electrical conductivity of expressed pore solutions with time

Quaternary mixtures of Qfa and Qs have the lowest conductivity due to their lower average content in mono-valence ions in comparison to other mixtures, as previously shown in Figures 6.71 and 6.72. Also, these quaternary mixtures have lower K-ion content, which is about 1.5 times more conductive than Na-ion [SNYDER et al., 2003]. Furthermore, this test requires more precautions to avoid misinterpretation of results. The volumes of extracted solutions and the difference between those volumes must be reported to assess the effect of this difference on results. The gradual reduction in volume with time is also due to the progress of hydration with time. The hydration of binary mixtures containing 25 and 50% GF seems to consume more water than the other mixtures, as they give less volume of extracted pore water, which was discussed in studying the stoichiometry of GF with NaOH and $Ca(OH)_2$ (refer to 5.13). Consequently, an important question related to extracted pore water arises: is it mainly

composed of only pore water or pore water and chemically combined water, because of applied pressure? This part of pore solution chemistry needs further verification tests.

6.13 Pore-size distribution analysis

Porosity and microstructure are two important structural characteristics of hydrated cement pastes. Both influence the mechanical properties of materials, as well as the transport behaviour of water and aggressive agents. A better control of the development and evolution of microstructure during hydration and setting is still needed to improve these properties. Microstructure is mainly characterized by the specific surface area, pore-size distribution, tortuosity, and pores connectivity. However, characterization of the porosity in this micropore range is so far poorly described because most of the existing methods are invasive and disturbing. The microstructure of Portland cement pastes is complex and, in many respects, has not been characterized quantitatively. The main hydration product, calcium silicate hydrate (C-S-H), has a complex internal pore structure with a high specific surface area. As cement grains recede due to hydration, stable hydrates may or may not form within the boundaries of the original cement particles. Different types of intrinsic pores exist in cement paste and concrete: gel pores and capillary pores. Mercury intrusion porosimetry (MIP) has been used to assess the porosity of different cementitious systems. The composition of the different cementitious systems investigated and their pore compositions are given in Table 6.5 and Figure 6.B1-6.B12 (Appendix 6.B); from which significant information can be extracted such as total porosity, average pore radius, total cumulative volume, and total specific surface area. Table 6.5 shows that the total cumulative volume of the control samples increases with increasing water-to-binder ratio because of increased porosity. Also, the total cumulative volume decreases by replacing fly ash with slag and maintaining the same replacement level and W/B ratio of 0.35, due to the slow early pozzolanic reactivity of fly ash in comparison with that of slag, particularly at 28 days. The average pore radius increases with an increase in porosity of the system. The most important thing to note is that 50% GF mixture has lower porosity than that of 25% GF, which partially explains why an increase in GF replacement decreases ASR expansion. Therefore, the importance of this part of the study is that it explains ASR expansion phenomena in a way that supports the assumption of increased porosity in the binary mixture containing 25% GF and its role in ASR expansion.

TABLE 6.5 PORE COMPOSITIONS OF DIFFERENT CEMENTITIOUS SYSTEMS CURED AT 38±2°C FOR 28 DAYS

Mixtures	w/c	Total cumulative pore volume (mm^3/g)	Total porosity (%)	Average pore radius (μm)
Control	0.4	153.97	25.68	0.035
Control	0.45	166.27	27.19	0.040
Control	0.5	181.31	28.38	0.070
B25GF	0.5	178.81	28.04	0.060
B50GF	0.5	129.44	21.68	0.040
T20GF5SF	0.35	95.27	15.67	0.022
T20GF5SF	0.5	137.39	20.33	0.030
T25GF15S	0.35	96.89	16.85	0.019
T25GF15S	0.45	171.72	25.68	0.052
T20GF15FA	0.35	110.22	18.33	0.020
T20GF15FA	0.40	144.48	22.89	0.037
Q20GF25FA5SF	0.5	168.48	24.22	0.010
Q25GF30S5SF	0.5	137.29	20.77	0.004

6.13.1 Comparison between the main binary, ternary, and quaternary mixtures

As pozzolanic reactivity depends on the nature of pozzolanic materials used and on their physical and chemical properties, they consequently have different rates of pozzolanic reactivity, that is to say, reaction with free lime. Silica fume is the most reactive and well-known pozzolanic material, while slag and class F fly ash are of moderate reactivity. On the other hand, GF, the main material of the current study, shows advanced pozzolanic reactivity. The pore size distribution in a series of paste mixtures are shown in Figures 6.78 and 6.79. The quaternary mixtures definitely have higher SCMs replacement levels that need additional time to react with free lime compared to the ternary and binary mixtures. For that reason, their mixtures gave slightly higher values in the coarser pore sizes (some of them are located in the area of air-entrained pores), which are located on the right side, than what is obtained with GF binary mixtures and even with the control. The mixtures shown in Figures 6.78 and 6.79 have different total cumulative volumes, which are classified in a descending manner as follows (for W/B of 0.5):

Control 0.5 > B25GF > Qfa > Qs = Tsf > B50GF

These mixtures have nearly the same order with respect to specific volumes and some insignificant difference in order with respect to relative volumes. With respect to the overall total porosity, they may have the same order as that with total cumulative volumes, as previously shown in Table 6.5 and as shown in Figure 6.79. It is well noted that the mixtures of T20GF5SF, Q20GF25FA5SF, and Q25GF30S5SF have pore sizes located in the area of less than 10 nm with the highest relative volumes. Therefore, the ternary and quaternary mixtures have a great effect on the refinement of the pore system. It is also noted that the same mixtures of T20GF5SF, Q20GF25FA5SF, and Q25GF30S5SF have pore sizes located in the area of large pores, but with a relative volume of less than 2% of the total pore volume, as shown in Figure 6.78.

It is well established that the incorporation of pozzolanic materials such as FA, slag or SF affects the porosity and pore size distribution of cement paste. At normal curing temperature, the partial substitution between 10% and 70% (by mass) of cement with FA is reported to increase the porosity and pore size of the paste during the early stages of hydration [POON et al., 1997; PANDEY AND SHARMA, 2000; FRIAS AND SANCHEZ DE ROJAS, 1997; HASSAN et al., 2000] and up to a curing period of 28 days. As hydration continues beyond 28 days, this effect is much reduced as more additional calcium silicate hydrate gel is formed and therefore the presence of FA in a cement paste is beneficial [PANDEY AND SHARMA, 2000; FRIAS, SANCHEZ DE ROJAS, 1997; HASSAN et al., 2000]. The incorporation of SF is reported to positively contribute to the short and long-term properties of paste or concrete, i.e. reducing porosity. These properties include strength and porosity [HASSAN, 2000]. Also, the incorporation of slag is reported to densify the cementitious matrix lowering the capillary porosity [HOOTON, 2000]

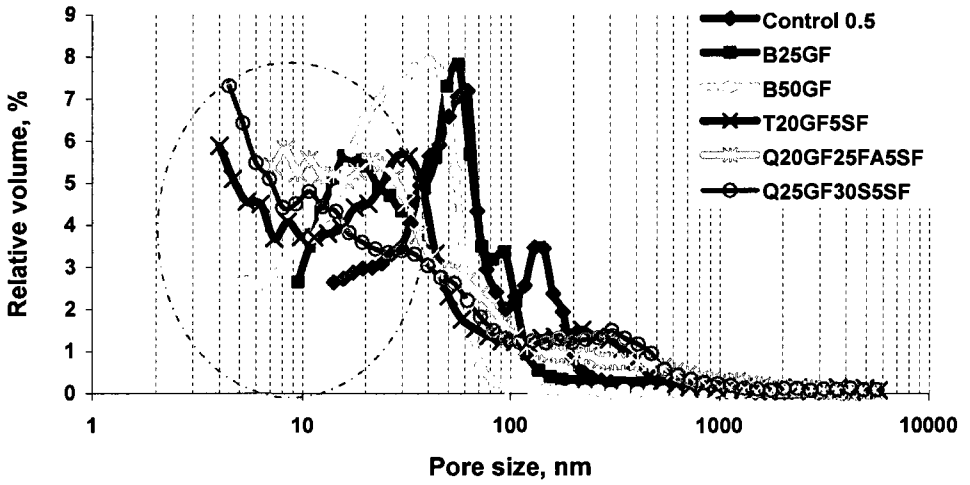

Figure 6.78 Pore size distribution as a function of specific volume (cementitious systems cured at 38°C for 28 days)

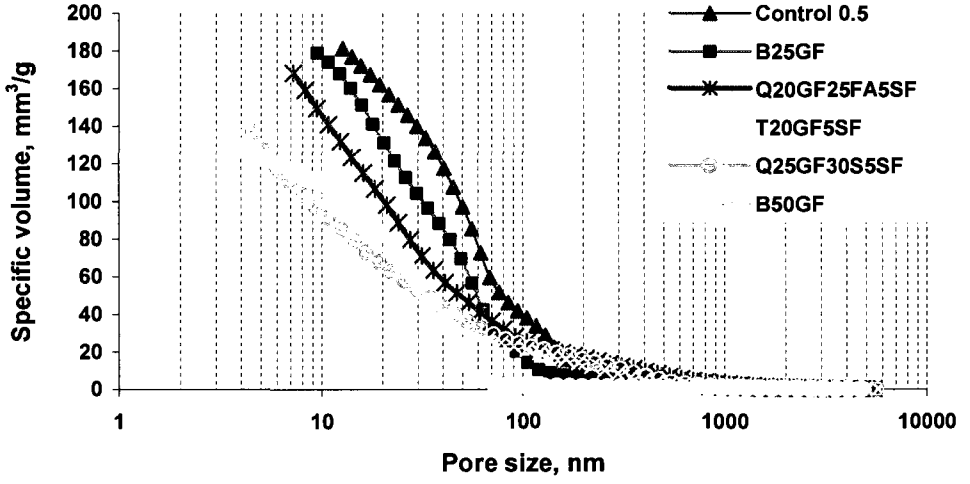

Figure 6.79 Pore size distribution as a function of relative volume(cementitious systems cured at 38°C for 28 days)

Therefore, the use of mineral admixtures resulted in pore-size and grain-size refinement, which leads to lower permeability, and consequently, reduction of the migration of alkalis towards the reactive aggregate. Also, mineral admixtures reduce the $Ca(OH)_2$ content of the cement paste, as a consequence reducing the pH and increasing the compactness of the cementitious matrix due to the formation of new extra C-S-H with improved properties. It is also important to mention that the the mixture containing 25% GF, at the same water content when compared with the mixture containing 50% GF, gives a system with a higher porosity

even in comparison with control mixture, as shown in Figure 6.80. This result possibly explains why the mixture containing 25% GF gives higher accelerated mortar bar expansion at early ages in comparison with the control mixture. Therefore, the use of 25% GF with the same water content as with the control mixture causes an increase in the coarser pores and leads to significant mortar bar expansion at early ages.

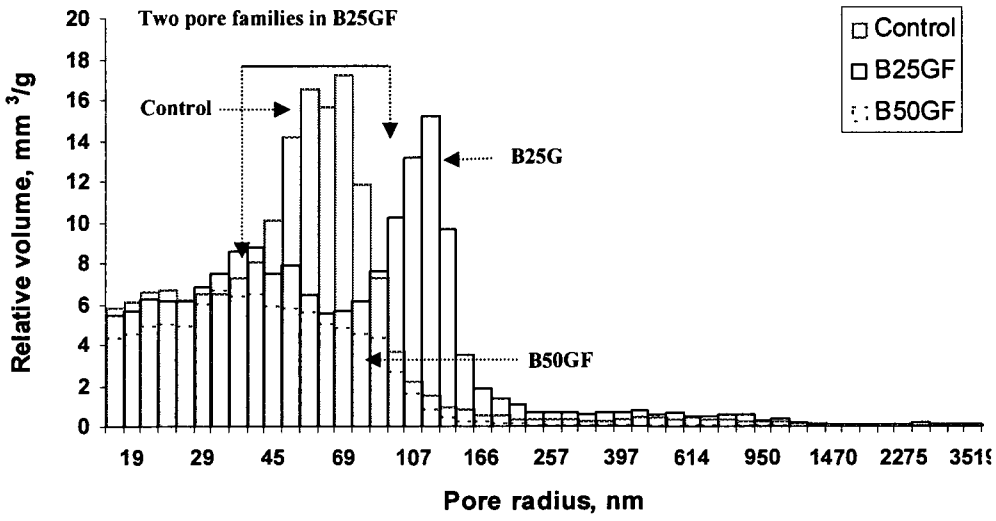

Figure 6. 80 The effect of using GF (replacement of OPC) on the pore system of the GF-binary system

The highlighted area shown in Figure 6.78 is of great importance as it is the area of the particular features characteristic to different cementitious materials. There are indeed particular pore radius ranges with higher relative volumes specific to definite cementitious systems, as shown in Figure 6.81 and as follows:

- At the range of 500-600 nm, the Q25GF30S5SF quaternary system gives higher relative pore volume, which is somewhat similar to that obtained from the B25GF binary and T20GF5SF ternary systems give nearly the same volume. However, the control, B50GF binary, and Qfa quaternary systems give lower relative pore volumes, nearly less than half of what are given by the preceding mixtures.

- At the range of 500-400 nm, the control and Q20GF25FA5SF quaternary systems give the same relative pore volumes (i.e. quite low) as that given in the previous pore range. The other systems give higher relative pore volumes.

- At the range of 400-350 to 250-150 nm, the different cementitious systems behave the same: the Qs, B25GF, and T20GF5SF systems give higher relative pore volumes, while control, Q20GF25FA5SF and B50GF systems give lower values.

- At the range of 150-100 nm, all mixtures, except the binary B50GF system, give nearly the same (i.e. quite high) relative pore volumes.

- At the range of 100-50 to 20-10 nm, all mixtures behave about the same and give higher relative pore volumes in comparison to the range of 600-100 nm.

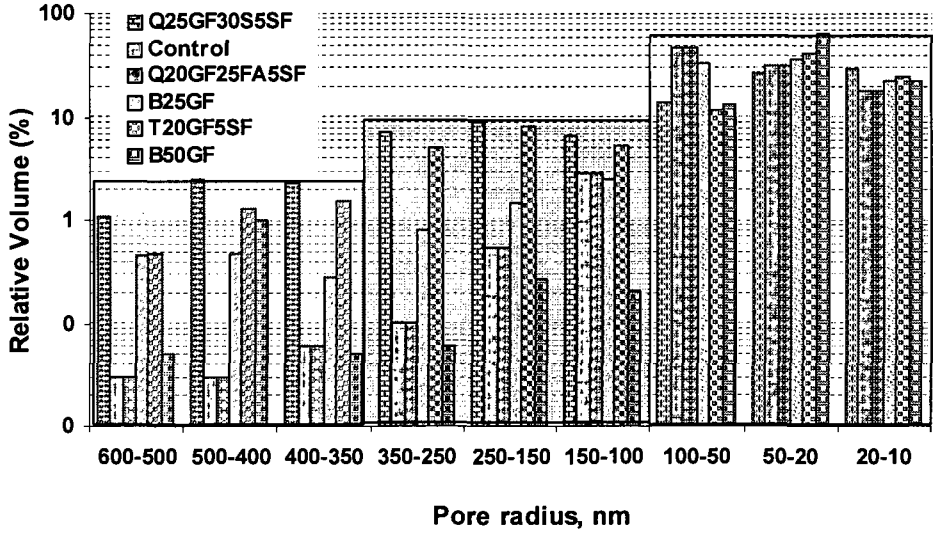

Figure 6. 81 The effect of different cementitious system on the relative volume of different pore radius

6.14 Microstructure analysis

An understanding of the performance of Portland cement-based materials requires knowledge at the microstructural level: SEM with EDS unit is one of the most powerful microstructural analyzing tools used for evaluating the development of microstructure change in cementitious matrix due to the presence of different cementitious materials. The same mixtures used in pore water extraction and pore-size distribution experiments were used in this part of the study. SEM/EDS microstructural analyses for different mixtures are shown in Figures 6.B13-6.B40

(Appendix 6.B). Special interest was shown towards the sample taken from mixtures used for pore water extraction, which were cured at 38 ± 2°C for different curing ages.

6.14.1 C/S ratio in C-S-H from different cementitious mixtures

The hydration products of the ternary and quaternary systems have a higher binding affinity towards alkalis than those of Portland cement. The typical C/S ratio of C-S-H in Portland cements is about 1.75 [THOMAS et al, 2003; HONG AND GLASSER, 2002; FAUCON et al., 1997], as previously shown, but reduced ratios are observed when mineral admixtures are used. The potential surface charge on C-S-H depends on its C/S ratio. When the C/S ratio is high, the surface charge of C-S-H is positive, then anions, with negative charges, are adsorbed on the C-S-H polymer; while when C/S ratio is lower than 1.3, the surface charge of C-S-H becomes negative and alkali cations, with positive charges, are captured in the C-S-H structure [MONTEIRO et al., 1997]. Therefore, alkali binding appears to be sensitive to the C/S ratio in the C-S-H gel, where it decreases as this ratio increases; therefore, there is a link between C-S-H composition and sorption of alkali. Different C/S ratios in different C-S-H gels from the previous mixtures tested at curing temperature of 38°C for 28 days and 6 months were examined.

A number of paste specimens with different cementitious matrices and a fixed water-to-binder ratio of 0.50, as shown in Table 6.6, were fabricated and cured at 38°C in a closed system (140 ml cylindrical sealed-plastic containers) to prevent evaporation or interaction with surrounding environment. The C/S ratios in the initial materials were calculated, as shown in Table 6.6. Hence, the cementitious materials evaluated can be classified in decreasing order of C/S as follows:

$$\text{Control} > \text{B25} > \text{TSF} > \text{B50} > \text{Qs} > \text{QFa}$$

2-mm thin-sections were cut at the middle of the sample height, vacuum dried and metalized with Au-Pd coat. The average C/S ratios from 3 different analyzed areas of the same sample were calculated, as shown in Table 6.6. These calculated values were plotted against the C/S value calculated from the chemical analysis. The other mixtures, whose compositions are

previously mentioned in Table 6.5, were also tested and their results are shown in Figures 6.B13-6.B40 (Appendix 6.B).

TABLE 6.6. DIFFERENT C/S RATIOS CALCULATED FROM AVERAGE AREA ANALYSIS FOR EACH MIXTURE

Average C/S ratio (out of area analysis)			
Identification	initial products	hydrated products	
		28 days	180 days
Control	2.88	3.6	3.71
B25	2.05	2.54	1.93
TSF	1.8	1.86	1.8
B50	1.4	2	1.53
QS	1.3	1.42	0.8
QFa	1.02	1.48	0.74

A list of figures representing area analysis for different C-S-H formed in different tested mixtures can be found in Figures 6.B41-6.B46 (Appendix 6.B). Total C/S ratios for different mixtures were calculated from the elemental area analysis of each mixture, as shown in Appendix. C/S ratios at 28 days and 180 days were plotted against the composition of each mixture and presented in Figure 6.82. The results show a reduction in C/S ratio with an increase in replacement level, which is always accompanied by an increase in silica content. For this reason, the initial C/S ratio for the total materials in each mixture (calculated from their chemical composition) was calculated and plotted against the C/S obtained from the elemental area analysis done on these hydrated materials in each mixture. A linear relationship between the initial C/S in unhydrated materials and the final C/S in the hydrated materials was obtained, as shown in Figure 6.83. and from which two mathematical equations were derived (28 and 180 days). These equations can be developed and integrated into an overall equation, which estimates the future C-S-H composition from the initial chemical composition and hydration conditions. This part of the study provides new ideas for future investigation of how to characterize a new source of supplementary cementitious material to reach potential utilization.

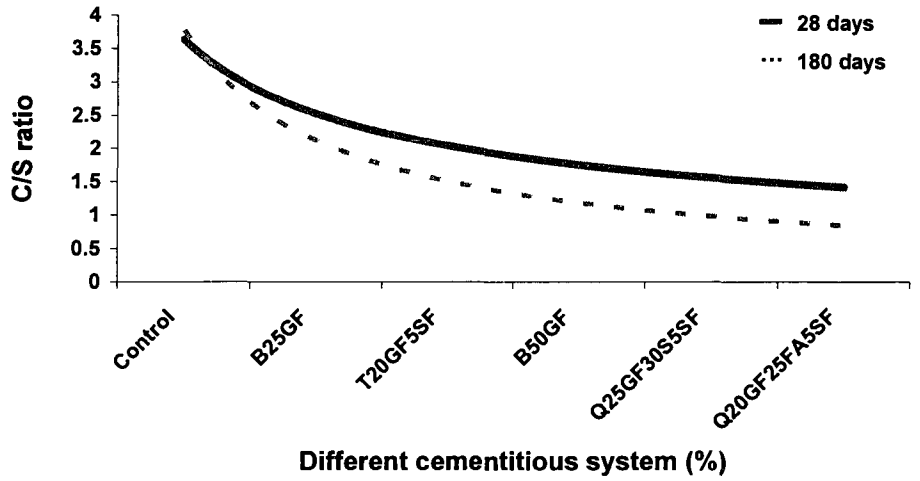

Figure 6.82 Change of C/S ratio with change of silica content (replacement level of SCMs)

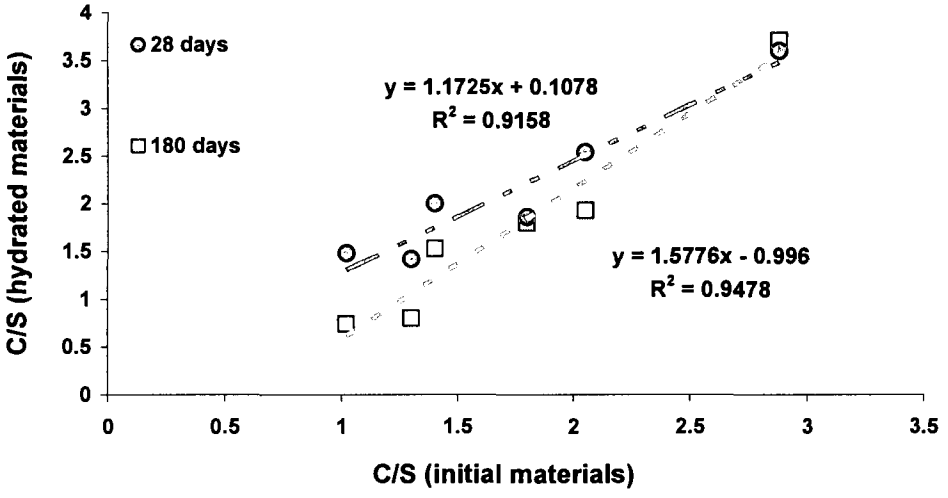

Figure 6.83 Relationship between the C/S of the initial and final products

6.15 Conclusions

Finally, in this part of the study, an inter-correlation between results from the alkali-activated GF (Chapter 5) and alkali-silica reaction studies (Chapter 6) can be established. The alkali content of GF is not that much a matter of concern if GF is well formulated with other mineral admixtures. GF can be used alone, but with higher replacement level. Considerable work has been done on GF; most of tests related to ASR reaction in mortar and concrete have been conducted. Insightful microscale analysis including microprobe analysis and pore size distribution contributes directly to interpretation of results obtained from ASR expansion tests.

The drawback observed with binary mixture with 25% GF in the accelerated mortar bar test is attributed to the total porosity of that binary system, which is confirmed by studying its pore system and microstructure, which was completely different from that of the binary mixture with 50% GF, as previously shown. This difference was attributed to the free water in the binary mixture containing 25% GF, as this dosage decreases water demand, therefore, keeping the same w/b ratio increases total porosity. The different microstructural properties of 50% GF binary mixture was first attributed to the optimum dosage of GF, which seems to match the replacement level of 50% GF. The newly formed C-S-H has promising features that chemically entrap alkalis inside its structure, though it does not look like physical adsorption, as proved by SEM-EDS analysis. The increase in pore alkalis due to the presence of GF is attributed largely to the alkalis from the cement itself as the mixture with GF gives lower volume of pore solution than that given by the control mixture. Therefore, dilution is another factor that has to be taken into account. The difference in pore solution volumes is attributed to the nature of the newly formed phases that consume large quantity of water. As well, this test can be taken as another proof of the stability of alkalis inside the structure, which needs extremely high pressure to squeeze alkalis out of the C-S-H structure. The results obtained from the accelerated mortar bar test carried out on the binary mixture containing 90% GF were promising. This binary mixture reduced ASR expansion largely in the short and long term under very severe conditions. The cement used in this mixture (10%) served as an activator. Despite the presence of Spratt aggregate, which is highly reactive, expansion was reduced in the long term to more than 88%. Therefore, the inorganic soluble salts present in cement work as a combination of a group of activators that favors the presence of external heat input, which is the case in precast concrete (our unpublished fieldwork).

General Conclusions

Spent pot-liner waste produced by aluminium smelters accumulates with time into a considerable amount threatening the Canadian environment, especially that of Quebec. A new-engineered material, known as Glass frit (GF), has been developed through the chemical treatment of such waste. GF being more than 99% amorphous possesses strong binding potential as cement. When ground to cement Blaine and combined with an alkaline activator, it hydrates and becomes an effective hydraulic binder enabling its use in highly durable concretes. When mixed with cement, GF participates indirectly in reducing CO_2 emission. When optimally mixed with other mineral admixtures, it gives synergetic mixtures, which withstand ASR reaction. The technology of engineering new cementitious materials is promising and it has many future applications.

The aim of the present study was to evaluate GF as a clinkerless binder and as a new cementitious material. Therefore, this research work has been divided into two main parts: in the first part GF was evaluated as a clinkerless binder while in the second part GF was evaluated as a new cementitious material mainly its effect on ASR expansion due to its alkali content.

This research work has instigated with some characterization tests related to GF powder, pastes, and mortars. These tests were, then, followed by intensive work done on GF as a clinkerless binder using different activators and temperatures of activation. A trial to convert GF into a new binder (clinker-free) using a chemo-thermal activation process was undertaken. Different paste, mortar, and concrete mixtures have been fabricated and evaluated. Different combinations of GF-slag and GF-fly ash were activated to investigate the beneficial effect of their presence. At the same time and in parallel with the first part, intensive ASR expansion studies have performed to evaluate the effect of alkali content of GF on the alkali-silica reaction (ASR) in mortar and concrete, especially when an alkali-active constituent exists. Different Canadian and American test methods with and without modifications were applied using different GF-based cementitious materials.

The initial characterization tests have proved that GF is an amorphous powder, which reacts with hydrated lime and sodium hydroxide as both pozzolanic and hydraulic material, respectively. The mortar mixture with 50% GF as partial replacement to cement has shown effective resistance to the deterioration due to sulfate attack. The rheological properties of GF pastes are highly affected by GF content. The flowability of GF pastes decreases with an increase in GF content.

Due to its higher amorphicity and chemical composition, GF has a great potential for conversion into cementitious binder. Choosing different inorganic activators with different combinations capable of performing safe GF activation was undertaken. The best optimal activator concentrations were chosen. Different temperatures of activation were investigated. The best sand-to-GF ratio of 1.5 was found and different concrete mixtures were made. NaOH activator, with a concentration varies from 1.5 to 3% Na_2O and the temperature of 60°C were chosen as the best activator concentration and optimal temperature of activation, respectively. The best sand-to-GF ratio of 1.5 was found and different concrete mixtures were made.

Different inorganic activators have shown dissimilar behavior with GF. Sulfate-based activators have synergistically reacted with GF forming stable sulfate compounds, as confirmed by XRD-analysis. The presence of other mineral admixtures, such as slag and fly ash, improved the mechanical properties of the binders obtained. Therefore, partial replacement of GF with small amounts of these admixtures can results in great changes in physical and mechanical properties of the binders obtained.

The mechanism of GF activation reaction with NaOH was assumed and confirmed by SEM-EDS analysis. It has been shown that the outer particle surface of GF was attacked first by NaOH solution. Thereafter, melting of the particle's surface has taken place, which fused the particles together, forming the initial binding effect. Finally, rearrangement with recrystallization took place to produce the last cementing solid form.

In the second part of the study, GF has been assessed as a new cementitious material. Since GF has high alkali content, therefore; different tests and specifications related to alkali silica

reaction (ASR) to evaluate the effect of GF alkali content on ASR expansions were used. Some of these specifications have many advantages, while the others have some drawbacks. For example, ASTM C227 specification has many drawbacks, including long period of time to obtain results, alkali leaching in the control mixture due to humidity of the testing conditions and to the small cross-sectional area of the tested mortar bars. All of these factors lead to an overall low expansion value from the control mixtures compared to the blended mixtures. It is also highly recommended, when planning to use ASTM C227 specification, to increase the amount of alkali to an extent that guarantees a sufficient level of alkalis in the cementitious system to disregard alkali leaching. The recommended percentage of alkali in cement is above 1.25%, according to the results obtained during this study. The modification done on ASTM C227 specification has led to a contraction of testing time from 180 days to about 33 days. This modification can successfully lead to a proposal for a new standard, as a new modification to ASTM C227.

However, and according to CSA A23.2 25A specification, the addition of GF decreases the ASR expansion, despite its high alkali content. This test method should be taken with more caution due to the effect of a high concentration of NaOH solution used in this method. The successfully obtained synergistic ternary diagrams of GF with silica fume, fly ash, and slag are promising. The importance of the synergistic ternary diagrams resides in their use as a guide for designing different ternary GF-based concrete binder to ensure minimum risk of the occurrence of ASR expansion.

As well, CSA A23.2-14A (equivalent to ASTM C1293) has many advantages. Moreover, it is also a popular test, as is the accelerated mortar bar test. Different 19 concrete mixtures were evaluated for their efficiency to mitigate ASR expansion in 2 years. These concrete mixtures have included different control, binary, ternary, and quaternary-based cementitious binders. The ASR expansion studies were carried out for these mixtures in presence and absence of added alkali. The results have shown that the presence of GF did not enhance ASR expansion in concrete mixtures with high and low GF contents with respect to the control mixtures. The GF-based ternary and quaternary mixtures have shown improved results.

The use of GF in the binary and ternary systems tested has shown limited efficacy in controlling ASR expansion. The GF did not enhance expansion due to ASR; however, it did not reduce expansion to a level similar to that obtained with a material of similar nature (ground granulated blast-furnace slag). This is likely attributed to some alkali contribution by the GF to the pore solution. Consequently, higher replacement levels (in binary systems) of combination with other SCMs (in ternary and quaternary systems) are needed.

Microstructural studies have shown that 50% GF binary mixture seems to be the optimum GF dosage. The newly formed C-S-H has promising features that chemically entrap alkalis inside its structure, though it does not look like physical adsorption, as proved by SEM-EDS analysis. The increase in pore alkalis due to the presence of GF was attributed to the alkali squeezed with the C-S-H.

Finally, the alkali content of GF is not that much a matter of concern, if GF is well formulated with other mineral admixtures (with intensive precautions and investigations). The inorganic soluble salts present in cement can be considered as a combination of a group of activators that favors the presence of external heat input, which is the case with precast concrete. The presence of GF with cement supported with an optimized input heat has the both advantages of GF, namely, it reacts both as a hydraulic and pozzolanic binder. Therefore, this work can be considered as a fruitful introduction to the engineering properties and chemistry of GF, as the major or minor constituent, in concrete.

Recommendations

Despite the systematic investigation reported in this thesis, more extensive study is still needed to establish a fine-tuned guideline for the development of new engineered supplementary cementitious materials (ESCMs) designated for "green" concrete. Concrete that satisfies the most basic requirements such as workability, compressive strength, scaling resistance, freeze-thaw resistance, and resistance to chloride penetration may not provide good resistance to sulfate attack or even corrosion of steel reinforcement used in that concrete. Approving any new ESCM requires extensive research to assess potential durability exposures that go beyond one particular application. The following research program can be recommended in the near future:

- Experimental work should be extended to assess potential durability of concrete made using activated GF binder. Other concrete mixtures should be fabricated to study the effect of GF-to-coarse aggregate ratio as well as the effect of changing GF-to-water ratio on fresh and hardened properties of these mixtures.

- Experimental work should be also extended to establish other activators, which may also be composed of a group of activators, capable of activating GF without need for external thermal effect. Testing of resulting binder in paste, mortar, and concrete would then be required as a second step.

- It is significant to study the kinetics of the reaction of GF with different activators; this study is important in establishing a mathematical model capable of predicting the physical and chemical properties of the hydrated cementitious material.

- Studying ASR expansion in alkali-activated GF mortar and concrete in the short and long term is highly recommended in presence and absence of active aggregate. The effect of temperature of activation and concentration of activator on ASR expansion should be investigated.

- Other points are needed to extend the area of effectiveness in the synergistic diagrams and to cover most of the efficient mixtures that can be used safely in mortar and concrete.

- The efficient ternary mortar mixtures in the accelerated mortar bar test should be tested in concrete prism test to assess the expansion behavior of these mixtures in long-term concrete testing.

- Further tests are still needed to evaluate the efficiency of the quaternary system in suppressing ASR expansion in concrete prism test.

- Further studies of pore-solution expression technique are still needed to investigate the effect of applied pressure on extracted volume of pore water and concentration of ions in this volume, as well as to determine whether the extracted pore water is only pore water or pore water and combined water, using available techniques.

- Further experimental studies are needed to determine a manner of fixing alkalis in C-S-H matrix of GF-based systems.

References

ACI COMMITTEE 201 (1992) *Guide to Durable Concrete* (ACI 201.2R-92).

ALUMINUM INDUSTRY ASSOCIATION (1st March, 1999) *The aluminium industry today for the needs of tomorrow*, Industry Canada.

ASGEIRSSON, H., GRDMUNDSSON, G. (1979) *Pozzolanic activity of silica dust.* Cement and Concrete Research, Vol. 9, No. 2, pp. 249-252.

ASTM C1012-04 Standard Test Method for Length Change of Hydraulic-Cement Mortars Exposed to a Sulfate Solution, Annual Book of ASTM Standard.

ASTM C1073-97a(2003) Standard Test Method for Hydraulic Activity of Ground Slag by Reaction with Alkali, Annual Book of ASTM Standard.

ASTM C1074-04 Standard Practice for Estimating Concrete Strength by the Maturity Method, Annual Book of ASTM Standard.

ASTM C109/C109M-07 Standard Test Method for Compressive Strength of Hydraulic Cement Mortars (Using 2-in. or [50-mm] Cube Specimens), Annual Book of ASTM Standard.

ASTM C125-00a (2000) *Standard terminology relating to concrete and concrete aggregates*, Annual Book of standard.

ASTM C1260 (1994) *Standard test method for potential alkali reactivity of aggregates (mortar-bar method)*, Annual Book of ASTM Standard, Section 4, Vol. 04.02 (Concrete and Aggregates).

ASTM C1293 (99) *Standard test method for concrete aggregates by determination of length change of concrete due to alkali-silica reaction*, Annual Book of ASTM Standard, Section 4, Vol. 04.02 (Concrete and Aggregates).

ASTM C227-03 Standard Test Method for Potential Alkali Reactivity of Cement-Aggregate Combinations (Mortar-Bar Method), Annual Book of ASTM Standard.

ASTM C289-03 Standard Test Method for Potential Alkali-Silica Reactivity of Aggregates (Chemical Method), Annual Book of ASTM Standard.

ASTM C311-98 Standard Test Methods for Sampling and Testing Fly Ash or Natural Pozzolans for Use as a Mineral Admixture in Portland-Cement Concentrate , Annual Book of ASTM Standard.

ASTM C33-03 Standard Specification for Concrete Aggregates, Annual Book of ASTM Standard.

ASTM C441-05 Standard Test Method for Effectiveness of Pozzolans or Ground Blast-Furnace Slag in Preventing Excessive Expansion of Concrete Due to the Alkali-Silica Reaction, Annual Book of ASTM Standard.

ASTM C490-07 Standard Practice for Use of Apparatus for the Determination of Length Change of Hardened Cement Paste, Mortar, and Concrete, Annual Book of ASTM Standard.

ASTM C593-06 Standard Specification for Fly Ash and Other Pozzolans for Use With Lime for Soil Stabilization, Annual Book of ASTM Standard.

ASTM C618-05 Standard Specification for Coal Fly Ash and Raw or Calcined Natural Pozzolan for Use in Concrete, Annual Book of ASTM Standard.

ASTM C989 - 06 Standard Specification for Ground Granulated Blast-Furnace Slag for Use in Concrete and Mortars, Annual Book of ASTM Standard.

BAKHAREV, T. (2005) Geopolymeric materials prepared using Class F fly ash and elevated temperature curing, Cement Concrete Research, Vol. 35, No. 6, pp. 961-974.

BAKHAREV, T., SANJAYAN, J.G., CHENG, Y.-B. (January 1999) Alkali activation of Australian slag cements, Cement and Concrete Research, Vol. 29, No. 1, pp. 113-120.

BAKHAREV, T., SANJAYAN, J.G., YI-BING CHENG, Y.-B. (1999) *Alkali activation of Australian slag cements*, Cement and Concrete Research, Vol. 29, No. 1,pp. 113-120

BAKHAREV, T., SANJAYAN, J.G., YI-BING CHENG, Y.-B. (2002) *Sulfate attack on alkali-activated slag concrete*, Cement and Concrete Research, Vol. 32, No. 2, pp. 211-216.

BAKKER, R.F.M. (1981) *About the cause of the resistance of blast furnace cement concrete to the alkali-silica reaction.* Proceedings of The Fifth International conference on Alkali-Aggregate Reaction in Concrete, Cape Town, South Africa, 30 March–3 April 1981, Pretoria, S252/29, 7p.

BALL M. C. CARROLL R. A. (1999) *Studies of hydrothermal reactions of UK pulverized fuel ashes. Part 1: reactions between pulverized fuel ash and calcium hydroxide*, Advances in cement research, vol. 11, No. 2, pp. 53-61.

BARLOW, D.F., JACKSON, P.J. (1987) *The release of alkalis from pulverized-fuel ashes and ground granulated blast furnace slags in the presence of Portland cement*, Cement and Concrete Research, Vol. 18, No. 2, pp. 235-248.

BEKMURATOV, A., DOBRYNINA, T. A. (1971) *Solubility in the ternary system NaF-H2O2-H2O*, Chemistry and material science, Russian Chemical Bulletin, Vol. 20, No. 20, pp. 2214-2216.

BERKE, N.S., SCALI,M.J., REGAN, J.C., SHEN, D.F. (1991) *Long-term corrosion resistance of steel in silica fume and/or fly ash containing concretes*, 2nd International Conference on Concrete Durability, Montreal, Canada 1991, ACI, SP-126, pp 393-422.

BERRY, E.E. (1980) *Strength Development of Some Blended Cement Mortars*, Cement and Concrete Research, Vol. 10, No. 1, pp. 1-11.

Berry, E. E., Malhotra, V. M. (1980) Fly Ash for Use in concrete-A Critical Review, ACI Journal, proceedings Vol. 77, No. 8, pp. 59-73.

BIERNACKI, J.J., WILLIAMS, P.J., STUTZMAN, P.E.(2001) *Kinetics of reaction of calcium hydroxide and fly ash*, ACI Mater. J. Vol. 98, No. 4, pp. 380–391.

BIJEN, J. (1996) *Benefits of slag and fly ash*, Construction and Building Materials, Vol. 10, No. 5, pp. 309-314.

BLACKWELL, B.Q., THOMAS, M.D.A., NIXON, P.J., PETTIFER, K. (1992) *The use of fly ash to suppress deleterious expansion due to AAR in concrete containing greywacke aggregate*, The 9th International Conference on Alkali Aggregate Reaction in Concrete, Concrete Society, Vol. I, pp. 103-109.

BOGUE, R.H. (1955) *The Chemistry of Portland Cement*. Reinhold Publication Corp., New York.

BONEN, D., DIAMOND, S. (1992*) Investigation on the coarse fraction of commercial silica fume*, Proceedings, 14th International Conference on Cement Microscopy, ICMA, Duncanville, TX, pp.103-113.

BOUZOUBAÂ N., FOURNIER, B. (2005) *Current situation with the production and use of* supplementary cementitious materials (SCMs) in concrete construction in Canada, Can. J. Civ. Eng. Vol.32, pp. 129–143.

BROUGH, A. R., ATKINSON, A. (2002) *Sodium silicate-based, alkali-activated slag mortars Part I. Strength, hydration and microstructure*, Cement and Concrete Research, Vol. 32, No. 6, pp. 865-879.

BUTTLER, F.G., MORGAN, S.R., WALKER, E.J. (1981) *Studies of the rate and Extent of reaction between calcium hydroxide and pulverized fuel ash at 38°C*, Proceedings of The 5th International Conference on Alkali-Aggregate Reaction in Concrete, Cape Town, South Africa, 30 March–3 April 1981, Pretoria, S252/38, 6p.

CANHAM, C.L., NIXON, P.J. (1987) *Aspects of the pore solution chemistry of blended cements related to the control of alkali silica reaction*, Cement and Concrete Research, Vol. 17, No. 5, pp. 839-844.

CATHERINE, J. S. (1987) *Chemical Durability of Fluoride Glasses: II The effect of Solution pH*, J. Am. Cer. Soc., Vol. 70, No. 9, pp. 654-661.

CATHERINE, J.S., JOSEPH, H.S. (1986) *Chemical Durability of Fluoride Glasses: I, Reaction of Fluorozirconate Glasses with Water*, Vol. 69, No. 9, J. Am. Cer. Soc., pp. 661-669.

CHAN, W.W.J., WU, C.M.I. (June 2000) *Durability of Concrete with High Cement Replacement*, Cement and Concrete Research. Vol. 30, No. 6, pp. 865 - 879.

CHATTERJI, S., CLAUSSON-KASS, N.F (1984) *Prevention of alkali-silica expansion by using slag-Portland cement*, Cement and Concrete Research, Vol. 14, No. 6, pp. 816-818.

CHATTERJI, S., THAULOW, N., JENSEN, A.D. (1988) *Studies of alkali-silica reactions: part6. practical implications of a proposed reaction mechanism*, Cement and Concrete Research, Vol. 18, pp. 363-366.

CHELLIAH, H.K., LAZZARINI, A.K., WANIAGARATHNE, P.C., LINTERIS, G.T. (2002) *Inhibition of premixed and non-premixed flame with fine droplets of water and solutions*, Proceedings of the combustion Institute, Vol. 29, pp. 1-8

COLLINS, F. (1999) *Alkali activation of Australian slag*, Department of Civil Engineering, Monash University, PhD Thesis, Clayton, Victoria 3168, Australia.

COLLINS, F., SANJAYAN, J.G. (2001) *Early age strength and workability of slag pastes activated by sodium silicates*, Magazine of Concrete Research, Vol. 53, No. 5, pp. 321-326.

CONSTANS, D.L. (1998) *Primary aluminum production wastes spent aluminum potliner*, K088, GCI Tech Notes, A Gossman Consulting Inc. Publication, Vol. 4, No. 09.

COX, H.P., COLEMAN, R.B. AND WHITE, L. (1950) *Effect of blast-furnace slag cement on the alkali-aggregate reaction in concrete*, Pit and Quarry, Vol. 45, pp. 95-96.

CRIADO, M., FERNANDEZ-JIMENEZ, A., de la TORRE, A.G., ARANDA, M.A.G., PALOMO, A., (2007) *An XRD study of the effect of the SiO_2/Na_2O ratio on the alkali activation of fly ash*, Cement and Concrete Research, Vol. 37, pp.671-679.

CRIADO, M., PALOMO, A., FERNANDEZ-JIMENEZ, A. (2005) *Alkali activation of fly ashes. Part 1: Effect of curing conditions on carbonation of the reaction products*, Fuel, Vol. 84, pp.2048-2054.

CSA A23.2-14A (1994) *Potential expansivity of aggregates (procedure for length change due to AAR in concrete prism*, CSA A23.2-94 - Methods of Test for Concrete, Canadian Standards Association, Rexdale, Ontario, Canada, pp. 205-214.

CSA A23.2-25A (1994) *Test method for detection of alkali-silica reactive aggregate by accelerated expansion of mortar bars*. CSA A23.2-94 - Methods of Test for Concrete. Canadian Standards Association, Rexdale, Ontario, Canada, pp. 236-242.

CSA A23.2-27A (2000) *Standard practice to identify degree of alkali-reactivity of aggregates and to identify measures to avoid deleterious expansion in concrete*. Final Draft Versions of A23.1-00/A23.2-00, Canadian Standard Association, Rexdale, Ontario, Canada, spring 2000, pp. 260-269.

CSA A23.2-28A (2000) *Standard practice for laboratory testing to demonstrate the effectiveness of supplementary cementing materials and chemical admixture to prevent alkali-silica reaction in concrete*, Final Draft Versions of A23.1-00/A23.2-00, Canadian Standard Association, Rexdale, Ontario, Canada, spring 2000, pp. 270-273.

DAVIES, D., OBERHOLSTER, R.E. (1988) *Alkali-silica reaction products and their development*, Cement and Concrete Research, Vol. 18, pp.621-635.

DAY, R.L (1988) *Natural pozzolans for building in Latin America*, in proceedings of project identification meeting on local building materials, Nairobi, Kenya, British Council, U.K.

DAY, R.L. (January 1992) *Pozzolans for use in low-cost housing: A state of the art Report*, Department of Civil Engineering, The University of Calgary, Research Report No. CE92-1, Calgary, Canada.

DAY, R.L., SHI, C. (1994) *Influence of the fineness of pozzolan on the strength of lime natural-pozzolan cement pastes*, Cement and Concrete Research, Vol. 24, No. 8, pp. 1485-1491.

DIAMOND, S. (1981) *effect of two Danish fly ashes on alkali contents of pore solutions of cement-fly ash pastes*, Cement and Concrete Research, Vol. 11, No. 3, pp. 383-394.

DIAMOND, S. (1983) *Alkali reactions in concrete-pore solution effects*, Proceedings of 6th International Conference, Alkalis in Concrete, Research and Practice, Technical University of Denmark, Copenhagen, 23-25 June 1983, pp. 155-166.

DIAMOND, S. (1986) *Particle morphologies in fly ash*, Cement and Concrete Research, Vol. 16, No. 4, pp. 569-579.

DIAMOND, S. (1989) *ASR-another look at mechanism*, 8th International Conference on Alkali-Aggregate Reaction, Kyoto (Japan), pp. 83-94.

DIAMOND, S., (1997) *Alkali Silica Reactions – Some paradoxes*, Cement and Concrete Composites, Vol. 19, pp. 391-401

DOUGLAS, E., BILDODEAU, A., BRANDSTETR, J., MALHOTRA, V.M. (January 1991) *Alkali activated ground granulated blast furnace slag concrete: Preliminary Investigation*, Cement and Concrete Research, Vol. 21, No. 1, pp. 101-108.

DOUGLAS, E., BILDODEAU, A., MALHOTRA, V.M. (1992) *Properties and durability of alkali-activated slag concrete,* ACI Materials Journal, Vol. 89, No. 5, pp. 509-516.

DOUGLAS, E., BRANSTETR, J. (1990) *A preliminary study on the alkali-activation of ground granulated blast furnace slag*, Cement and Concrete Research, Vol. 20, No. 5, pp. 746-756.

DUCHESNE, J., BÉRUBÉ, M.-A. (1992) *An autoclave mortar bar test for assessing the effectiveness of mineral admixtures in suppressing expansion due to AAR.* The 9th International Conference on Alkali Aggregate Reaction in Concrete, Concrete Society, Vol. I, pp. 279-286.

DUCHESNE, J., BÉRUBÉ, M.-A. (1994) The effectiveness of supplementary cementing materials in suppressing expansion due to ASR: another look at the reaction mechanisms part 2: pore solution chemistry, Cement and Concrete Research, Vol. 24, No. 2, pp. 221-230.

DUCHESNE, J., BÉRUBÉ, M.-A. (2000) *Long term effectiveness of supplementary cementing materials against ASR.* Proceedings of 11th International Conference on Alkali-Aggregate Reaction in Concrete, Edited by BÉRUBÉ, M.A., FOURNIER, B., DURAND, B., Québec city, Qc., Canada, pp. 613-622.

DUNCAN, M.A.G, SWENSON, E.G., GILLOT, J.E., FORAN, M.R. (1973) *Alkali-aggregate reaction in Nova Scotia, I. summary of a five-year study*, Cement Concrete Research, Vol. 3, No. 1, pp. 55-69.

FAUCON, P. CHARPENTIER, T., HENOCQ, P., PETIT, J.C., VIRLET, J., ADENOT, F. (1997) *Interaction of alkalis (Cs^+) with calcium silicates hydrates*, Materials Research Society Symposium - Proceedings of the 1997 Symposium on Scientific Basis for Nuclear Waste Management XXI, Sep 28-Oct 3 1997, DAVOS, SWITZ, Sponsor and Publisher: MRS, Vol. 506, pp. 551-559.

FENG, N., JIA, H., CHEN, E. (1998) *Study on the suppression effect of natural zeolite on expansion of concrete due to alkali-aggregate reaction*, Magazine of Concrete Research , Vol. 50, No. 1, pp. 17-24.

FENG, N., TINGYU, H. (1998) *Mechanism of natural zeolite powder in preventing alkali-silica reaction in concrete*, Advances in Cement Research, Vol. 10, No. 3, pp. 101-108.

FERNÁNDEZ-JIMÉNEZ A., PALOMO A., CRIADO, M. (2005*) Microstructural development of alkali-activated fly ash cement. A descriptive model*, Cement and Concrete Research, Vol 35, pp.1204-1209.

FERNANDEZ-JIMENEZ, A., de la TORRE, A.G., PALOMO, A.., LOPEZ-OLMO, G., ALOSO, M.M., ARANDA, M.A.G. (2006) *Quantitative determination of phases in the alkali activation of fly ash. Part I. Potential ash reactivity*, FUEL, Vol. 85, pp. 625-634.

FERNANDEZ-JIMENEZ, A., PALOMO, A. (2004) *Alkaline activation of fly ashes. manufacture of concretes not containing Portland cement*, International RILEM Conference on the Use of Recycled Materials in Building and Structures, VÁZQUEZ, E., HENDRIKS, CH. F., JANSSEN, G.M.T. (Eds.), pp. 863-870.

FERNANDEZ-JIMENEZ, A., PALOMO, A. (2005) *Composition and microstructure of alkali activated fly ash binder: Effect of activator*, Cement and Concrete Research, Vol. 35, pp.1984-1992.

FERNANDEZ-JIMENEZ, A., PUERTAS, F. (2002) *The alkali-silica reaction in alkali-activated granulated slag mortars with reactive aggregate*, Cement and Concrete Research, Vol. 32, pp.1019-1024.

FIGG, J.W. (1981) *Reaction between cement and artificial glass in concrete*, Proceedings of The Fifth International conference on Alkali-Aggregate Reaction in Concrete, Cape Town, South Africa, 30 March–3 April 1981, Pretoria, S252/7, 19p.

FOURNIER, B., BÉRUBÉ, M.-A. (2000) *Alkali–aggregate reaction in concrete: a review of basic concepts and engineering implications*, Can. J. Civ. Eng., Vol. 27, pp. 167–191.

FOURNIER, B., BÉRUBÉ, M., ROGERS, C. A. (2000) *Canadian standards associations (CSA) standard practice to evaluate potential alkali-reactivity of aggregates and to select preventive measures against alkali-aggregate reaction in new concrete structures*, Proceedings of 11th

International Conference on AAR in Concrete, Québec (Canada), June 2000. BÉRUBÉ, M.A. (Ed.), pp. 632-642.

FOURNIER, B., FERRO, A., SIVASUNDARAM, V. (2001) CANMET/Industry Research Consortium on Alkali-Aggregate Reactivity in Concrete, Technical Report, 1004031.

FRAAY, L.A., BIJEN, J.M., HAAN, Y.M. (1989) *The reaction of fly ash in concrete- a critical examination*, Cement and Concrete Research, Vol. 19, No. 2, pp. 235-246.

FREYER, D., VOIGT, W. (2003) *Crystallization and Phase Stability of CaSO4 and CaSO4 – Based Salts*, Monatchefte für Chemie / Chemical Monthly, Vol. 134, No. 5, pp. 693-719.

FRIAS, M., SANCHEZ DE ROJAS, M.I. (1997) *Microstructural alterations in fly ash mortar: study on phenomena affecting particle and pore size.* Cem. Concr. Res. Vol. 27, No. 4, pp. 619–628.

FU, X., WANG, Z., TAO, W., YANG, C., HOU, W., DONG, Y., WU, X. (2002) Studied on blended cement with a large amount of fly ash, Cement and Concrete Research, Vol. 32, No. , pp. 1153-1159.

GAZE, M. E., NIXON, P. J.(1983) *The effect of pfa upon alkali-aggregate reaction.* Magazine of Concrete Research, Vol. 35, No.123. June 1983. pp. 107-110.

GIFFORD, P.M. (1995) *Alkali-aggregate reaction and freeze-thaw durability of activated blast furnace slag cement concrete*, Ph.D. dissertation, Department of Civil Engineering, the University of Calgary, Calgary, Alta., Canada.

GIFFORD, P.M., GILLOT, J.E. (1994) *Strength development of activated blast furnace slag cement mortar and concrete using various alkaline activators and curing regimes.* Proceedings of the Annual Conference of the Canadian Society for Civil Engineering, Winnipeg, Manitoba (Canada), Vol. 2, pp. 494-503.

GIFFORD, P.M., GILLOT, J.E. (1996A) *Freeze-thaw durability of activated blast furnace slag cement concrete.* ACI Material Journal, Vol. 93, No. 3, pp. 242-245.

GIFFORD, P.M., GILLOT,J.E. (1996B) *Alkali-silica reaction (ASR) and alkali-carbonate reaction (ACR) in activated blast furnace slag cement (ABFSC) concrete.* Cement Concrete Research, Vol. 26, No. 1, pp. 21-26.

GLASSER, F.P., MARR, J. (1984) *The effect of mineral additives on the composition of cement pore fluids*. Chemistry and Chemical Related Properties of Cement, London, 12-13 April 1984. British Ceramic Society, Proceedings, Vol. 35. GLASSER, F.P. (Ed.), pp. 419-429.

GLUCHOWSKY, V.D., ROSTOVSKAJA, G.S., RUMYNA, G.V. (1980) *High strength slag-alkaline cements,* Proceedings of the 7th International Conference on Chemistry of Cement, Vol. 1, pp. 164-168.

GRATTAN-BELLEW, P.E., BEAUDOIN, J.J., VALLEE, V.-G.(1998) *Effect of aggregate particle size and composition on expansion of mortar bars due to delayed ettringite formation*, Cement and Concrete Research, Vol. 28, No. 8, pp. 1147-1156.

GRATTAN-BELLEW, P.E., MITCHELL, L. (2002) Preventing Concrete Deterioration Due to Alkali-Aggregate Reaction, Construction technology update, No. 52.

GREENBERG, S. A., CHANG, T. N. (1965) *Investigation of colloidal hydrated calcium silicates. II. Solubility relationships in the calcium oxide–silica–water system at 25°C, Journal Physical Chemistry*, Vol. 69, No. 1, pp. 182–188.

GUDMUNDSSON, G., HALFDANARSON, J., MOLLER, J. (2000) Effect of silica fume properties on mitigation of ASR reactivity in concrete. Proceedings of 11th International Conference on AAR in Concrete, Québec (Canada), June 2000. Bérubé, M.A. (Ed), pp. 643-651.

GUTIERREZ, B., PAZOS, C., COCA, J. (1993) *Characterization and leaching of coal fly ash*, Waste Manage. Res. Vol. 11, pp. 279–286.

HASSAN, K.E., CABRERA, J.G., MALIEHE, R.S. (2000) *the effect of mineral admixtures on the properties of high-performance concrete.* Cem. Concr. Res. Vol. 22, No. 4, pp. 267–271.

HOBBS, D.W. (1982) *Influence of pulverized fuel ash and granulated blast furnace slag upon expansion caused by the alkali-silica reaction.* Magazine of Concrete Research, Vol 34, No. 119, pp. 83-94.

HOBBS, D.W. (1986) *Deleterious expansion of concrete due to alkali-silica reaction: influence of pfa and slag.* Magazine of Concrete Research, Vol. 38, No. 137, pp. 191-205.

HOGAN, F. J. (1983) *The effect of blast furnace slag cement on alkali aggregate reactivity. A literature review. Cement,* Concrete and Aggregates. Vol. 7, No.2, pp. 100-107.

HONG, S.-Y., GLASSER, F.P. (2002) *Alkali sorption by C-S-H and S-A-S-H gels Part II Role of alumina,* Cement and Concrete Research, Vol. 32, pp. 1101-1111.

HOOTON, R.H. (2000) *Canadian use of ground granulated blast-furnace slag as a supplementary cementing material for enhanced performance of concrete.* Can. J. Civ. Eng. Vol. 27, pp. 754-760

HUANHAI, Z., XUEQUAN, W., ZHONGZI, X., MINGSHU, T. (1993) *Kinetic study on hydration of alkali-activated slag,* Cement and Concrete Research, Vol. 23, No. 6, pp. 1253-1258

HUDEC, P.P., GHAMARI, R.C. (2000) *Ground waste glass as an alkali-silica reaction inhibitor,* The 11Th International Conference on Alkali Aggregate Reaction in Concrete, Québec (Canada), June 2000, BÉRUBÉ, M.A. (Ed.), pp.663-672.

HUSSAIN, S.E., RASHEEDUZZAFAR (1994) *Corrosion resistance performance of fly ash blended cement concrete,* ACI Materials Journal, Vol. 91, No. 3,pp. 264-272.

HWANG, C.L., SHEN, D.H. (1988) *The effect of blast furnace slag and fly ash on the hydration of Portland cement.* Cement Concrete Research, Vol. 21, No. 4, pp. 410-425.

ICHIKAWA, T., MIURA, M. (2007) *Modified model of alkali silica reaction,* Cement Concrete Research, Vol. 37, No. 9, pp. 1291-1297.

JAMES, J., RAO, M.S. (1986) *Reaction product of lime and silica from rice husk ash.* Cement Concrete Research, Vol. 16, No. 1, pp. 67-73.

JAMBOR, J. (1963) *Relation between composition, over-all porosity and strength of hardened lime-pozzolana pastes,* Magazine of Concrete Research, Vol. 15, No. 45, pp. 131-142.

JOHN EGGERS, P.E. (2002) Evaluation of Ground Granulated Iron Blast-Furnace Slag: Grade 100, LTRC Project No. 00-4C, State Project No. 736-99-0786, Louisiana Transportation Research Center, pp. 35.

JOHNSTON, C.D. (1974) Waste glass as coarse aggregate for concrete, Journal of Testing and Evaluation, Vol. 2, No. 5, pp. 344-350.

JOLICOEUR, C., SIMARD, M.A., TO, T.C., SHARMAN, J., ZAMOJSKA, R., DUPUIS, M., SPIRATORS, N., DOUGLAS, E., MALHOTRA, V.M. (1992) *Chemical activation of blast furnace slag: An overview and systematic experimental investigations,* Proceedings of the CANMET/ACI, International Conference on Advances in Concrete Technology, ACI SP-154, pp. 471-502

JUENGER, M.C.G., OSTERTAG, C.P. (2004) *Alkali-silica reactivity of large silica fume-derived particles,* Cement Concrete Research, Vol. 34, No. 8, pp. 1389-1402.

KECK, R.H. (2001) *Improving concrete durability with cementitious materials,* ACI, Concrete International, Vol. 23, No. 7, pp. 47-51.

KERENIDIS, K. (2007) Mitigating alkali silica reaction in concrete with supplementary cementing materials when used in conjunction withportland cements having alkali contents in excess of 1.0%, A Mater's thesis, Applied Science, Graduate Department of Civil Engineering, University of Toronto, September 2007, 235p.

KHEDR, S.A., ABOU-ZEID, M.N. (1994) Characteristics of Silica-Fume Concrete, J. Mat. in Civ. Engrg., Vol. 6, N. 3, pp. 357-375.

KIMMERLE, F.M., KASIREDDY, V., TELLIER, J.-G. (2003) *SPL treatment by LCL & L process: Pilot study of two-stage leaching,* From a presentation in Alcan International Ltd., Arvida Research Development Centre

KOJIMA, T, TAKAGI, N., HARUTA, K. (2000) *Expanding characteristics of mortar with glass powder produced from waste bottles,* The 11Th International Conf. on Alkali Aggregate Reaction in Concrete, Québec (Canada), June 2000. BÉRUBÉ, M.A. (Ed.), pp.673-682.

KOUKOUZAS, N., ZENG, R., PERDIKATSIS, V., XU, W., KAKARAS, E.K. (2006) *Mineralogy and geochemistry of Greek and Chinese coal fly ash,* Fuel, Vol. 85, pp. 2301-2309.

KRIZAN, D., ZIVANOVIC, B. (2002) *Effect of dosage and modulus of water glass on early hydration of alkali-slag cements*, Cement and Concrete Research, Vol. 32, No. 8, pp. 1181-1188.

KURODA, K., NISHIBAYASHI, S, INOUE, S.,YOSHINO, A.(2000) *Effects of the particle size of reactive fine aggregate and accelerated test conditions on ASR expansion of mortar bar*, Source: Transactions of the Japan Concrete Institute, Vol. 22, p 113-118

LAFAVE, J.M., PFEIFER, D.W., SUND, D.J., LOVETT, D., CIVIAN, S.A. (August 2002) *Using mineral and chemical durability-enhancing admixtures in structural concrete*, ACI, Concrete International, pp. 71-78.

LALDJI, S., FARES, G., TAGNIT-HAMOU A. (2004) *Glass Frit in Concrete as a New Alternative Cementitious Material,* RILEM, Conference on the " Use of Recycled Materials in Building and Structures", 9-11 November 2004, Barcelona, Spain.

LALDJI, S., TAGNIT-HAMOU A. (March 2006) *Properties of ternary and quaternary concrete incorporating new alternative cementitious material,* ACI, Mat., Jr., Vol. 103, No. 2, pp. 83-89.

LALDJI, S., TAGNIT-HAMOU, A. (July 2007) *Glass frit for concrete structures: a new, alternative cementitious material*, Canadian Journal of Civil Engineering Vol. 34, No. 7, pp. 793-802.

LANE, D.S., OZYILDIRIM, C. (1999) Preventive measures for alkali-silica reactions (binary and ternary systems), Cement and Concrete Research, Vol. 29, No. 8, pp. 1281-1288.

LEA, F.M. (1938) *The chemistry of pozzolans*, In proceedings of 3rd Symposium on the Chemistry of Cements, Stockholm, pp. 460-490.

LEA, F.M. (1974) *The Chemistry of Cement and Concrete*, 3rd Edition, Edward Arnold, New York.

LI, D., ZHONGZI, X., ZHIMIN, L., ZHIHUA, P., LIN, C. (2002) *The activation and hydration of glassy cementitious materials*. Cement and Concrete Research, Vol. 32, No. 7, pp. 1145-1152.

LI, S., ROY, D.M., KUMAR, A. (November 1985) *Quantitative determination of pozzolans in hydrated systems of cement or Ca(OH)2 with fly ash or silica fume*. Cement Concrete Research, Vol. 15, No. 6, pp. 1079-1086.

LI, Z., LIU, S. (2007) *Influence of slag as additive on compressive strength of fly ash-based geopolymer*, J. Mat. Civ. Eng., Vol. 19, No. 6, pp. 470-474

LI, Z., MU, B., AND PENG, J. (1999) *The combined influence of chemical and mineral admixture on the alkal-silica reaction*, Magazine of Concrete Research, Vol. 51, No. 3, pp. 163-169.

LOTHENBACH, B., GRUSKOVNJAK, A. (2007) *Hydration of alkali-activated slag: thermodynamic modelling*, Advances in Cement Research, Vol. 19, No. 2, pp. 81-92.

LUMLEY, S.J. (1992) *The ASR expansion of concrete prisms made from cements partially replaced by ground granulated blast furnace slag*. The 9th International Conference on Alkali-Silica Reaction in Concrete, Concrete Society, London (UK), pp. 662-629.

LUXAN, M.P., SANCHEZ DE ROHAS, M.I., FRIAS, M. (1989) *Investigations on the fly ash–calcium hydroxide reactions*, Cement and Concrete Research, Vol. 19, pp. 69–80.

MA, W., BROWN, P.W. (1997) *Hydrothermal reactions of fly ash with $Ca(OH)_2$ and $CaSO_4 \cdot 2H_2O$*, Cement and Concrete Research, Vol. 27, No. 8, pp. 1237–1248.

MA, W., LIU, C., BROWN, P.W., KOMARNENI, S. (1995) *Pore structure of fly ashes activated by $Ca(OH)_2$ and $CaSO_4.2H_2O$*, Cement and Concrete Research, Vol. 25, No. 2, pp. 417-425.

MALHOTRA, V.M. (2000) *Role of supplementary cementing materials in reducing greenhouse gas emissions*, Concrete Technology for a Sustainable development in the 21st Century, Edited by GJORV, O.E., SAKAI, K., pp. 226-235.

MALINOWSKI, R., GARFINKEL, Y. (1991) *Prehistory of concrete*, concrete international: Design and Construction, Vol. 13, No. 3, pp. 62-68.

MALQUORI, G. (1960) *Portland-Pozzolan cement*, Proceedings of the 4thInternational Symposium on the Chemistry of Cement, Washington, Vol. II, pp. 983-1000.

MALVAR, L.J., CLINE, G.D., BURKE, D.F., ROLLINGS, R., SHERMAN, T.W., GREENE, J. (2002) *Alkali-silica reaction mitigation: state-of-the-art and recommendations.* ACI, Materials Journal, Vol. 99, No. 5, pp.1-21.

MANTEL, D.G. (September 1994) *Investigation into the hydraulic activity of five granulated blast furnace slags with eight different Portland cements*. ACI Materials Journal. Vol. 91. No. 5 pp.471-477.

MARSH, B.K., DAY, R.L., BONNER, D.G. (March 1986) *Strength gain and calcium hydroxide depletion in hardened cement pastes containing fly ash*. Magazine of Concrete research, Vol. 38, No. 134, pp. 23-29.

MARSH, B.K., DAY. R.L. (1988) *Pozzolanic and cementitious reactions of fly ash in blended cement pastes*. Cement and Concrete Research, Vol. 18, No. 2, pp. 301-310.

MARUSIN, S.L., SHOTWELL, L.B. (1995) *Alkali-silica reaction in concrete study,* 5th *CANMET*/ACI international conference on fly ash, silica fume, slag and natural pozzolans in concrete, Waukee, M., pp. 45-59 (Volume of supplementary papers).

MATSUKAWA, K. (1991) *Quantitative analysis of interactions between Portland cements and superplasticizers,* PhD thesis, Purdue University, 1991.

MCCARTER, W.J., EZIRIN, H.C. (October 1998) *Monitoring the early hydration of pozzolan-Ca(OH)2 mixtures using electrical methods*. Advances in Cement Research, Vol.10, No. 4, pp. 161-168.

MEHTA, K.P.(1983) *Pozzolanic and cementitious byproduct as mineral admixture for concrete – a critical review*. CANMET/ACI Proceedings on the Use of Fly Ash, Silica Fume, Slag and other Mineral Byproducts in Concrete, ACI SP-79, 46 p.

MEHTA, P.K. (1989) *Pozzolanic and cementitious by products in concrete-another look*, Fly Ash, Silica Fume, Slag, and Natural Pozzolans in Concrete, Proceedings of the Third International Conference, Trondheim, Norway, American Concrete Institute, MALHOTRA, V.M. Ed., ACI, SP-114, pp. 1-43.

MEMON, A.H., RADIN, S.S., ZAIN, M.F.M, TORTTIER, J.-F. (2002) *Effect of mineral and chemical admixtures on high-strength concrete in seawater*, Cement and Concrete Research, Vol. 32, No. 3, pp. 373-377.

MINTO, R. (2003) *Environmental issue in the aluminum industry*, CRU 8th world aluminium Conference, Montreal, Canada.

MIURA, T., IWAKI,I. (2000) *Strength development of concrete incorporating high levels of ground granulated blast-furnace slag at low temperatures. ACI Materials Journal*. Vol. 97, no. 1, pp. 66 - 70.

MOHD ZAIN, M.F., S.S. RADIN.(2000) *Physical Properties of High-Performance Concrete with Admixtures Exposed to a Medium Temperature Range 20°C to 50°C*. Cement and Concrete Research. Vol. 30, No. 8, pp. 1283 - 1287.

MONTEIRO, P.J.M. WANG, K. SPOSITO, G. SANTOS, M.C. ANDRADE, W.P. (1997) *Influence of mineral admixture on the alkali aggregate reaction*, Cement and Concrete Research, Vol. 27, No 12, pp. 1899-1909.

MORALES, J. W., GALLEGUILLOS, H.R., HERNANDEZ-LUIS, F. (2007) *Solubility of NaF in NaF + NaX + H2O (X=ClO4 and NO3) Ternary systems and density and refractive index of the saturated solutions at 298.15K*, J. Chem. Eng. Data, Vol. 52, pp. 687-690.

MOSTAFA, N. Y., EL-HEMALY, S. A. S., AL-WAKEEL, E.I., EL-KORASHY, S.A., BROWN, P.W. (2001) *Hydraulic activity of water-cooled slag and air-cooled slag at different temperatures*. Cement and Concrete Research. Vol. 31, no. 3, pp. 475 - 484.

MOUKWA, M. (1990) *Cobalt furnace slag: A latent hydraulic binder*, Cement Concrete Research, Vol. 20, No. 2, pp. 253-258.

NAIK, T.R., RAMME, B.W. (1989) *High-Strength Concrete Containing Large Quantities of Fly Ash*. ACI Materials Journal. Vol. 86, no. 2, pp. 111 - 116.

NIXON, P. J. and GAZE, M. E. (1983) *The effectiveness of fly-ashes and granulated blast furnace slags in preventing AAR*. Proceedings of the Sixth International Conference on Alkalis in Concrete, Copenhagen, 22-25 June 1983, DORN, G.M, ROSTRUM, S. (Eds.), Danish Concrete Association, December 1983, pp. 61-68.

NIXON, P. J., GAZE, M. W. (1981) *The use of fly ash and granulated blast furnace slag to reduce expansion due to the alkali-aggregate reaction*, Proceedings of the Fifth International Conference on Alkali-aggregate Reaction in Concrete, Cape Town, 30 March-3 April 1981. Pretoria, National Building Research Institute, Paper S252/32, pp. 10.

NIXON, P.J., PAGE, C.L., BOLLINGHAUS, R., CANHAM, I. (1984) *The effect of PFA with high alkali content on pore solution composition and alkali-silica reaction*, Magazine of Concrete Research, Vol. 38, No. 134, pp.30-35.

OBERHOLSTER, R.E., WESTRA, M.B. (1981) *The effectiveness of mineral admixture in reducing expansion due to alkali-aggregate reaction with malmesburry group aggregates*, Proceedings of the 5th International Conference on alkali-aggregate Reaction in Concrete, Cape Town, S252/31, 11p.

OHSAWA, S., ASAGA, K., GOTO, S., DAIMON, M. (1985) *Quantitative determination of fly ash in the hydrated fly ash-CaSO4.2H2O- Ca(OH)2 system*, Cement Concrete Research, Vol. 15, No. 2, pp. 357-366.

PALOMO, A., FERNÁNDEZ-JIMÉNEZ, A., KOVALCHUK, G., ORDOÑEZ, L. M., NARANJO, M. C. (2007) *Opc-fly ash cementitious systems: study of gel binders produced during alkaline hydration, Jr. Mt. Science, Vol. 42, No. 9, pp. 2958-2966.*

PAN, Z., CHEN, L., LU, Y., YANG, N. (2002) *Hydration products of alkali-activated slag red mud cementitious material*, Cement and Concrete Research, Vol. 32. No. 3, pp. 211-216.

PANDEY, S.P., SHARMA, R.L. (2000) *The influence of mineral additives on the strength and porosity of OPC mortar.* Cem. Concr. Res. Vol. 30, No. 1, pp. 19–23.

PAPADAKIS, V.G.(1999) *Experimental Investigation and Theoretical Modeling of Silica Fume Activity in Concrete.* Cement and Concrete Research. Vol. 29, no. 1, pp. 79 - 86.

PAPAYIANNI, J. (1987) *An investigation of the pozzolanicity and hydraulic reactivity of a high-lime fly ash.* Magazine of Concrete Research, Vol. 39, No. 138, pp.19-28.

PARADIS, G. (1998) *La Gestion des brasques usées au Canada*, Mémoire de Maîtrise, Sherbrooke, Qc., Université de Sherbrooke, 60 p.

PAUL, T. SEIKO, M. (1991) *Durability of Fluoride Glasses in Water.* J. Am. Cer. Soc., Vol. 74, No. 3, pp. 481-490.

PERRY, C., GILLOT, J.E. (1985) *Feasibility of using silica fume to control expansion due to alkali-aggregate reactions*, Durability of Building Materials, Vol. 3, pp. 133-146.

PETTERSON, K., (1992) *Effect of silica fume on alkali-silica expansion on mortar specimens*, Cement Concrete Research, Vol. 22, No. 1, pp. 15-22.

PIETERSEN, H.S., FRAAY, L.A., BIJEN, J.M. (1990) *Reactivity of fly ash at high pH*, Material Research Society Symp. Proc., Vol, 178, pp. 139-157.

POLLEY, C, CRAMER,S.N., CRUZ, R.U. (November 1998) *Potential for using waste glass in Portland cement concrete.* J. Mat. Civ. Eng., pp. 210-219.

POON, C.S., WONG, Y.L., LAM, L. (1997) *The influence of different curing conditions on the pore structure and related properties of fly-ash cement pastes and mortars. Constr Building Mater* Vol. 11, No. 7–8, pp. 383–393.

PRICE, W.H. (1975) *Pozzolans-A Review.* ACI, Materials Journal, Vol. 65, pp. 225-232.

PU, X. (1999) *Investigation on pozzolanic effect of mineral additives in cement and concrete by specific strength index.* Cement Concrete Research, Vol. 29, No. 6, pp. 951-955.

PUERTAS, F., MARTÍNEZ-RAMÍREZ, S., ALONSO, S., VÁZQUEZ, T. (2000) *Alkali-activated fly ash/slag cements Strength behaviour and hydration products*, Cement and Concrete Research, Vo. 30, No. 10, pp. 1625-1632.

PURDON, A.O. (1940) *The action of alkalis on blast furnace slag*, Journal Society of Chemical Industry, Vol. 59, No. 5, pp. 191-202.

QING-HUA, C., SARKAR, S.A. (1994) *A study of rheology and mechanical properties of mixed alkali activated slag pastes*, Advanced Cement Based Material, Vol. 1, pp. 178-184.

QING-HUA, C., TAGNIT-HAMOU, A., SAKAR, S.L. (1992) *Strength and microstructural properties of water glass activated slag*, GLASSER, F.P., YOUNG, G.J., YOUNG, J.F., MASON,

T.O., PRATT, P.L. (Eds), Advanced Cementitious Systems: Mechanisms and Properties, Pittsburg, Pennsylvania, Material Research Society Symposia Proc., Vol. 245, pp. 49-54.

RAMYAR, K., TOPAL, A., ANDIC, Ö. (2005) *Effects of aggregate size and angularity on alkali-silica reaction*, Cement and Concrete Research, Vol. 35, No. 11, pp. 2165-2169.

RANC, R., ISABELLE, H., CLEMENT, J.Y., SORRENTINO, D. (1994) *Reactivity Limits of application of the ASTM C 227 mortar bar test. Comparison with two other standards on alkali aggregate Cement*, Concrete and Aggregates, Vol. 16, No. 1, pp. 63-72

RAO, A.G.(2001) *Development of strength with age of mortars containing silica fume.* Cement and Concrete Research. Vol. 31, No. 8, pp. 1141 - 1146.

RICHARDSON, J.M., BIENACKI, J.J. (2002) *Stoichiometry of slag hydration with calcium hydroxide*, Journal of American Ceramic Society, Vol. 85, No. 4, pp.947-953.

RIVARD, P., BÉRUBÉ, M-A., OLLIVIER, J-P., BALLIVY, G. (2003) *Alkali mass balance during the accelerated concrete prism test for alkali-aggregate reactivity*, Cement and Concrete Research, Vol. 33, No. 8, pp. 1147-1153.

RODRIGUEZ-CAMACHO, R.E., URIBE-AFIF, R. (2002) *Importance of using the natural pozzolans on concrete durability.* Cement and Concrete Research, Vol. 32, No. 12, pp. 1854-1858.

ROGERS, C.A., HOOTON, R.D. (1991) *Reduction in mortar and concrete expansion with reactive aggregate due to alkali leaching*, Cement and Concrete Research, Vol. 13, No. 1, pp. 42-49.

ROY, D.M. (1989) *Hydration, microstructure, and chloride diffusion of slag-cement pastes and mortars.* Proceedings Third International Conference on the use of Fly Ash, Silica Fume, Slag and Natural Pozzolans in Concrete, Trondheim, Norway, Vol. 2,ACI SP 114-61, pp. 1265-1281.

ROY, D.M. (1999) *Alkali-activated cements. Opportunities and challenges*, Cement and Concrete Research, Vol. 29, No. 2, pp. 249-254.

SAINT-PIERRE, F., RIVARD, P., BALLIVY, G. (2007) Measurement of alkali-silica reaction progression by ultrasonic waves attenuation, Cement Concrete Research, Vol. 37, No. 6, pp. 948-956.

SAUMAN, Z. (1989) *Study of the possibilities of using industrial gypsum as a setting regulator for cement*, Proceedings of the Second International Symposium on cement and Concrete September 5-8, Beijing, China, pp. 328-337.

SCHMIDT, A., SAIA, W.H.F (1963) *Alkali-aggregate reaction tests on glass used for exposed aggregate wall panel work*, ACI, Material Journal, Vol. 60, pp. 1235-1236.

SHANBA, W., ZHONGHUI, Z. (1989) *Effect of fluorine on hydration of C3S*, Proceedings of the Second International Symposium on cement and Concrete September 5-8, Beijing, China, pp. 185-191.

SHAYAN, A., DIGGINS, R., IVANUSEC, I. (1996) *Long-term effectiveness of fly ash in preventing deleterious expansion due to alkali-aggregate reaction in concrete*, A. SHAYAN (Ed.), Proc. of the 10th International conference on Alkali-Aggregate Reaction in Concrete, Melbourne, Australia, 1996, pp. 538–545.

SHAYAN, A., QUICK, G.W., LANCUCKI, C.J. (1993) *Morphology, mineralogical and chemical feature of steam-cured concretes containing densified silica fume and various alkali levels*, Advaces in Cement Research, Vol. 5, pp. 151-162.

SHAYAN, A., XU, A. (2004) *Value-added utilisation of waste glass in concrete*, Cement and Concrete Research, Vol. 34, No. 1, pp. 81–89.

SHEHATA, M.H., THOMAS, D.A. (2002) *Use of ternary blends containing silica fume and fly ash to suppress expansion due to alkali-silica reaction in concrete*, Cement and Concrete Research, Vol. 32, No. 3, pp. 341-349.

SHI, C. (1992) Activation of natural pozzolans fly ashes and blast furnace slag, Ph.D. Thesis, Department of Civil Engineering, the University of Calgary, Calgary, Alta., Canada.

SHI, C. (2001) *An overview on the Activation of Reactivity of Natural Pozzolans.* Con. J. Civ. Eng. Vol. 28, pp. 778-786.

SHI, C., DAY, R.L. (1995) *Acceleration of the reactivity of fly ash by chemical activation*, Cement and Concrete Research, Vol. 25, No. 1, pp. 15-21.

SHI, C., DAY, R.L. (1996a) *Selectivity of Alkaline Activators for the Activation of Slags*, Cement, Concrete and Aggregates, Vol. 18, No. 1, pp. 8-14.

SHI, C., DAY, R.L. (1996b) *Some factors affecting early hydration of alkali-slag cements*, Cement and Concrete Research, Vol. 26, No. 3, pp. 439-447.

SHI, C., DAY, R.L. (1993a) Acceleration of strength gain of lime-natural pozzolan cements by thermal activation. Cement and concrete research, Vol. 23,No. 4 pp.824-832

SHI, C., DAY, R.L., (1999) *Early strength development and hydration of alkali-activated blast furnace slag/fly ash blends*, Advances in Cement Research, *Vol.* 11, No. 4, pp.189–196.

SHI, C., DAY, R.L., WU, X., TANG, M. (1992) *Comparison of the microstructure and performance of alkali-slag and Portland cement pastes*, Proceedings of the 9th International Congress on the Chemistry of Cement, New Delhi, India, Vol. III, Theme II B, pp. 298-304.

SHI, C., KRIVENKO, P.V., ROY, D. (2006) *Alkali-activated cements and concretes*, Great Britain, 1 st Edition, Taylor and Francis Group, 376 p.

SHI, C., LI, Y. (1989) *Investigation on some factors affecting the characteristics of alkali-phosphorus slag cement*, Cement and Concrete Research, Vol. 19, pp. 527-533.

SHI, C., WU, Y., RIEFLER, C., WANG, H. (2005) *Characteristics and pozzolanic reactivity of glass powders*, Cement and Concrete Research, Vol. 35, No. 5, pp. 987-993.

SIBBICK, R.G., NIXON, P.J.(2000) *Investigation into the effect of metakaolin as a cement replacement material in ASR reactive concrete.* Proceedings of 11th International Conference on Alkali-Aggregate Reaction in Concrete, Edited by BÉRUBÉ, M.A., Fournier, B., Durand, B., Québec city, Qc., Canada.

SIVASUNDARAM, V., MALHOTRA, V.M. (1992) *Properties of concrete incorporating low quantity of cement and high volumes of ground granulated slag, ACI* Materials Journal. Vol. 89, No. 6, pp. 554 - 563.

SLOTA, R.J. (1987) *Utilization of water glass as an activator in the manufacturing of cementitious materials from waste by-products.* Cement Concrete Research, Vol. 17, No. 5, pp. 703-708.

SNYDER, K.A., FENG, X., KEEN, B.D., MASON, T.O. (2003) Estimating the electrical conductivity of cement paste pore solutions from OR-, K+ and Na + concentrations, Cement and Concrete Research Vol. 33, pp. 793- 798.

SONG, S., JENNINGS, H.M. (1999) *Pore solution chemistry of alkali-activated ground granulated blast furnace slag*, Cement Concrete Research, Vol. 29,No. 2, pp. 159-170.

STANTON, T.E. (1940) *Expansion of concrete through reaction between cement and aggregate.* Proceedings of the American Society of Civil Engineering, Vol. 66, No. 10, pp. 1781-1811.

LANE, D.L. (2000) *Preventive measures for alkali-silica reactions used in Virginia, USA*, The 11Th International Conference on Alkali Aggregate Reaction in Concrete, Québec (Canada), June 2000. BÉRUBÉ, M.A.(Ed.), pp. 693-702.

SUGAMA, T. (2007) *Advanced cements for geothermal wells*, Final report, Report No. BNL-77901-2007IR, July 2006, Energy Resources Division Energy Science and Technology Department, Brookhaven National Laboratory, Upton, NY, Prepared for The US Department of Energies Office of Geothermal Technologies, Washington, D.C., pp.1-80.

TAGNIT-HAMOU, A., LALDJI, S. (2004) Development of a new binder using thermally-treated spent pot liners from aluminium smelters, ACI SP219-11, March, pp.145-162.

TALLING, B., BRANDSTETS, J. (1989) *Present state and future of alkali-activated slag concrete*, Proceedings 3rd international Symposium on Fly ash, Silica Fume, Slag, and Natural Pozzolans in Concrete, Trondheim, Norway, ACI SP-114-74, MALHOTRA, V.M. (Ed.), Vol. 2, pp. 1519-1545.

TEMIZ, H., KARAKECI, A.Y. (2002) *An investigation on microstructure of cement paste containing fly ash and silica fume*, Cement and Concrete Research, Vol. 32, No. 7, pp. 1131-1132.

THOMAS, J. J., CHEN, J.J. JENNINGS M.H. (2003) *Ca-OH bonding in the C-S-H gel phase of tricalcium silicate and white Portland cement pastes measured by inelastic neutron scattering*, Chem. Mater. Vol. 15, pp. 3813-3817.

THOMAS, M.D.A. (1996) *Field studies of fly ash concrete structures containing reactive aggregates*, Magazine of Concrete Research, Vol. 48, No. 177, pp. 265-279.

THOMAS, M.D.A., BLESZYNSKI, R.F. (2000) *The use of silica fume to control expansion due to alkali-aggregate reactivity in concrete- A review*. Material Science of Concrete(Edited by SKANLY AND MINDESS), Vol. 6, American ceramics Society.

THOMAS, M.D.A., NIXON, P.J., PETTIFER, K. (1991) *The effect of pulverized fuel ash with a high total alkali content on alkali-silica reaction in concrete containing natural U.K. aggregate*, 2nd International Conference on the Durability of Concrete, MALHOTRA, V.M. (Ed.), ACI Sp-126, Vol. 11, American Concrete Institute, Detroit, pp. 919-940.

TOUTANJI, H.A., BAYASI, Z. (1999) *Effect of Curing Procedures on Properties of Silica Fume Concrete*, Cement and Concrete Research, Vol. 29, No. 4, pp. 497 - 501.

UCHIKAWA, H., OKOMUR, T. (1993) *Binary and ternary components blended cements in : mineral admixtures in cement and concrete*, Edited by GHOSH, S.N., HARSH,S., ABI Books Pvt. Ltd. New Delhi, Vol.4, pp. 1-83.

VAN AARDT, J.H.P., VISSER, S. (1977) *Formation of hydrogarnets: Calcium hydroxide attack on clays and feldspars*, Cement and Concrete Research, Vol. 7, No.1, pp. 39-44.

WANG S.D., SCRIVENER, K.L, PRATT, P.L. (1994) *Factors affecting the strength of alkali-activated slag*, Cement and Concrete Research, Vol. 24, No. 6, pp. 1033-1043.

WANG, H, GILLOT, J.E. (JULY 1992) *Combined effect of an air-entraining agent and silica fume on alkali-silica reaction*, The 9th International Conference on Alkali-aggregate Reaction in Concrete, London (UK), Concrete Society, 27-31 July 1992, Conference papers Vol. 2, pp. 1100-1106.

WANG, S.D. (1991) *Review of recent research on alkali-activated concrete in China*, Magazine of Concrete Research, Vol. 43, No. 154, pp. 29-35.

WANG, S.-D. (2000) *Alkali-Activated Slag: Hydration Process and Development of Microstructure*, Advances in Cement Research, Vol. 12, No. 4, pp.163-172.

WANG, S.D., SCRIVENER, K.L. (1995) *Hydration products of alkali activated slag cement*, Cement and Concrete Research, Vol. 25, No. 3, pp. 561-571.

WENG, J.K., LANGAN, B.W., WARD, M.A. (1997) *Pozzolanic reaction in Portland cement, silica fume, and fly ash mixtures*, Canadian journal of civil engineering., Vol. 24, pp. 754-760.

WIGUM, B.J., FRENCH, W.J., HOWARTH, R.J., HILLS, C. (1997) Accelerated Tests for Assessing the Potential Exhibited by Concrete Aggregates for Alkali Aggregate Reaction, Cement and Concrete Composites, Vol. 19, No. 5/6, pp. 451-476.

WILLIAMS, P.J., BIERNACKI, J.J., WALKER, L.R., MEYER, H.M, RAWN, C.J., BAI, J. (2002) *Microanalysis of alkali-activated fly ash–CH pastes*, Cement and Concrete Research, Vol. 32, No. 6, pp. 963-972.

WU, X., JIANG, W., ROY, D.M. (1990) *Early activation and properties of slag cement,* Cement and Concrete Research, Vol. 20, No. 6, pp. 961-974.

XINCHENG, P. (1992) *Structure and properties of high strength alkali slag concrete,* Proceedings of the fourth International Conference on fly ash, slag, and natural pozzolans in concrete, Istanbul, Turkey, ACI SP-132, pp. 689-707.

YAMAMOTO, T., KANAZU, T. (2000) *Chemical assessment method for the preventive effect of fly ash on alkali-silica reaction*, Proceedings of 11th International Conference on AAR in Concrete, Québec (Canada), BÉRUBÉ, M.A. (Ed.).

ZHANG, C., WANG, A., TANG, M., WU, B., ZHANG, N. (1999*) Influence of aggregate size and aggregate size grading on ASR expansion*, Cement and Concrete Research, Vol. 29, No.9, pp.1393-1396.

ZHAO, F.-Q., NI, W., WANG, H.-J., LIU, H. GLASSER, F.P., MARR, J. (2007) *Activated fly ash/slag blended cement*, Resources, Conservation and Recycling, Vol. 52, No. 2, pp. 303-313.

Appendices

Appendix 5.A Alkali-Activated GF binder

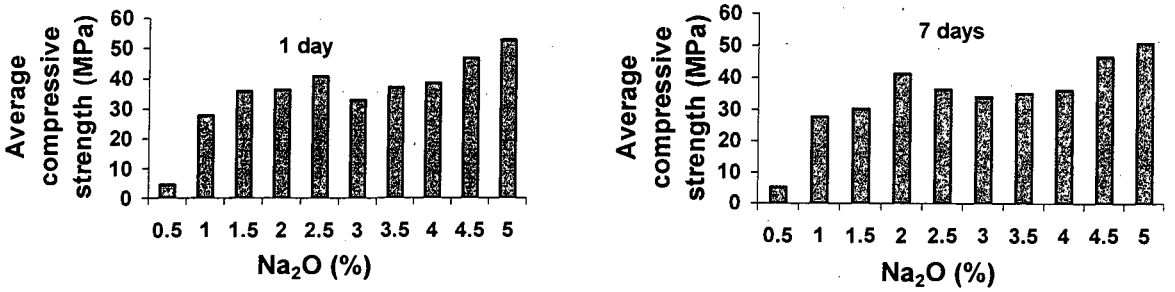

Figure 5.A 1 Compressive strengths of 1 and 7-day samples activated at 50°C

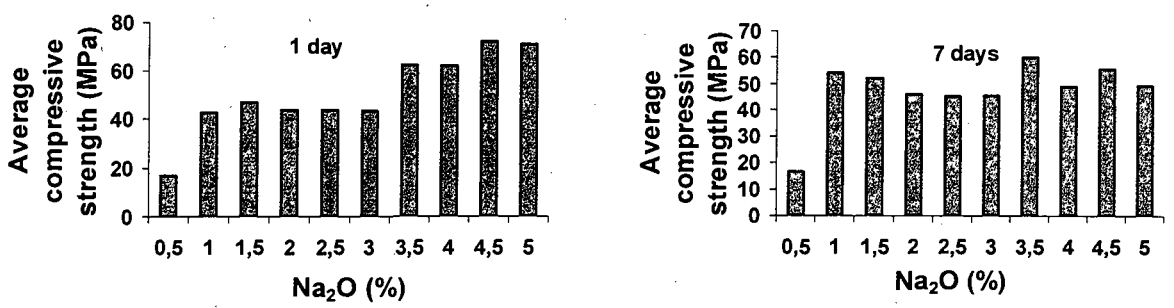

Figure 5.A 2 Compressive strengths of 1 and 7-day samples activated at 60°C

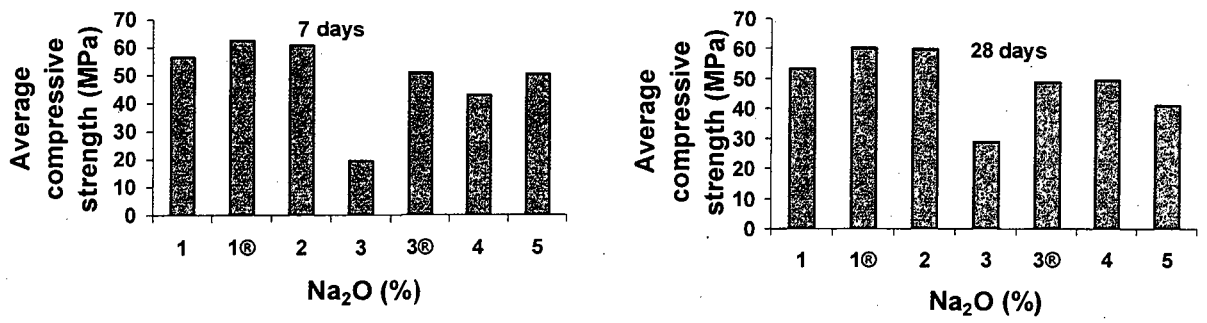

Figure 5.A 3 Compressive strengths of 7 and 28-day samples activated at 80°C

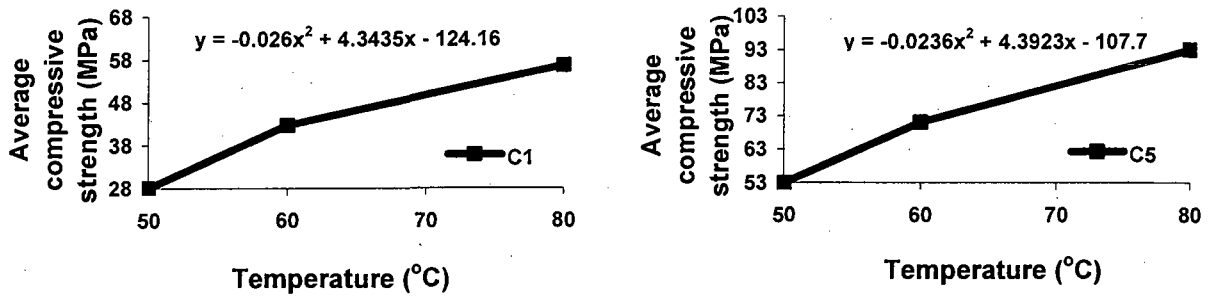

Appendices

Appendix 5.A Alkali-Activated GF binder

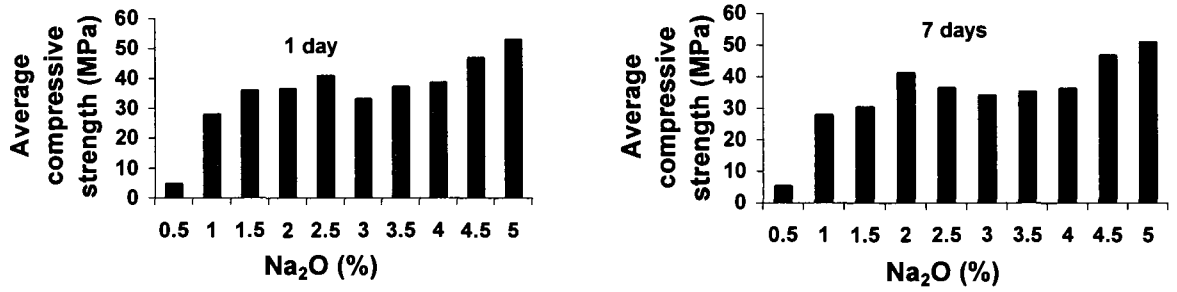

Figure 5.A 1 Compressive strengths of 1 and 7-day samples activated at 50°C

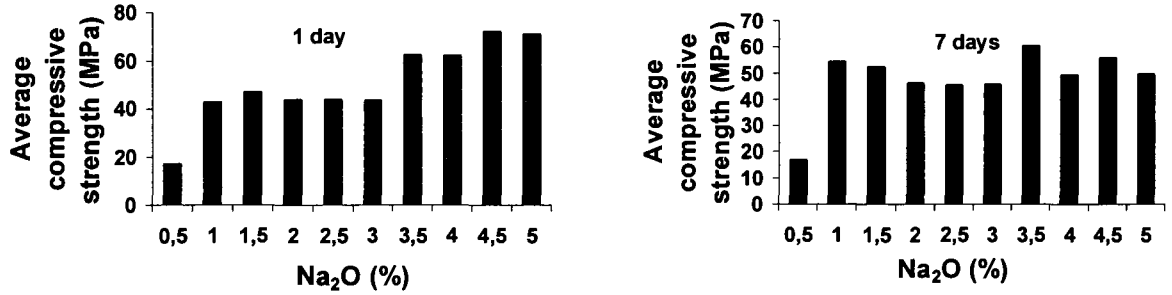

Figure 5.A 2 Compressive strengths of 1 and 7-day samples activated at 60°C

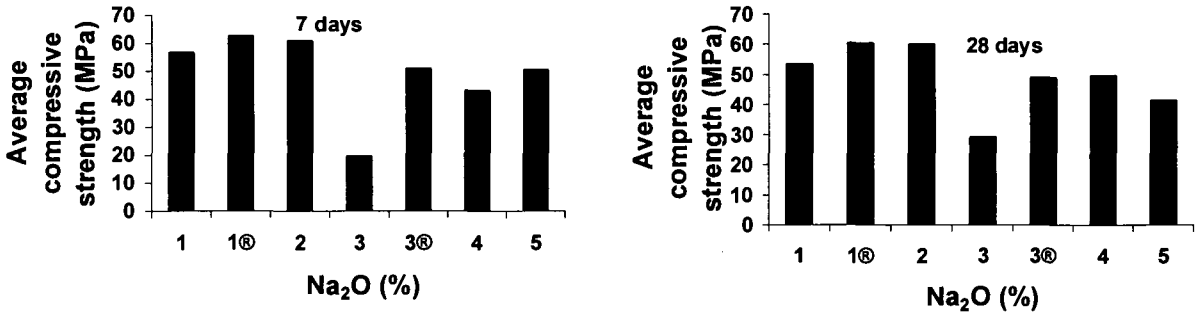

Figure 5.A 3 Compressive strengths of 7 and 28-day samples activated at 80°C

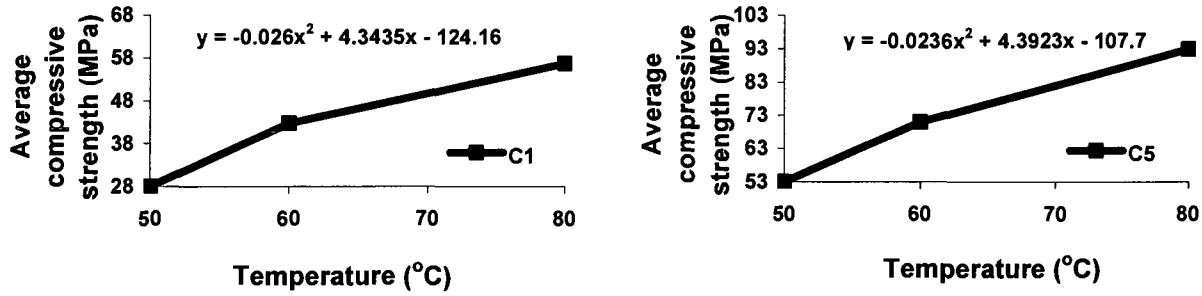

Figure 5.A 4 Rate of compressive strength gain at C1 and C5 concentrations

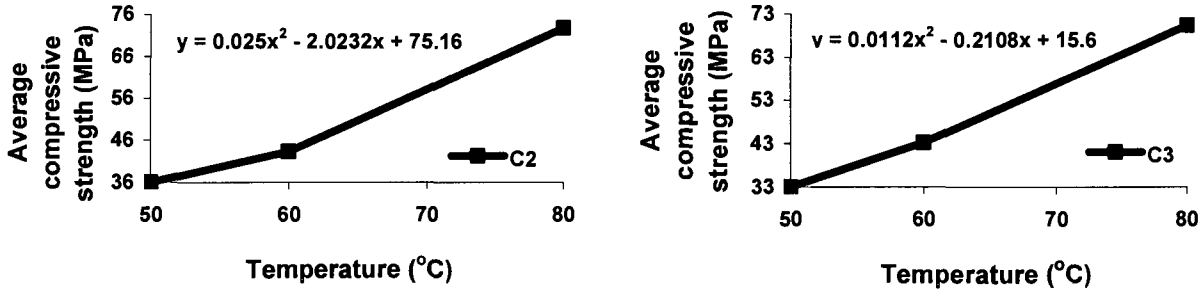

Figure 5.A 5 Rate of compressive strength gain at C2 and C3 concentrations

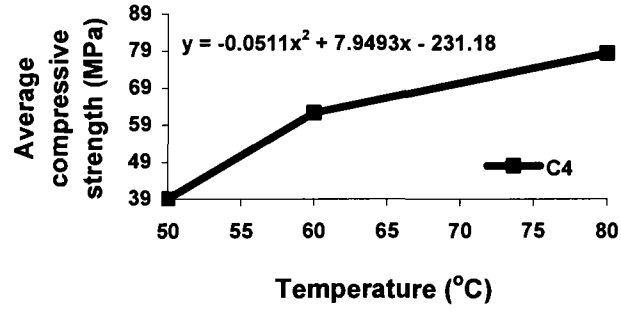

Figure 5.A 6 Rate of compressive strength gain at C4 concentration

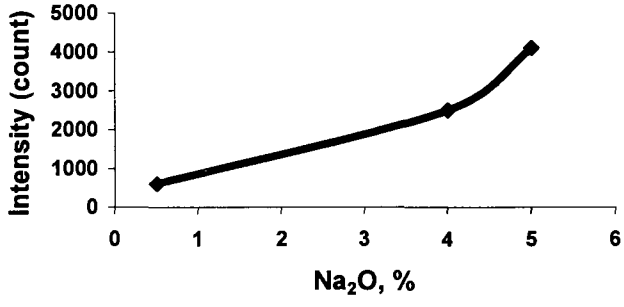

Figure 5.A7 Intensity of silica as a function of NaOH concentration

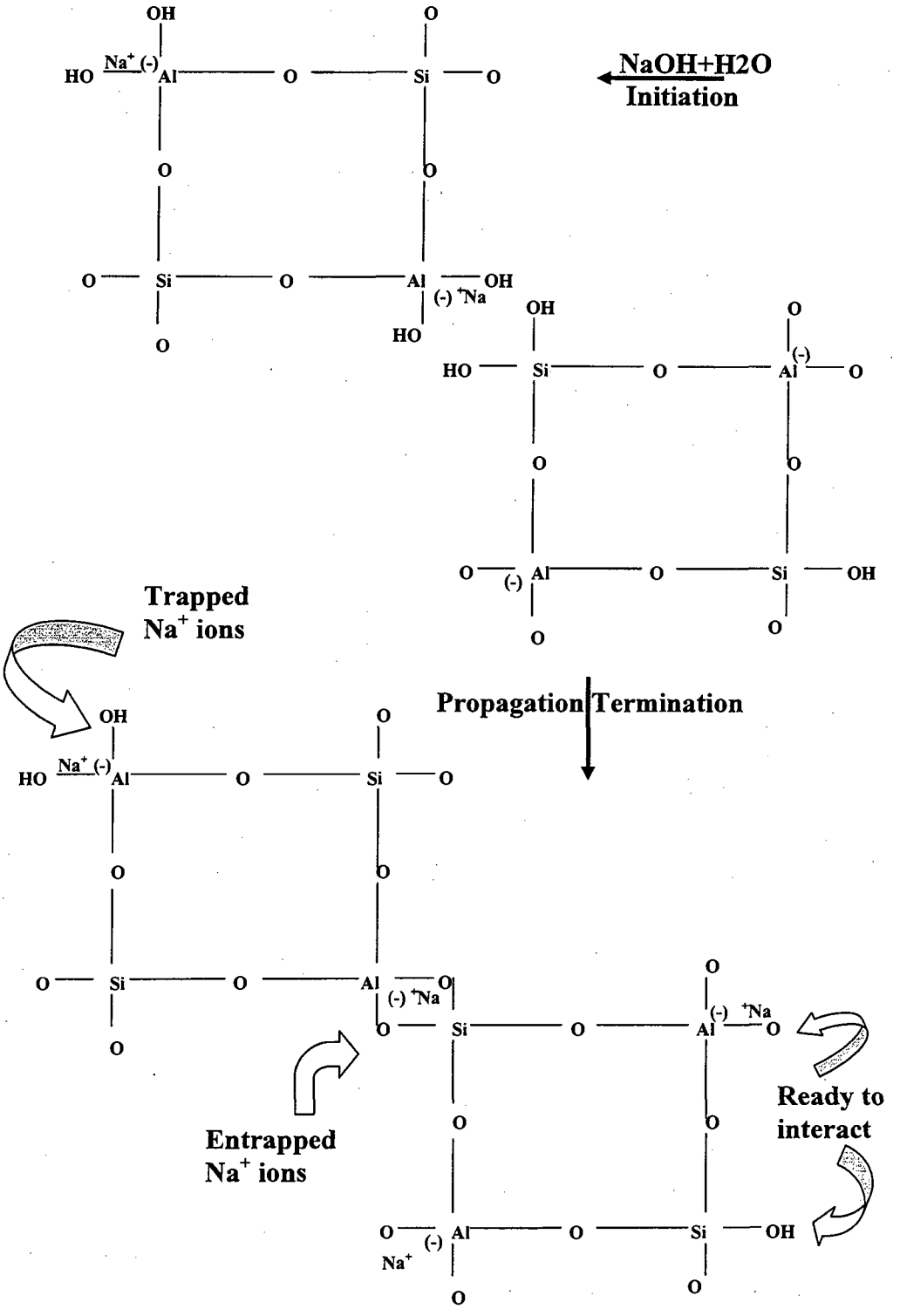

Figure 5.A 9 Formation of alumino-silicate hydrate polymer

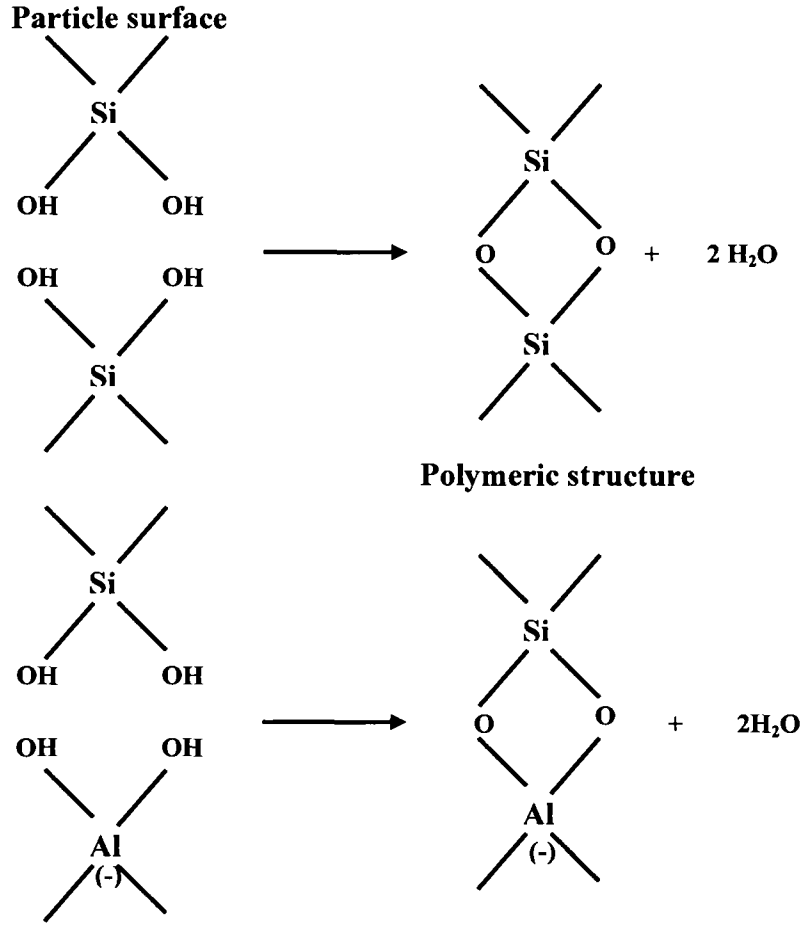

Figure 5.A 8 Formations of new polymeric structures

Figure 5.A 9 Formation of alumino-silicate hydrate polymer

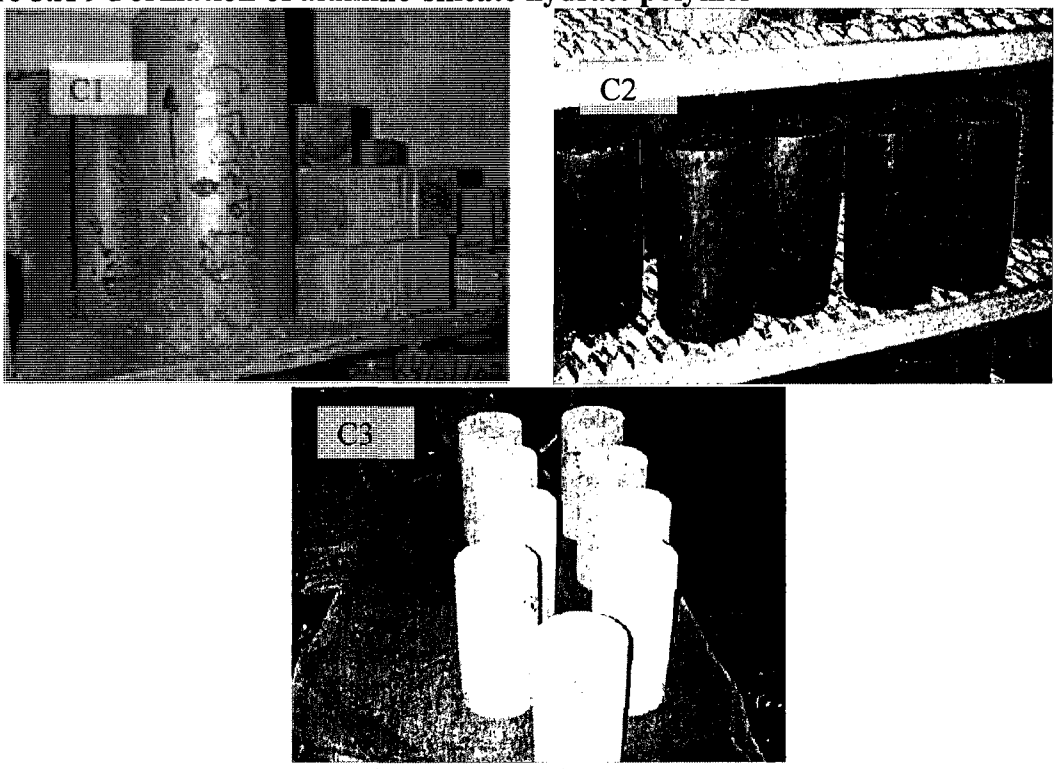

Figure 5.A 10 Activated C1, C2, and C3 concrete mixtures

5. B A proposal for a new method to determine the pozzolanic activity

A new method for quantitative determination of pozzolanic activity using XRD analysis was established. In this method different calibration curves of the dry mixtures of different concentrations of hydrated lime (CH) with fixed amount of GF at different temperatures (20-80°C), based on the intensities of the mean peak of CH, were drawn. Then, to these dry GF-CH mixtures known amount of water has to be added followed by homogeneous mixing and curing at a temperature equivalent to the temperature used in creating the calibration curve for 24 hours. Consquently, the mixture has to be ground and weighed followed by vacuum and oven dry to avoid carbonation, to remove humidity and to be weighed again to calculate free water. At that time, final grinding is necessary to carry out another XRD analysis. From which the intensity of the remaining CH is calculated and the amount of unreacted CH can be estimated by extrapolation from the calibration curve (CH-intensity) corresponding to the accelerating temperature. This method was tested using different cementitious materials and

calibrated with different differential and thermogravimetrical methods (DTA and TGA). It was found that this method is reliable and it gives reproducible results. This method and its results will be published in detail in different papers.

Appendix 6A. Concrete Prism Test (CPT) CSA A23.2-14A

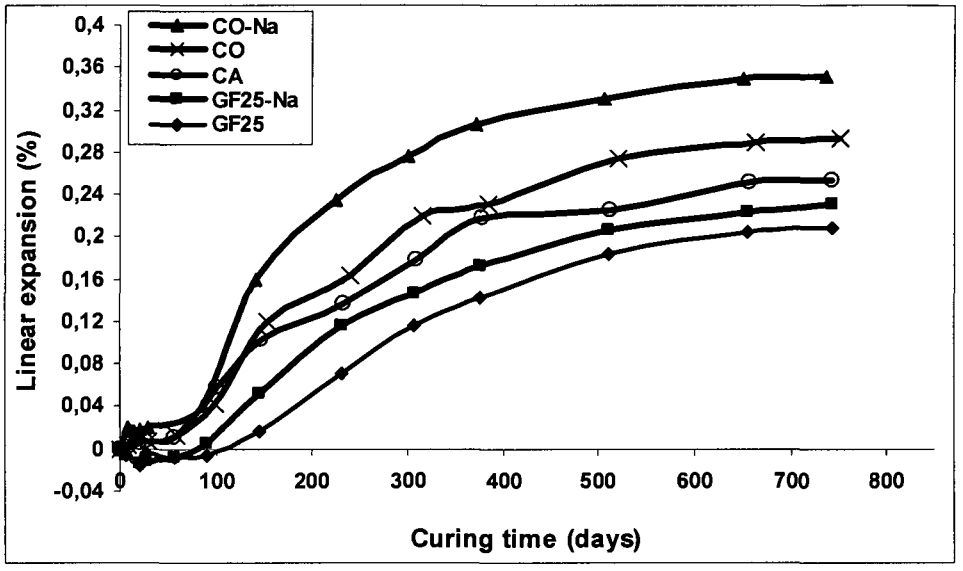

Figure 6.A 1 Binary concrete mix after 2 years containing 25%GF with and without alkali

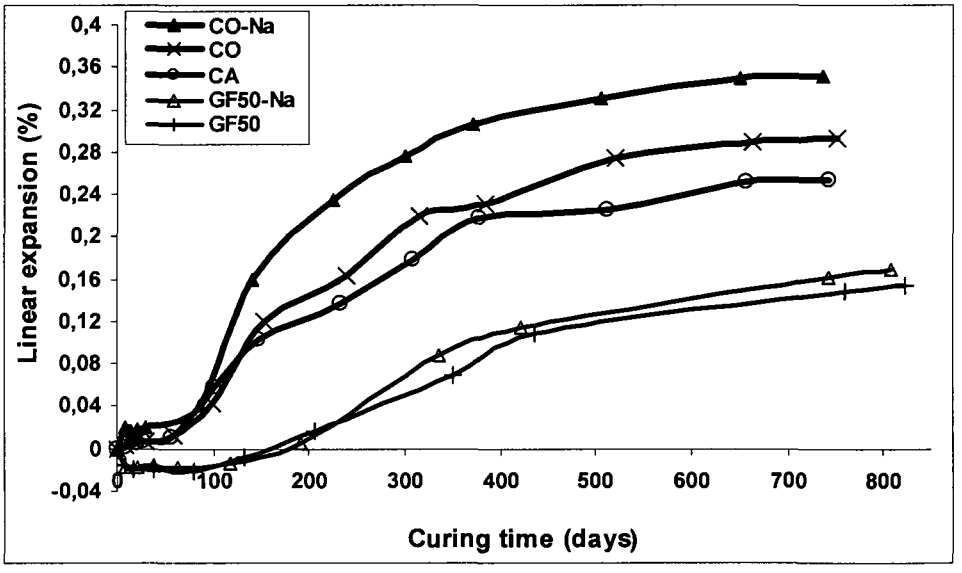

Figure 6.A 2 Binary concrete mix after 2 years containing 50%GF with and without alkali

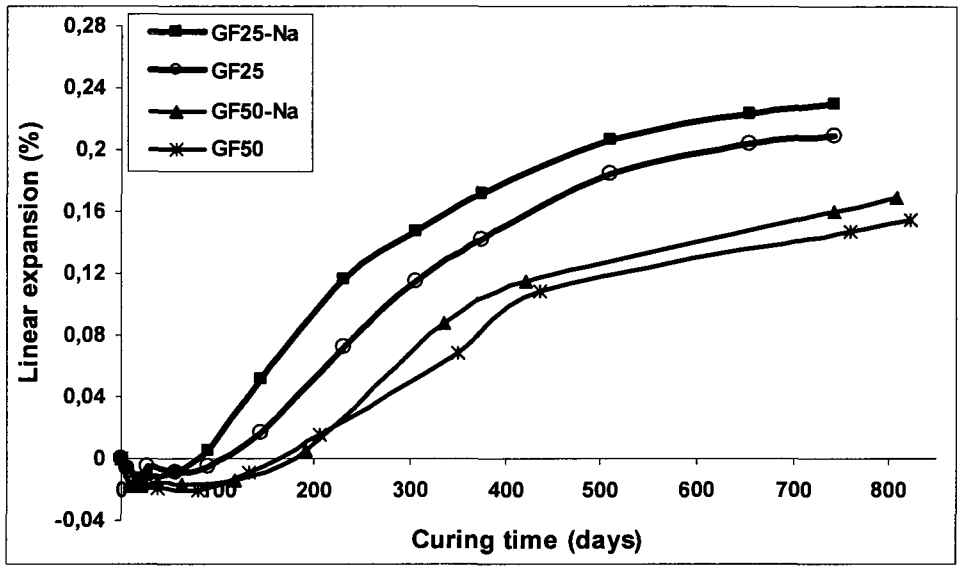

Figure 6.A 3 Comparison between 25 and 50 % binary GF concrete mix with and without alkali

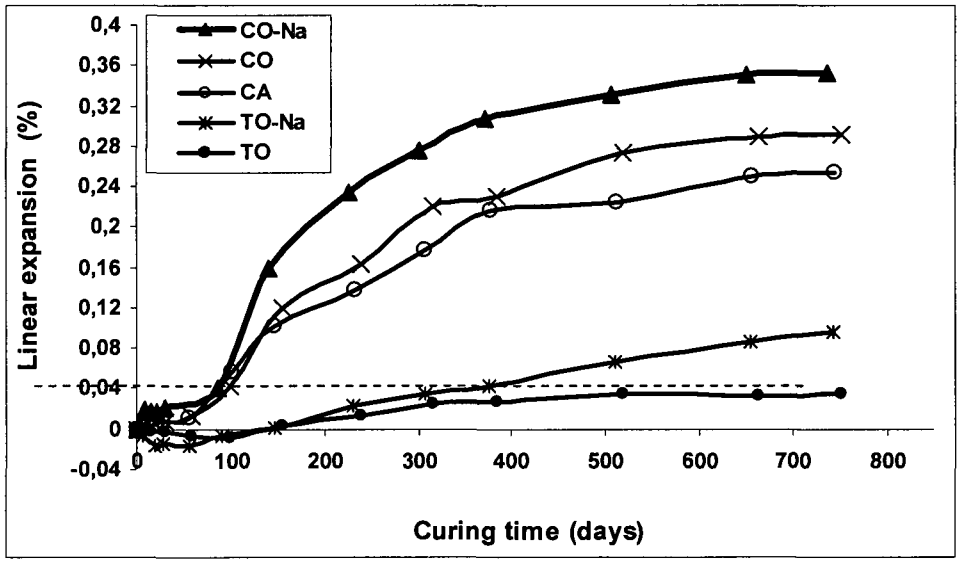

Figure 6.A 4 Comparison between control and GF-ternary concrete mixtures with and without alkali

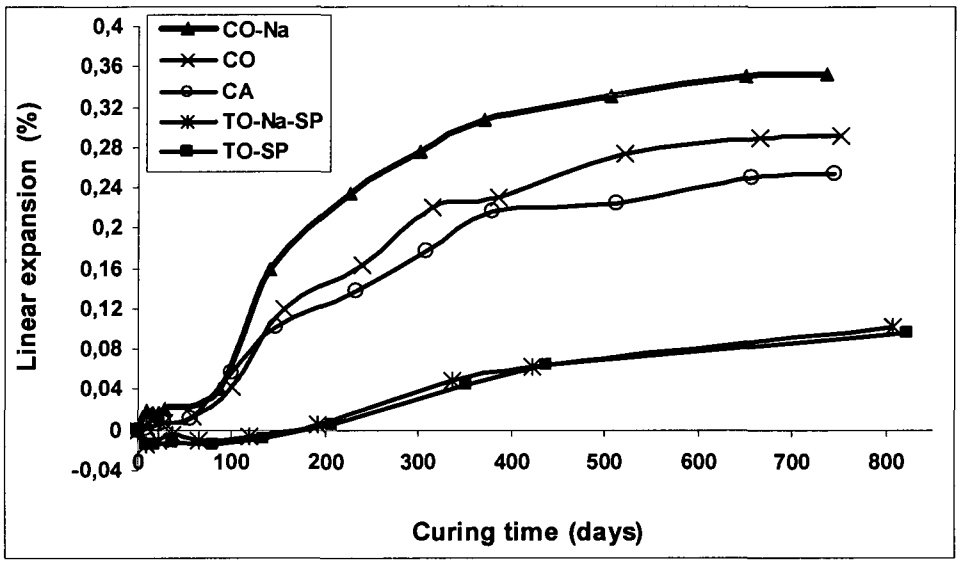

Figure 6.A 5 Comparison between control and GF-ternary concrete mixtures with and without both alkali and superplasticizer

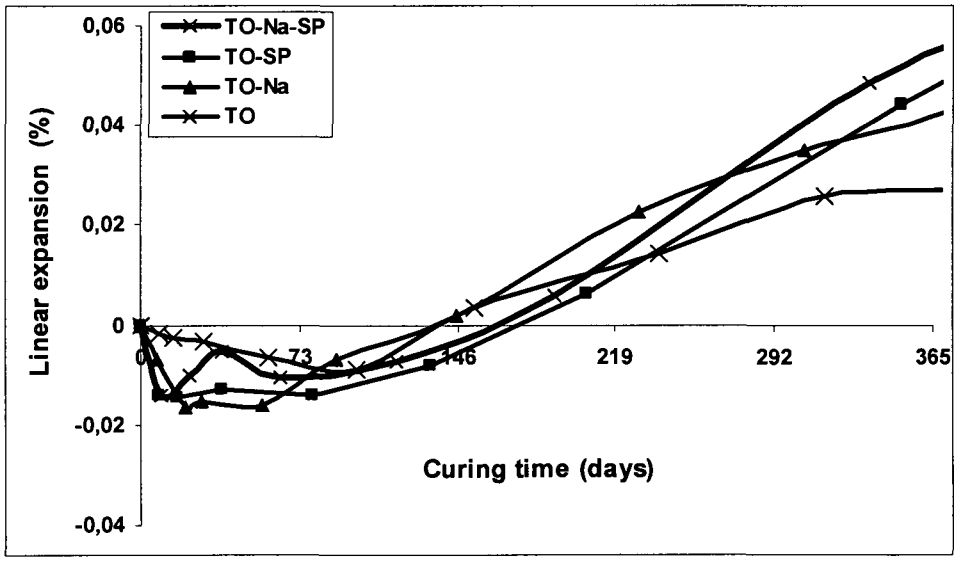

Figure 6.A 6 Comparison between control and GF-ternary concrete mixtures with and without both alkali and superplasticizer after one year

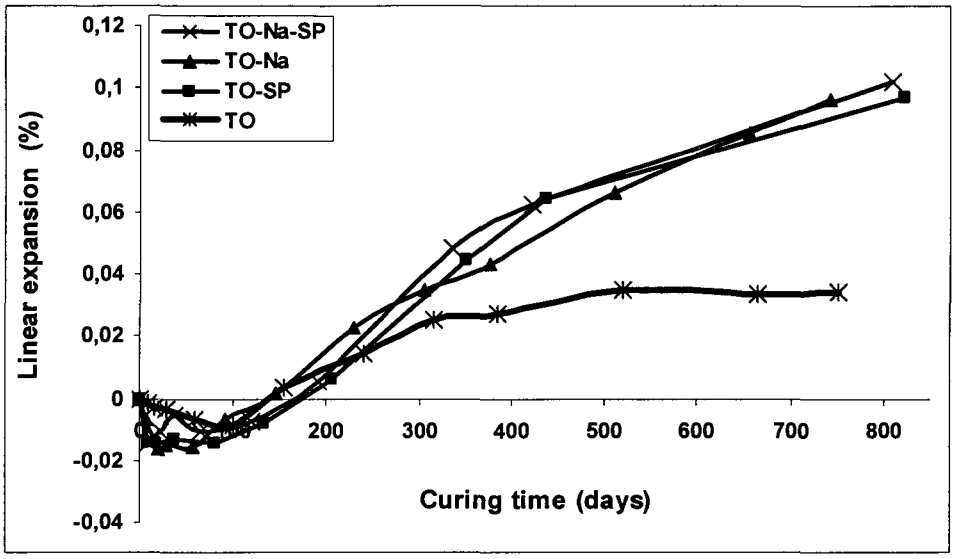

Figure 6.A 7 Comparison among control and GF-ternary concrete mix with and without both alkali and superplasticizer after two years

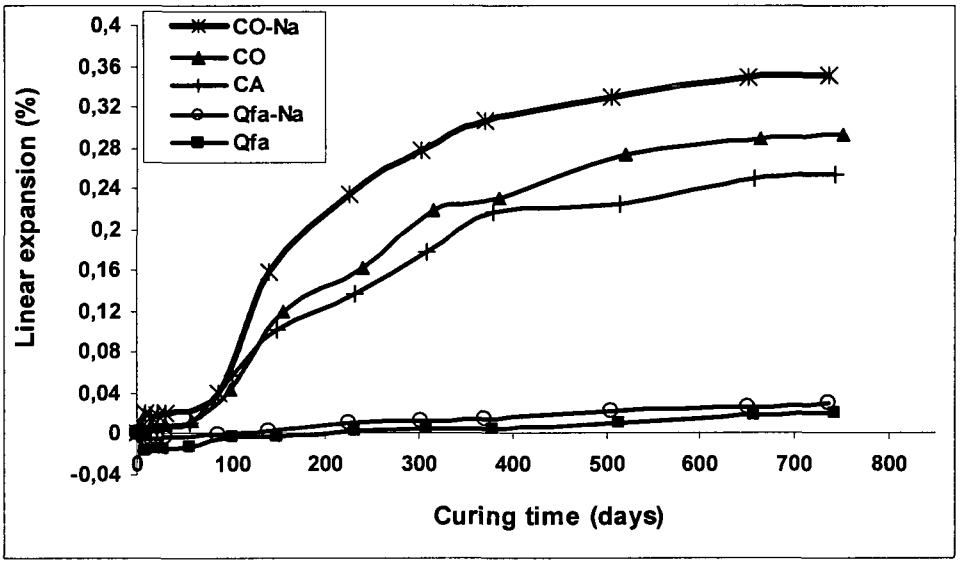

Figure 6.A 8 Comparison between control and GF-Pfa quaternary concrete mixtures with and without alkali after two years

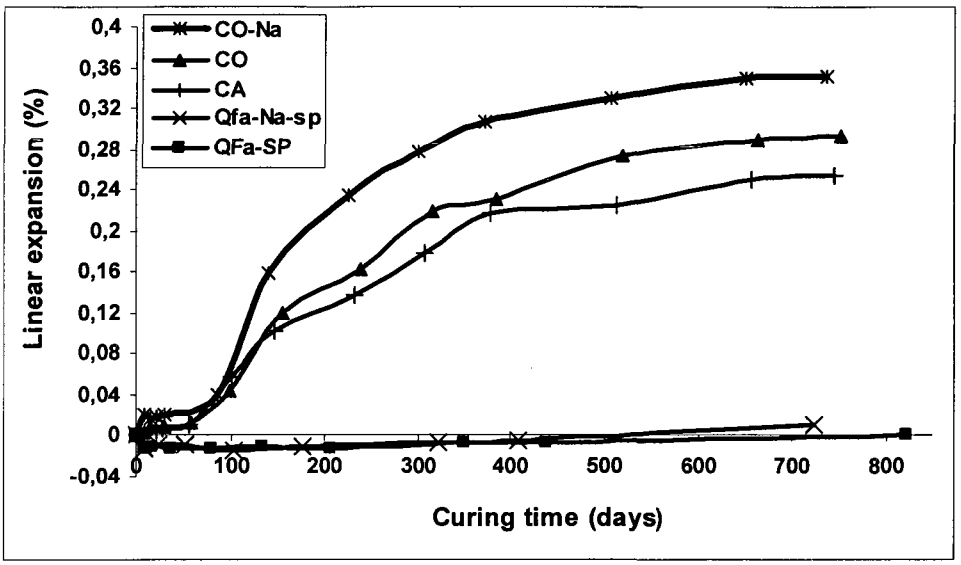

Figure 6.A 9 Comparison between control and GF-Pfa quaternary concrete mixtures with and without both alkali and superplasticizer after two years

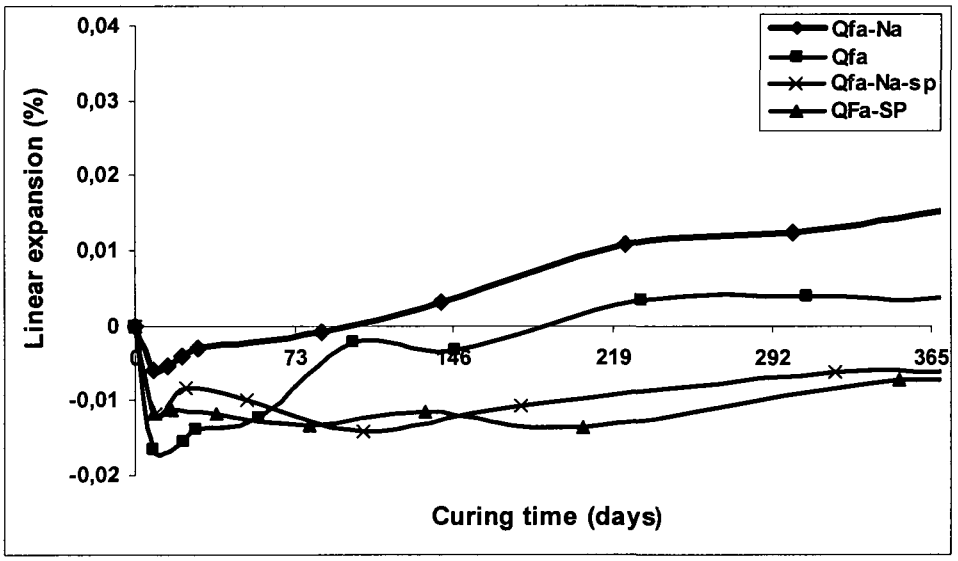

Figure 6.A 10 Comparison between GF-Pfa quaternary concrete mixtures with and without both alkali and superplasticizer, after one year

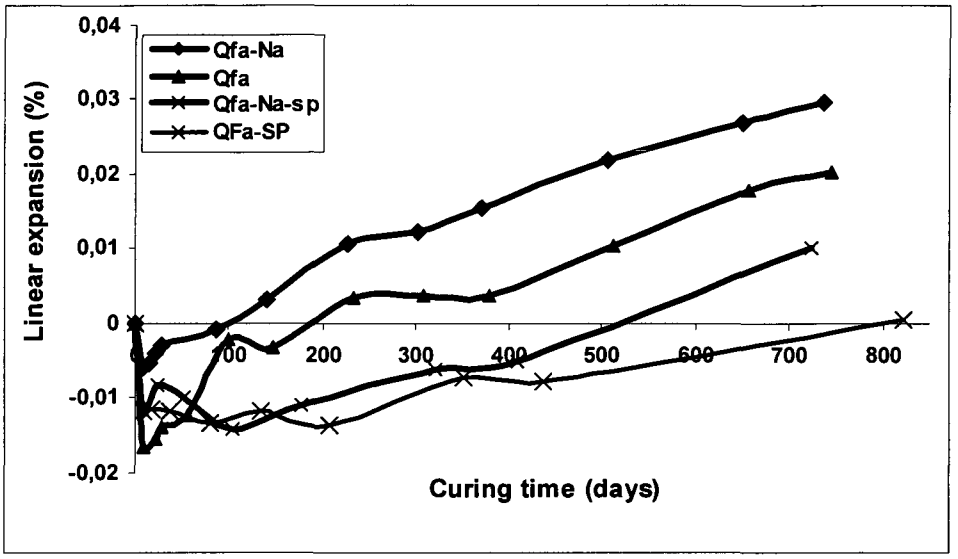

Figure 6.A 11 Comparison between GF-Pfa quaternary concrete mixtures with and without both alkali and superplasticizer, after two years

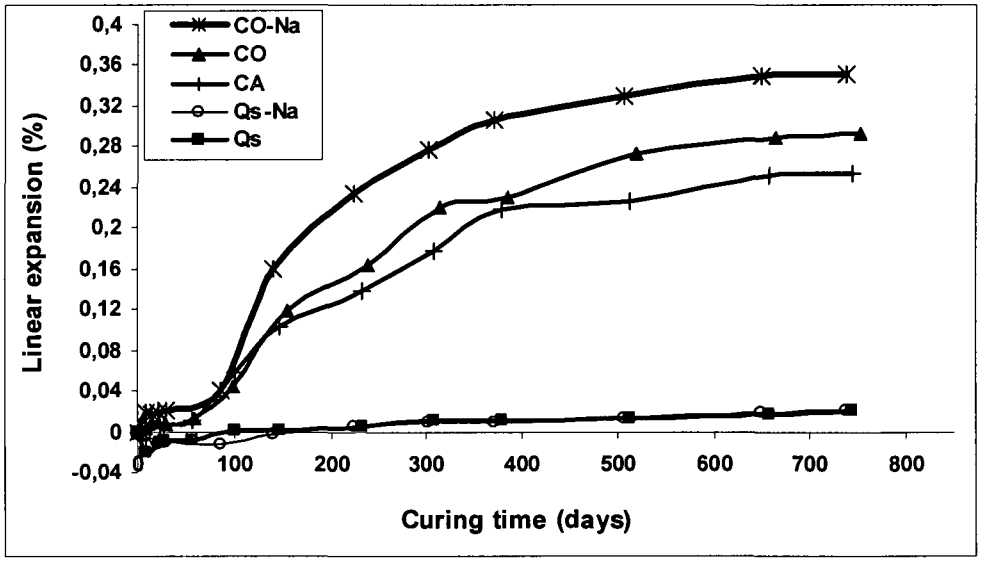

Figure 6.A 12 Comparison between GF-slag quaternary concrete mixtures with and without alkali, after two years

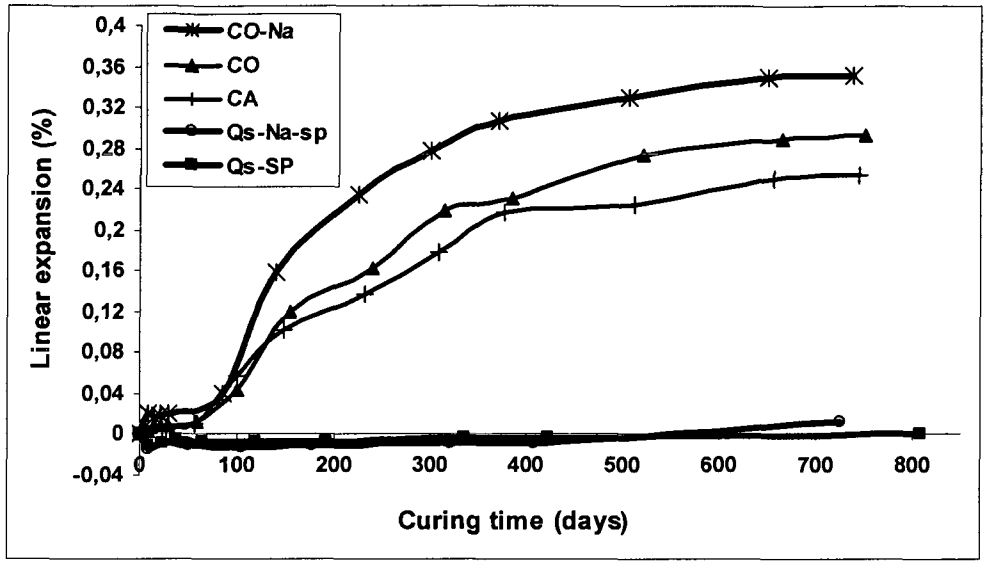

Figure 6.A 13 Comparison between GF-slag quaternary concrete mixtures with and without both alkali and superplasticizer, after two years

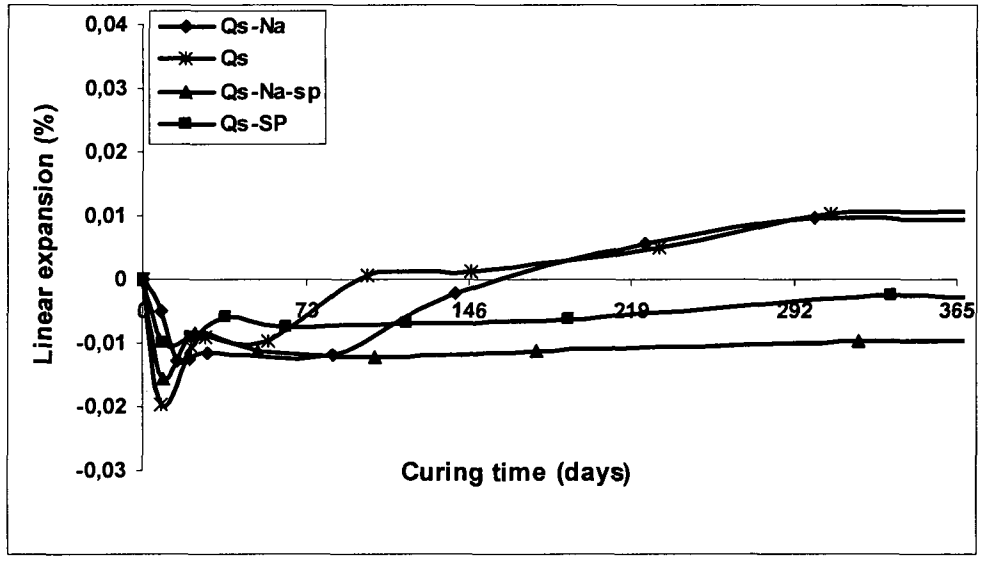

Figure 6.A 14 Comparison between GF-slag quaternary concrete mixtures with and without both alkali and superplasticizer, after one year

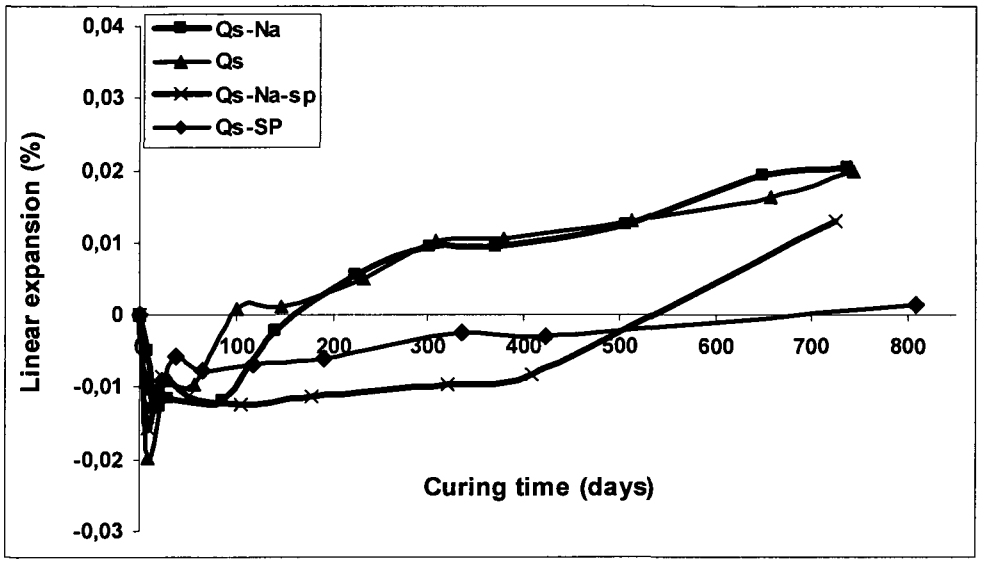

Figure 6.A 15 Comparison between GF-slag quaternary concrete mixtures with and without both alkali and superplasticizer, after two years

Appendix 6.B Pore-size distribution and microstructure analysis

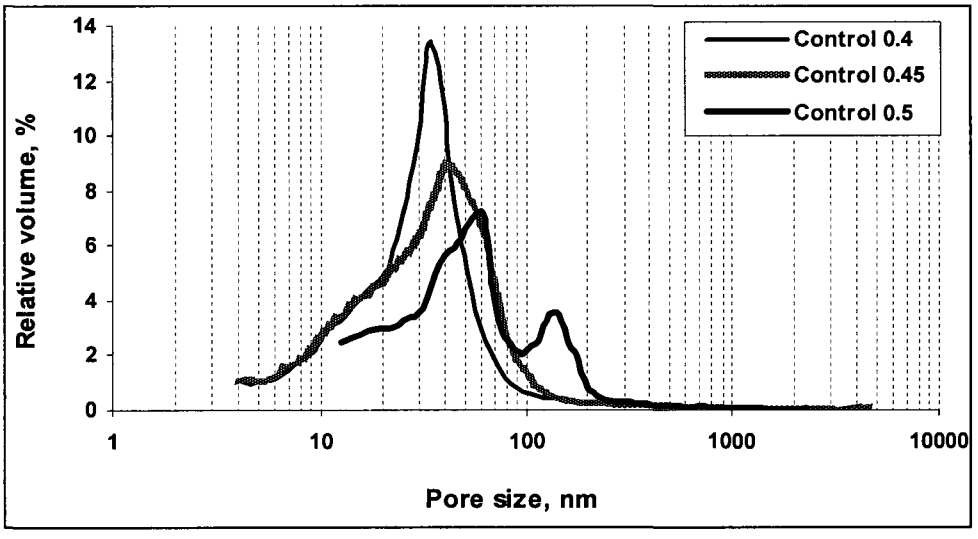

Figure 6.B 1 Pore size distribution as a function of relative volume

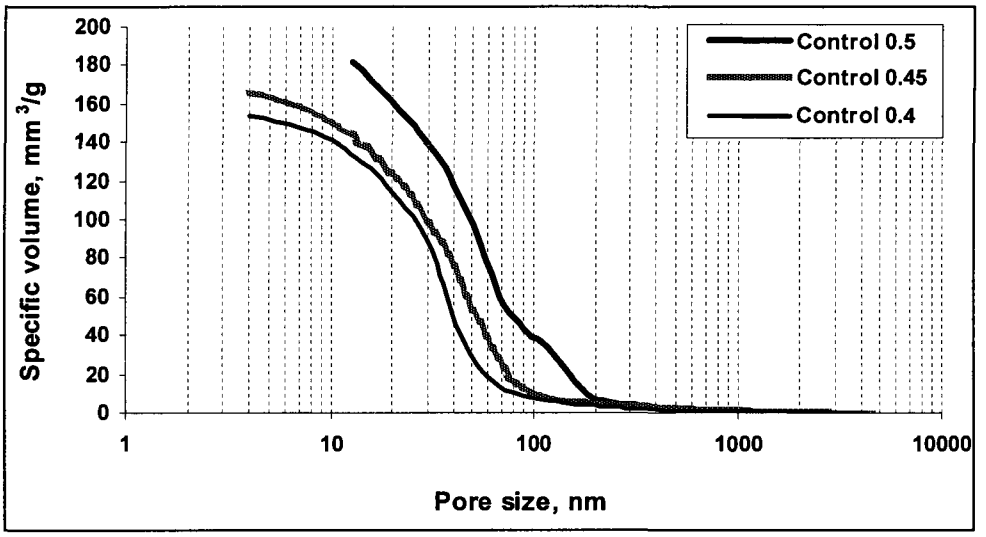

Figure 6.B 2 Pore size distribution as a function of specific volume

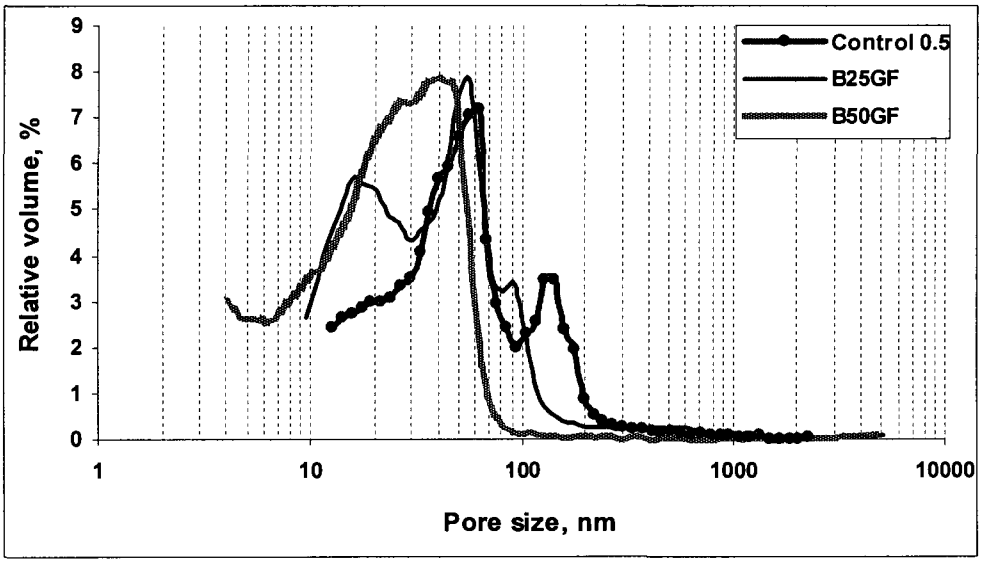

Figure 6.B 3 Pore size distribution as a function of relative volume

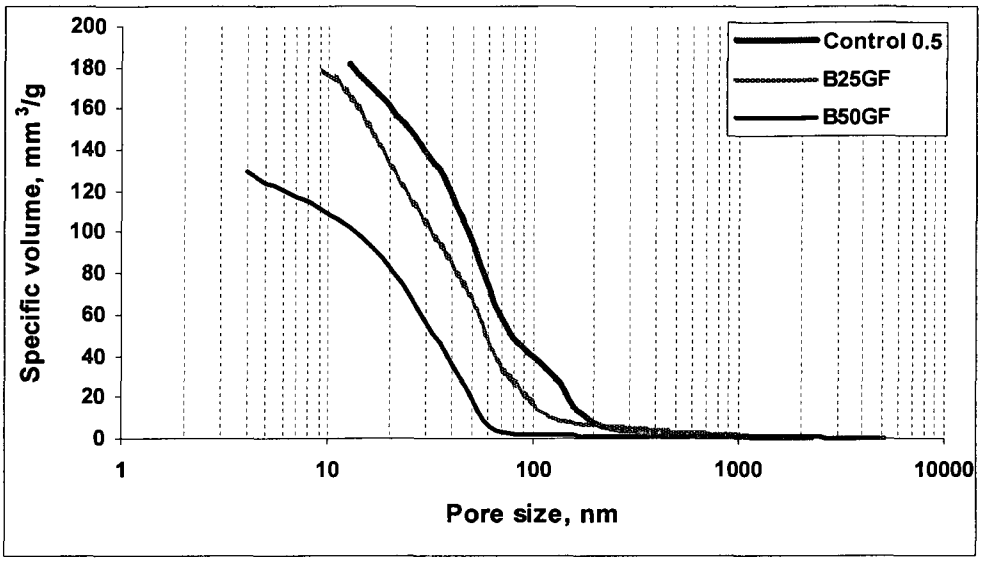

Figure 6.B 4 Pore size distribution as a function of specific volume

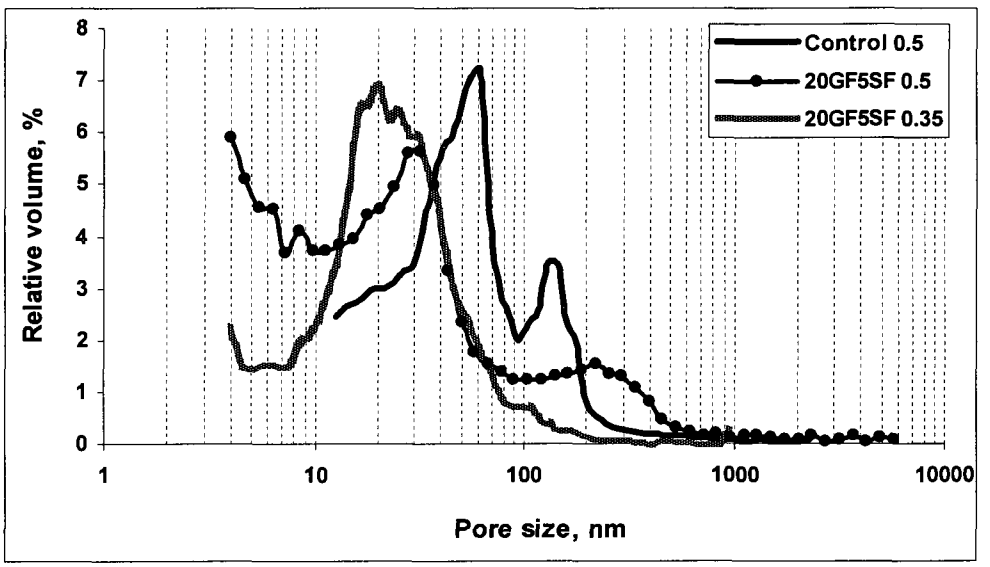

Figure 6.B 5 Pore size distribution as a function of relative volume

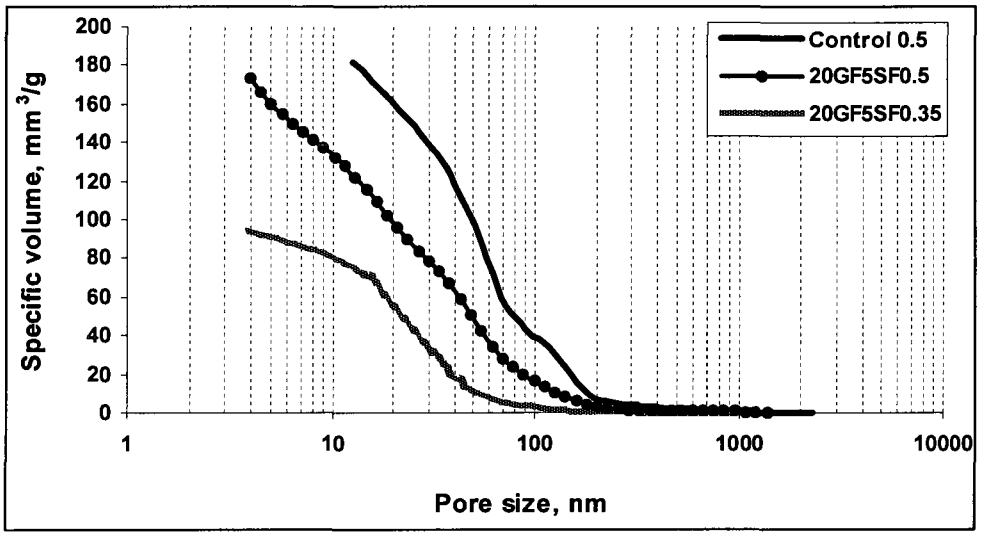

Figure 6.B 6 Pore size distribution as a function of specific volume

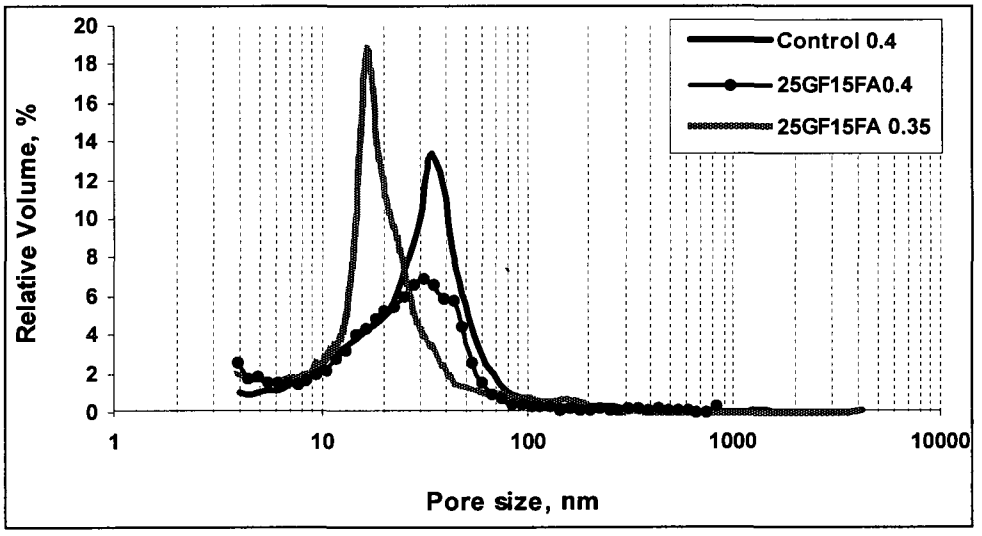

Figure 6.B 7 Pore size distribution as a function of relative volume

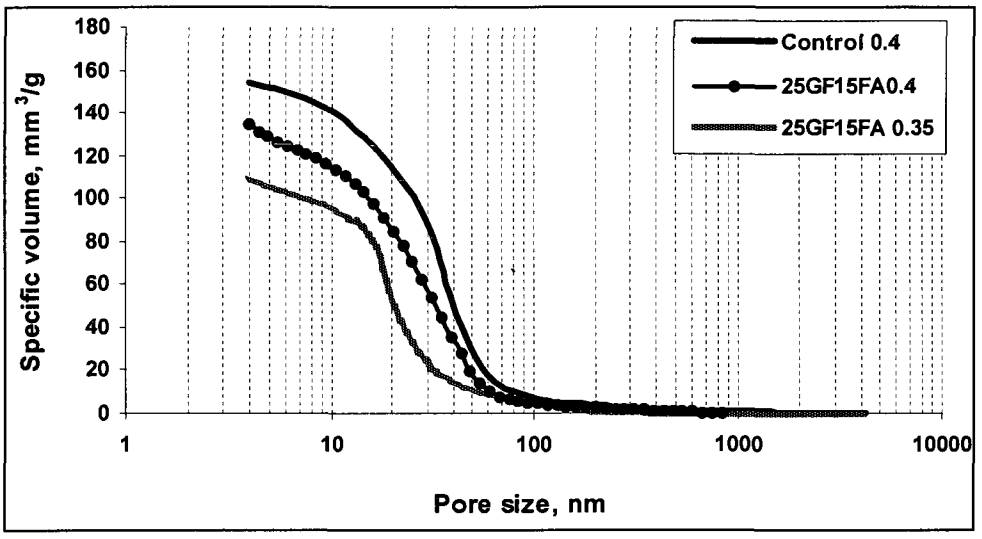

Figure 6.B 8 Pore size distribution as a function of specific volume

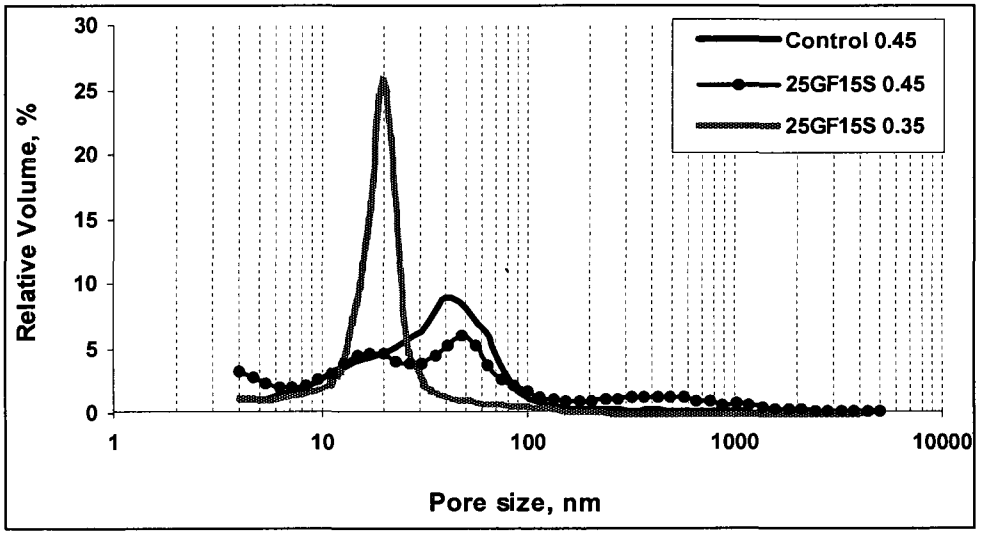

Figure 6.B 9 Pore size distribution as a function of relative volume

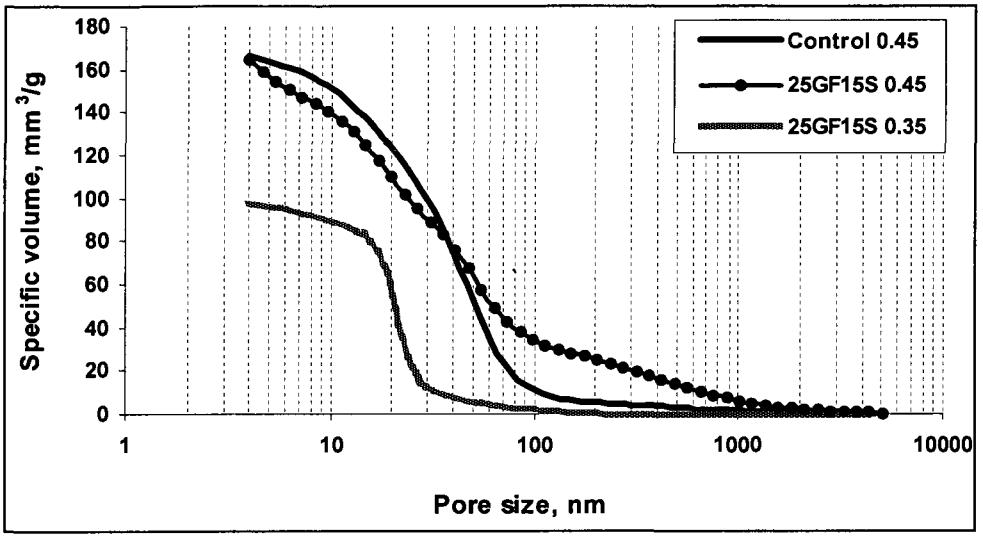

Figure 6.B 10 Pore size distribution as a function of specific volume

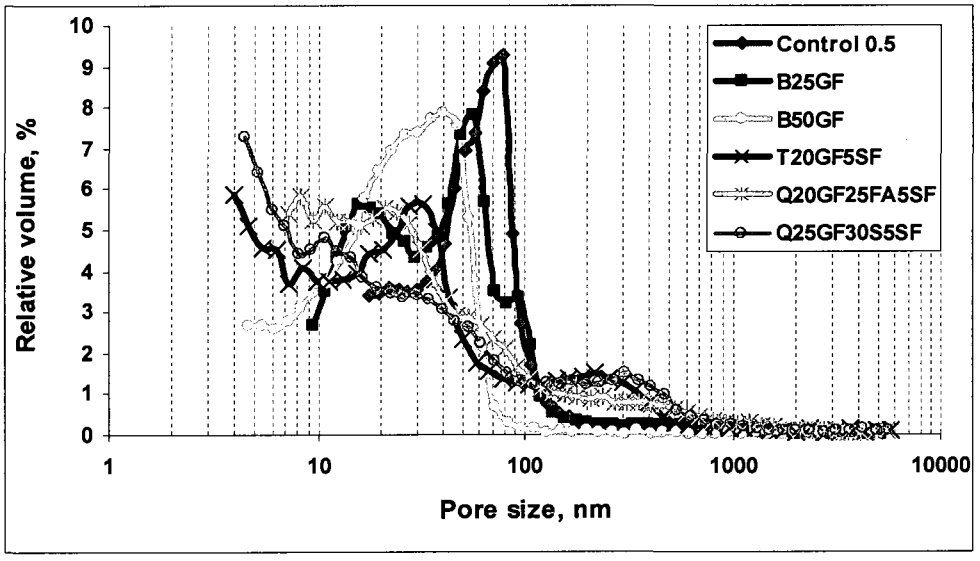

Figure 6.B 11 Pore size distribution as a function of specific volume

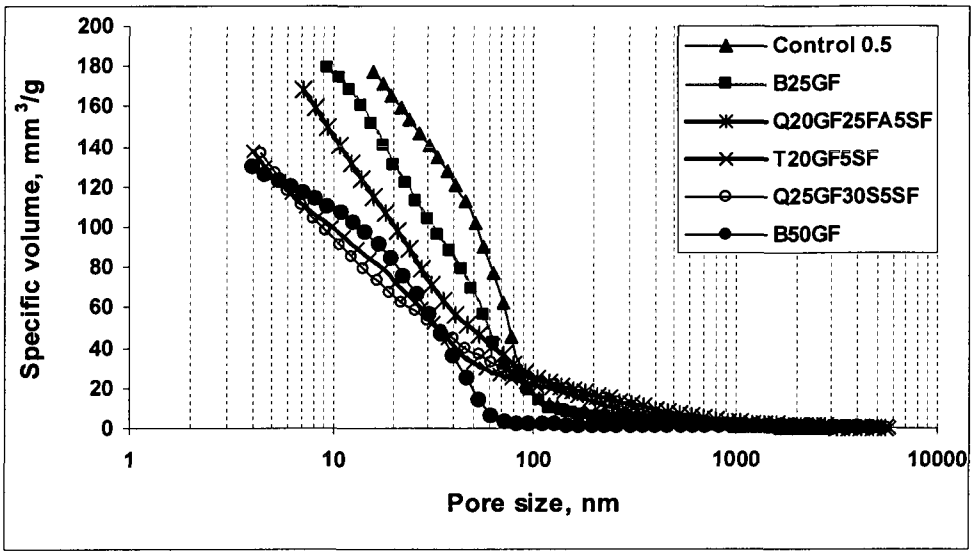

Figure 6.B 12 Pore size distribution as a function of relative volume

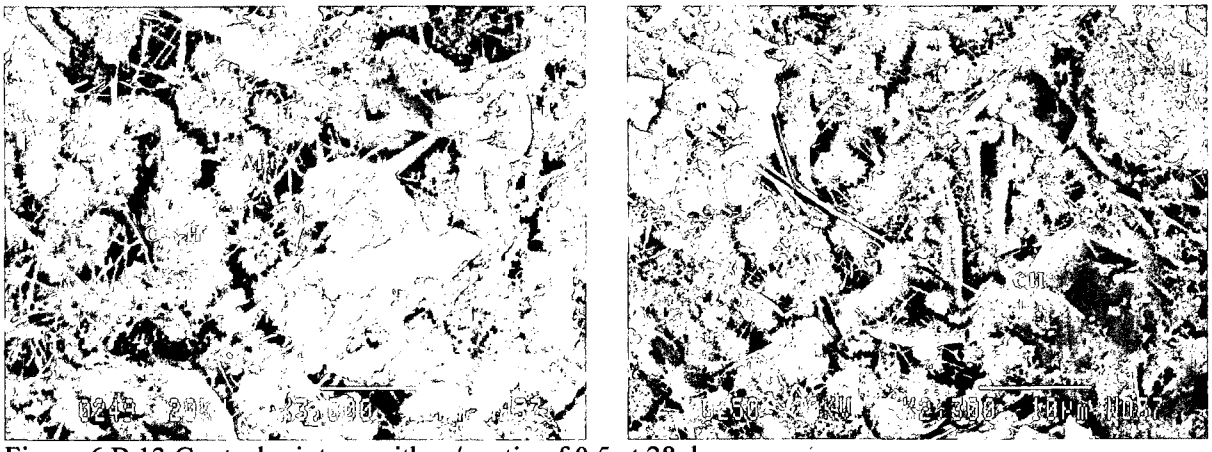

Figure 6.B 13 Control mixture with w/c ratio of 0.5 at 28 days

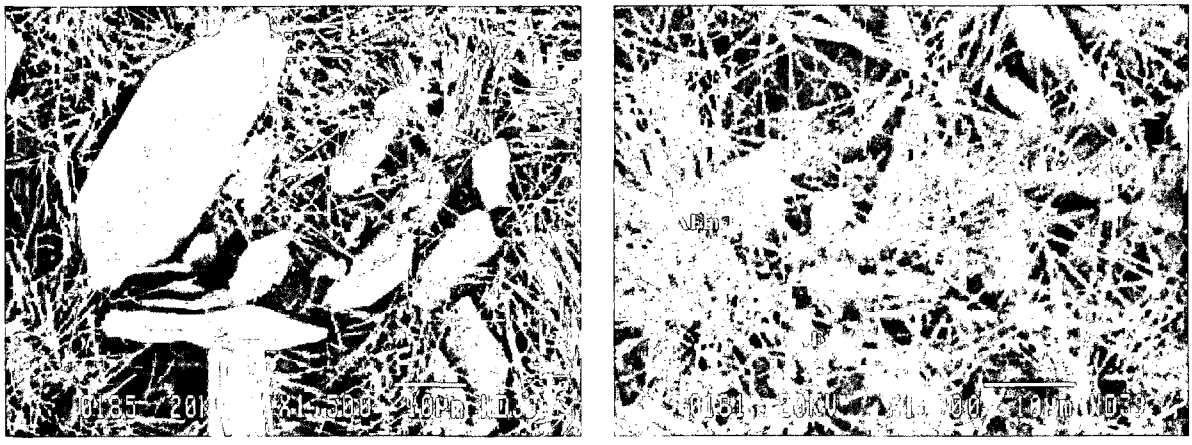

Figure 6.B 14 Control mixture with w/c ratio of 0.5 at 28 days

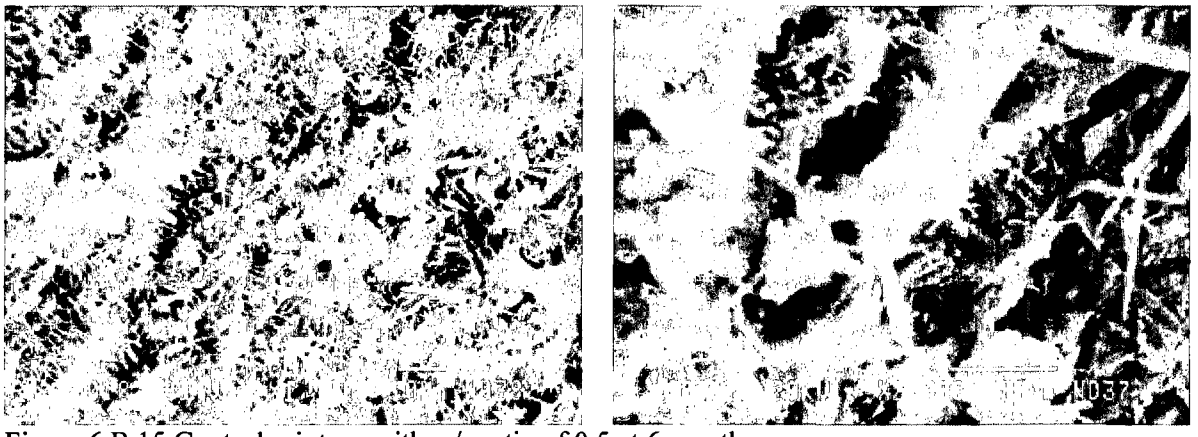

Figure 6.B 15 Control mixture with w/c ratio of 0.5 at 6 months

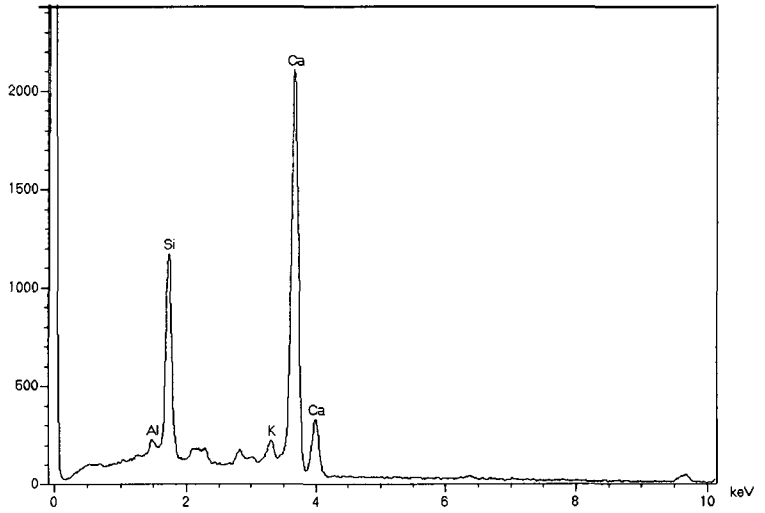

Figure 6.B 16 Elemental spot analysis for the control mixture, with w/c ratio of 0.5, showed that Ca/Si ratio is 1.75, at 28 days

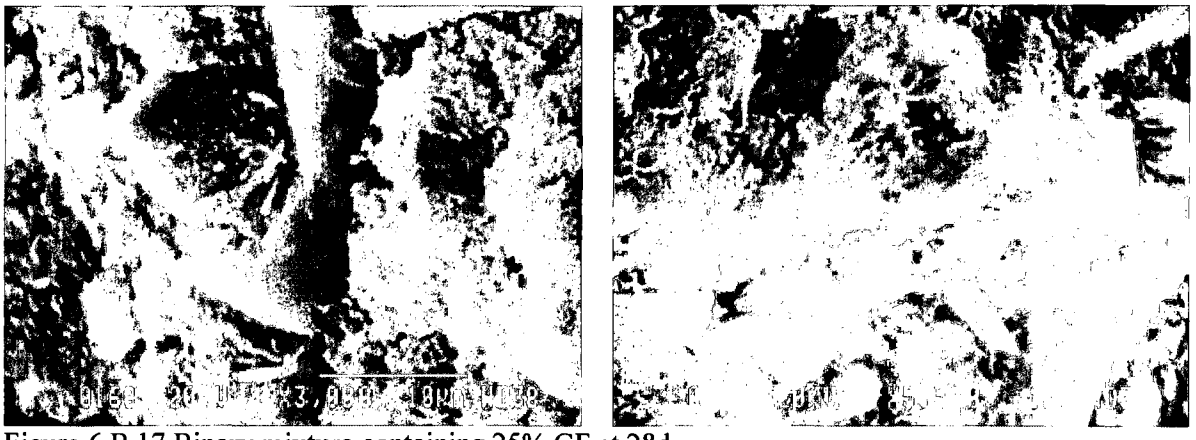

Figure 6.B 17 Binary mixture containing 25% GF at 28d

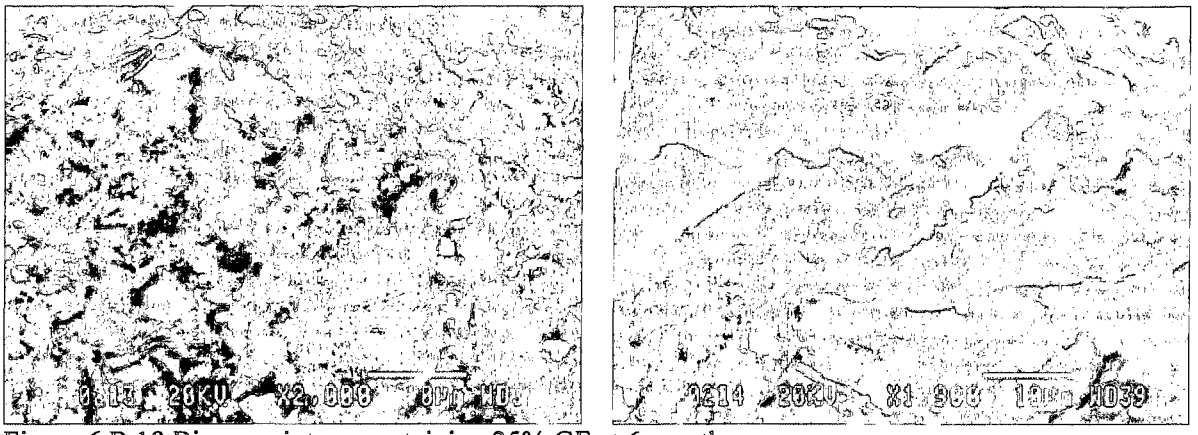

Figure 6.B 18 Binary mixture containing 25% GF at 6 months

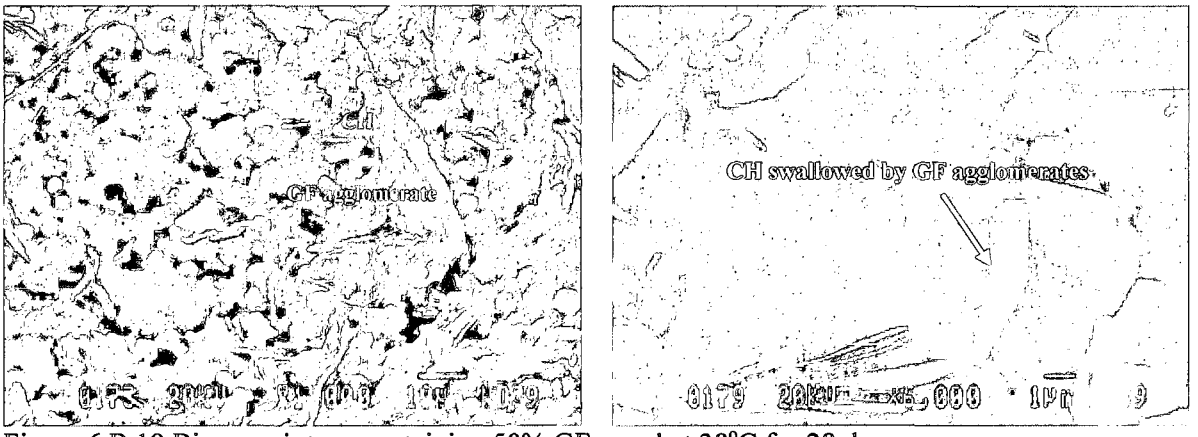

Figure 6.B 19 Binary mixture containing 50% GF cured at 38°C for 28 days

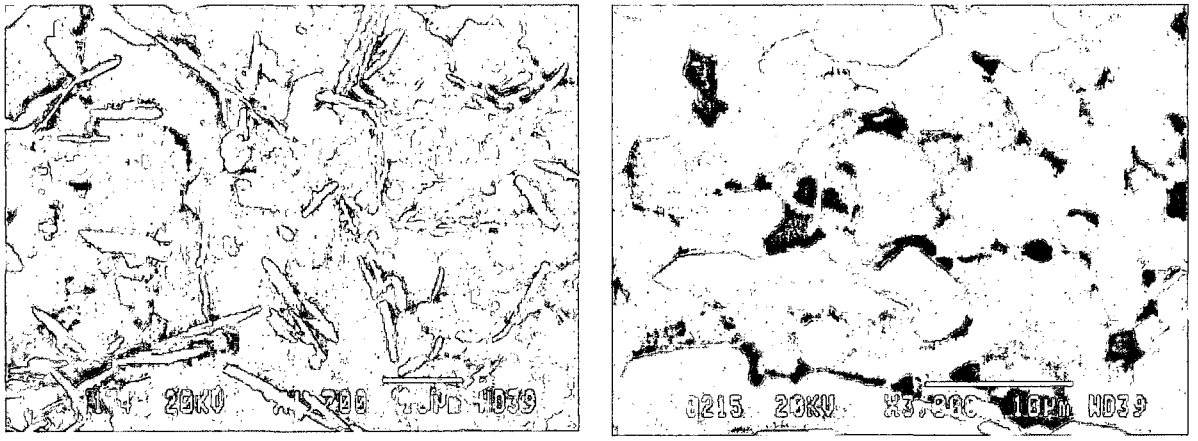

Figure 6.B 20 Binary mixture containing 50% GF cured at 38°C for 28 days, showed CH particles swallowed by new GF agglomerate

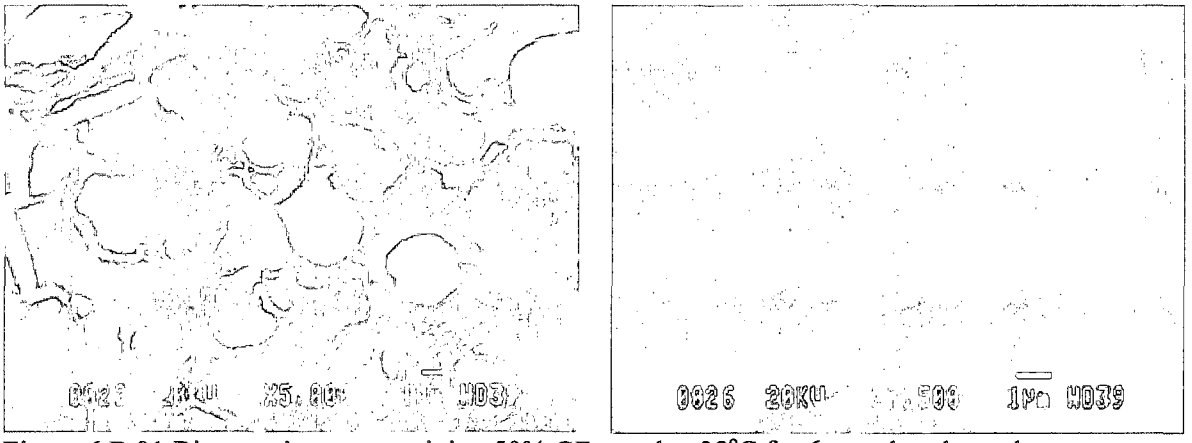

Figure 6.B 21 Binary mixture containing 50% GF cured at 38°C for 6 months, showed compete dissolution of GF and CH particles with very condensed structure

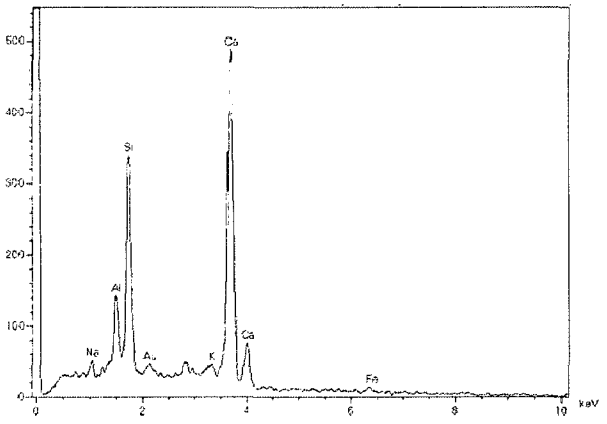

Figure 6.B 22 Spherical agglomeration of GF with high alkali content of the binary mixture containing 50% GF cured at 38°C for 6 months with C/S of 1.42

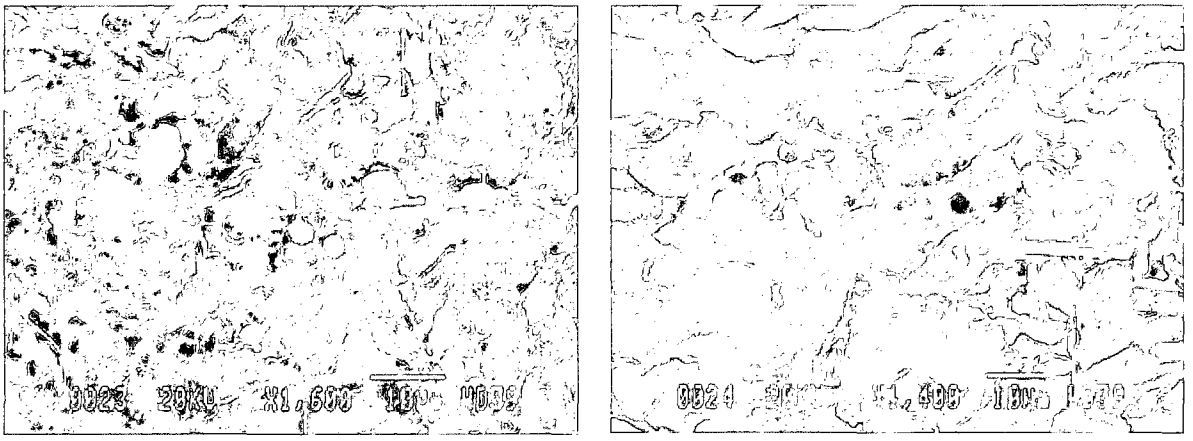

Figure 6.B 23 Microstructure development and closure of the pores of the binary mixture containing 50% GF cured at 38°C for 6 months

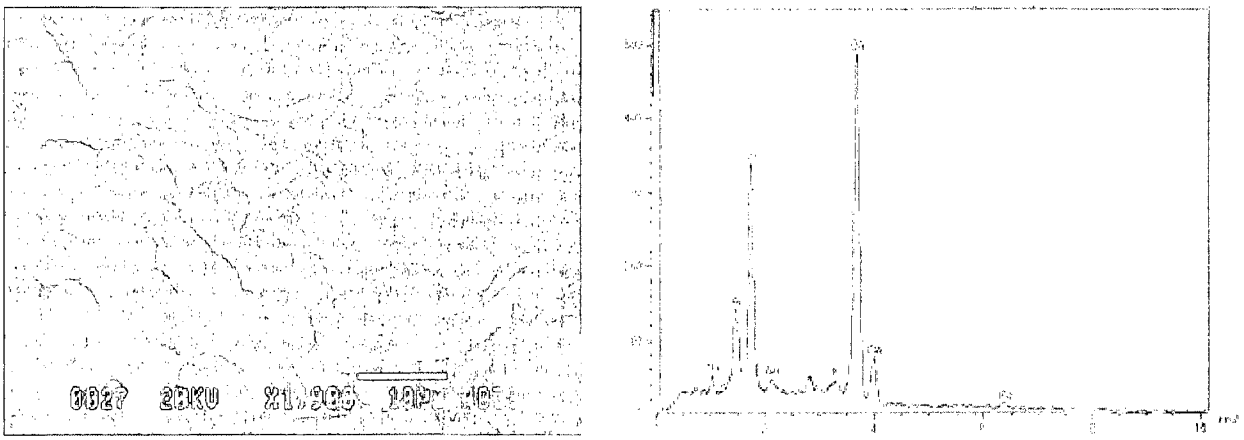

Figure 6.B 24 Microstructure development of the binary mixture with 50% GF cured at 38°C for 6 months

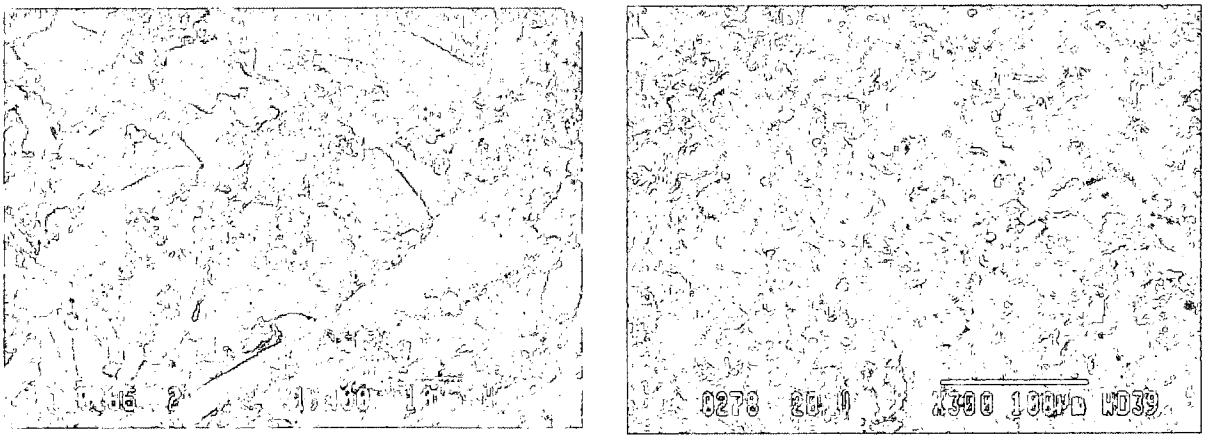

Figure 6.B 25 Microstructure development of the ternary mixture containing 20% GF and 5% SF with w/c ratio of 0.35, cured at 38°C for 28 days

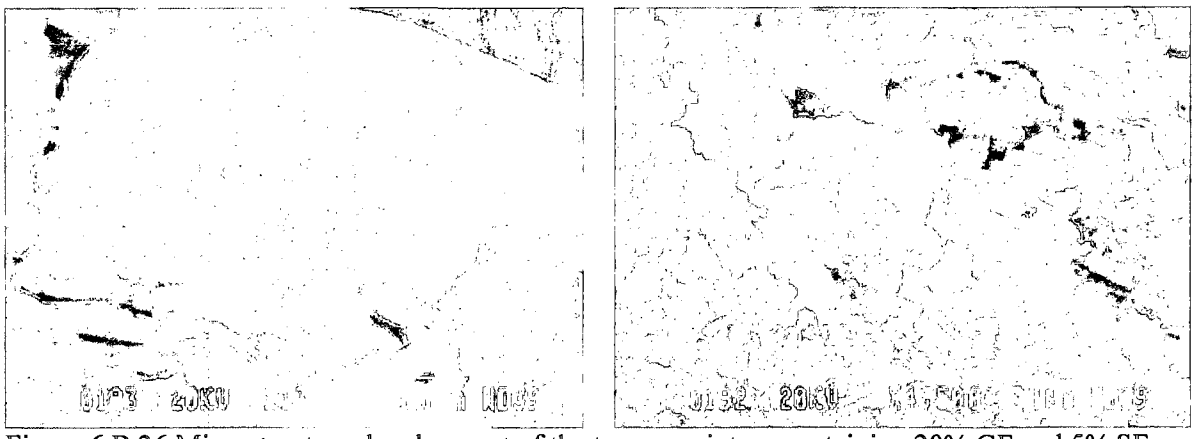

Figure 6.B 26 Microstructure development of the ternary mixture containing 20% GF and 5% SF cured at 38°C for 28 days

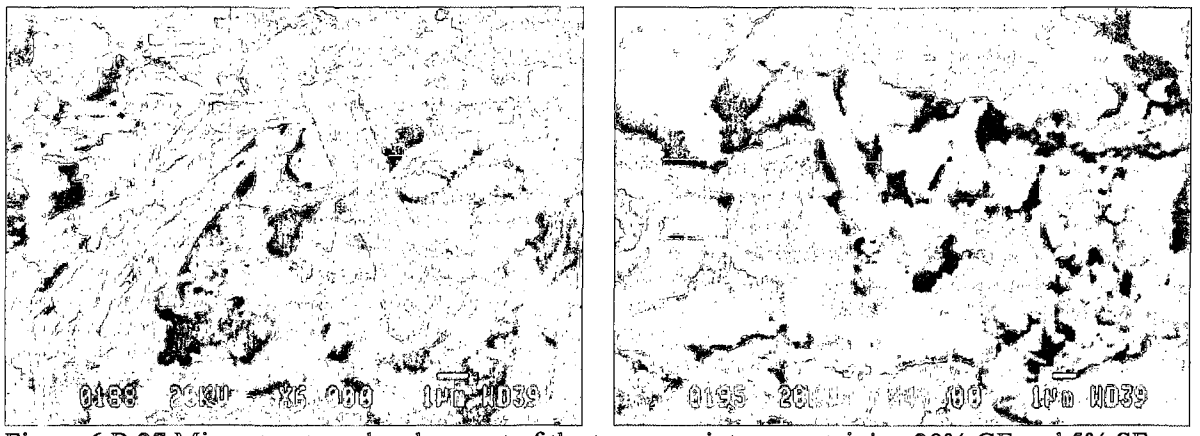

Figure 6.B 27 Microstructure development of the ternary mixture containing 20% GF and 5% SF cured at 38°C for 28 days

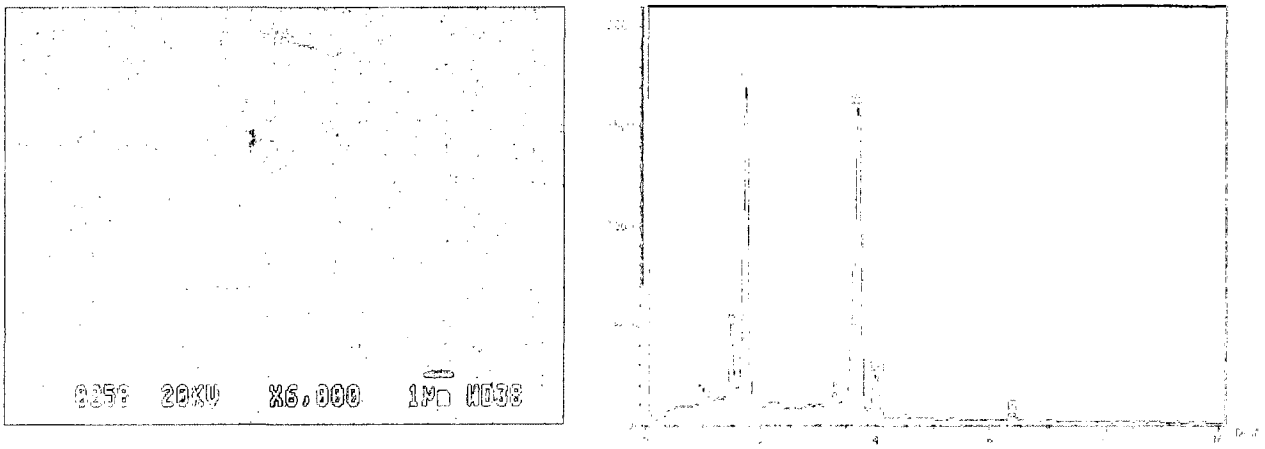

Figure 6.B 28 C-S-H formed from reaction of GF, silica fume and CH, giving Ca/Si ratio of 0.92, at 28 days

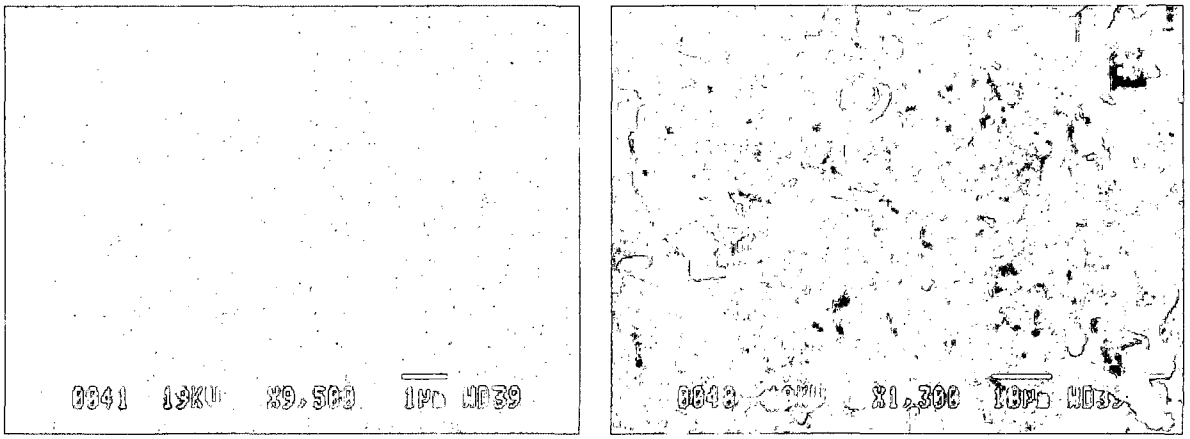

Figure 6.B 29 Microstructure development of the ternary mixture contaning 20% GF and 5% SF cured at 38°C for 6 months

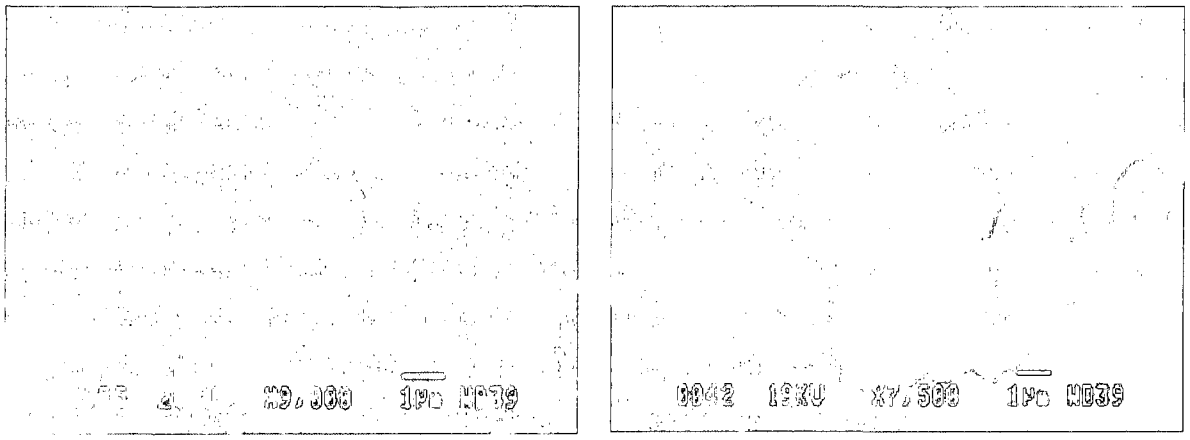

Figure 6.B 30 Microstructure development of the ternary mixture containing 20% GF and 5% SF cured at 38°C for 6 months

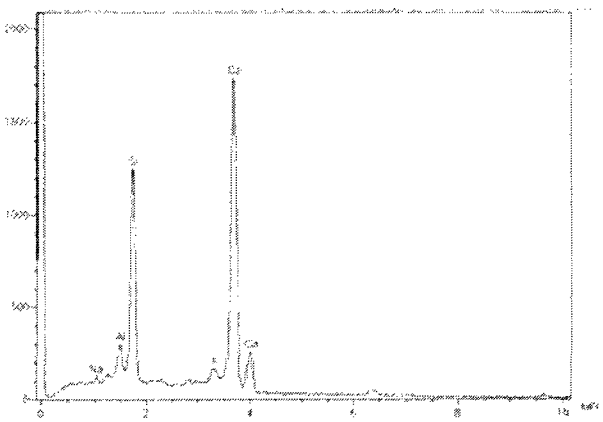

Figure 6.B 31 Small Spherical agglomeration embedded in the ternary GF and SF matrix with high alkali content cured at 38°C for 6 months, with C/S of 1.38

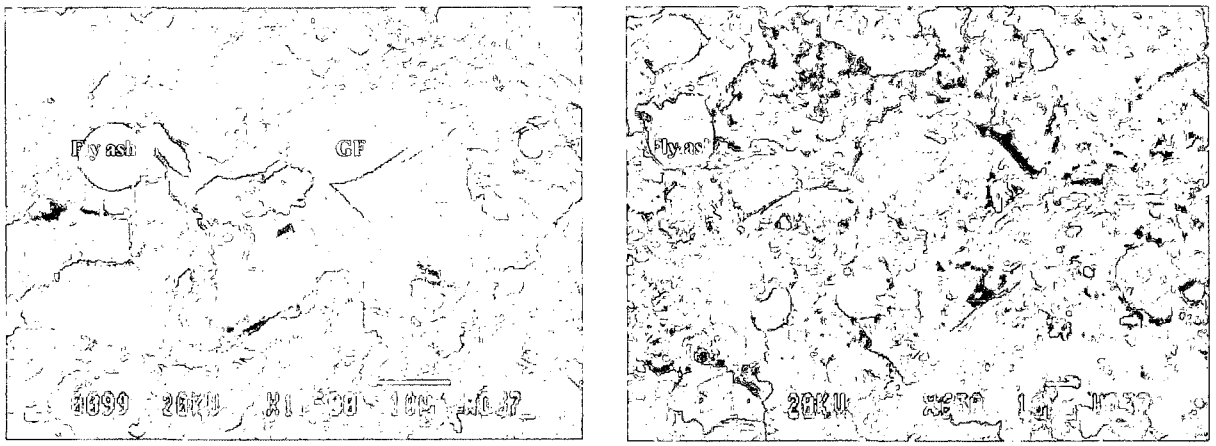

Figure 6.B 32 Ternary mixture of 25%GF and 15% FA with water-to-cement ratio of 0.35, cured at 38°C for 28 days

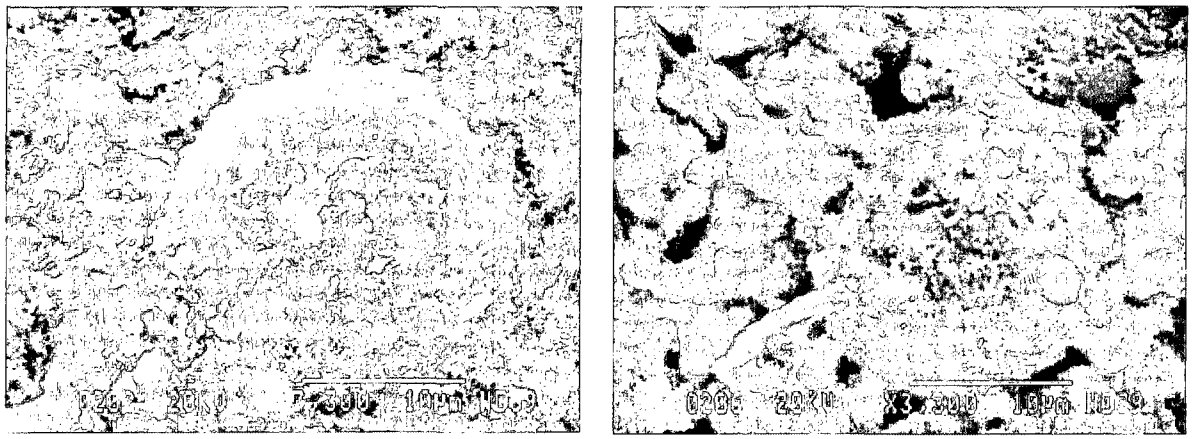

Figure 6.B 33 Coverage of the fly ash particle by reaction product in the quaternary GF-FA-SF system at 38°C for 28 days

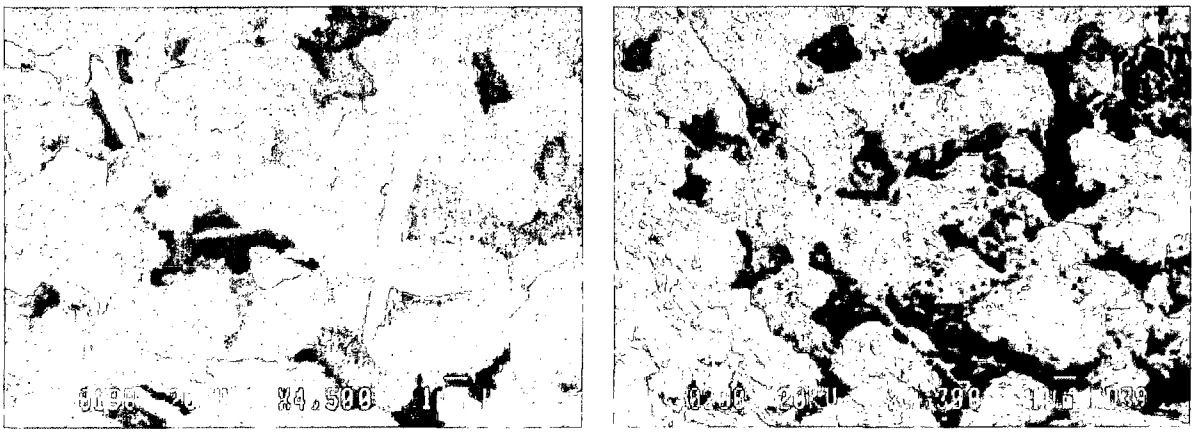

Figure 6.B 34 Polymerization reaction attacking portlandite crystals and covering the surface of the quaternary GF-FA-SF system at 38°C, at 6 months

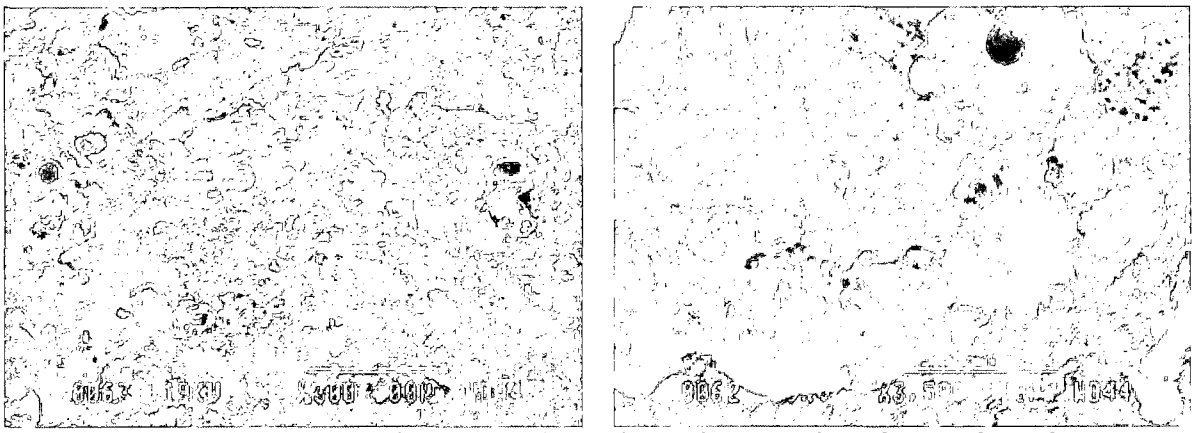

Figure 6.B 35 Complete polymerization reaction and complete covering of the surface of the quaternary GF-FA-SF system at 38°C, at 6 months

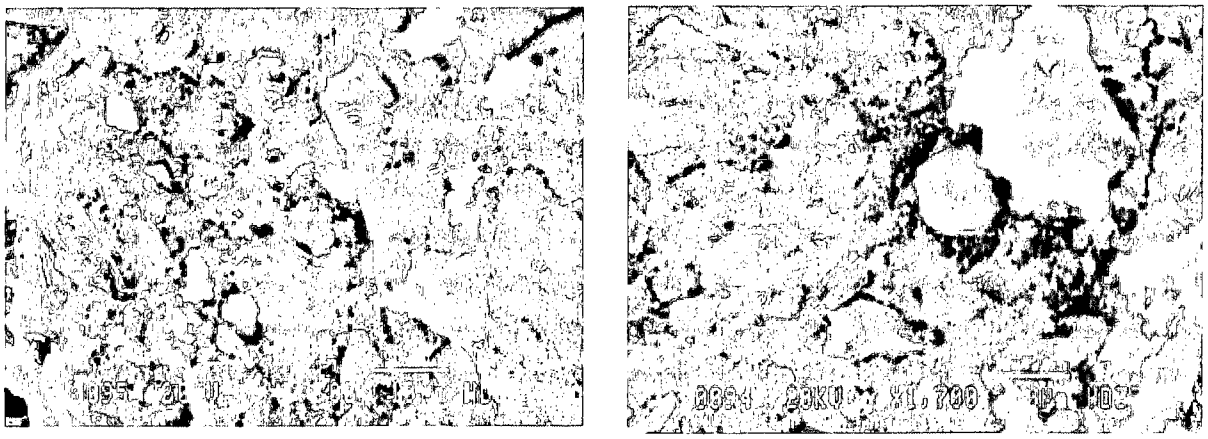

Figure 6.B 36 Ternary GF-slag mixture with water cement ratio of 0.35 at 28 days

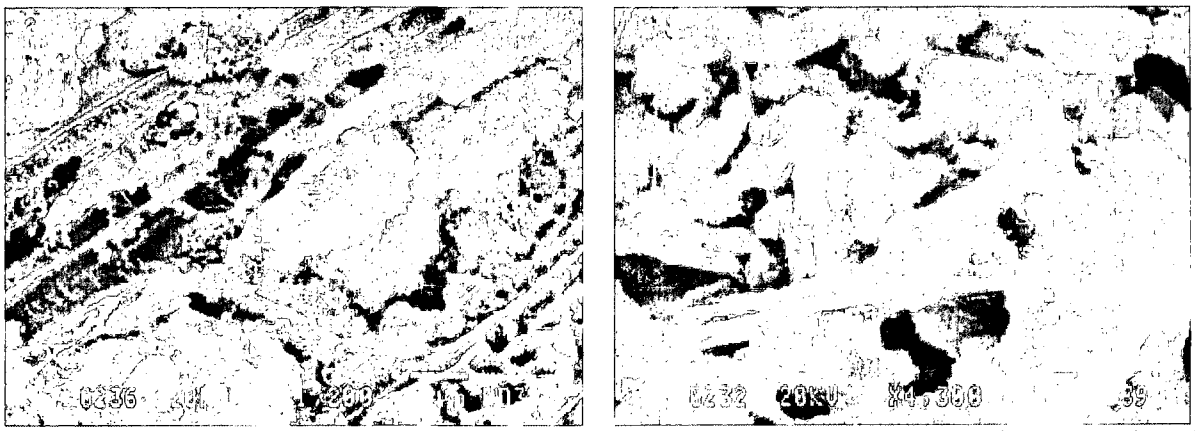

Figure 6.B 37 Microstructure development of the GF-slag-silica fume quaternary mixture cured at 28 days, at 38°C

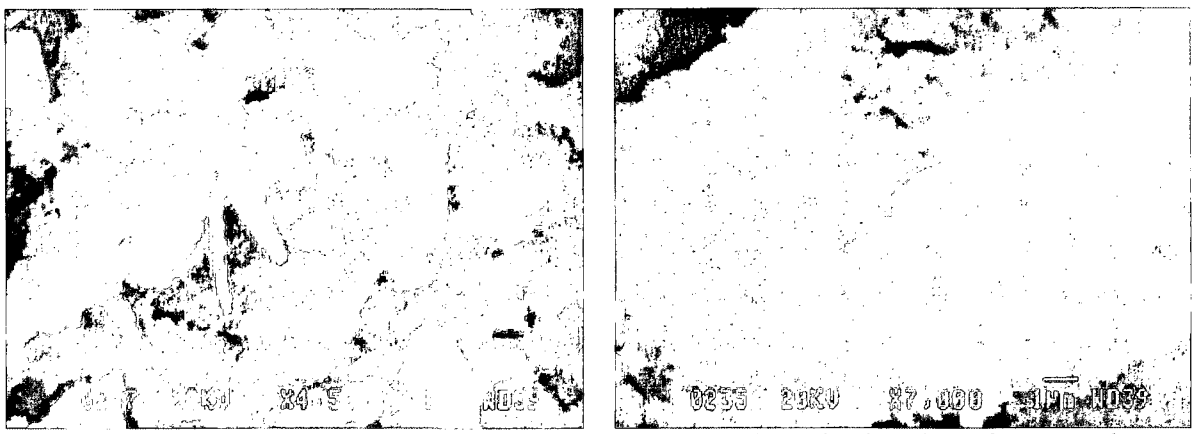

Figure 6.B 38 Microstructure development and formation of polymerization sites of the GF-slag-silica fume quaternary mixture cured at 28 days, at 38°C

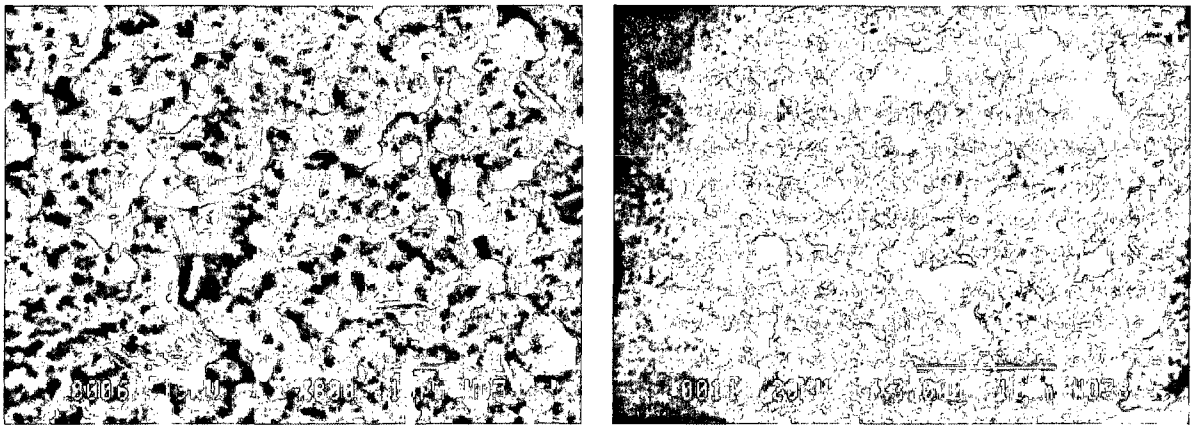

Figure 6.B 39 Microstructure development and propagation of polymerizing sites of the GF-slag-silica fume quaternary mixture cured at 6 months, at 38°C

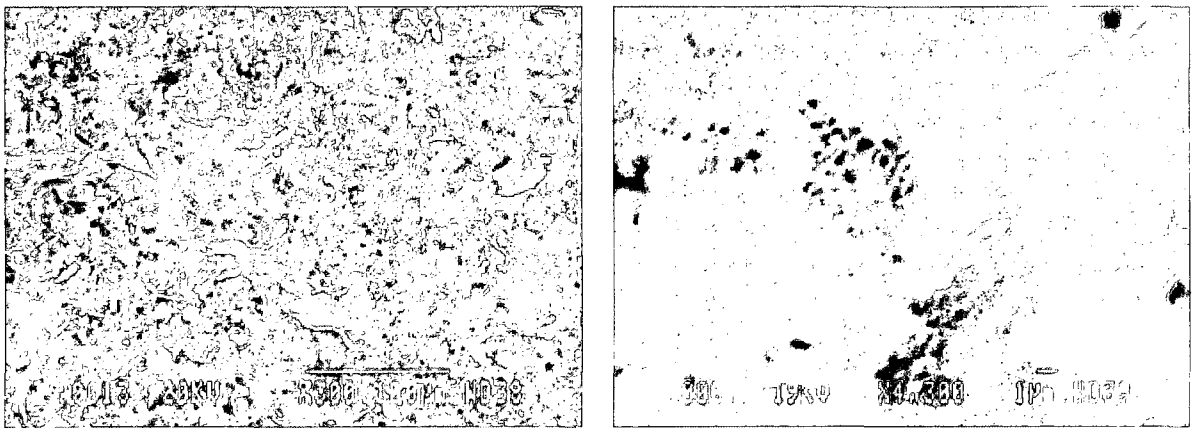

Figure 6.B 40 Microstructure development and start of surface covering of the GF-slag-silica fume quaternary mixture cured at 6 months, at 38°C

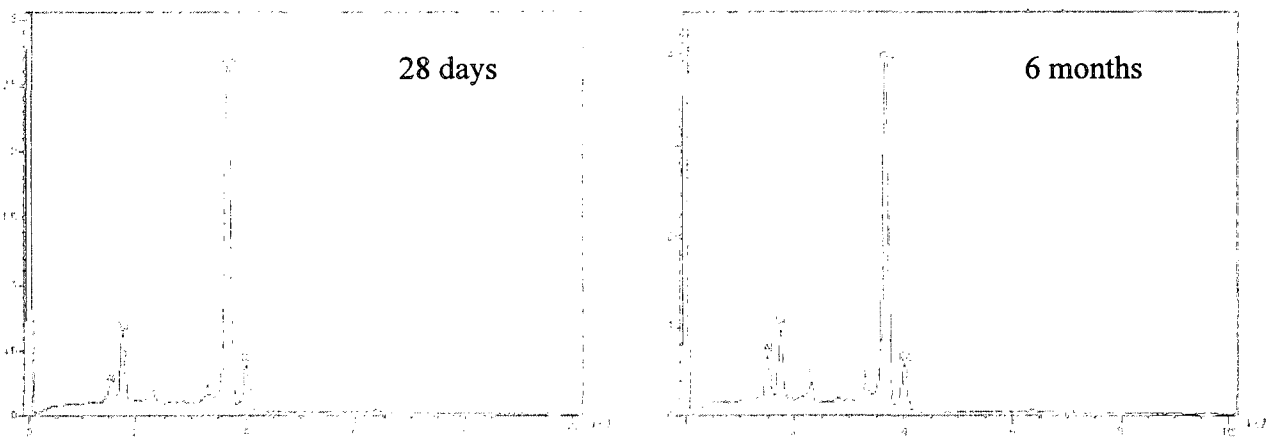

Figure 6.B 41 Control mixture at 28 days and 6 months

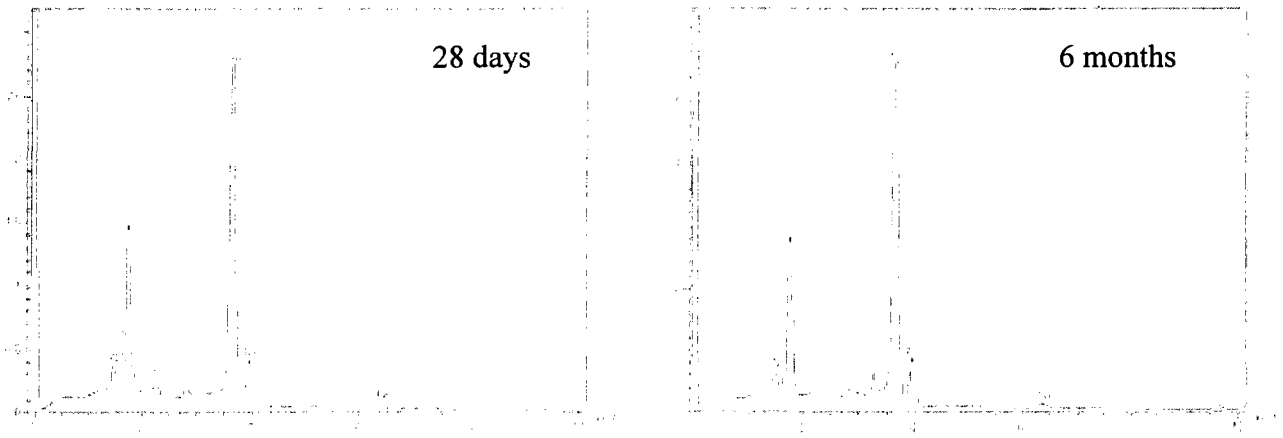

Figure 6.B 42 Binary mixture with 25% GF at 28 days and 6 months

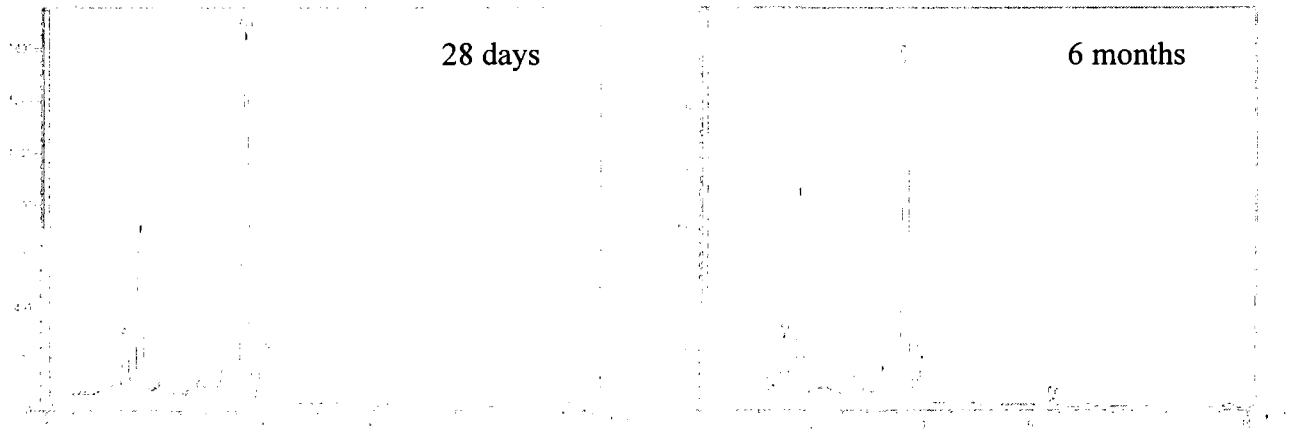

Figure 6.B 43 Binary mixture with 50% GF at 28 days and 6 months

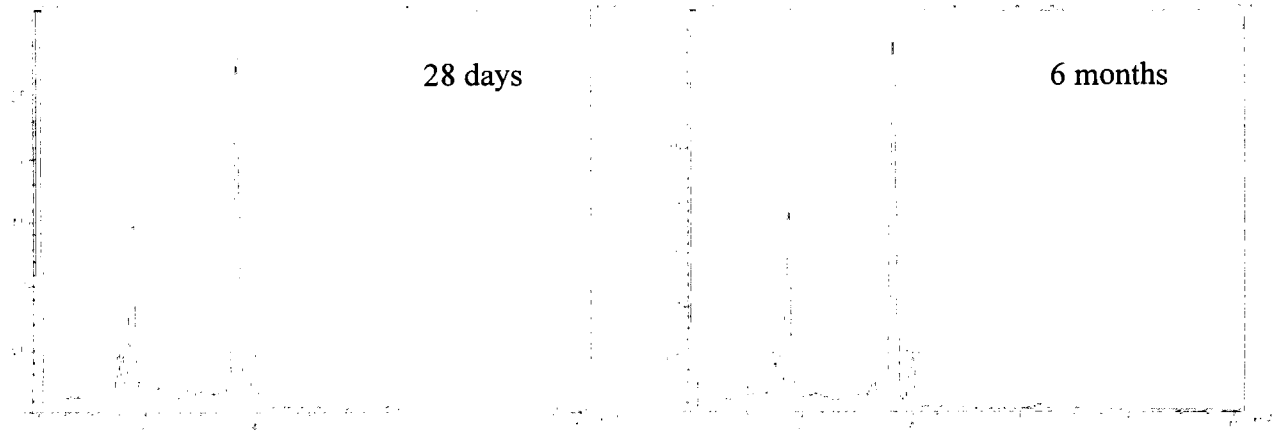

Figure 6.B 44 Ternary mixture with 20%GF5%SF at 28 days and 6 months

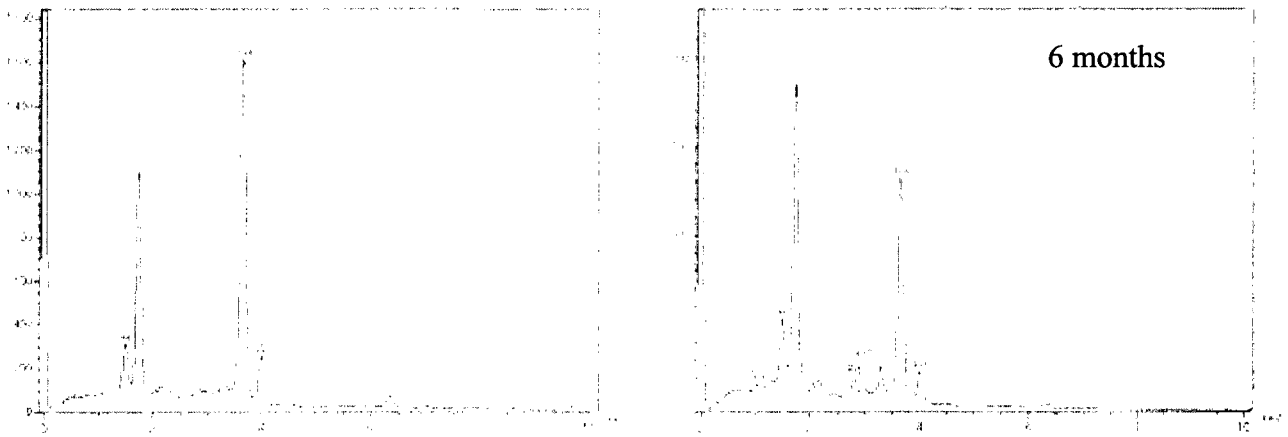

Figure 6.B 45 Quaternary mixture with 20%GF25%FA5%SF at 28 days and 6 months

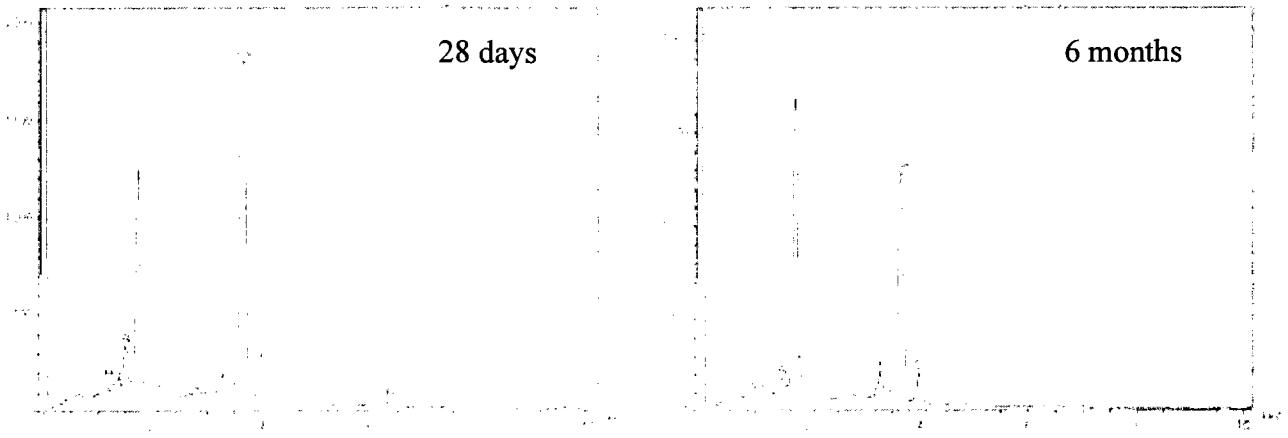

Figure 6.B 46 Quaternary mixture with 25%GF30%S5%SF at 28 days and 6 months